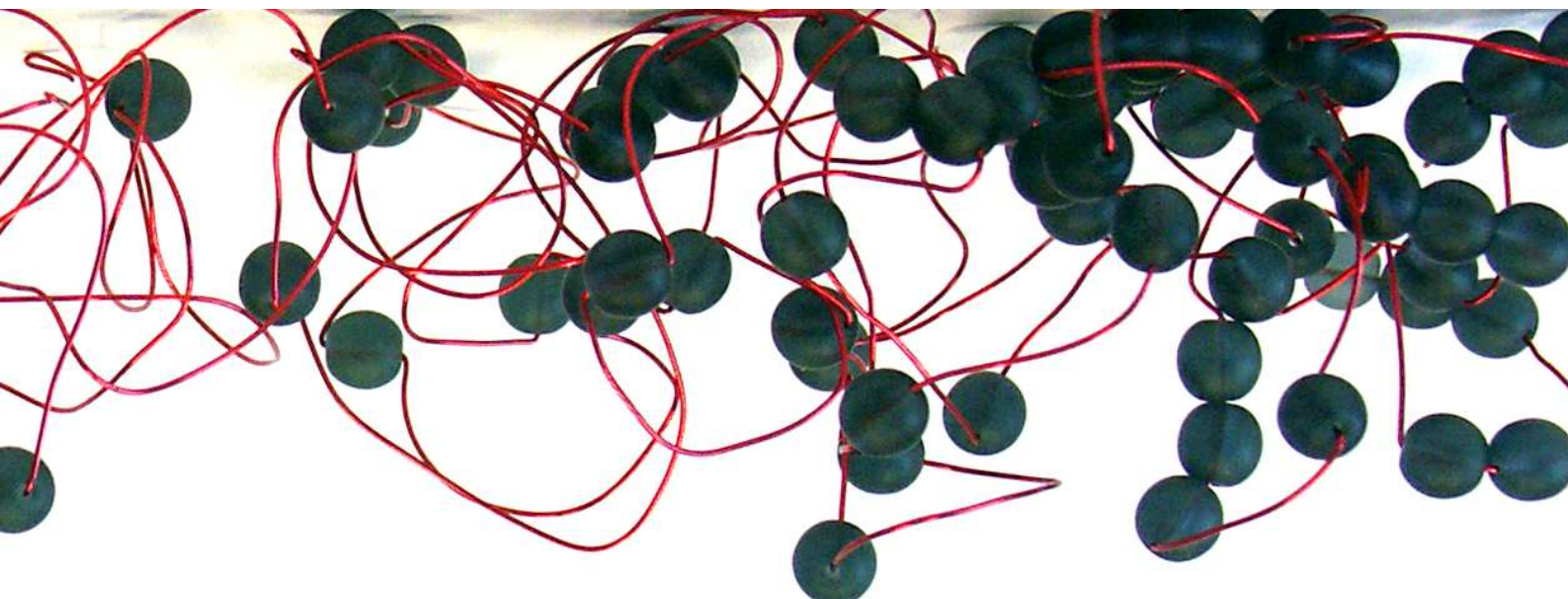


Protein/polysaccharide complexes at air/water interfaces



Renate A. Ganzevles

Promotoren:	Prof. dr. M.A. Cohen Stuart hoogleraar fysische chemie met bijzondere aandacht voor de kolloïdchemie
	Prof. dr. ir. A.G.J. Voragen hoogleraar levensmiddelenchemie
Co-promotoren:	Dr. ir. H.H.J. de Jongh projectleider WCFS TNO quality of life
	Dr. ir. T. van Vliet projectleider WCFS Wageningen Universiteit
Promotiecommissie:	Prof. dr. C.G. de Kruif (Universiteit Utrecht/NIZO food research, Ede) Prof. P. Dubin (University of Massachusetts, USA) Prof. dr. ir. R.M. Boom (Wageningen Universiteit) Dr. T.J. Foster (Unilever Research and Development, Vlaardingen)

Dit onderzoek is uitgevoerd binnen de onderzoeksschool VLAG

Protein/polysaccharide complexes at air/water interfaces

Renate A. Ganzevles

Proefschrift
ter verkrijging van de graad van doctor
op gezag van de rector magnificus
van Wageningen Universiteit,
Prof. dr. M.J. Kropff,
in het openbaar te verdedigen
op vrijdag 30 maart 2007
des namiddags te half twee in de Aula

Ganzevles, Renate A.

Protein/polysaccharide complexes at air/water interfaces,

Ph.D. Thesis Wageningen University, The Netherlands, 2007

ISBN: 90-8504-614-9

Abstract

Proteins are often used to create and stabilise foams and emulsions and therefore their adsorption behaviour to air/water and oil/water interfaces is extensively studied. Interaction of protein and polysaccharides in bulk solution can lead to the formation of soluble or insoluble complexes. The aim of this thesis was to understand the influence of (attractive and non-covalent) protein/polysaccharide interaction on adsorption behaviour at air/water interfaces (and oil/water interfaces) in terms of adsorption kinetics, and rheological and spectroscopic characterisation of the adsorbed layers. The approach was to first identify the relevant parameters (like charge density, charge distribution or molecular weight of the ingredients) in the mixed protein/polysaccharide adsorption process. Subsequently, for each parameter a range of ingredients was selected/prepared allowing variation of only this single parameter. After investigation of the phase behaviour in bulk solution of the different protein/polysaccharide mixtures to be used, the role of each parameter in mixed protein/polysaccharide adsorption was studied. The parameters most thoroughly assessed were: protein/polysaccharide mixing ratio, polysaccharide charge density and molecular weight and the sequence of adsorption. The majority of the measurements were performed with β -lactoglobulin (in combination with various polysaccharides e.g. pectin or carboxylated pullulan) at air/water interfaces, at standard conditions of pH 4.5 and low ionic strength (< 10 mM). In addition, experiments were performed at higher ionic strengths, different pH's, with different proteins or at an oil/water interface, to extend the insight in mixed protein/polysaccharide adsorption. This results obtained lead to a generic mechanistic model of mixed protein/polysaccharide adsorption.

In conclusion, protein/polysaccharide interaction can be exploited to control protein adsorption at air/water interfaces. Any parameter affecting protein/polysaccharide interaction (e.g. ingredient parameters like polysaccharide molecular weight, charge density and distribution or system parameters like charge ratio, pH and ionic strength) may be varied to obtain the desired adsorption kinetics, surface rheological behaviour, or net charge of the surface layer. The choice of simultaneous protein/polysaccharide adsorption (in the form of complexes) versus sequential adsorption (first the protein, than the polysaccharide) provides an extra control parameter regarding the functionality of mixed adsorbed layers.

KEYWORDS: protein, polysaccharide, β -lactoglobulin, pectin, electrostatic interaction, complex coacervation, adsorption, air/water interface, oil/water interface, surface pressure, surface rheology, spectroscopy

Table of contents

Abstract	5
Table of contents	7
Chapter 1: General introduction	11
1.1 Biopolymers	11
1.2 Protein adsorption	13
1.3 Protein/polysaccharide interaction in solution	14
1.4 Characterisation of adsorbed layers	16
1.4.1 Tensiometry	16
1.4.2 Surface rheology	16
1.4.3 Spectroscopy	17
1.5 Aim and outline of the thesis	18
References	19
Chapter 2: Dynamic surface pressure of protein/polysaccharide complexes at air/water interfaces	21
2.1 Introduction	22
2.2 Materials and methods	23
2.2.1 Materials	23
2.2.2 Drop tensiometry	24
2.2.3 Dynamic light scattering	24
2.3 Results	24
2.4 Discussion	27
References	30
Chapter 3: Modulating surface rheology by electrostatic protein/polysaccharide interactions	33
3.1 Introduction	34
3.2 Materials and methods	35
3.2.1 Materials	35
3.2.2 Light scattering	35
3.2.3 Determination of ζ -potential	36
3.2.4 Drop tensiometry/ surface dilatational rheology	36
3.2.5 Surface shear rheology	36
3.3 Results	37
3.3.1 β -Lactoglobulin/pectin complexes in solution	38
3.3.2 Surface dilatational rheology	40
3.3.3 Surface shear rheology	42
3.4 Discussion	44
References	47

Chapter 4: Adsorption of protein/polysaccharide complexes; a comparison between air/water and oil/water interfaces	49
4.1 Introduction	50
4.2 Experimental	51
4.2.1 Materials	51
4.2.2 Dynamic light scattering	51
4.2.3 Drop tensiometry	52
4.3 Adsorption kinetics	52
4.4 Surface rheology and structure of adsorbed layers	56
4.5 Concluding remarks	58
References	58
Chapter 5: Structure of mixed β-lactoglobulin/ pectin adsorbed layers at air/water interfaces; a spectroscopy study	61
5.1 Introduction	62
5.2 Materials and methods	63
5.2.1 Materials	63
5.2.2 Neutron reflection	64
5.2.3 Time Resolved Fluorescence Anisotropy	65
5.3 Results	67
5.3.1 Neutron reflection measurements	67
5.3.2 Pure protein film	67
5.3.3 Effect of complex net charge on layer density profile	68
5.3.4 Simultaneous versus sequential adsorption	70
5.3.5 Time resolved fluorescence anisotropy	71
5.4 Discussion	73
5.5 Conclusions	75
References	76
Chapter 6: Pullulan charge density controlled β-lactoglobulin complexation in relation to surface activity	79
6.1 Introduction	80
6.2 Materials and methods	81
6.2.1 Pullulan oxidation and characterization	81
6.2.2 Sample preparation	82
6.2.3 Light scattering	82
6.2.4 Electrophoretic mobility	83
6.2.5 Drop tensiometry/surface dilatational rheology	83
6.2.6 Surface shear rheology	83
6.3 Results	84
6.3.1 β -lactoglobulin pullulan complexation	84
6.3.2 Effect of charge density on surface rheology	86
6.3.3 Effect of charge ratio on surface rheology	87
6.4 Discussion	89
6.4.1 Bulk complexation	89
6.4.2 Complexes at interfaces	90
6.5 Conclusions	92
References	93

Chapter 7: Complex coacervate morphology controlled by polysaccharide charge density	95
7.1 Introduction	96
7.2 Materials and methods	96
7.2.1 Materials	96
7.2.2 Small angle X-ray scattering	97
7.2.3 Microscopy	97
7.3 Results and discussion	97
7.3.1 Charge density dependence	98
7.3.2 Charge ratio dependence	99
7.3.3 Light microscopy	100
7.4 Conclusions	101
References	102
Chapter 8: Polysaccharides as a kinetic barrier for protein accumulation at air/water interfaces	103
8.1 Introduction	104
8.2 Materials and methods	104
8.2.1 Materials	104
8.2.2 Dynamic light scattering	105
8.2.3 Determination of ζ -potential	106
8.2.4 Ellipsometry & Surface tensiometry	106
8.3 Results	107
8.3.1 Selection of materials	107
8.3.2 Complex charge ratio	108
8.3.3 Polysaccharide molecular weight	109
8.3.4 Polysaccharide charge density	110
8.3.5 Equation of state	111
8.4 Discussion	112
8.4.1 Accumulation of mass at the interface	112
8.4.2 Equation of state	115
8.5 Conclusions	116
References	116
Chapter 9: General discussion	119
9.1 Schematic model polysaccharide controlled protein adsorption	119
9.2 Complex dynamics	123
9.2.1 Results	123
9.2.2 Discussion	128
9.3 Applications	132
References	135
Summary	137
Samenvatting	141
Dankwoord	145
List of publications	149
Curriculum vitae	150
Overview of completed training activities	151

General introduction

The properties of emulsions (liquid-in-liquid dispersions) and foams (air-in-liquid dispersions) are to a large extent determined by the properties of the fluid-fluid interfaces they contain. Many food emulsions and foams contain proteins. Adsorption of proteins at air/water and oil/water interfaces changes the properties of these interfaces and with that enables the formation and stabilisation of foams and emulsions. A lot of work has been done to understand the exact role of proteins in this respect. Fast adsorption of components to the created interface during bubble/droplet formation providing surface pressure, surface elasticity and colloidal repulsion enhances foam and emulsion formation. Surface elasticity in combination with electrostatic and steric repulsion contributes to long term stability. Foods are complex systems containing also other ingredients besides protein. Polysaccharides are often used for their water holding and thickening or gelling properties. If different ingredients in a product interact, the functionality of the mixture is not a simple sum of the functionality of the separate ingredients. The understanding of interactions between the different ingredients is relevant to prevent undesired effects. Moreover, insight in these interactions may be used to control and even improve the functionality of a combination of ingredients. A classical application of protein/polysaccharide interaction is the use of pectin adsorption on casein micelles to prevent their aggregation¹. In a similar way polysaccharides may affect interaction between emulsion droplets or air bubbles by adsorption on the protein layer covering the droplets/bubbles². Before further defining the aim of this thesis, we will discuss some basic aspects of protein adsorption, protein/polysaccharide interaction and the relevant ingredient parameters that are important in both processes.

1.1 BIOPOLYMERS

Two types of biopolymers are used in this thesis: proteins and polysaccharides. Both types are present in nature in a wide variety. With few exceptions, protein and polysaccharides consist of long linear (or branched for some polysaccharides) chains of covalently linked subunits. In this respect the two classes may be similar. They differ, however, in the kind of subunits and consequently in the structure they adopt in aqueous solution. The flexibility of the polysaccharide chain depends on the linkage type (through which carbon atoms the sugar rings are connected, e.g. 1,4 or 1,6) and the anomeric form of the linkage (α or β). Depending

on the flexibility a polysaccharide may adopt a stiff linear, helical or random coil conformation in solution. The latter conformation makes the polysaccharide a very bulky and diffuse object. As opposed to polysaccharides, which commonly show only limited differences (or no difference at all) between subunits, protein chains are build up from many (up to 20) different amino acids for every protein in a unique sequence as encoded by genetic material. These amino acids can be neutral, acidic or basic and furthermore they differ in their polarity (and thus hydrophobicity). Besides by their primary structure (amino acid sequence), proteins are characterised by their conformation (or native structure or protein folding) at a secondary, tertiary and sometimes quaternary level. The secondary structure is defined as the local organisation of the linear chain in α -helices, β -sheets and β -turns. The tertiary structure is the way the secondary structures are organised in a defined spatial arrangement, possibly stabilised by disulphide bridges. Some proteins can also adopt a quaternary structure, which is defined as the association of two or more protein molecules to a dimer or trimer or an even larger aggregate, but in a specific orientation. On the basis of their conformation, proteins can be subdivided in globular and random-coil like. A globular conformation makes the protein molecules much more compact than (random-coil like) polysaccharides. Proteins are generally surface active, polysaccharides, besides some exceptions, are not. In principle all protein molecules (of one type) are identical, as opposed to polysaccharides which are heterodisperse in molecular weight and distribution of subunits. The molecular weight of polysaccharides (100 – 1 000 kDa) is often much larger than that of proteins (10 – 60 kDa).

The main protein used in this thesis is β -lactoglobulin (Figure 1.1). It is a globular protein, the most abundant protein in bovine whey, and a common ingredient in food products. At the conditions used in this thesis, it is predominately present in dimeric form. The dimer has a mass of 36.6 kDa consisting of two molecules of 18.3 kDa. The iso-electric pH is 5.1; at this pH the net charge (the number of positively charged groups minus the number of negatively charged groups) of the protein is zero. Below this pH the protein is positively charged; above this pH the net charge is negative.

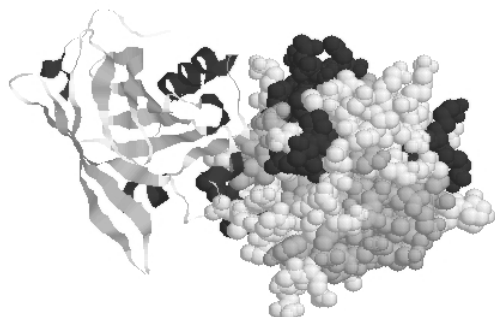
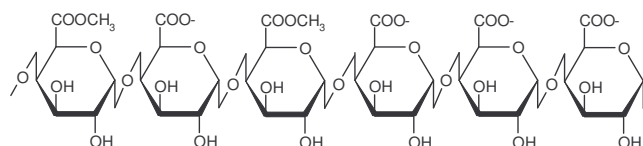


Figure 1.1: Schematic representation of a β -lactoglobulin dimer; the left half is a ribbon presentation showing β -sheets (grey) and α -helices (black), the right half is a space filling model.

Two types of anionic polysaccharides are used: pectin and carboxylated pullulan. Pectin is a common constituent of plant cell walls. We used pectin isolated from lemon peel of which branches are removed during the acid extraction. Pectin consists of a linear α -1,4 galacturonic acid backbone of which a fraction of the carboxylic acids is substituted with methoxyl groups

(Figure 1.2a). If more than 50% of the galacturonic acid residues are substituted (the degree of methoxylation $> 50\%$) it is denoted as high methoxyl pectin (hmp) and with less than 50% substitution it is called low methoxyl pectin (lmp). Pullulan is produced from starch by the fungus *Aureobasidium pullulans* and consists of a linear chain of a repeating trimer of glucose units. The trimers are connected by α -1,6 bonds and the glucose units within the trimers are connected by α -1,4 bonds. The C6 carbon atom can be chemically carboxylated (Figure 1.2b)³.

a) Low methoxyl pectin



b) carboxylated pullulan

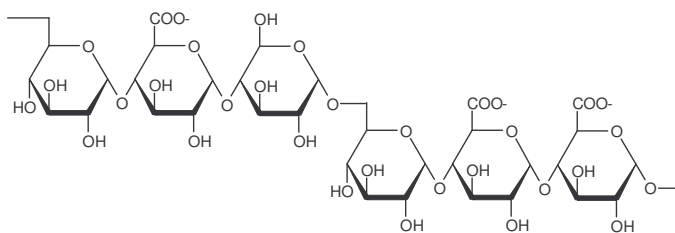


Figure 1.2: Typical example of an oligosaccharide sequence as could be part of a) a low methoxyl pectin chain and b) a carboxylated pullulan chain; the substitutions do not follow the same pattern throughout the polysaccharide chain.

1.2 PROTEIN ADSORPTION

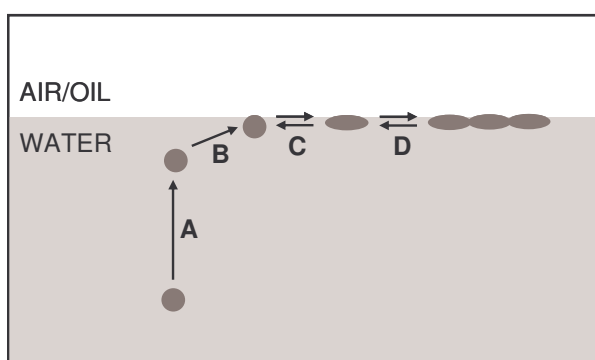


Figure 1.3: Overview of different steps in the formation of an adsorbed protein layer: A) transport of the protein molecule to the interface, B) adsorption of the protein molecule, C) conformational changes and D) interaction between neighbouring protein molecules.

The fact that proteins consist of amino acids with different polarity gives them a high affinity for air- and oil/water interfaces. Hydrophobic parts may gain energy by residing at interfaces with lower dielectric constant. Hydrophilic and charged parts remain in the water phase. Adsorption of proteins to an air- or oil/water interface reduces - like any adsorption - the surface (or interfacial) tension (γ). Figure 1.3 gives a pictorial representation of various steps that may occur in the formation of an adsorbed protein layer. The steps need not be sharply separated; they may overlap or occur at the same time. Step A represents transport of proteins to the interface. This can be diffusive or convective. The rate of diffusive transport is

inversely proportional to the radius of the globule. Whereas transport may be dominated by diffusion in typical adsorption experiments (depending on the measurement setup and the concentration), convection is often dominating during the formation of a foam/emulsion. Since different globular proteins often do not differ much in size, large differences in their adsorption kinetics cannot be attributed to a difference in transport rate (assuming that transport depends only on size). Step B refers to the actual attachment of the protein once it is in close vicinity of the interface. This process depends on the balance between the net charge and the exposed hydrophobicity on the surface of a protein. Increasing the exposed hydrophobicity on a protein reduces its kinetic barrier for adsorption⁴ and increasing the net charge increases the kinetic barrier⁵. This makes step B a discriminating step between different proteins. Step C represents unfolding/refolding of proteins. The extent to which this happens depends on the folding stability of the protein molecules^{6, 7}. Typically random coil polymers can unfold easily, assuming a conformation containing monomer sequences in the surface layer (trains) as well as protrusions away from the surface (loops, tails). Globular protein unfold less easily due to their internal cohesion⁸. They may partly spread at the air/water interface adopting a larger area per molecule, but retain a large part of their native conformation upon adsorption^{6, 7, 9, 10}. Fainerman et al. described a model for protein adsorption in which the area occupied by protein molecules can vary between a maximum and minimum value, depending on the surface pressure¹¹. Proteins are thus considered as compressible or soft¹² particles, in which the term compressible refers to the area occupied by the protein, not to the volume of a protein. Finally step D refers to the colloidal interaction between proteins at the interface. This interaction can be repulsive, due to a high net charge on the proteins or attractive, in the absence of strong electrostatic repulsion, e.g. due to hydrophobic interaction. The combination of the molecular structure of the proteins, adsorbed amount (or area per molecule) and the interaction between the proteins determines the rheological behaviour of the adsorbed layer. This surface rheological behaviour is important for the stability of emulsions and foams¹³⁻¹⁵. The rate of protein adsorption (and the resulting decrease in surface tension and increase in surface elasticity) is believed to be important for the formation of foams and emulsions^{16, 17}.

1.3 PROTEIN/POLYSACCHARIDE INTERACTION IN SOLUTION

When proteins and polysaccharides, or polyelectrolytes are mixed, three different scenarios are possible (Figure 1.4): (i) segregative phase separation; the ingredients repel each other and two phases appear, one rich in polysaccharide and poor in protein and one rich in protein and poor in polysaccharide, (ii) cosolubility; the ingredients mix well and the solution is stable and (iii) associative phase separation or complex coacervation; protein and polysaccharide attract each other and form a concentrated protein/polysaccharide phase and a dilute phase. On changing ingredient and/or solvent properties a system may shift from one scenario to another (see arrows).

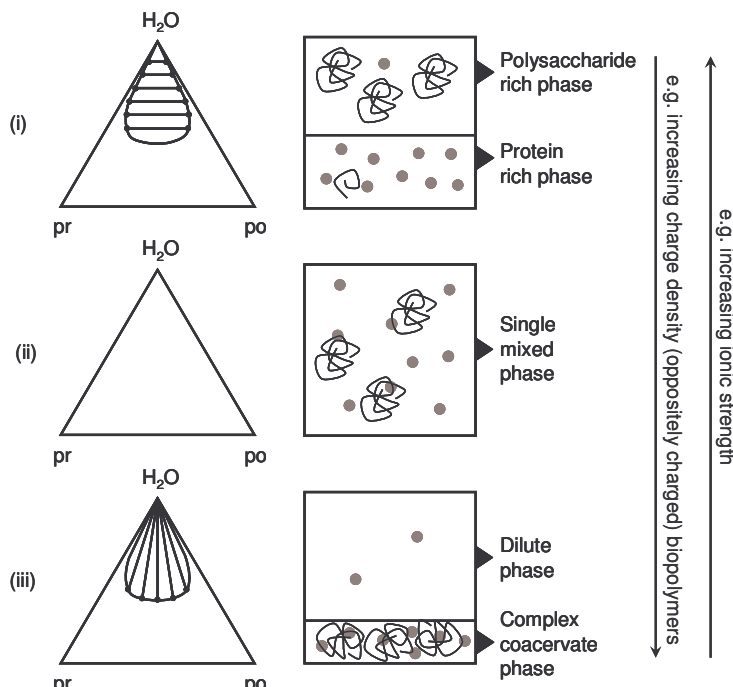


Figure 1.4 left: Schematic phase diagrams of protein (pr) and polysaccharide (po) in three different interaction scenarios in aqueous solvent (H_2O) (i) segregative phase separation (as characterised by horizontal tie-lines), (ii) cosolubility and (iii) associative phase separation (as characterised by vertical tie-lines), right: Schematic depictions of the corresponding present phases, protein is represented as (grey) spheres and polysaccharide as (black) coils.

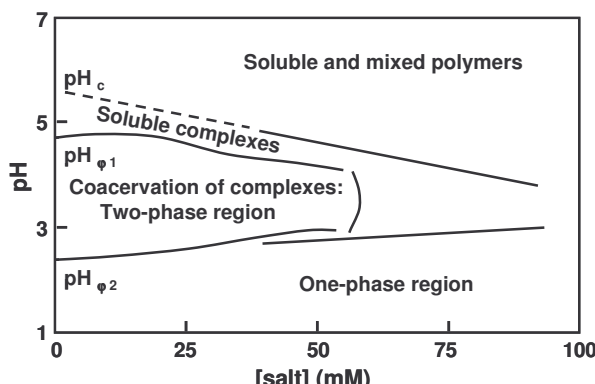


Figure 1.5: Schematic state diagram of an anionic polyelectrolyte and a globular protein (based on De Kruif et al.¹⁸).

In figure 1.5 a state diagram is shown for a weak anionic polysaccharide with a globular protein. Interaction of proteins with anionic polysaccharides is often described along the pH-axis through this state diagram. Moving from high to low pH (or from low to high pH in case of cationic polyelectrolytes) through this diagram (at constant composition – protein/polysaccharide mixing ratio), in general at least three regimes are distinguished: solubility of both polymers above pH_c , starting at pH_c and lower formation of soluble or intrapolymer complexes (carrying excess net charge), below $pH_{\phi 1}$ aggregation of these soluble complexes (to interpolymer complexes) as a result of decreasing net charge, finally resulting in the formation of coacervate droplets¹⁸⁻²¹. Whether the formation of interpolymer complexes and the formation of coacervate droplets can be identified separately depends on

the technique used²². At pH below pH_{φ2} (this value depends on the pK_a of the polysaccharide) complexation is suppressed by protonation of the acidic groups on the polysaccharides. This brings the system back to a one phase system. The ionic strength at which coacervation or complexation ‘ends’ presumably depends on the charge density of the protein and polysaccharide. The thermodynamic nature of interaction is still a matter of debate. Some authors report that electrostatic complexation is enthalpically driven due to a decrease of electrostatic energy in the system^{23, 24}, others claim that it is entropically driven due to liberation of counter ions and water molecules^{25, 26}. De Kruif et al. ascribe the discrepancy to differences in the ionic strength involved in the study. At low ionic strength the interaction may be enthalpic, because dissociation of carboxylic groups on the polysaccharides and possibly also protonation of the protein is suppressed. At higher ionic strength (>10 mM) the interaction may be entropic.¹⁸ However, with β -lactoglobulin/low methoxyl pectin complexation (at pH 4.25) was observed to be enthalpic up to an ionic strength of 30 mM²⁷. The formation of soluble intrapolymer complexes and the aggregation of these to finally form a coacervate phase should be distinguished in this respect²³. These two regimes are also addressed when titrating an anionic polysaccharide (low methoxyl pectin) with a protein (β -lactoglobulin) below the iso-electric point of the protein (i.e. varying composition at constant pH and ionic strength). Soluble complexes are formed as long as the negative charge on the polysaccharide is in excess to the net positive charge on the protein. Upon decreasing the net charge of the complexes - the complexes lose their negative net charge by further uptake of proteins in the complexes - they can aggregate and become insoluble (complex coacervation)²³. The final appearance of the concentrated phase depends on the strength of interaction between the protein and polysaccharide; weak (carboxylated) polysaccharides form a liquid coacervate phase, whereas strong (sulphated) polysaccharides form precipitates¹⁸.

1.4 CHARACTERISATION OF ADSORBED LAYERS

Several techniques can be used to characterise adsorbed layers of proteins. The techniques used in this thesis are classified in three main categories: tensiometry, surface rheology and spectroscopy.

1.4.1 Tensiometry

The interfacial tension of the air- or oil/water interface changes upon protein adsorption (or adsorption of any other surfactant). Therefore, the most simple way to examine adsorption is measuring surface tension (γ) in time. This can be done by using a Wilhelmy plate pending in the interface in combination with a pressure sensor. Alternatively, surface tension can be determined from the shape of a droplet, using a drop tensiometer. The change in surface tension due to protein adsorption is expressed in terms of surface pressure (Π), using $\Pi = \gamma_0 - \gamma$ where γ_0 is the surface tension of the clean interface and γ is the measured surface tension.

1.4.2 Surface rheology

Surface rheology refers to techniques used to probe the resistance of the adsorbed layer against deformation and can be classified in two types: surface dilatational rheology and

surface shear rheology. With surface dilatational rheology changes in surface pressure upon deformations (sinusoidal compressions and expansions) of the size of the interfacial area (A) are recorded. The shape of the interface remains constant during these measurements. The surface dilatational modulus (E) is defined as $E = -d\Pi/d\ln A$ ($= d\gamma/d\ln A$). With surface shear rheology the shear stress in the interface is measured as a result of continuous shearing deformation of the shape of the interface (at a given shear rate). Because the size of the interfacial area, and therefore also the surface pressure, remains constant in this experiment, this type of surface rheology is more sensitive to the interaction between adsorbed molecules in the interface, in particular to the extent of cohesion in the interfacial layer.

1.4.3 Spectroscopy

Spectroscopy is the study of the interaction between radiation and matter. Depending on the timescale of the measurement and the wavelength of the radiation, different characteristics of a material can be determined. If the material is an adsorbed layer at an air/water interface, measurements are performed in reflective mode. From a change in polarisation of the reflected light from the interface, as measured with ellipsometry, the thickness (d) and refractive index (n) of an adsorbed layer can be obtained²⁸. The adsorbed amount is directly related to d and n. The fact that the retrieval of one data point takes only 10 seconds makes ellipsometry a suitable technique to follow a slow adsorption process in time. With infra-red reflection adsorption spectroscopy (IRRAS) in principle the same information can be obtained²⁹. In addition, the spectral resolution of this technique enables distinguishing protein and polysaccharide (or other constituents like fats) at the interface, based on the vibration and stretching of different chemical bonds. However, the intensity in the wavelength region of the polysaccharide is too low to provide quantitative information on the amount of polysaccharide adsorbed. The advantage of neutron reflection is that the contrast between the adsorbed layer and the bulk solution can be varied by making use of the H/D isotope effect on scattering; by varying the H₂O/D₂O ratio of the solvent. Comparison of experiments carried out at different contrast gives information on the adsorbed amount and on the distribution of adsorbed mass perpendicular to the interface³⁰. The limited time resolution makes the technique less suitable to probe adsorption kinetics. In contrast to previous described methods time resolved fluorescence anisotropy (TRFA) does not aim to retrieve the amount of material in the interface; it gives information on the dynamic character of the macromolecules in the layer. It determines rotational mobility of e.g. (fluorescently labelled) protein molecules by comparing polarisation of the excitation beam and (non-specular) emitted light³¹.

Techniques to characterise complexes in bulk solution are (among others) dynamic light scattering (DLS), electrophoretic mobility and Small angle X-ray scattering (SAXS). With DLS the scattering of light by a sample in a cuvette is followed in time. From this information the diffusion coefficient and the size of complexes in the sample is deduced. When the mobility of the complexes is measured in an electric field (electrophoretic mobility), the ζ -potential of the complexes (a measure of the ‘mobile’ net charge) is retrieved. SAXS gives information on characteristic distances in the sample. From SAXS measurements on a coacervate phase the spatial distribution of protein molecules in the coacervate can be

deduced. No quantitative information on the spatial distribution of protein in soluble complexes can be obtained due to limited intensity.

1.5 AIM AND OUTLINE OF THE THESIS

The aim of this thesis is to understand the influence of (attractive and non-covalent) protein/polysaccharide interaction on the adsorption behaviour at air/water interfaces. To make progress, important parameters need to be identified and their roles need to be assessed separately and systematically. The phase behaviour in solution should be studied to identify the conditions where protein and polysaccharide or protein/polysaccharide complexes are soluble. Next, insight in the mechanism of mixed protein/polysaccharide adsorption should provide suggestions or predictions to control adsorption kinetics and the functional behaviour of the adsorbed layers. This may help to identify problems in more complex systems like food products, and to solve them by selecting ingredients with suitable chemical properties or by adapting the physical conditions.

In chapter 2 we investigate how complexation of proteins to anionic polysaccharides affects adsorption kinetics at the air/water interface – as monitored by surface pressure. Parameters involved in protein/polysaccharide interaction and thus in mixed adsorption kinetics are identified. In chapter 3 the effect of protein/polysaccharide mixing ratio on surface rheology is evaluated using β -lactoglobulin/low-methoxyl-pectin as a model system. Furthermore, we compare adsorption of existing protein/polysaccharide complexes at the air/water interface (simultaneous adsorption) to adsorption of polysaccharides onto a previously adsorbed protein layer (sequential adsorption). A schematic representation on a molecular level of the different adsorbed layer structures is proposed. In chapter 4 we investigate whether the mechanism of complex adsorption at oil/water interfaces is similar to that at the air/water interface. Both adsorption kinetics and surface rheology are evaluated in this respect.

The layer structures at the air/water interface, which we infer from surface rheological measurements, are probed on a more molecular level by means of neutron reflection and time resolved fluorescence anisotropy in chapter 5. Since protein/polysaccharide interaction is predominately electrostatic, a large effect of charge density on the complex behaviour in solution and at the interface is expected. This is examined in chapter 6, using β -lactoglobulin with four pullulan samples that are carboxylated to a different degree. Since pullulan charge density has a large effect on the rheological behaviour of the mixed adsorbed layers, it is expected that also the structure of a bulk coacervate phase depends on charge density. In chapter 7 the distance between protein molecules in coacervate phases with pectin and the four pullulan samples is probed using small angle x-ray scattering. Understanding the structure of coacervates may help understanding the structure of soluble complexes and adsorbed complex layers.

Protein/polysaccharide mixing ratio, polysaccharide charge density and polysaccharide molecular weight are expected to affect adsorption kinetics. Adsorption kinetics was monitored by following surface pressure as a function of time. When comparing adsorption

kinetics however, one should consider adsorbed amount rather than surface pressure. The relation between surface pressure and adsorbed amount (equation of state) may differ between different samples. Therefore in chapter 8 the adsorbed amount is followed as a function of time using ellipsometry while systematically varying all parameters that are expected to affect adsorption kinetics. In chapter 9, entitled ‘general discussion’, the proposed mechanism for mixed adsorption and layer formation is discussed and extended. We present some more speculative ideas on the dynamic character of different protein/polysaccharide complexes inferred from surface dilatational modulus and phase angle data (viscous/elastic contribution). Finally we consider possible applications of the newly gained insights.

REFERENCES

- (1) Maroziene, A.; de Kruif, C. G., Interactions of pectin and casein micelles. *Food Hydrocolloids* **2000**, 14, (4), 391-394.
- (2) Tokaev, E. S.; Gurov, A. N.; Rogov, I. A.; Tolstoguzov, V. B., Properties of oil/water emulsions stabilized by casein-acid polysaccharide mixtures. *Nahrung* **1987**, 31, (8), 825-834.
- (3) de Nooy, A. E. J.; Besemer, A. C.; van Bekkum, H.; van Dijk, J. A. P. P.; Smit, J. A. M., TEMPO-Mediated Oxidation of Pullulan and Influence of Ionic Strength and Linear Charge Density on the Dimensions of the Obtained Polyelectrolyte Chains. *Macromolecules* **1996**, 29, (20), 6541-6547.
- (4) Wierenga, P. A.; Meinders, M. B. J.; Egmond, M. R.; Voragen, F. A. G. J.; de Jongh, H. H. J., Protein exposed hydrophobicity reduces the kinetic barrier for adsorption of ovalbumin to the air-water interface. *Langmuir* **2003**, 19, (21), 8964-8970.
- (5) Wierenga, P. A.; Meinders, M. B. J.; Egmond, M. R.; Voragen, A. G. J.; de Jongh, H. H. J., Quantitative description of the relation between protein net charge and protein adsorption to air-water interfaces. *Journal of Physical Chemistry B* **2005**, 109, (35), 16946-16952.
- (6) Meinders, M. B. J.; De Jongh, H. H. J., Limited conformational change of beta-lactoglobulin when adsorbed at the air-water interface. *Biopolymers* **2002**, 67, (4-5), 319-322.
- (7) Wierenga, P. A.; Egmond, M. R.; Voragen, A. G. J.; de Jongh, H. H., The adsorption and unfolding kinetics determines the folding state of proteins at the air-water interface and thereby the equation of state. *Journal of Colloid and Interface Science* **2006**, 299, (2), 850-857.
- (8) Cohen Stuart, M. A.; Norde, W.; Kleijn, J. M.; van Aken, G. A., Formation and properties of adsorbed protein films: importance of conformational stability. In *Food Colloids: interaction, microstructure and processing*, Dickinson, E., Ed. The Royal Society of Chemistry: Cambridge, 2005; pp 99-119.
- (9) Lad, M. D.; Birembaut, F.; Matthew, J. M.; Frazier, R. A.; Green, R. J., The adsorbed conformation of globular proteins at the air/water interface. *Physical Chemistry Chemical Physics* **2006**, 8, (18), 2179-2186.
- (10) Martin, A. H.; Meinders, M. B. J.; Bos, M. A.; Cohen Stuart, M. A.; van Vliet, T., Conformational aspects of proteins at the air/water interface studied by infrared reflection-absorption spectroscopy. *Langmuir* **2003**, 19, (7), 2922-2928.
- (11) Fainerman, V. B.; Lucassen-Reynders, E. H.; Miller, R., Description of the adsorption behaviour of proteins at water/fluid interfaces in the framework of a two-dimensional solution model. *Advances in Colloid and Interface Science* **2003**, 106, 237-259.
- (12) de Feijter, J. A.; Benjamins, J., Soft-Particle Model Of Compact Macromolecules At Interfaces. *Journal of Colloid and Interface Science* **1982**, 90, (1), 289-292.
- (13) Dickinson, E., Adsorbed protein layers at fluid interfaces: interactions, structure and surface rheology. *Colloids and Surfaces B-Biointerfaces* **1999**, 15, (2), 161-176.

- (14) Izmailova, V. N.; Yampolskaya, G. P.; Tulovskaya, Z. D., Development of the Rehbinder's concept on structure-mechanical barrier in stability of dispersions stabilized with proteins. *Colloids and Surfaces A-Physicochemical and Engineering Aspects* **1999**, 160, (2), 89-106.
- (15) Wilde, P. J., Interfaces: their role in foam and emulsion behaviour. *Current Opinion in Colloid & Interface Science* **2000**, 5, (3-4), 176-181.
- (16) Martin, A. H.; Grolle, K.; Bos, M. A.; Cohen Stuart, M. A.; van Vliet, T., Network forming properties of various proteins adsorbed at the air/water interface in relation to foam stability. *Journal of Colloid and Interface Science* **2002**, 254, (1), 175-183.
- (17) Graham, D. E.; Phillips, M. C., The Conformation of Proteins at the Air/Water Interface and their role in Stabilizing Foams. In *Foams*, Akers, R. J., Ed. Academic Press: London, 1976; p 237.
- (18) de Kruif, C. G.; Weinbreck, F.; de Vries, R., Complex coacervation of proteins and anionic polysaccharides. *Current Opinion in Colloid & Interface Science* **2004**, 9, (5), 340-349.
- (19) Cooper, C. L.; Dubin, P. L.; Kayitmazer, A. B.; Turksen, S., Polyelectrolyte-protein complexes. *Current Opinion in Colloid & Interface Science* **2005**, 10, (1-2), 52-78.
- (20) Kaibara, K.; Okazaki, T.; Bohidar, H. B.; Dubin, P. L., pH-Induced Coacervation in Complexes of Bovine Serum Albumin and Cationic Polyelectrolytes. *Biomacromolecules* **2000**, 1, (1), 100-107.
- (21) Turgeon, S. L.; Beaulieu, M.; Schmitt, C.; Sanchez, C., Protein-polysaccharide interactions: phase-ordering kinetics, thermodynamic and structural aspects. *Current Opinion in Colloid & Interface Science* **2003**, 8, (4-5), 401-414.
- (22) Mekhloufi, G.; Sanchez, C.; Renard, D.; Guillemin, S.; Hardy, J., pH-induced structural transitions during complexation and coacervation of beta-lactoglobulin and acacia gum. *Langmuir* **2005**, 21, (1), 386-394.
- (23) Girard, M.; Turgeon, S. L.; Gauthier, S. F., Thermodynamic parameters of beta-lactoglobulin-pectin complexes assessed by isothermal titration calorimetry. *Journal of Agricultural and Food Chemistry* **2003**, 51, (15), 4450-4455.
- (24) Schmitt, C.; da Silva, T. P.; Bovay, C.; Rami-Shojaei, S.; Frossard, P.; Kolodziejczyk, E.; Leser, M. E., Effect of time on the interfacial and foaming properties of beta-lactoglobulin/acacia gum electrostatic complexes and coacervates at pH 4.2. *Langmuir* **2005**, 21, (17), 7786-7795.
- (25) Ball, V.; Winterhalter, M.; Schwinte, P.; Lavalle, P.; Voegel, J. C.; Schaaf, P., Complexation mechanism of bovine serum albumin and poly(allylamine hydrochloride). *Journal of Physical Chemistry B* **2002**, 106, (9), 2357-2364.
- (26) Dautzenberg, H., Polyelectrolyte complex formation and highly aggregating systems: methodical aspects and general tendencies. In *Physical Chemistry of Polyelectrolytes*, Radeva, T., Ed. Marcel Dekker: New York, 2001; Vol. 99, pp 743-792.
- (27) Sperber, B. unpublished results. Wageningen University.
- (28) de Feijter, J. A.; Benjamins, J.; Veer, F. A., Ellipsometry As A Tool To Study Adsorption Behavior Of Synthetic And Biopolymers At Air-Water-Interface. *Biopolymers* **1978**, 17, (7), 1759-1772.
- (29) Meinders, M. B. J.; van den Bosch, G. G. M.; de Jongh, H. H. J., IRRAS, a new tool in food science. *Trends in Food Science & Technology* **2000**, 11, (6), 218-225.
- (30) Lu, J. R.; Perumal, S.; Zhao, X. B.; Miano, F.; Enea, V.; Heenan, R. R.; Penfold, J., Surface-induced unfolding of human lactoferrin. *Langmuir* **2005**, 21, (8), 3354-3361.
- (31) Kudryashova, E. V.; Meinders, M. B. J.; Visser, A.; van Hoek, A.; de Jongh, H. H. J., Structure and dynamics of egg white ovalbumin adsorbed at the air/water interface. *European Biophysics Journal with Biophysics Letters* **2003**, 32, (6), 553-562.

Dynamic surface pressure of protein/polysaccharide complexes at air/water interfaces

Renate A. Ganzevles, Martien A. Cohen Stuart, Ton van Vliet, and Harmen H.J. de Jongh
Food Hydrocolloids 2006, 20 (6), 872

ABSTRACT

In order to understand foaming behaviour of mixed protein/anionic polysaccharide solutions, we investigated the effect of β -lactoglobulin/pectin interaction in the bulk on β -lactoglobulin adsorption to the air/water interface. Adsorption kinetics were evaluated by following surface pressure development in time of several pure protein solutions and of mixed protein/polysaccharide solutions using an Automated Drop Tensiometer (ADT). It was found that complexation of proteins with polysaccharides can slow down the kinetics of surface pressure development by at least a factor 100, and greatly diminish foam formation. In contrast, a five times acceleration in the increase of surface pressure was observed in other cases. We propose a mechanism for protein adsorption from mixed protein/polysaccharide solutions. Effects of ionic strength, pH and mixing ratio on this mechanism were studied for mixtures of β -lactoglobulin and low methoxyl pectin, whereas other proteins and anionic polysaccharides were used to explore the role of protein and polysaccharide charge density and distribution. Whereas the possibilities to change system parameters like ionic strength or pH are limited in food related systems, selecting a suitable combination of protein and polysaccharide offers a broad opportunity to control protein adsorption kinetics and with that foam formation.

2.1 INTRODUCTION

The ability to create foams from aqueous protein solutions largely depends on the protein adsorption kinetics to the air/water interface. Adsorption kinetics of proteins have been extensively studied and large differences have been found between different proteins (e.g. β -lactoglobulin is known to quickly increase surface pressure¹, whereas for lysozyme the process is much slower²). Several steps in protein adsorption have been identified³⁻⁵: transport of the molecule to the interface by diffusion/convection, adsorption to the interface and possible conformational changes once adsorbed at the interface. The relation between adsorbed amount of protein at the interface, Γ (mg/m²) and the resulting surface pressure, Π (mN/m) is not linear. Below a certain minimum surface concentration, (depending on properties of the protein, e.g. net charge⁶, between 0.5 and 1 mg/m²) the surface pressure does not measurably deviate from zero and the surface pressure can be described by treating the adsorbed molecules as a two dimensional ideal gas. When the surface concentration exceeds this typical minimum value, a steep increase in surface pressure is seen on further adsorption. Once Γ has increased until full monolayer coverage, the Π - Γ curve flattens⁷. Obviously all this holds for pure protein solutions; but what happens when there are also polysaccharides, which are typically added to food systems to increase viscosity, present in the solution? This is likely to depend on the way the proteins and polysaccharides interact.

Protein/polysaccharide interaction is intensively investigated in a diversity of contexts: heparin and blood coagulation⁸; protection of enzymes against high pressure or temperature; enzyme substrate binding and recovery and fractionation of milk proteins. A classical example from the food industry is the use of pectin to stabilize casein micelles in acidified milk drinks. Due to electrostatic interaction negatively charged pectin molecules adsorb at the casein micelles and prevent them from acid induced aggregation by electrostatic and steric repulsion⁹⁻¹¹. Also in food emulsions polysaccharides are used to prevent aggregation and creaming of emulsion droplets^{12, 13}. However, only little is known about the effect of protein/polysaccharide interactions on protein adsorption kinetics^{14, 15}. On mixing an anionic polysaccharide like pectin with a protein, four different regimes can be distinguished, depending on pH, ionic strength and mixing ratio, as described for mixtures of whey protein and arabic gum by Weinbreck, de Vries, Schrooyen & de Kruif¹⁶. At neutral pH and low ionic strength (less than 50 mM) both the protein and the polysaccharide are negatively charged and although there can be some attractive interaction between the positively charged groups on the protein and the negatively charged polysaccharide, the components are cosoluble (I). On decreasing the pH close to the iso-electric pH of the protein or below, soluble protein/polysaccharide complexes are formed (II). Further decrease of the pH leads to aggregation of the soluble complexes and subsequently complex coacervation (III). At pH values below 2.5 complexation can be suppressed by protonation of the acidic groups on the polysaccharide (IV)¹⁶. From the work of Girard, Turgeon and Gauthier¹⁷ it is known that also β -lactoglobulin and pectin can form soluble complexes around pH 4.5. Protein adsorption kinetics to the air/water interface from mixed protein/polysaccharide solutions depend on the

extent of protein complexation to pectin in the bulk, which in turn depends on parameters like pH, ionic strength, mixing ratio and charge density of the ingredients. This chapter aims at understanding how one can control protein adsorption kinetics (as monitored by drop tensiometry) and, with that, foam formation by manipulating protein/polysaccharide interaction in the bulk.

2.2 MATERIALS AND METHODS

2.2.1 Materials

Acetate buffer and NaCl solutions were prepared from analytical grade chemicals and deionised water. Bovine β -lactoglobulin was purified using a non denaturing method as described previously¹⁸. Ovalbumin was isolated as described before¹⁹. Lysozyme L-6878 was purchased from Sigma-Aldrich (St. Louis, Missouri, USA) and used without further purification. Stock solutions of 0.2 mg/ml protein were prepared by dissolving protein in deionised water and subsequently diluting with concentrated acetate buffer solution to 5 mM acetate, ionic strength 1 mM, pH 4.5. The protein solutions were kept at -40°C until further use. For pH dependency experiments, protein was dissolved in water, adjusted to the desired pH values with concentrated HCl or NaOH and subsequently the conductivity was set at 0.4 mS/cm in all samples by addition of NaCl solution. For the experiments with various proteins and polysaccharides at pH 7, a 5 mM phosphate buffer with an ionic strength of 8 mM was used. The corresponding samples at pH 4.5 were adjusted to this ionic strength with NaCl. Two pectins with different degree of methyl esterification: low methoxyl pectin (LMP) and high methoxyl pectin (HMP) were used (CP Kelco, Lille Skensved, Denmark; table 2.1). Only the non-methylated galacturonic acid monomers have a free carboxyl group (weak acid, $\text{pKa} \sim 4.5$). l -carrageenan (Copenhagen Pectin A/S, Lille Skensved, Denmark) has one sulphate group (strong acid, $\text{pKa} \sim 2$) per monosaccharide. Polysaccharide solutions were prepared by first wetting the powder with ethanol (only for l -carrageenan no ethanol was used), than dissolving in buffer and subsequently heating at 70°C for 30 minutes. After overnight storage in the fridge, the samples were centrifuged at 6000 g at room temperature for 10 minutes. Number averaged molecular weight (M_n) and polydispersity of the polysaccharides were determined using size exclusion chromatography (5000, 4000, 3000 PW columns and 0.2M sodium nitrate as eluens, flow rate 0.5 mL/min, refractive index detection) in combination with multi-angle laser light scattering (DAWN-F MALLS photometer, equipped with K5 flow cell and a linearly polarized He-Ne laser light source, 14 detectors used). M_n and M_w were calculated using Astra for Windows, using a d_n/dc of 0.152 mL/g).

Table 2.1: Characteristics of polysaccharides

Characteristics of polysaccharides	low methoxyl pectin	high methoxyl pectin	l -carrageenan
Degree of methylation (% of monomers) ²⁰	30.4	74	0
Degree of blockiness (-) ²⁰	16.5	2	0
Uronic acid content (w/w%) ²⁰	78.5	85	-
M_n (* 10^5 g/mol)	1.5	-	0.5
Polydispersity M_w/M_n (-)	2.4	-	2.6

2.2.2 Drop tensiometry

Surface tension as a function of time was measured for single component and mixed solutions of protein and polysaccharide using an automated drop tensiometer (ITCONCEPT, Longessaigne, France). Samples were freshly prepared for each experiment and equilibrated for 30 minutes. Each experiment started with a clean interface of a newly formed air bubble (7 μL) in a cuvette containing the sample solution. Surface tension was determined by bubble shape analysis. The setup is described in detail elsewhere²¹. Temperature was controlled at 22 ± 1 °C. All results are presented in terms of surface pressure $\Pi = \gamma_0 - \gamma$, where γ_0 is the surface tension of the solvent (72 mN/m) and γ is the measured surface tension.

2.2.3 Dynamic light scattering

Second cumulant diffusion coefficients of the pectins and the β -lactoglobulin/pectin complexes were determined by dynamic light scattering²², using an ALV light scattering instrument equipped with a 400 mW argon laser tuned at a wavelength of 514.5 nm, as described by van der Burgh, de Keizer & Cohen Stuart²³. Hydrodynamic radii were calculated according to Stokes-Einstein, assuming that the pectin molecules and the complexes are spherical. Temperature was controlled at 20 ± 1 °C. Protein concentration was 0.1 g/L for all samples and pectin concentrations varied from protein/pectin mixing ratio 0 to 15 w/w.

2.3 RESULTS

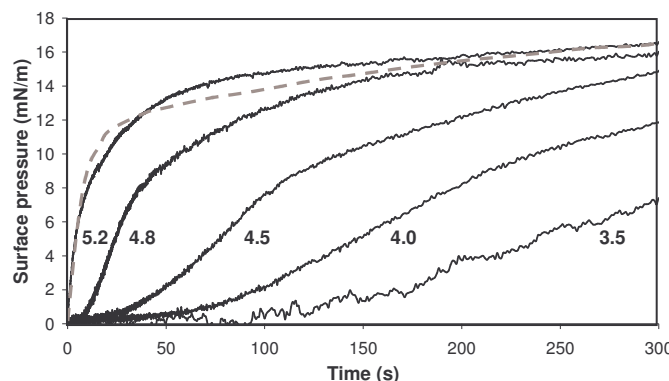


Figure 2.1: Surface pressure at the air/water interface as a function of time at various pH values for β -lactoglobulin (dashed grey), and a mixture of β -lactoglobulin and low methoxyl pectin, w/w ratio 2 (black), pH values as indicated.

To monitor the adsorption kinetics of protein in presence and absence of polysaccharides, surface pressure at the air/water interface was measured as a function of time for β -lactoglobulin (β -Lg) solutions and mixed β -lactoglobulin/pectin solutions, at various pH values (figure 2.1). The protein concentration of all samples was 0.1 g/L, protein/polysaccharide mixing ratio was kept constant at 2 w/w and ionic strength was kept low (on the order of 1 mM, samples were matched on the basis of a conductivity of 0.4 mS/cm) to optimise electrostatic interactions. At pH 3.5 the presence of low methoxyl pectin (LMP) clearly delays the increase in surface pressure. We defined a 'lag time' as the time from the start of an experiment - with a clean interface - until the surface pressure starts increasing, or more precise: the time at the cross section between the initial horizontal line

and the steepest slope in the surface pressure versus time curve. On increasing the pH starting from 3.5, the lag time diminishes until it completely disappears at pH 5.2, just above the iso-electric point of the protein. Surface pressure versus time curves for β -Lg solutions in the absence of pectin also vary with pH (not shown), but the differences are very small compared to the effect of the presence of pectin; at a concentration of 0.1 g/L there is no lag time at any of the pH values. Compared to proteins, the polysaccharides on their own do not give a significant increase in surface pressure at the concentrations used (less than 2 mN/m in 20000 s for a concentration of 0.05 g/L, data not shown).

The pH dependent behaviour suggests that electrostatic interactions play a role in the delaying effect caused by the polysaccharides. To confirm this, we measured lag time as a function of ionic strength for mixtures of β -Lg/LMP, at a mixing ratio of 2 w/w, pH 4.5. Increasing the NaCl concentration leads to a gradual decrease in lag time until it has completely vanished at 80 mM NaCl (figure 2.2).

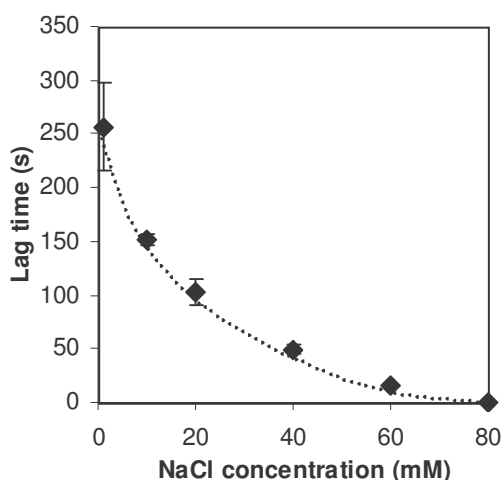


Figure 2.2: Influence of ionic strength (by NaCl addition) on the lag time for the increase in surface pressure; 0.1 g/l β -lactoglobulin and 0.05 g/l low methoxyl pectin, pH 4.5. Dashed line is to guide the eye. Error bars represent largest deviation from average.

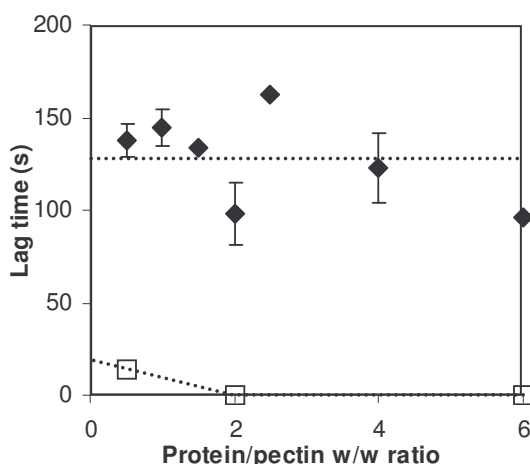


Figure 2.3: Lag time for the increase in surface pressure at various β -lactoglobulin/pectin mixing ratios, β -lactoglobulin concentration was constant at 0.1 g/L, pH 4.5, ionic strength 1 mM; low methoxyl pectin (◆) and high methoxyl pectin (□). Dashed lines are to guide the eye. Error bars represent largest deviation from average (for the data with high methoxyl pectin, error bars are smaller than the data symbols).

If the delaying effect of the polysaccharides is indeed governed by electrostatic interactions with the proteins, the protein/pectin mixing ratio is expected to play a role. Figure 2.3 shows lag times for different mixing ratios. Surprisingly, with low methoxyl pectin the lag time does not correlate with the mixing ratio. With high methoxyl pectin a small lag time is observed at a mixing ratio of 0.5, but at higher mixing ratio this lag time disappears.

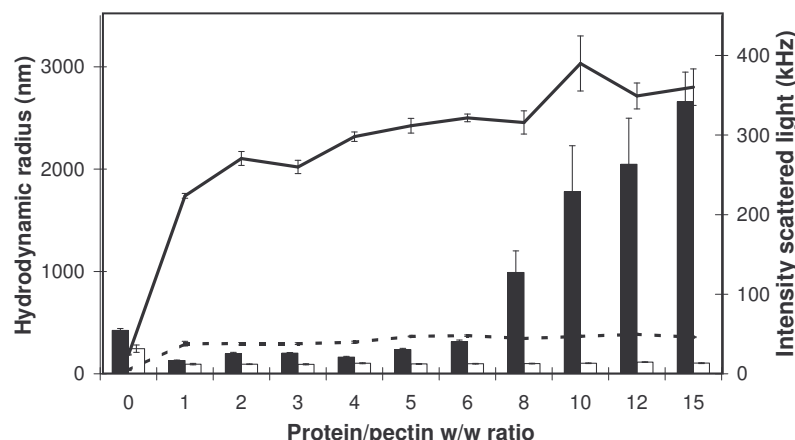


Figure 2.4: Dynamic light scattering at various β -lactoglobulin/pectin mixing ratios, protein concentration was constant at 0.1 g/L, pH 4.5, ionic strength 1 mM. Hydrodynamic radius (black bars) and intensity scattered light (black line) for low methoxyl pectin; hydrodynamic radius (open bars) and intensity scattered light (dashed line) for high methoxyl pectin.

From dynamic light scattering experiments (figure 2.4) it can be deduced that the hydrodynamic radius of pectin decreases on addition of protein. In a range between ratio 1 and 6 the radius seems not to depend on the protein/pectin mixing ratio. In the case of LMP, increasing the mixing ratio to more than 6 w/w leads to the formation of large aggregates. A rough estimation of the total charge on protein and pectin confirms that at these mixing ratios there is enough protein present to completely compensate the negative charge on the pectin (if all protein takes part in the complexation), which can lead to macroscopic phase separation. Although HMP has less negative charges than LMP, and charge compensation occurs already at lower mixing ratio, no large (with a hydrodynamic radius larger than 500 nm) aggregates are formed.

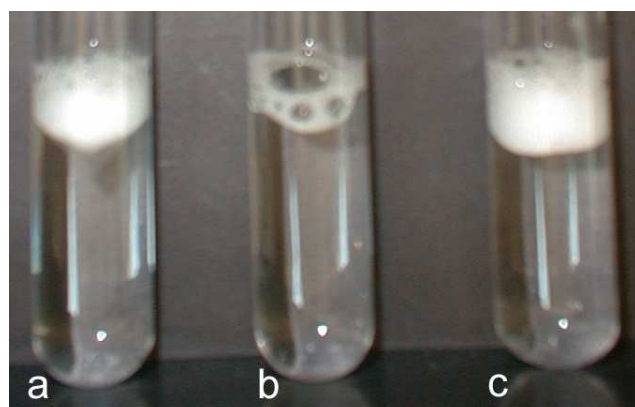


Figure 2.5: Foam 10 minutes after shaking a tube with a) β -lactoglobulin solution, b) a mixture of β -lactoglobulin and low methoxyl pectin and c) a mixture of β -lactoglobulin and high methoxyl pectin; protein concentration kept constant at 0.03 g/L, protein/pectin mixing ratio 2 w/w, pH 4.5, ionic strength 1mM.

In order to illustrate the relevance of these lag times, figure 2.5a shows that shaking a test tube (40 times vigorously up and down by hand, all samples at the same time) with 0.03 g/L β -lactoglobulin solution (pH 4.5, ionic strength 1mM) resulted in a foam layer on top of the solution. The presence of 0.015 mg/mL low methoxyl pectin almost completely prevented foam formation (b), whereas the presence of high methoxyl pectin did not have this effect (c). This is consistent with the results presented in figure 2.3, where LMP causes a lag time at a mixing ratio of 2 w/w whereas HMP does not. Although a foam stabilising effect of complexation is expected, adsorption kinetics determine whether a foam can be formed or not. The final appearance of a foam depends on the combination of both effects.

Table 2.2 shows that the mechanism is not specific for β -Lg and LMP, but that in many cases the presence of a polysaccharide affects the surface pressure versus time curve of a protein. Not only pectin, but also ι -carrageenan can cause a lag time with β -lactoglobulin. LMP delays the increase in surface pressure not only for β -Lg, but also for ovalbumin, both at pH 4.5 and at pH 7. Conversely, in the case of lysozyme, the increase in surface pressure is accelerated instead of delayed by the presence of pectin.

Table 2.2: Lag time (ks) for increase in surface pressure for different protein solutions, 0.1 g/L, and mixed protein/polysaccharide solutions, w/w ratio 2, at pH 4.5 and pH 7, ionic strength 8 mM

Protein	pH 4.5 (ks)	pH 7 (ks)	Protein & Polysaccharide	pH 4.5 (ks)	pH 7 (ks)
β -lactoglobulin	-	-	β -lactoglobulin & LM pectin	0.10 ± 0.009	-
β -lactoglobulin	-	-	β -lactoglobulin & HM pectin	-	-
β -lactoglobulin	-	-	β -lactoglobulin & ι -carrageenan	0.24 ± 0.05	-
ovalbumin	-	0.53 ± 0.02	ovalbumin & LM pectin	0.0058 ± 0.0007	0.63 ± 0.03
ovalbumin	-	0.53 ± 0.02	ovalbumin & HM pectin	-	0.68 ± 0.1
lysozyme	5.3 ± 1	1.9 ± 5	lysozyme & LM pectin	2.4 ± 0.5	1.3 ± 0.4
lysozyme	5.3 ± 1	1.9 ± 5	lysozyme & HM pectin	0.73 ± 0	0.50 ± 0.1

2.4 DISCUSSION

Since in the pH region (II) above the pK of a polysaccharide and below the iso electric point of the protein both components are oppositely charged, they electrostatically attract each other. From literature it is known that this can lead to the formation of soluble complexes¹⁶. Complexation of protein molecules to pectin reduces the internal repulsion of the pectin molecule leading to a smaller hydrodynamic radius and an increase in the intensity of scattered light as illustrated in figure 2.4 for β -Lg with LMP and with HMP. When the amount of positive net charge on the protein and negative charge on the polysaccharide are equal, full charge compensation could lead to aggregation of the soluble complexes and, finally, to complex coacervation/precipitation. This is observed only with the mixture of β -Lg and LMP. Most likely, interaction with HMP is not strong enough to encourage coacervation/precipitation at these conditions. The fact that complexation occurs is likely to affect the protein adsorption rate at air/water interfaces. Various factors may contribute to this: (i) due to complexation the protein molecules are partitioning over polysaccharide bound and the free state, implying that less proteins are ‘available’ for direct adsorption; (ii) the bound state diffuses much more slowly than the free state, because of the larger hydrodynamic radius of the polysaccharide ‘carrier’ and (iii) the attachment of the bound protein to the air/water interface may be hindered by the presence of the surrounding

polysaccharide. These options are summarized in figure 2.6 and discussed below. One may argue that a possible increased viscosity due to the presence of a polysaccharide might also explain the delay in the increase in surface pressure. This can be ruled out by the fact that at pH 7 no delay is observed due to the presence of polysaccharides, as was stated in the results section.

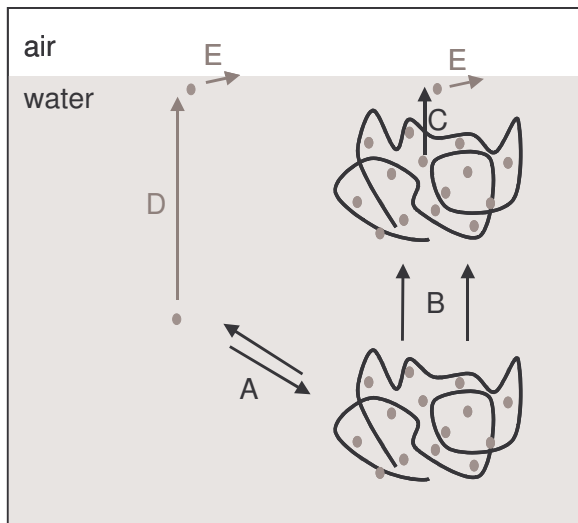


Figure 2.6: Model for polysaccharide controlled protein adsorption at the air/water interface; A = partition free protein and protein bound to polysaccharide, B = diffusion of protein/polysaccharide complexes in bulk, C = availability of complexed protein for interface, D = diffusion of free protein in bulk, E = kinetic barrier for protein adsorption.

Several scenarios can be considered to account for the data. To explain the delay in increase of surface pressure we might at first assume that since part of the β -Lg is bound to LMP, we have an effectively reduced protein concentration. Let us suppose that only the free β -Lg would be responsible for the increase in surface pressure (figure 2.6, route D, E). Upon going from pH 3.5 to pH 5.2 (figure 2.1), or from low to high ionic strength (figure 2.2) more protein would become dissociated from the complex, and therefore give rise to a faster increase in surface pressure. This is qualitatively supported by the data (figure 2.1 and 2.2). However, one would also have to conclude from this assumption that the lag time decreases on increasing the β -Lg to LMP mixing ratio, which is not observed (figure 2.3). Hence we propose that at low ionic strength all protein is bound to the low methoxyl pectin, which is theoretically possible since the total negative charge on the polysaccharide exceeds in all cases the total net positive charge on the protein. This rules out the first scenario. Moreover, if only free protein was responsible for the increase in surface pressure, surface pressure versus time curve of a protein/polysaccharide mixture would coincide with that of a pure β -Lg solution at lower concentration. However, whereas the β -Lg/LMP (2 w/w) mixture has the same lag time as a pure protein solution at a 10 times lower concentration, the lag time for the mixture is followed by a much steeper increase in surface pressure (not shown). Compared to a sole protein solution at the same concentration, the equilibrium surface pressure of the mixture is slightly higher (for β -Lg 25 ± 1 mN/m, for mixtures 27 ± 1 mN/m). This leads to the conclusion that not only β -Lg, but also some pectin must adsorb to the interface.

A second possibility illustrated in figure 2.6 is the adsorption of protein/pectin complexes (route B) possibly combined with some additional adsorption of free protein (route A, D). Protein/pectin complexes have a much larger hydrodynamic radius and with that lower diffusion coefficient than free proteins (figure 2.6, process B). To calculate whether the delay in surface pressure development can be caused solely by the slower diffusion of protein in complexes, we have to consider adsorbed amount in addition to surface pressure. Since we are working with mixed systems of proteins and polysaccharides, we cannot obtain well-defined values for the adsorbed amount from ellipsometry or reflectometry. The adsorbed amount of protein from where surface pressure starts to increase, Γ^* , is on the order of 1 mg/m^2 for most globular proteins. Ellipsometric measurements (results not shown) of adsorbed amount at this stage of adsorption where the concentration of pectin at the interface is still expected to be relatively low confirm this value. Knowing the time at which surface pressure starts increasing, earlier defined as the 'lag time', t^* , we can roughly estimate an effective diffusion coefficient, D_{eff} , using the equation of Ward and Tordai²⁴: $\Gamma^* = 2c\sqrt{(D_{\text{eff}}t^*/\pi)}$, where c is the total protein bulk concentration. The effective diffusion coefficient obtained for a mixture of β -Lg (0.1 g/l) and LMP (mixing ratio 2 w/w) is $3 \cdot 10^{-13} \text{ m}^2/\text{s}$. The diffusion coefficient, D_{DLS} , obtained from dynamic light scattering of the complexes equals $1 \cdot 10^{-12} \text{ m}^2/\text{s}$. If all β -Lg is complexed to pectin, the experimentally obtained effective diffusion coefficient should be equal to the one obtained by dynamic light scattering, since all protein diffuses as complexes in this case. However, D_{eff} appears to be about 3 times smaller than D_{DLS} . Since dynamic light scattering is biased to the larger components in a polydisperse sample²⁵, it is likely that there are smaller complexes with an even larger D_{DLS} . Hence, although diffusion rate seems to play an important role, it is not likely that retarded diffusion is the only reason for a delayed increase in surface pressure. A possible contribution of convection to transport of complexes to the interface would mean that the true diffusion coefficient is smaller than the value obtained for D_{eff} . The effective diffusion coefficient for β -Lactoglobulin obtained with this method (determined using a β -Lg concentration range of 0.002 g/L – 0.02 g/L) is $1 \cdot 10^{-10} \text{ m}^2/\text{s}$, which corresponds well with the value reported by Le Bon, Nicolai, Kuil and Hollander²⁶. It cannot entirely be excluded that proteins crosslink pectin molecules to form larger aggregates, but this does not appear from the DLS results: the average size of pectin molecules decreases rather than increases on addition of pectin (figure 2.4).

Finally, we consider the association/dissociation step in adsorption of protein from complexes, step C (figure 2.6): if a protein in a complex with a polysaccharide is present in close proximity to the interface, it might be available for adsorption to the interface. If so, how rapid is this process? Presumably this depends on how rapidly protein can move within the complex and how rapidly it is released to the air/water interface. Both processes depend on the interaction affinity between the protein and the polysaccharide carrier and is thus related to charge densities of both polymers. Consequently, this latter step seems to explain the different behaviour of different polysaccharides and different proteins (table 2.2). Although the molecular weight of ι -carrageenan is smaller than that of low methoxyl pectin, it causes a similar lag time. This could be explained by the larger affinity of ι -carrageenan for

β -Lg, compared to the affinity of low methoxyl pectin for β -Lg; τ -carrageenan (containing sulphate groups) is a strong poly-acid whereas pectin (containing carboxyl groups) is a weak poly-acid. High methoxyl pectin does not cause a lag time at a ratio of 2 w/w. The fact that a small lag time is observed at a mixing ratio of 0.5 w/w, that disappears on increasing mixing ratio (figure 2.3), suggests that in this case not all protein is bound to pectin, implying that the binding-affinity is limited. The lower charge density of this polysaccharide explains this. With ovalbumin, as opposed to β -Lg, low methoxyl pectin can cause a lag time even at pH 7. Apparently, either the affinity of the pectin for ovalbumin is larger than the affinity for β -lactoglobulin at pH 7, or the affinity of ovalbumin for the interface is lower than the affinity of β -lactoglobulin for the interface. Presumably this depends on the charge distribution on the protein surface because the amount of positive charges on a β -Lg dimer is similar to that on ovalbumin. For lysozyme, that is known to adsorb very slowly compared to β -Lg (presumably due to its highly positive net charge providing a kinetic barrier for adsorption), step E is important: crossing of the kinetic barrier for adsorption, once the protein is situated just beneath the interface. In this case it could be shown that the presence of pectin can enhance the adsorption rate (table 2.2); if the kinetic barrier is indeed of an electrostatic nature, complexation of the strongly charged protein with an oppositely charged polysaccharide will lower this barrier and hence accelerate adsorption, as is observed in this case.

The carrier-mediated protein adsorption mechanism proposed in this work, provides a broad opportunity to control foam formation by protein/polysaccharide interaction in the bulk. Small changes in ionic strength or pH can change protein adsorption kinetics by changing the amount of complexed/free protein or the binding strength. In addition to generic parameters like ionic strength and pH, the mechanism can be controlled with molecular properties like charge density and distribution of the protein, and charge density of the polysaccharide. Charge distribution along the polysaccharide chain is also expected to play a role, but this needs to be further explored. All parameters mentioned above influence processes A and C in figure 2.6. Moreover, since diffusion of the complexes plays such a dominant role, also the hydrodynamic radius of the polysaccharide molecules can affect adsorption kinetics (process B in figure 2.6).

ACKNOWLEDGEMENTS

We acknowledge Bram Sperber from the Laboratory of Food Chemistry, Wageningen University, the Netherlands for his assistance with dynamic light scattering measurements.

REFERENCES

- (1) Paulsson, M.; Dejmek, P., Surface-Film Pressure of Beta-Lactoglobulin, Alpha-Lactalbumin and Bovine Serum-Albumin at the Air-Water-Interface Studied by Wilhelmy Plate and Drop Volume. *Journal of Colloid and Interface Science* **1992**, 150, (2), 394-403.
- (2) Tripp, B. C.; Magda, J. J.; Andrade, J. D., Adsorption of Globular-Proteins at the Air/Water Interface as Measured Via Dynamic Surface-Tension - Concentration-Dependence, Mass-Transfer Considerations, and Adsorption-Kinetics. *Journal of Colloid and Interface Science* **1995**, 173, (1), 16-27.

- (3) MacRitchie, F.; Alexander, A. E., Kinetics of Adsorption of Proteins at Interfaces.1. Role of Bulk Diffusion in Adsorption. *Journal of Colloid Science* **1963a**, 18, (5), 453-457.
- (4) MacRitchie, F.; Alexander, A. E., Kinetics of Adsorption of Proteins at Interfaces.2. Role of Pressure Barriers in Adsorption. *Journal of Colloid Science* **1963b**, 18, (5), 458-463.
- (5) Graham, D. E.; Phillips, M. C., Proteins at Liquid Interfaces.1. Kinetics of Adsorption and Surface Denaturation. *Journal of Colloid and Interface Science* **1979**, 70, (3), 403-414.
- (6) Wierenga, P. A.; Meinders, M. B. J.; Egmond, M. R.; Voragen, A. G. J.; de Jongh, H. H. J., Quantitative description of the relation between protein net charge and protein adsorption to air-water interfaces. *Journal of Physical Chemistry B* **2005**, in press.
- (7) Benjamins, J. Static and dynamic properties of proteins adsorbed at liquid interfaces. PhD, Thesis, Wageningen University, Wageningen, The Netherlands, 2000.
- (8) Lee, Y. C.; Lee, R. T., Carbohydrate-Protein Interactions - Basis of Glycobiology. *Accounts of Chemical Research* **1995**, 28, (8), 321-327.
- (9) Pereyra, R.; Schmidt, K. A.; Wicker, L., Interaction and stabilization of acidified casein dispersions with low and high methoxyl pectins. *Journal of Agricultural and Food Chemistry* **1997**, 45, (9), 3448-3451.
- (10) Syrbe, A.; Bauer, W. J.; Klostermeyer, H., Polymer science concepts in dairy systems - An overview of milk protein and food hydrocolloid interaction. *International Dairy Journal* **1998**, 8, (3), 179-193.
- (11) Maroziene, A.; de Kruif, C. G., Interactions of pectin and casein micelles. *Food Hydrocolloids* **2000**, 14, (4), 391-394.
- (12) Dickinson, E., Hydrocolloids at interfaces and the influence on the properties of dispersed systems. *Food Hydrocolloids* **2003**, 17, (1), 25-39.
- (13) Benichou, A.; Aserin, A.; Garti, N., Protein-polysaccharide interactions for stabilization of food emulsions. *Journal of Dispersion Science and Technology* **2002**, 23, (1-3), 93-123.
- (14) Dickinson, E.; Pawlowsky, K., Effect of l-carrageenan on flocculation, creaming, and rheology of a protein-stabilized emulsion. *Journal of Agricultural and Food Chemistry* **1997**, 45, (10), 3799-3806.
- (15) Baeza, R.; Sanchez, C. C.; Pilosof, A. M. R.; Patino, J. M. R., Interactions of polysaccharides with beta-lactoglobulin adsorbed films at the air-water interface. *Food Hydrocolloids* **2005**, 19, (2), 239-248.
- (16) Weinbreck, F.; de Vries, R.; Schrooyen, P.; de Kruif, C. G., Complex coacervation of whey proteins and gum arabic. *Biomacromolecules* **2003**, 4, (2), 293-303.
- (17) Girard, M.; Turgeon, S. L.; Gauthier, S. F., Quantification of the interactions between beta-lactoglobulin and pectin through capillary electrophoresis analysis. *Journal of Agricultural and Food Chemistry* **2003**, 51, (20), 6043-6049.
- (18) de Jongh, H. H. J.; Groneveld, T.; de Groot, J., Mild isolation procedure discloses new protein structural properties of beta-lactoglobulin. *Journal of Dairy Science* **2001**, 84, (3), 562-571.
- (19) Wierenga, P. A.; Meinders, M. B. J.; Egmond, M. R.; Voragen, A. G. J.; de Jongh, H. H. J., Protein exposed hydrophobicity reduces the kinetic barrier for adsorption of ovalbumin to the air-water interface. *Langmuir* **2003**, 19, (21), 8964-8970.
- (20) Daas, P. J. H.; Boxma, B.; Hopman, A. M. C. P.; Voragen, A. G. J.; Schols, H. A., Nonesterified galacturonic acid sequence homology of pectins. *Biopolymers* **2001**, 58, (1), 1-8.
- (21) Benjamins, J.; Cagna, A.; Lucassen-Reynders, E. H., Viscoelastic properties of triacylglycerol/water interfaces covered by proteins. *Colloids and Surfaces A* **1996**, 114, 245-254.
- (22) Berne, B. J.; Pecora, R., *Dynamic Light Scattering: with applications to Chemistry, biology, and Physics*. 2000 ed.; General Publishing Company, Ltd.: Toronto, 1976.

- (23) van der Burgh, S.; de Keizer, A.; Cohen Stuart, M. A., Complex coacervation core micelles. Colloidal stability and aggregation mechanism. *Langmuir* **2004**, 20, (4), 1073-1084.
- (24) Ward, A. F. H.; Tordai, L., Time-Dependence of Boundary Tensions of Solutions.1. The Role of Diffusion in Time-Effects. *Journal of Chemical Physics* **1946**, 14, (7), 453-461.
- (25) Axelos, M. A. V.; Lefebvre, J.; Thibault, J. F., Conformation of a low methoxyl citrus pectin in aqueous solution. *Food Hydrocolloids* **1987**, 1, (5/6), 569-570.
- (26) Le Bon, C.; Nicolai, T.; Kuil, M. E.; Hollander, J. G., Self-diffusion and cooperative diffusion of globular proteins in solution. *Journal of Physical Chemistry B* **1999**, 103, (46), 10294-10299.

Modulating surface rheology by electrostatic protein/polysaccharide interactions

Renate A. Ganzevles, Kyriaki Zinoviadou, Ton van Vliet, Martien A. Cohen Stuart and Harmen H.J. de Jongh, Langmuir 2006, 22 (24), 10089

ABSTRACT

There is a large interest in mixed protein/polysaccharide layers at air/water- and oil/water interfaces because of their ability to stabilize foams and emulsions. Mixed protein/polysaccharide adsorbed layers at air/water interfaces can be prepared either by adsorption of soluble protein/polysaccharide complexes or by sequential adsorption of complexes or polysaccharides to a previously formed protein layer. Even though final protein and polysaccharide bulk concentrations are the same, the behaviour of the adsorbed layers can be very different, depending on the way of preparation. The surface shear modulus of a sequentially formed β -lactoglobulin/pectin layer can be up to a factor 6 higher than a layer made by simultaneous adsorption. Furthermore surface dilatational modulus and surface shear modulus strongly (up to a factor of 2 and 7, respectively) depend on the bulk β -lactoglobulin/pectin mixing ratio. Based on the surface rheological behaviour, a mechanistic understanding of how the structure of adsorbed layers depends on protein polysaccharide interaction in bulk solution, mixing ratio, ionic strength and on the order of adsorption to the interface (simultaneously or sequential) is derived. Insight in the effect of protein polysaccharide interactions on the properties of adsorbed layers provides a solid basis to modulate surface rheological behaviour.

3.1 INTRODUCTION

A classical application of electrostatic protein polysaccharide interaction in the food industry is the use of pectin to stabilize casein micelles in acidified milk drinks. Due to electrostatic interaction negatively charged pectin molecules adsorb to the positively charged casein micelles. As a consequence electrostatic and steric repulsion prevent the micelles from acid-induced aggregation¹⁻³. Polysaccharides are also used in food emulsions to prevent aggregation and creaming of emulsion droplets⁴⁻⁷. By layer-by-layer deposition of oppositely charged proteins, polysaccharides and surfactants on emulsion droplets^{8, 9} one can control the net charge on the droplets and enhance emulsion stability by electrostatic repulsion. However, depending on relative concentrations, polysaccharides can also decrease emulsion stability due to bridging flocculation¹⁰.

Besides establishing electrostatic and/or steric repulsion, adsorbed layers at the air/water or oil/water interface may also affect foam and emulsion stability by their elastic behaviour¹¹. In this context ample attention has been paid to surface rheological behaviour of different proteins depending on pH, ionic strength and aging of the interface¹²⁻¹⁶. When dealing with complex systems (e.g. protein/polysaccharide mixtures) it is important to understand how the functional behaviour of the individual components, like surface activity, rheology, etc. is affected by interactions between the components. Furthermore, rheological measurements can provide insight in the build-up of mixed protein/polysaccharide layers at liquid interfaces.

Electrostatically driven coadsorption of non-surface-active anionic polysaccharides with proteins can affect surface rheological properties¹⁷⁻¹⁹. Ducel and coauthors report that (oil/water-) interfacial rheological properties of plant protein-arabic gum coacervates is related to the interfacial rheological properties of the protein used²⁰. Schmitt et al. describe an effect of aging time of β -lactoglobulin/acacia gum complexes on (air/water-) surface rheology in terms of reorganization of the complexes at the interface²¹. However, it is not known how the surface properties are related to structure of/and interactions within the complex surface layer.

When mixing an anionic polysaccharide like pectin with a protein at low ionic strength and above the pK_a of the polysaccharide, one can form protein/polysaccharide complexes. Depending on protein/polysaccharide mixing ratio and protein/polysaccharide binding affinity, these soluble complexes can either be soluble or they can aggregate and phase separate (as a liquid coacervate phase or precipitate)²². From chapter 2 it is known that soluble β -lactoglobulin/low methoxyl pectin complexes (at pH 4.5) adsorb at air/water interfaces and that protein polysaccharide interactions can be used to control adsorption kinetics at the air/water interface.

This chapter aims to provide a mechanistic understanding of how surface dilatation and surface shear rheological behaviour depends on electrostatic protein polysaccharides interaction in the bulk solution, mixing ratio, ionic strength and on the order of adsorption to the air/water interface (simultaneously or sequential). Based on all observations a model is

proposed of how the parameters mentioned above could be used to control the build-up of protein/polysaccharide layers and, as a result, tune the surface rheological behaviour at the air/water interface. In chapter 4 is shown that the model is also valid for oil/water interfaces.

3.2 MATERIALS AND METHODS

3.2.1 Materials

Acetate buffers (pH 4.5, ionic strength 9 mM) were prepared from analytical grade chemicals and deionised water (Barnstead EASYpure UV, USA). Please note that values for ionic strength mentioned in the text represent ionic strength of the buffer. Bovine β -lactoglobulin (isoelectric point 5.1) was purified using a non denaturing method as described previously²³. Low methoxyl pectin was supplied by CP Kelco (Lille Skensved, Denmark). The degree of methylation is 30.4 % (only the non-methylated galacturonic acid subunits have a free carboxyl group, pKa ~4.5), the uronic acid content is 78.5 %²⁴, number averaged molar mass (M_n) $1.5 \cdot 10^5$ g/mol, polydispersity (M_w/M_n) 2.4 (chapter 2). Pectin solutions were prepared by wetting the powder with ethanol and subsequent dispersion in deionised water, followed by heating at 70 °C for 30 minutes. After overnight storage, the samples were centrifuged at 6000 g for 10 minutes and stored at 4 °C until further use. Protein stock solutions (for ζ -potential 20 g/l, all other measurements 1 or 2 g/l) were prepared freshly every day by dissolving the freeze dried protein in deionised water, allowing at least 30 min for dissolving. The pH of the protein stock solutions was 6.8 ± 0.2 . After diluting pectin stock solution with buffer, addition of protein stock solution to a protein concentration of 0.1 g/L and mixing, protein/polysaccharide samples were equilibrated for 30 min before use in order to allow formation of protein/polysaccharide complexes.

3.2.2 Light scattering

Second cumulant diffusion coefficients and scattered light intensities (at 90°) of the pectins and the β -lactoglobulin/pectin complexes were determined by light scattering²⁵, using an ALV 5000 light scattering instrument (Langen, Germany) equipped with a 400 mW argon laser tuned at a wavelength of 514.5 nm, as described before²⁶. From dynamic light scattering hydrodynamic radii were calculated according to the Stokes-Einstein relation, assuming that the pectin molecules and the complexes are spherical. Averages and standard deviations were calculated from sets of 10 measurements. Temperature was controlled at 20 ± 0.1 °C. Stock protein (2 g/L), pectin (2 g/L) and buffer solutions (25 mM acetate buffer, ionic strength 9 mM, pH 4.5) were filtered through 0.45 μ m filters (Acrodisc, Gelman Sciences, MI, USA). For each mixing ratio a separate sample was prepared by subsequent addition of stock pectin and stock protein solution to the buffer solution. Protein concentration was 0.1 g/L for all samples and pectin concentrations varied from protein/pectin mixing ratio 1 to 15 w/w. The 0 w/w sample is a 0.1 g/L pectin solution, without protein, in the same buffer. Protein/polysaccharide samples were equilibrated for 30 min before use in order to allow formation of protein/polysaccharide complexes.

3.2.3 Determination of ζ -potential

The electrophoretic mobility of soluble protein/polysaccharide complexes was measured using a zetasizer 2000 HS (Malvern instruments Ltd., UK) at 150 V applied voltage, using a He-Ne laser at 633 nm. The ζ -potential was calculated using the Helmholtz-Smoluchovski equation. Protein concentration could not be kept constant (but varied from 0.01 to 0.05 g/L) in these measurements because the scattered light intensity varies too much between the different mixing ratios to allow determination of ζ -potential. Stock β -lactoglobulin and stock pectin solutions were mixed with buffer (ionic strength 9 mM, pH 4.5) to a final total concentration - depending on mixing ratio - such that the signal retrieved was optimal and only a single narrow peak was observed in the scattered light intensity versus electrophoretic mobility curve. Average values and standard deviations were calculated over sets of 5 to 10 measurements. A duplicate set of samples was measured and differences were within 5%.

3.2.4 Drop tensiometry/ surface dilatational rheology

Surface tension as a function of time was measured (for single component and mixed solutions of protein and polysaccharide) using a Profile Analysis Tensiometer (PAT1, SINTERFACE technology, Berlin, Germany). Each experiment started with a clean interface of a freshly formed sample solution droplet (14 μ L) pending on the tip of a double concentrical needle connected to two separate syringes. Injection through the inner syringe, while withdrawing liquid through the outer syringe such that the droplet surface area is kept constant, allows to rinse the solution inside the droplet while keeping a previously formed adsorbed layer intact. The rinsing velocity was 1 μ L/s. Surface tension was determined by bubble shape analysis. All results are presented in terms of surface pressure $\Pi = \gamma_0 - \gamma$, where γ_0 is the surface tension of the solvent (72 mN/m) and γ is the measured surface tension.

Surface dilatational moduli (ϵ) were determined by subsequent expansion and compression of the interfacial area A (amplitude in area oscillation 6 %, frequencies 0.01, 0.05 and 0.1 s^{-1} , respectively) and recording the resulting change in surface tension: $\epsilon = d\gamma/d\ln A = -d\Pi/d\ln A$. Measurements of dilatational modulus as a function of time were performed using a different drop tensiometer setup (ADT, ITCONCEPT, Longessaigne, France), where immediately before the start of the experiment an air bubble (7 μ L) is formed on the tip of a needle in the sample solution as described before²⁷. Periods of 5 oscillations (amplitude in area oscillation 4 %, frequency 0.1 s^{-1}) were alternated with equally long resting periods. Average dilatational moduli, as well as average surface tension during oscillations, were determined using the last three oscillations of each oscillation set. All experiments were performed at least in duplicate; differences were within 5 to 10%. Temperature was controlled at 21 ± 1 °C. Experiments were performed at 2 mM ionic strength in addition to 9 mM, as indicated in the text, to enhance differences between the different samples.

3.2.5 Surface shear rheology

Surface shear rheological behaviour of adsorbed protein/polysaccharide layers at air/water interfaces was investigated using a strain-controlled Couette-type interfacial shear rheometer, as described elsewhere^{28, 29}. Buffer solution was poured into the sample holder and

subsequently, at time zero, a 10 times concentrated protein or protein/polysaccharide solution was injected in the bulk solution at the bottom of the sample beaker to a final protein concentration of 0.1 mg/mL. Immediately after injection, a disc was suspended from a torsion wire until it just touched the interface. The sample was left to adsorb and equilibrate for 20 hours at 21 ± 1 °C, during which surface tension was monitored using a Wilhelmy plate. Deformation of the interface is achieved by turning the sample container at an angular velocity of $1.27 \cdot 10^{-3}$ rad/s and the resulting stress on the interfacial layer near the disc was calculated from the rotation of the disc. Stress-strain curves were calculated from these values. Since the relative deformation of the interface is not uniform due to the large gap width relative to the disc diameter, the ratio of stress and strain is to be considered as an apparent surface shear modulus. All experiments were performed in duplicate or triplicate.

3.3 RESULTS

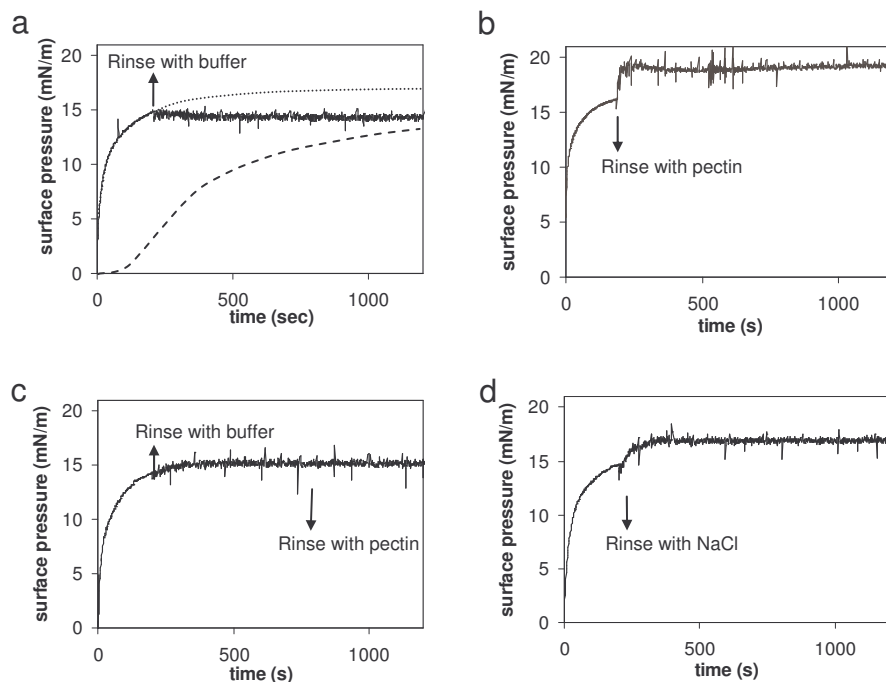


Figure 3.1: Surface pressure (at the air/water interface) versus time curves for a 0.1 g/L β -lactoglobulin solution pH 4.5, I 2 mM, flushed (from 200 s) with a: buffer (dotted line represents β -lactoglobulin curve without rinsing, dashed line represents β -lactoglobulin/pectin curve in case β -lactoglobulin and pectin were mixed before the experiment started, also without rinsing), b: pectin solution, c: first buffer then pectin (from 750 s), d: 50 mM NaCl solution.

In order to investigate how protein/polysaccharide interactions affect the properties of mixed protein/polysaccharide adsorbed layers we first consider exerted surface pressures. Figure 3.1a shows a typical surface pressure versus time curve for a pure β -lactoglobulin solution (0.1 g/L, pH 4.5, I 2 mM, dotted line) and for a mixture of β -lactoglobulin and pectin (protein/polysaccharide mixing ratio 2 w/w, dashed line) measured with a pendant drop tensiometer. Pectin alone does not increase surface pressure by more than 0.5 mN/m in 30000 seconds at the concentrations used (not shown). The double syringe setup enables one to replace the protein solution inside the droplet with buffer solution. When this option is

employed one observes an instantaneous inhibition of surface pressure development (Figure 3.1a, solid curve). It appears that the increase in surface pressure due to protein adsorption can be stopped at any value by rinsing with buffer, after which surface pressure remains constant in time (the fluctuations in surface pressure are due to vibrations caused by the rinsing and disappear when the rinsing stops). Because in the case of simultaneous adsorption the major part of the β -lactoglobulin is bound to pectin, adsorption kinetics to the air/water interface in the presence of pectin are different from the pure protein case (chapter 2). In particular, the exact amount of protein in the mixed layers is unknown and the role of pectin is unclear. In order to elucidate this, it is important to separate protein and polysaccharide effects. Using the rinsing method one can compare interfaces with and without pectin starting from the same β -lactoglobulin layer. Rinsing a droplet - after formation of a protein layer - with a pectin solution (0.05 g/L, pH 4.5, I 2 mM) instead of with buffer, results in a 3 mN/m increase in the surface pressure (Figure 3.1b). Interestingly when the droplet was first rinsed with buffer to remove remaining protein from the bulk solution and subsequently rinsed with the same pectin solution, surface pressure remained constant (Figure 3.1c). Rinsing with a 50 mM NaCl solution (Figure 3.1d) resulted in a similar increase in surface pressure as observed after rinsing with pectin.

Table 3.1: Dilatational moduli and phase angles (at various frequencies as indicated in the table) of different β -lactoglobulin/pectin layers adsorbed to an air/water interface, β -lactoglobulin bulk concentration was 0.1 g/L, pH 4.5, ionic strength 2 mM, experimental error $\pm 5\%$

type of adsorbed layer	dilatational modulus (mN/m)			phase angle (°)		
	0.1 (s ⁻¹)	0.05 (s ⁻¹)	0.01 (s ⁻¹)	0.1 (s ⁻¹)	0.05 (s ⁻¹)	0.01 (s ⁻¹)
protein rinsed with buffer	68	66	57	10	12	13
protein rinsed with 0.05 g/L pectin	108	103	86	12	13	18
protein rinsed with buffer, then with 0.05 g/L pectin	109	104	92	11	12	15
protein rinsed with 50 mM NaCl solution	79	76	62	10	11	17
simultaneously adsorbed 2 w/w protein/pectin	61	56	43	13	14	16

Besides surface pressure, one can compare surface rheological behaviour of the different adsorbed layers using this setup. Dilatational moduli of all samples at three different frequencies were measured after the rinsing procedure, at ~ 30 min after the formation of the droplet (Table 3.1). Adsorption of pectin on a previously formed protein layer results in a 60 % increase in modulus. In contrast, the presence of pectin in the protein solution before exposure to the interface, leads to a 10 % lower modulus than that of a pure protein layer. With decreasing oscillation frequency all layers exhibit a decrease in dilatational modulus, which is coincided with an increase in phase angle. This behaviour suggests that when there is more time available, the molecules may relax to a larger extent.

3.3.1 β -Lactoglobulin/pectin complexes in solution

Before we attempt to understand the behaviour of the mixed adsorbed layers from simultaneous protein/polysaccharide adsorption, it is useful to have information about the mixing behaviour of the components in bulk. Figure 3.2 shows results of light scattering

measurements; scattered light intensity and hydrodynamic radius as a function of protein/polysaccharide mixing ratio at pH 4.5, 9 mM ionic strength (ratio 0 is pure pectin, for all other mixing ratios protein concentration was 0.1 g/L). The scattered light intensity in the presence of protein, from ratio 1 w/w upwards, is much higher than at ratio 0 w/w, in the absence of protein (Figure 3.2). The presence of protein does not influence the hydrodynamic radius until a mixing ratio of 6 w/w. Furthermore, from a previously measured decrease in adsorption kinetics it is known that at least 90% of the protein is bound up to a ratio of 6 w/w (chapter 2). Based on these observations it is concluded that soluble β -lactoglobulin/pectin complexes are formed. The soluble complexes aggregate and become insoluble (complex coacervation) at protein/polysaccharide mixing ratios from 7 w/w upwards, as concluded from the steep increase in hydrodynamic radius and a strong increase in turbidity (as observed with the naked eye). The increased turbidity (that prevents the light to go through the sample) could account for the decrease in intensity observed at 90° from ratio 8 w/w upwards. Furthermore, the amount of phase separated material decreases with the decrease in pectin concentration on increasing mixing ratio. Comparing the number of charges on β -lactoglobulin and pectin based on their proton titrations curves (data not shown) suggests that, if all molecules take part in the soluble complex formation, the total positive net charge on the protein molecules just compensates the total negative charge on the polysaccharides at the transition at ratio 7 w/w. Apparently the complexes aggregate and become insoluble when their net charge approaches neutrality and an excess charge at lower mixing ratio prevents this. Small fractions of insoluble aggregated complexes below mixing ratio 7, due to heterogeneity in stoichiometry, could heavily increase the average hydrodynamic radius and can account for the variation in hydrodynamic radius in the soluble complexes regime.

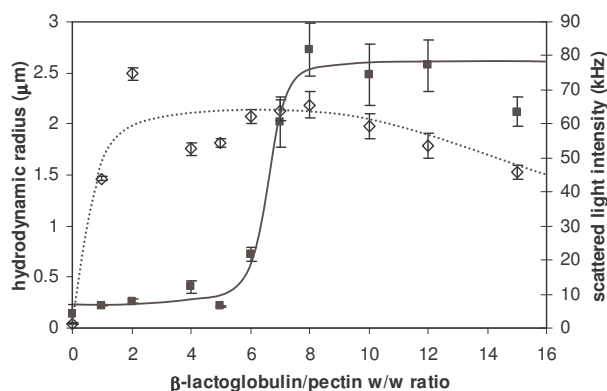


Figure 3.2: Dynamic light scattering of β -lactoglobulin/pectin mixtures at different w/w mixing ratios, (■) hydrodynamic radius, (○) scattered light intensity, lines serve to guide the eye; for all samples protein concentration was 0.1 g/L pH 4.5, 19 mM

The ζ -potential of the protein/polysaccharide complexes was measured to determine whether the net charge of the protein/polysaccharide complexes indeed decreases with increasing mixing ratio (Figure 3.3). On addition of protein to a pectin solution (at pH 4.5, I 9 mM) the ζ -potential, which is -40 mV for pure pectin, increases. First a linear increase in ζ -potential is observed until a value of -8 mV is reached for a protein/polysaccharide mixing ratio of 8 w/w. Upon further increase of the mixing ratio the ζ -potential only slightly increases. As appears

from figure 3.2 and 3.3, a ζ -potential as small as -8 mV is not capable to prevent the complexes from aggregating and becoming insoluble. Although β -lactoglobulin is slightly positively charged at pH 4.5 (as known from titration curves, data not shown), the ζ -potential measured for the protein is 0 ± 1 mV.

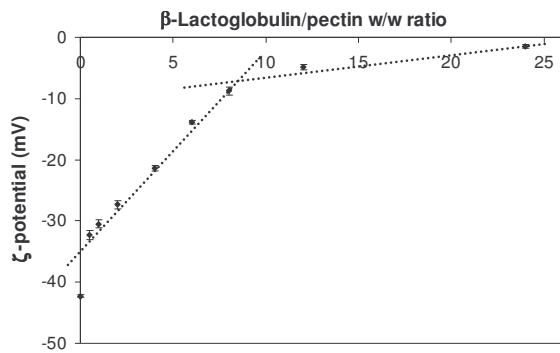


Figure 3.3: ζ -potential as a function of β -lactoglobulin/pectin w/w ratio; concentrations were adapted to optimal signal, pH 4.5, 19 mM, lines serve to guide the eye

3.3.2 Surface dilatational rheology

As mentioned before the rate of surface pressure development at air/water interfaces can be affected by complexation of protein with polysaccharide in the bulk solution (Figure 3.1a). Furthermore, the presence of pectin in the interface appears to affect rheological behaviour of the adsorbed layer (Table 3.1). Because the net charge of the complexes depends on the mixing ratio and might affect surface rheology, we measured the dilatational modulus (at 0.1 s $^{-1}$) of mixed β -lactoglobulin/pectin layers for different bulk mixing ratios (Figure 3.4). Figure 3.4a shows that the higher the protein/polysaccharide mixing ratio, the faster the surface pressure levels off to a constant value; at a mixing ratio of 8 w/w, the surface pressure versus time curve comes close to that of β -lactoglobulin alone (at this large time scale, initial slopes are not resolved). This trend with mixing ratio is more pronounced for the development of the dilatational modulus. For the lower mixing ratios no steady state value of the dilatational modulus is reached within 11 hours (Figure 3.4b).

In order to compare the rheological properties of the interface in a way independent of adsorption kinetics, the modulus is plotted as a function of surface pressure in figure 3.4c. The shape of the curves, with a minimum in dilatational modulus at a surface pressure between 15 and 20 mN/m, is not unique for the mixed systems, but is also observed for pure β -lactoglobulin layers (depending on bulk concentration). The minimum in dilatational modulus, coupled with a maximum in phase angle (chapter 9), can presumably be attributed to structural reorganisations of the protein molecules at the interface. With increasing protein bulk concentration the minimum in dilatational modulus becomes deeper (chapter 9), the maximum in phase angle becomes higher, and the whole modulus versus surface pressure curve shifts to slightly lower dilatational modulus. We tentatively interpret these differences in terms of layer structure. When protein adsorbs from low concentrations, it has the time to

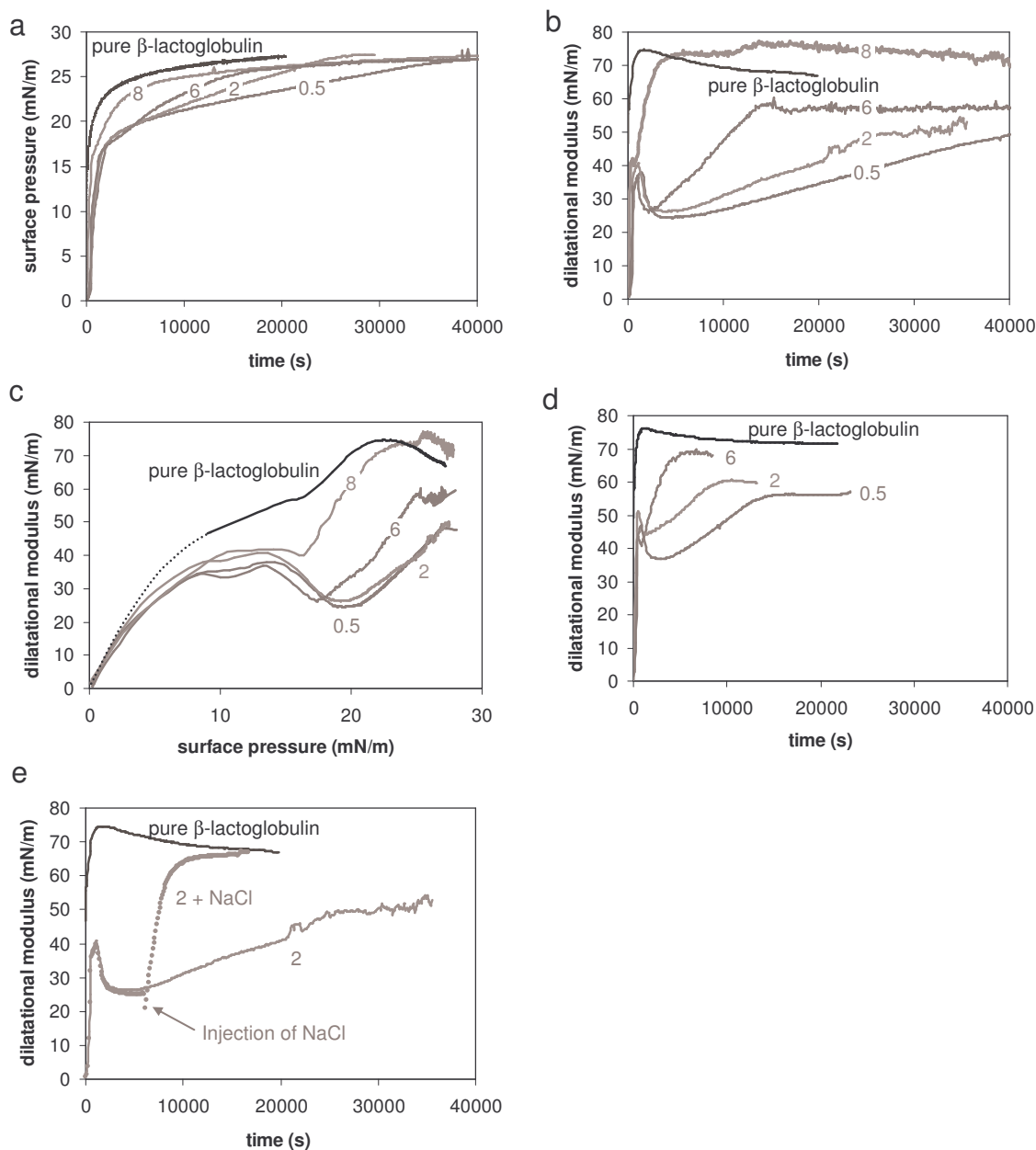


Figure 3.4: a) surface pressure (at the air/water interface) versus time curves of β -lactoglobulin and β -lactoglobulin/pectin mixtures at different ratios (as indicated in graphs), for all samples protein concentration was 0.1 g/L, pH 4.5, 1 2 mM b) dilatational modulus versus time curves for the same samples, pH 4.5, 1 2 mM, c) dilatational modulus versus surface pressure curves, dotted part of β -lactoglobulin curve is estimated, d) dilatational modulus versus time curves at 9 mM ionic strength, pH 4.5 e) dilatational modulus of a 2 w/w β -lactoglobulin/pectin mixture as a function of time with and without NaCl injection up to 100 mM after two hours.

adopt a more favourable conformation at the interface before the layer is jammed, whereas on adsorption from higher concentrations the system is jammed before these conformational changes can occur. The latter layer structure is less ordered and less compact at $\Pi \approx 17$ mN/m, allowing for less pressure increase upon compression, i.e. a lower modulus. Possibly some partial desorption occurs too. At saturation, a similar steady state value of the modulus for all concentrations is reached (~ 70 mN/m) at steady state surface pressure values increasing with concentration. The shift in surface pressure versus surface load curves to higher surface

loads upon increasing β -lactoglobulin bulk concentration, as observed by Wierenga et al., supports this hypothesis³⁰. The time scale at which the dilatational modulus goes through this minimum is orders of magnitude larger for the protein/polysaccharide mixtures as compared to the pure protein case. For the protein/polysaccharide mixtures, the minimum in dilatational modulus could possibly be interpreted as conformational changes of protein molecules, or as rearrangements of the protein/polysaccharide complexes or a combination of both. This discussion will be extended in chapter 9.

Comparing the mixed β -lactoglobulin/pectin layers in figure 3.4c at a given value of surface pressure above 15 mN/m, one observes an increase of the dilatational modulus with increasing mixing ratio. At an ionic strength of 9 mM (instead of 2 mM), the difference between the different mixing ratios diminishes and for all ratios a steady state dilatational modulus is reached faster (Figure 3.4d). In figure 3.4e, NaCl was injected in a 2 w/w β -lactoglobulin/pectin mixture up to an ionic strength of 100 mM two hours after the start of the experiment. The dilatational modulus instantaneously increased approximately to the steady state value of a pure protein layer, suggesting that protein liberated from its complex with pectin adsorbed rapidly.

3.3.3 Surface shear rheology

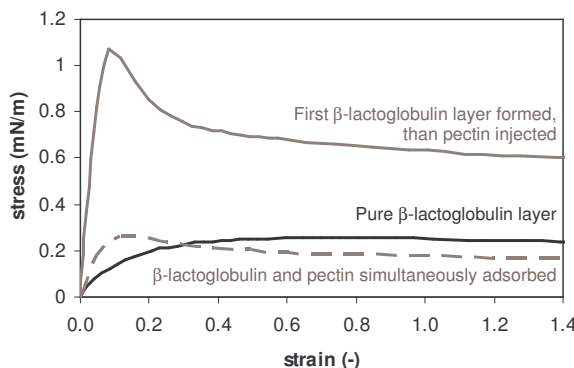


Figure 3.5: Typical examples of stress/strain curves of a pure β -lactoglobulin adsorbed layer at the air/water interface, a β -lactoglobulin/pectin layer simultaneously adsorbed from 2 w/w mixture and a mixed layer where β -lactoglobulin/pectin complexes adsorbed under a previously adsorbed protein layer (after \sim 150 minutes), final overall mixing ratio 2 w/w; for all samples protein concentration was 0.1 g/L, pH 4.5 and I 9 mM

Surface shear deformation is different from surface dilatation in the sense that the area of the interface remains constant during shear deformation. This means there is no contribution of changing surface pressure during deformation and therefore the surface shear modulus is, compared to dilatational modulus, more sensitive to elastic or viscous forces within the adsorbed layer. Surface shear stress was measured as a function of strain for the different samples (Figure 3.5). A pure protein layer initially responds elastically; the stress increases with the strain. At higher strain, it becomes viscous; the stress levels off at a steady state value of 0.24 mN/m. The steady state shear stress for a mixture of 2 w/w β -lactoglobulin/pectin is not much different from that of a pure protein layer. However, the shape of the curves is different; the mixture exhibits a maximum stress, indicating yielding (or fracture) of the layer, which the pure protein layer does not. When a protein layer was adsorbed from a pure protein

solution (for ~150 minutes) prior to injection of pectin under the surface (into the bulk protein solution) much higher shear stresses were measured.

The initial slope of a stress/strain curve represents an apparent surface shear modulus, also called apparent Young's modulus. Figure 3.6a shows surface shear moduli for adsorbed layers of β -lactoglobulin/pectin mixtures at different bulk mixing ratios (solid triangles). Between ratio 2 and 6 the surface shear modulus strongly increased with increasing protein/polysaccharide mixing ratio. At a mixing ratio of 12 w/w, where the protein is in excess, surface shear modulus may be decreased. If protein and polysaccharide do not simultaneously adsorb, but a protein layer has been formed before pectin is injected in the bulk, this dependence on mixing ratio is not seen (open squares). At all mixing ratios the surface shear modulus is higher than the surface shear modulus of a pure protein layer (dotted line), indicating the presence of pectin in the interface. The steady state shear stress values at larger deformation show an effect of mixing ratio in case of simultaneous adsorption, which is very similar to that for the (apparent) modulus. Again, this trend is absent in case of sequential adsorption (Figure 3.6b).

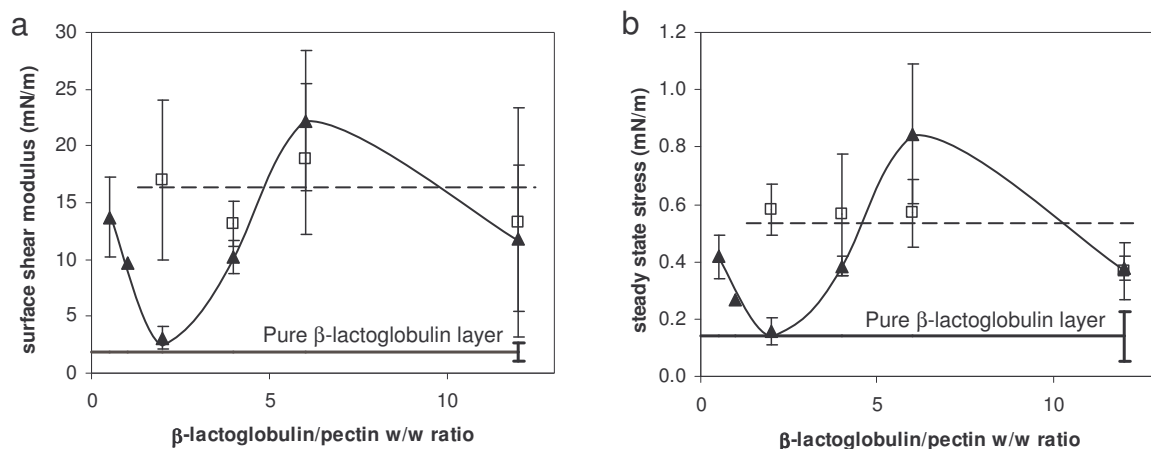


Figure 3.6. a: Apparent surface shear modulus and b: steady state shear stress as a function of β -lactoglobulin/pectin w/w mixing ratio in the bulk for (\blacktriangle) simultaneous adsorption and sequential adsorption (\square) at the air/water interface; for all samples protein concentration was 0.1 g/L, pH 4.5 and 19 mM, lines serve to guide the eye

Since the protein/polysaccharide complexes are formed due to electrostatic interaction, the dependence of surface shear modulus and steady state shear stress on ionic strength was studied (Figure 3.7). The β -lactoglobulin/pectin complex (w/w ratio 6) layer has a much higher surface shear modulus and steady state surface shear stress than a pure protein layer under the same conditions at ionic strengths up to 300 mM. Pure pectin does not cause any surface shear elasticity at any ionic strength (results not shown).

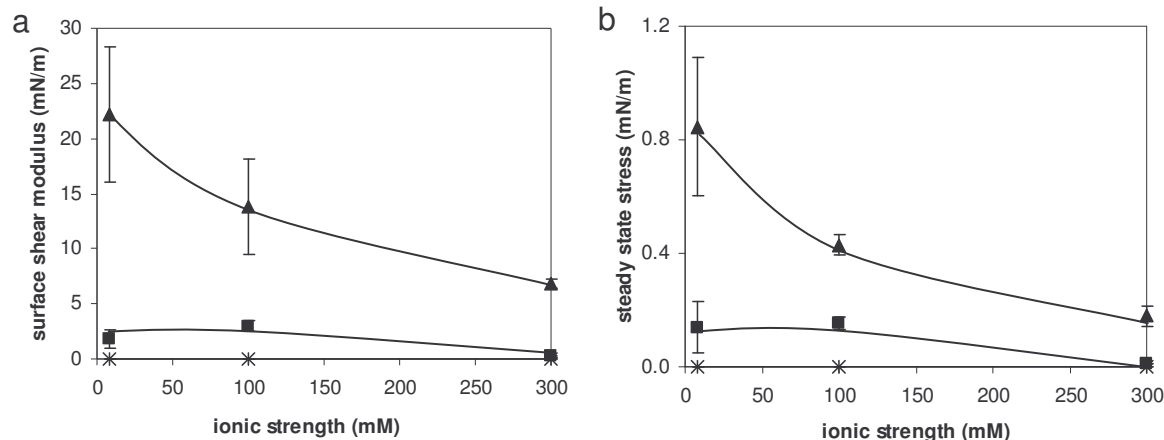


Figure 3.7: a) Apparent surface shear modulus and b) steady state shear stress as a function of ionic strength for 6 w/w ratio protein/polysaccharide complexes (▲), pure protein (■) and pure pectin (x) at the air/water interface; for all samples protein concentration was 0.1 g/L, pH 4.5 and 19 mM, lines serve to guide the eye.

3.4 DISCUSSION

With the rinsing experiments it was shown that pectin can adsorb to an adsorbed protein layer at the air/water interface and so affect surface rheology. The fact that surface pressure increased on rinsing with pectin, but did not increase when the bulk protein had been removed first by rinsing with buffer before the introduction of pectin (Figure 3.1), indicates that in the first case the increase in surface pressure is caused by additional protein adsorption; the injected pectin strongly attracts any protein it encounters in the droplet under these conditions, as demonstrated by dynamic light scattering and ζ -potential data. In a similar way as an increased ionic strength^{31, 32}, the presence of negatively charged pectin may reduce electrostatic repulsion between the positive protein molecules at the interface and in this way facilitate a denser protein packing. The higher dilatational modulus after rinsing with pectin, as compared to rinsing with NaCl (Table 3.1), may be explained by the formation of thicker layers upon pectin injection (chapter 5) as compared to NaCl injection.

We propose the layer compositions as depicted in figure 3.8 to account for the data. In the absence of pectin, a pure protein layer is formed (Figure 3.8A). Using neutron reflection the thickness of this layer was found to be approximately 4 nm, corresponding to a monolayer of β -lactoglobulin dimers (chapter 5). Comparing the values for the dilatational modulus obtained from sequential protein/polysaccharide adsorption with those obtained from simultaneous adsorption (Table 3.1) shows that, on the one hand, adsorption of pectin (alone or in combination with extra protein) can reinforce an already existing protein layer at the interface, as in figure 3.8D. On the other hand, when the pectin is present from the start it seems to prevent the formation of a compact layer due to electrostatic repulsion between the net negatively charged protein/polysaccharide complexes, figure 3.8B. In effect, the protein/polysaccharide complex constitutes a barrier against adsorption of protein molecules. The extent to which the latter effect occurs decreases with increasing protein/polysaccharide mixing ratio until the ζ -potential of the complexes is (close to) neutral. This is depicted in figure 3.8 as going from B to C. Increasing ionic strength, and with that decreasing

electrostatic repulsion between strongly negatively charged complexes (and finally break up of the complexes) was demonstrated to counteract the effect of pectin.

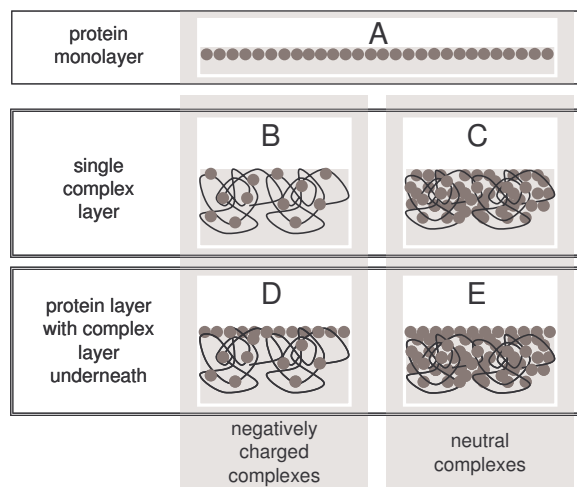


Figure 3.8: Schematic representation of different adsorbed layers at the air/water interface (A) protein monolayer, (B) and (C) mixed layers from simultaneous protein/polysaccharide adsorption where (B) is from negatively charged complexes and (C) from net neutral complexes, (D) and (E) protein/polysaccharide complexes adsorbed at previously formed protein layer where (D) concerns negatively charged complexes and (E) net neutral complexes.

Results of surface shear measurements support this mechanistic view on structure and composition of mixed protein/polysaccharide adsorbed layers. The surface shear modulus of layers created by simultaneous protein/polysaccharide adsorption (Figure 3.6) strongly increases with the mixing ratio, between a mixing ratio of 2 and 6. Above this range, surface shear modulus does not further increase. Since above a mixing ratio of 6 the ζ -potential is close to zero, one can imagine that at this point more compact layers can be formed (Figure 3.8C), resulting in a higher surface shear modulus and a higher steady state stress as compared to a ratio of 2, where complexes are strongly negatively charged (Figure 3.8B). Monteux et al.³³ observed a similar dependence of surface shear and dilatation rheology on mixing ratio of oppositely charged polyelectrolytes and surfactants. Since soluble complexes aggregated at a mixing ratio of 7 or higher, as shown by dynamic light scattering (Figure 3.2), presumably this can also occur in the interface, possibly resulting in a macroscopic network. It is possible that the interface is wetted by a liquid coacervate phase in situation C and E, but the thermodynamic non-equilibrium character of protein adsorption might not allow the formation of a pure viscous layer. It is not clear yet why surface shear modulus and steady state shear stress were higher at w/w mixing ratio of 0.5 and 1, compared to a ratio of 2 (Figure 3.6); this trend is not observed with dilatational modulus. Possibly at these low mixing ratios the layers are thicker because the complexes are swollen due to strong electrostatic repulsion.

A pure protein layer (Figure 3.8A) exhibits only a low surface shear modulus and no maximum in the stress/strain curve. Possibly, individual protein molecules can easily be sheared along each other. When pectin is injected under the surface, it will complex with the remaining protein in the bulk. When these complexes are negatively charged, they will most

likely bind to the slightly positively charged protein layer at the interface. In this case a compact layer of protein molecules has already adsorbed before the polysaccharides have a chance to interfere. The existing protein layer can now be reinforced by adsorption of protein/polysaccharide complexes, resulting in a layer as in figure 3.8D. One can imagine why in this case the shear elasticity of sequential adsorbed layers does not depend on the mixing ratio (compare Figure 3.8D and E) as was observed for the layers formed from simultaneous adsorption (Figure 3.8 B and C); with sequential adsorption the mixing ratio primarily affects the second layers. Apparently as long as it is negative the absolute value of the net charge of the complexes in the second layer is not of primary importance. At a mixing ratio of 12 w/w, where protein is in excess and the complexes are net neutral (as shown by the ζ -potential experiments) the system becomes unstable (as appeared from light scattering); the soluble complexes aggregate and eventually phase separate. One might expect that in this case only free protein molecules would adsorb at the interface, but it appears that the formed layer still has a higher shear modulus than a pure protein layer, indicating the presence of complexes in the interface. Presumably after its injection in the bulk solution, pectin immediately forms complexes with protein in the bulk due to the high affinity. Eventually it could be more favourable for polysaccharides to complex with proteins at the interface, which have already lost much of their entropy, as compared to protein molecules that can freely move through the bulk solution. This hypothesis is supported by the observation that in the presence of 300 mM NaCl, at a mixing ratio of 6, the shear modulus is still higher than that of a pure protein layer, while in chapter 2 it was shown that the effect of the presence of pectin on protein adsorption kinetics disappears at an ionic strength of 80 mM. Apparently the electrostatic binding of pectin on an adsorbed protein layer at the interface can occur under circumstances where binding with protein molecules in bulk solution is no longer detectable. Presumably in this case binding is not so strong that the polysaccharide can prevent the formation of a densely packed protein layer at the interface as was observed at low ionic strength.

One might expect that in time a layer as depicted in figure 3.8B transforms into a layer as 8D, because overall bulk solution concentrations are the same in both cases; however, within the timescale of the experiments, up to 20 hours, this does not occur, indicating a thermodynamically non-equilibrium situation.

Insight in the mechanism of mixed protein/polysaccharide adsorption provides an opportunity to modulate surface rheological properties by manipulating protein polysaccharide interaction. Protein/polysaccharide mixing ratio and the order of adsorption at the interface are shown to be important parameters. A major advantage is that at the interface there is a net attraction between the protein and polysaccharide over a wider range of ionic strengths than in solution. Varying protein/polysaccharide binding affinity, e.g. by varying charge density and distribution on the protein or polysaccharide, is therefore expected to provide a broad opportunity to modulate surface rheological behaviour.

ACKNOWLEDGEMENTS

The authors thank Jan Benjamins for many valuable discussions and Hans Kosters for performing the light scattering measurements.

REFERENCES

- (1) Maroziene, A.; de Kruif, C. G., Interactions of pectin and casein micelles. *Food Hydrocolloids* **2000**, 14, (4), 391-394.
- (2) Pereyra, R.; Schmidt, K. A.; Wicker, L., Interaction and stabilization of acidified casein dispersions with low and high methoxyl pectins. *Journal of Agricultural and Food Chemistry* **1997**, 45, (9), 3448-3451.
- (3) Syrbe, A.; Bauer, W. J.; Klostermeyer, H., Polymer science concepts in dairy systems - An overview of milk protein and food hydrocolloid interaction. *International Dairy Journal* **1998**, 8, (3), 179-193.
- (4) Benichou, A.; Aserin, A.; Garti, N., Protein-polysaccharide interactions for stabilization of food emulsions. *Journal of Dispersion Science and Technology* **2002**, 23, (1-3), 93-123.
- (5) Dickinson, E., Hydrocolloids at interfaces and the influence on the properties of dispersed systems. *Food Hydrocolloids* **2003**, 17, (1), 25-39.
- (6) Einhorn-Stoll, U., Interactions of whey proteins with different pectins in O/W emulsions. *Nahrung* **1998**, 42, (3/4), 248-249.
- (7) Tokaev, E. S.; Gurov, A. N.; Rogov, I. A.; Tolstoguzov, V. B., Properties of oil/water emulsions stabilized by casein-acid polysaccharide mixtures. *Nahrung* **1987**, 31, (8), 825-834.
- (8) Ogawa, S.; Decker, E. A.; McClements, D. J., Production and characterization of O/W emulsions containing droplets stabilized by lecithin-chitosan-pectin multilayered membranes. *Journal of Agricultural and Food Chemistry* **2004**, 52, (11), 3595-3600.
- (9) Guzey, D.; Kim, H. J.; McClements, D. J., Factors influencing the production of o/w emulsions stabilized by β -lactoglobulin-pectin membranes. *Food Hydrocolloids* **2004**, 18, (6), 967.
- (10) Dickinson, E.; Pawlowsky, K., Effect of l-carrageenan on flocculation, creaming, and rheology of a protein-stabilized emulsion. *Journal of Agricultural and Food Chemistry* **1997**, 45, (10), 3799-3806.
- (11) Murray, B. S., Interfacial rheology of food emulsifiers and proteins. *Current Opinion in Colloid & Interface Science* **2002**, 7, (5-6), 426-431.
- (12) Patino, J. M. R.; Sanchez, C. C.; Nino, M. R. R.; Fernandez, M. C., Structural and dynamic properties of milk proteins spread at the air-water interface. *Journal of Colloid and Interface Science* **2001**, 242, (1), 141-151.
- (13) Dickinson, E., Adsorbed protein layers at fluid interfaces: interactions, structure and surface rheology. *Colloids and Surfaces B-Biointerfaces* **1999**, 15, (2), 161-176.
- (14) Martin, A. H.; Grolle, K.; Bos, M. A.; Cohen Stuart, M. A.; van Vliet, T., Network forming properties of various proteins adsorbed at the air/water interface in relation to foam stability. *Journal of Colloid and Interface Science* **2002**, 254, (1), 175-183.
- (15) Benjamins, J. Static and dynamic properties of proteins adsorbed at liquid interfaces. PhD, Thesis, Wageningen University, Wageningen, The Netherlands, 2000.
- (16) Lucassen-Reynders, E. H.; Fainerman, V. B.; Miller, R., Surface Dilatational Modulus or Gibbs' Elasticity of Protein Adsorption Layers. *Journal of Physical Chemistry B* **2004**, 108, (26), 9173-9176.
- (17) Dickinson, E.; Semenova, M. G.; Antipova, A. S.; Pelan, E. G., Effect of high-methoxy pectin on properties of casein-stabilized emulsions. *Food Hydrocolloids* **1998**, 12, 425-432.

- (18) Laplante, S.; Turgeon, S. L.; Paquin, P., Effect of pH, ionic strength, and composition on emulsion stabilising properties of chitosan in a model system containing whey protein isolate. *Food Hydrocolloids* **2005**, 19, (4), 721.
- (19) Baeza, R.; Sanchez, C. C.; Pilosof, A. M. R.; Patino, J. M. R., Interactions of polysaccharides with beta-lactoglobulin adsorbed films at the air-water interface. *Food Hydrocolloids* **2005**, 19, (2), 239-248.
- (20) Ducel, V.; Richard, J.; Popineau, Y.; Boury, F., Rheological interfacial properties of plant protein-arabic gum coacervates at the oil-water interface. *Biomacromolecules* **2005**, 6, (2), 790-796.
- (21) Schmitt, C.; da Silva, T. P.; Bovay, C.; Rami-Shojaei, S.; Frossard, P.; Kolodziejczyk, E.; Leser, M. E., Effect of time on the interfacial and foaming properties of beta-lactoglobulin/acacia gum electrostatic complexes and coacervates at pH 4.2. *Langmuir* **2005**, 21, (17), 7786-7795.
- (22) de Kruif, C. G.; Weinbreck, F.; de Vries, R., Complex coacervation of proteins and anionic polysaccharides. *Current Opinion in Colloid & Interface Science* **2004**, 9, (5), 340-349.
- (23) de Jongh, H. H. J.; Gröneveld, T.; de Groot, J., Mild isolation procedure discloses new protein structural properties of beta-lactoglobulin. *Journal of Dairy Science* **2001**, 84, (3), 562-571.
- (24) Daas, P. J. H.; Boxma, B.; Hopman, A. M. C. P.; Voragen, A. G. J.; Schols, H. A., Nonesterified galacturonic acid sequence homology of pectins. *Biopolymers* **2001**, 58, (1), 1-8.
- (25) Berne, B. J.; Pecora, R., *Dynamic Light Scattering: with applications to Chemistry, biology, and Physics*. 2000 ed.; General Publishing Company, Ltd.: Toronto, 1976.
- (26) van der Burgh, S.; de Keizer, A.; Cohen Stuart, M. A., Complex coacervation core micelles. Colloidal stability and aggregation mechanism. *Langmuir* **2004**, 20, (4), 1073-1084.
- (27) Benjamins, J.; Cagna, A.; Lucassen-Reynders, E. H., Viscoelastic properties of triacylglycerol/water interfaces covered by proteins. *Colloids and Surfaces A* **1996**, 114, 245-254.
- (28) Martin, A.; M., B.; Cohen Stuart, M.; Vliet, T. v., Stress-strain curves of adsorbed protein layers at the air/water interface measured with surface shear rheology. *Langmuir* **2002**, 18, 1238-1243.
- (29) Wierenga, P. A.; Kosters, H.; Egmond, M. R.; Voragen, A. G. J.; de Jongh, H. H. J., Importance of physical vs. chemical interactions in surface shear rheology. *Advances in Colloid and Interface Science* **2006**, 119, (2-3), 131.
- (30) Wierenga, P. A.; Egmond, M. R.; Voragen, A. G. J.; de Jongh, H. H., The adsorption and unfolding kinetics determines the folding state of proteins at the air-water interface and thereby the equation of state. *Journal of Colloid and Interface Science* **2006**, 299, (2), 850-857.
- (31) Cho, D.; Narsimhan, G.; Franses, E. I., Adsorption Dynamics of Native and Pentylated Bovine Serum Albumin at Air-Water Interfaces: Surface Concentration/ Surface Pressure Measurements. *Journal of Colloid and Interface Science* **1997**, 191, (2), 312.
- (32) Wierenga, P. A.; Meinders, M. B. J.; Egmond, M. R.; Voragen, A. G. J.; de Jongh, H. H. J., Quantitative description of the relation between protein net charge and protein adsorption to air-water interfaces. *Journal of Physical Chemistry B* **2005**, 109, (35), 16946-16952.
- (33) Monteux, C.; Fuller, G. G.; Bergeron, V., Shear and dilatational surface rheology of oppositely charged polyelectrolyte/surfactant microgels adsorbed at the air-water interface. Influence on foam stability. *Journal of Physical Chemistry B* **2004**, 108, (42), 16473-16482.

Adsorption of protein/polysaccharide complexes; a comparison between air/water and oil/water interfaces

Based on: Renate A. Ganzevles, Ton van Vliet, Martien A. Cohen Stuart and Harmen H.J. de Jongh in: Food Colloids; Self-Assembly and Material Science, Royal Society of Chemistry, Montreux, 2007

ABSTRACT

In chapter 2 and 3 it was shown how protein/polysaccharide interaction can be used to control adsorption kinetics and surface rheological behaviour of mixed protein/polysaccharide adsorbed layers at air/water interfaces. In this chapter surface pressure and dilatational modulus measurements as a function of time at oil/water interfaces are presented and discussed while focussing on the comparison of oil/water and air/water interfaces. Protein adsorption in the presence of polysaccharides is retarded to a similar extent (up to a factor of 300 with LMP and a factor of 10 with HMP) at oil/water and air/water interfaces. In addition to system properties (protein/polysaccharide mixing ratio, pH and ionic strength) the mechanism can be controlled by molecular properties; e.g. charge density of the polysaccharide. These parameters also affect the rheological behaviour of the adsorbed layers at oil/water interfaces, in a similar way as previously observed for air/water interfaces. Understanding the mechanism of mixed protein/polysaccharide adsorption is of great value to manipulate adsorption kinetics and surface rheological properties at both air/water and oil/water interfaces. This could help to better understand and control foam and emulsion formation and stability.

4.1 INTRODUCTION

Protein/polysaccharide interaction has been investigated in a diversity of contexts: heparin and blood coagulation¹; protection of enzymes against high pressure or temperature; enzyme substrate binding and recovery and fractionation of milk proteins. A classical example from the food industry is the use of pectin to stabilize casein micelles in acidified milk drinks. Due to electrostatic interaction negatively charged pectin molecules adsorb at the casein micelles and prevent them from acid induced aggregation by electrostatic and steric repulsion²⁻⁴. On mixing an anionic polysaccharide, like pectin, with a globular protein, four different interaction-regimes can be distinguished, depending on pH, ionic strength and mixing ratio, as described for mixtures of whey protein and arabic gum by Weinbreck, et al.⁵. (I) At neutral pH both the protein and the polysaccharide are net negatively charged and therefore co-soluble, although there can be some attractive interaction between the positively charged groups on the protein and the negatively charged polysaccharide. (II) On lowering the pH close to the iso-electric pH of the protein or below, soluble protein/polysaccharide complexes are formed at low ionic strength (less than approximately 100 mM, depending on binding affinity). (III) A further decrease of the pH leads to aggregation of the soluble complexes and subsequently complex coacervation. (IV) At pH values below 2.5 complexation can be suppressed by protonation of the acidic groups on the polysaccharide⁵.

Adsorption kinetics of proteins have been extensively studied in relation to foam- and emulsion formation. Several steps in protein adsorption have been identified⁶⁻⁸: 1) transport of the molecule to the interface by diffusion/convection, 2) adsorption to the interface and 3) possibly conformational changes once adsorbed at the interface. Large differences have been found between different proteins (e.g. β -lactoglobulin is known to quickly increase surface pressure⁹, whereas for lysozyme the process is much slower¹⁰). According to Wierenga and co-workers a kinetic barrier for protein adsorption can explain these differences; when a protein molecule approaches the air/water interface a balance between its hydrophobic exposure and net charge determines the chance by which it adsorbs^{11, 12}. Obviously all this holds for pure protein solutions; the presence of anionic polysaccharides that interact with the protein molecules affects adsorption kinetics to air/water interfaces¹³⁻¹⁵. Because protein adsorption kinetics to air/water and oil/water interfaces can be different¹⁶, also the impact of protein/polysaccharide interaction on adsorption kinetics could differ for both types of interfaces. In chapter 2 (Figure 2.6) a mechanistic model for mixed protein/polysaccharide adsorption at air/water interfaces was proposed. Retarded adsorption kinetics in the presence of polysaccharides were explained by a lower diffusion rate (due to the large hydrodynamic radius of complexes, compared to that of protein molecules) and a reduced protein mobility through the protein/polysaccharide complex.

Anionic polysaccharides can be used in combination with proteins to prevent aggregation and creaming of emulsion droplets¹⁷⁻²². However, depending on relative concentrations, polysaccharides can also decrease emulsion stability due to bridging flocculation¹³. By layer-by-layer deposition of oppositely charged proteins, polysaccharides

and surfactants on emulsion droplets^{23, 24} one can control the net charge on the droplets and enhance emulsion stability by electrostatic repulsion. Through electrostatic interaction with proteins, anionic polysaccharides that are not surface active are able to affect surface rheological properties by coadsorption^{14, 25}. Ducel and co-authors report that (oil/water-) interfacial rheological properties of plant protein-arabic gum coacervates is related to the interfacial rheological properties of the protein used²⁶. Schmitt et al. describe an effect of aging time of β -lactoglobulin/acacia gum complexes on (air/water-) surface rheology in terms of reorganisation of the complexes at the interface¹⁵. The elastic behaviour of adsorbed protein layers at the air/water or oil/water interface may affect foam and emulsion stabilizing ability²⁷. A mechanistic understanding of how surface rheological behaviour depends on parameters like charge density of the polysaccharides, protein/polysaccharide mixing ratio, ionic strength and on the order of adsorption to the interface (simultaneously or sequential) is still missing.

The aim of this chapter is to demonstrate how protein/polysaccharide interaction can be used to control both adsorption kinetics and surface rheological behaviour of mixed adsorbed layers at oil/water interfaces and which parameters are involved. The mechanism of mixed protein/polysaccharide adsorption (as proposed in chapter 2 and 3) to liquid interfaces is discussed while focussing on the comparison of air/water and oil/water interfaces.

4.2 EXPERIMENTAL

4.2.1 Materials

Acetate buffer (pH 4.5) was prepared from analytical grade chemicals and deionised water. Bovine β -lactoglobulin (β -Lg) was purified using a non denaturing method as described previously²⁸. Stock solutions of 0.2 mg/ml protein were prepared by dissolving the protein in deionised water and subsequently diluting with concentrated acetate buffer solution to a final acetate concentration of 5 mM with an ionic strength of 2 mM. The protein solutions were kept at -40 °C until further use. Two pectins with different degree of methyl esterification (DM) were used: low methoxyl pectin (LMP, DM 30; i.e. 30% of the galacturonic acid subunits is methyl esterified) and high methoxyl pectin (HMP, DM 70) supplied by CP Kelco (Lille Skensved, Denmark). Only the non-methylated galacturonic acid subunits have a free carboxyl group (weak acid, pKa ~ 4.5). Polysaccharide solutions were prepared by first wetting the powder with ethanol, than dissolving in buffer and subsequently heating at 70°C for 30 minutes. After overnight storage at 4 °C, the samples were centrifuged at 6000 g at room temperature for 10 minutes. Sunflower oil (Reddy, Vandermoortele, Roosendaal, the Netherlands) was purified by stirring it under vacuum with silicagel 60 (70-230 mesh, Merck, Germany) as described before²⁹. After performing this procedure twice, the oil was stored at -20 °C until use.

4.2.2 Dynamic light scattering

Second cumulant diffusion coefficients of β -lactoglobulin/pectin complexes were determined by dynamic light scattering³⁰, using an ALV light scattering instrument equipped with a 400 mW argon laser tuned at a wavelength of 514.5 nm, as described by van der Burgh, de Keizer

& Cohen Stuart³¹. Hydrodynamic radii were calculated according to Stokes-Einstein, assuming that the pectin molecules and the complexes adapt spherical conformation. Temperature was controlled at $23 \pm 0.3^\circ\text{C}$. Protein concentration was 0.1 g/L for all samples and pectin concentrations varied from protein/pectin mixing ratio 0 to 15 w/w.

4.2.3 Drop tensiometry

Surface tension at air/water and oil/water interface was measured as a function of time for single component and mixed solutions of protein and polysaccharide using an automated drop tensiometer (ITCONCEPT, Longessaigne, France). The setup is described in detail elsewhere³². Protein/polysaccharide mixtures were freshly prepared for each experiment and equilibrated for 30 minutes to allow formation of protein/polysaccharide complexes. Unless mentioned otherwise, protein concentration was always 0.1 g/L. Each experiment started with a clean interface of a newly formed air bubble (7 μL) or oil droplet (21 μL) in a cuvette containing the sample solution. Temperature was controlled at $22 \pm 1^\circ\text{C}$. Surface tension was determined by axisymmetric bubble shape analysis and results are presented in terms of surface pressure; $\Pi = \gamma_0 - \gamma$, where γ_0 is the air/solvent (72 mN/m) or oil/solvent (30 mN/m) interfacial tension and γ is the measured surface tension. Surface rheology measurements were performed with the same setup. By subsequent expansion and compression of the interfacial area A (amplitude in area oscillation 4%, frequency 0.1 Hz) and recording the resulting change in surface tension, dilatational modulus ϵ was calculated ($\epsilon = d\gamma/d\ln A$) and followed in time. Periods of 5 oscillations were alternated with equally long resting periods. Average dilatational moduli were measured using the last three oscillations of each period. All experiments were performed in duplicate.

4.3 ADSORPTION KINETICS

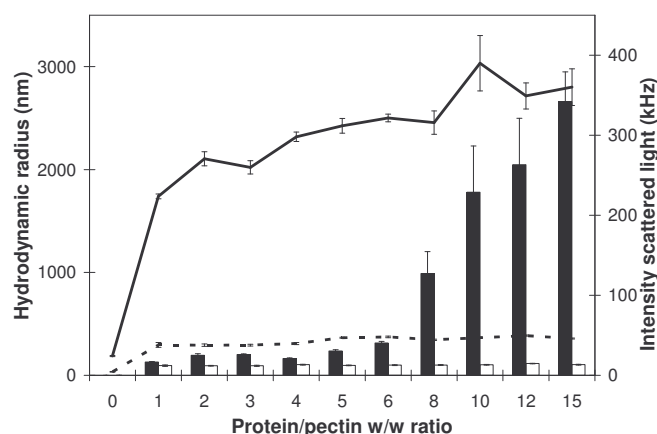


Figure 4.1: Dynamic light scattering at various β -lactoglobulin/pectin mixing ratios, protein concentration was constant at 0.1 g/L. Hydrodynamic radius (black bars) and intensity scattered light (—) for mixtures with LMP; hydrodynamic radius (open bars) and intensity scattered light (---) for mixtures with HMP; pH 4.5, 12 mM

In chapter 2 β -lactoglobulin/pectin interaction in bulk was characterised as a function of mixing ratio by dynamic light scattering (Figure 4.1). On addition of β -lactoglobulin to LMP scattered light intensity increased (Figure 4.1, mixing ratio 0 and 1 w/w) indicating formation of soluble protein/polysaccharide complexes as suggested previously⁵. On further increasing

the mixing ratio scattered light intensity slightly increases while the hydrodynamic radius remains fairly constant, indicating that the soluble complexes are gradually filled with protein. From the point where the positive charge on the protein compensates the negative charge on the polysaccharides and the net charge of the complexes approaches zero (chapter 3), the soluble complexes aggregate and phase separate. This is shown by the strongly increasing hydrodynamic radius at a mixing ratio of 8 and higher. In the case of HMP, an increase in scattered light intensity is observed as well. Based on the lower charge density of HMP as compared to LMP aggregation could be expected from a lower mixing ratio, but no aggregation is observed with this pectin.

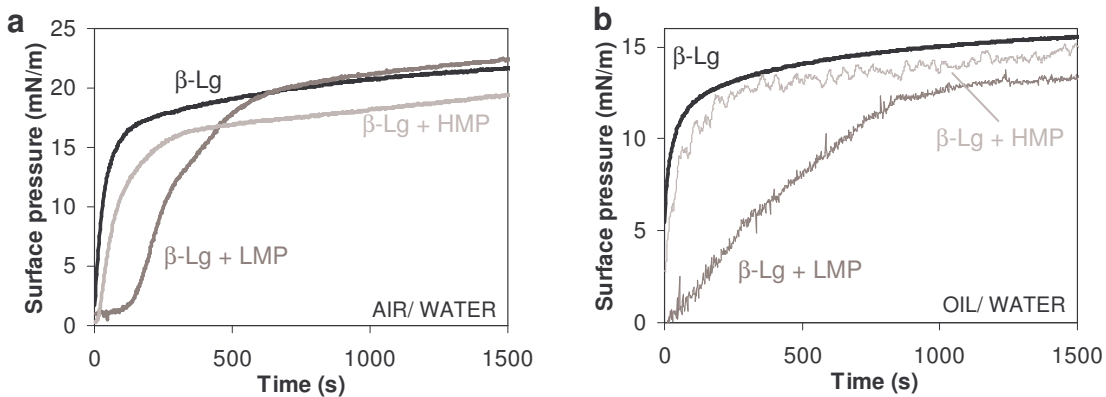


Figure 4.2: Surface pressure as a function of time for β -lactoglobulin and mixed β -lactoglobulin/LM- or HM- pectin solutions, mixing ratio 0.5 w/w at a) air/water interface and b) oil/water interface; pH 4.5, 12 mM

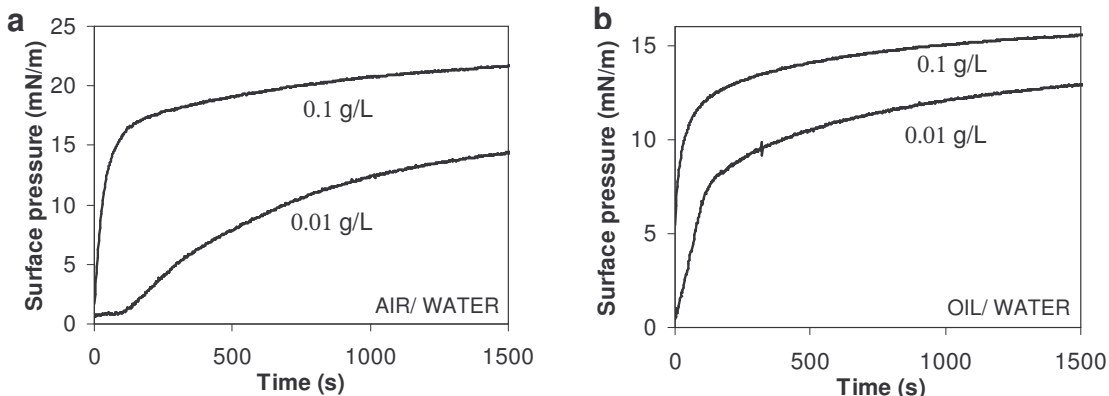


Figure 4.3: Surface pressure as a function of time for 0.1 en 0.01 g/L β -lactoglobulin solutions, at a) air/water interface and b) oil/water interface; pH 4.5, 12 mM

To study the impact of the presence of a polysaccharide on the adsorption kinetics of protein, the surface pressure was measured as a function of time for β -lactoglobulin solutions and mixed β -lactoglobulin/pectin solutions, both at the air/water interface (figure 4.2a) and at the oil/water interface (figure 4.2b). The β -lactoglobulin concentration of all samples was 0.1 g/L, and the β -lactoglobulin/pectin mixing ratio was 0.5 w/w. At these conditions the majority of the protein is present in soluble complexes with the pectin (at least 90% in case of LMP, as argued in chapter 2) as the charge on the polysaccharide is in excess (Figure 4.1). Both LMP and HMP were used to compare the effect of their different binding affinities (due to their

different charge densities) with β -lactoglobulin. Compared to proteins, the polysaccharides on their own do not give a significant increase in surface pressure at the concentrations used (less than 2 mN/m in 20000 s for a concentration of 0.05g/L, data not shown). A pure β -lactoglobulin solution demonstrates a fast increase in surface pressure at both types of interfaces. At the air/water interface the presence of LMP causes a 'lag time' before surface pressure increases. The presence of HMP causes a lag time at the air/water interface as well, but it is much shorter compared to the one with LMP. This can be explained by the lower charge density and thus lower binding affinity for β -lactoglobulin. At the oil/water interface this lag time is absent, but the increase in surface pressure is clearly delayed with LMP and to a lower extent with HMP. One could imagine that the difference in shape of the curves between the air/water interface and the oil/water interface is caused by a difference in the effect of pectin at both interfaces. However, figure 4.3 shows that the surface pressure versus time curve at the oil/water interface for a pure β -lactoglobulin solution at lower concentration also differs from the curve at the air/water interface. At the air/water interface a lag time is observed, whereas at the oil/water interface this lag time is absent and only the initial slope differs from the higher concentration. Both the adsorbed amount of protein as a function of time¹⁶ and the relation between surface pressure and adsorbed amount at the oil/water interface can differ from those at the air/water interface³³.

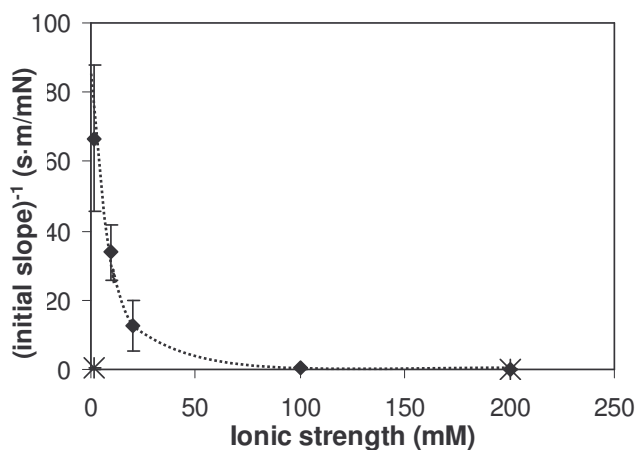


Figure 4.4: Inverse of initial slope of surface pressure versus time curves at the oil/water interface as a function of ionic strength for 2 w/w β -lactoglobulin/LMP mixtures (◆) and pure β -lactoglobulin solutions (★), β -lactoglobulin concentration 0.1 g/L; pH 4.5

Since the delay in surface pressure development as observed for the mixtures (Figure 4.2) is caused by electrostatic interaction of protein with the polysaccharide, it should reduce with increasing salt concentration. At the air/water interface it was demonstrated that the lag time indeed gradually diminished on increasing salt concentration until it completely disappeared at an ionic strength of 80 mM (chapter 2). At the oil/water interface the effect of pectin is manifested not as a lag time but as a lower initial slope of the surface pressure versus time curve. In figure 4.4 the inverse of this initial slope is plotted as a function of ionic strength for a 2 w/w β -lactoglobulin/LMP mixture and for pure β -lactoglobulin. It shows that

at the oil/water interface the effect of LMP also diminishes with increasing ionic strength and disappears at an ionic strength between 50 and 100 mM.

To get a semi-quantitative insight in the extent to which the increase in surface pressure is delayed by the polysaccharide, an apparent diffusion constant was calculated from the data for air/water interfaces. To compare adsorption kinetics, one should consider the adsorbed amount instead of the surface pressure. In lack of well defined values for the adsorbed amount of the mixed systems, only a rough calculation is made based on surface pressure and the relation between surface pressure and adsorbed amount of pure β -lactoglobulin at the air/water interface. The adsorbed amount of β -lactoglobulin at an air/water interface from where surface pressure starts to increase, Γ^* , is on the order of 1 mg/m² (data not shown). The value of Γ^* for the β -lactoglobulin/LMP mixture is on the same order of magnitude as observed from ellipsometry measurements (data not shown). Using the time at which surface pressure starts increasing, earlier defined as the 'lag time', t^* , we can roughly estimate an effective diffusion coefficient, D_{eff} , using the equation of Ward and Tordai³⁴: $\Gamma^* = 2c\sqrt{(D_{\text{eff}}t^*/\pi)}$, where c is the total protein bulk concentration. The effective diffusion coefficient for pure β -lactoglobulin obtained with this method (determined using a β -lactoglobulin concentration range of 0.002 g/L – 0.02 g/L, where a possible contribution of convection during droplet formation is relatively low) is $1 \cdot 10^{-10}$ m²/s. Also the observation that a Γ of ~1 mg/m² is reached within the first 20 seconds of an ellipsometry measurement (at the air/water interface of a sample in a Langmuir trough) at a protein bulk concentration of 0.02 g/L (chapter 8, e.g. figure 4.2a) leads to an effective diffusion constant of $1 \cdot 10^{-10}$ m²/s. This value corresponds well with the diffusion coefficient reported by Le Bon, et al.³⁵. From this it can be derived that adsorption of β -lactoglobulin is diffusion controlled and not significantly hindered by a kinetic barrier (as depicted by E in figure 2.6, chapter 2) for adsorption. Subsequently we conclude that adsorption rate to the oil/water interfaces is not significantly faster than to the air/water interface and that presumably the difference in the surface pressure versus time curves for β -lactoglobulin at air/water and oil/water interface is caused by a difference in the relation between surface pressure and adsorbed amount at both types of interfaces. A difference in this Π - Γ relation was previously suggested for BSA at air/water and tetradecane/water interface by Benjamins³³. The effective diffusion coefficient obtained for a mixture of β -lactoglobulin (0.1 g/l) and LMP (mixing ratio 2 w/w) is $3 \cdot 10^{-13}$ m²/s. The diffusion coefficient, D_{DLS} , obtained from dynamic light scattering of the complexes equals $1 \cdot 10^{-12}$ m²/s. If all β -lactoglobulin is complexed to LMP, the experimentally obtained effective diffusion coefficient should be equal to the one obtained by dynamic light scattering, since all protein diffuses as complexes in this case. However, D_{eff} appears to be about 3 times smaller than D_{DLS} . Since dynamic light scattering is biased to the larger components in a polydisperse sample³⁶ because it determines weight-averaged diffusion coefficients, it is likely that there are many smaller complexes with a much larger diffusion coefficient and hence faster adsorption kinetics. Although diffusion rate seems to play an important role, it is not likely that retarded diffusion is the only reason for a delayed increase

in surface pressure. In absence of a lag time for the oil/water interface we observe that the surface pressure for 0.1 g/L β -lactoglobulin at the oil/water interface has increased to 5 mN/m within the first second of the experiment, while for the 2 w/w β -lactoglobulin/LMP mixture it takes \sim 250 seconds before a surface pressure of 5 mN/m is reached (data not shown). Therefore the delay in surface pressure increase at the oil/water interface caused by the presence of LMP is on the same order of magnitude (\sim 300) as found for the air/water interface (assuming that possible differences in Π - Γ relation in presence and absence of pectin are small compared to this number). For HMP the delay is of the order of 10 for both types of interfaces. Although these calculations are only rough estimates, they show that the effect of the presence of pectin on protein adsorption kinetics at the air/water and oil/water interface may be comparable. When using a protein that has a kinetic barrier for adsorption, like chicken egg ovalbumin¹², the effect could be different for both types of interfaces. If the affinity of the protein differs for both interfaces, the balance of affinity of protein for the interface and for the polysaccharide may shift and different effects might come in to play.

In conclusion, β -lactoglobulin adsorption in the presence of pectin is retarded to a similar extent at air/water and oil/water interfaces. Most likely, retarded β -lactoglobulin diffusion as a result of the larger hydrodynamic radius of the β -lactoglobulin/pectin complexes contributes to the slower increase in surface pressure at both air/water and oil/water interfaces, as observed in the presence of polysaccharides. However, presumably a reduced availability of protein molecules in the complexes at the interface (Figure 2.6C, chapter 2) also plays an important role. This availability is expected to depend on the protein density (number of protein molecules per unit volume) in the complex and the mobility of the protein molecules through the complex.

4.4 SURFACE RHEOLOGY AND STRUCTURE OF ADSORBED LAYERS

If a polysaccharide in case of protein/polysaccharide complex adsorption can affect the protein density in the interface, this should be detectable by surface rheology. Presumably the protein density in the complexes in bulk depends on the protein/polysaccharide mixing ratio and with that on the net charge of the complexes. For β -lactoglobulin/LMP complexes of 0.5 w/w mixing ratio a ζ -potential of -32 ± 1 mV was measured and for mixing ratios of 2, 4 and 8 w/w -27 , -21 and -9 ± 1 mV respectively (chapter 3). The ζ -potential of the protein molecules was 0 ± 1 mV. Surface dilatational modulus at the oil/water interface of these complexes and of pure β -lactoglobulin was followed in time and plotted as a function of surface pressure (Figure 4.5a). In this way the different adsorbed layers can be compared independent of adsorption kinetics. The shape of the resulting modulus-surface pressure curves is very similar as found before for the air/water interface (chapter 3), where the minimum in dilatational modulus, depending on mixing ratio, is observed between surface pressures of 16 and 20 mN/m (data not shown). Comparison of the dilatational modulus for the different adsorbed layers at the air/water interface at a surface pressure of 20 mN/m, shows an increase with mixing ratio from \sim 25 mN/m for a mixing ratio of 2 w/w to \sim 62 mN/m for a mixing ratio of 8 w/w. A pure protein layer at the same surface pressure had a

dilatational modulus of 72 mN/m. Based on these results a schematic picture of the different layers was sketched (chapter 3, figure 3.8). The decreasing modulus with increasing negative net charge of the complexes was explained by the ability of pectin to prevent the formation of a densely packed protein layer. The fact that a resulting more diffuse layer is easily compressible, can account for the lower dilatational modulus. When the mixing ratio is such that the net charge of the complexes is close to neutral, electrostatic repulsion minimizes and a compact layer can be formed. The data for the oil/water interface show qualitatively the same trend as observed for the air/water interface; when comparing the dilatational modulus at the oil/water interface for the different mixing ratios at a surface pressure of 15 mN/m, it increases with increasing mixing ratio (Figure 4.5a; the measurements were terminated before the dilatational modulus reached a steady state value). The curve for the highest mixing ratio (4 w/w), which has the lowest net charge, comes closest to the curve for the pure protein layer.

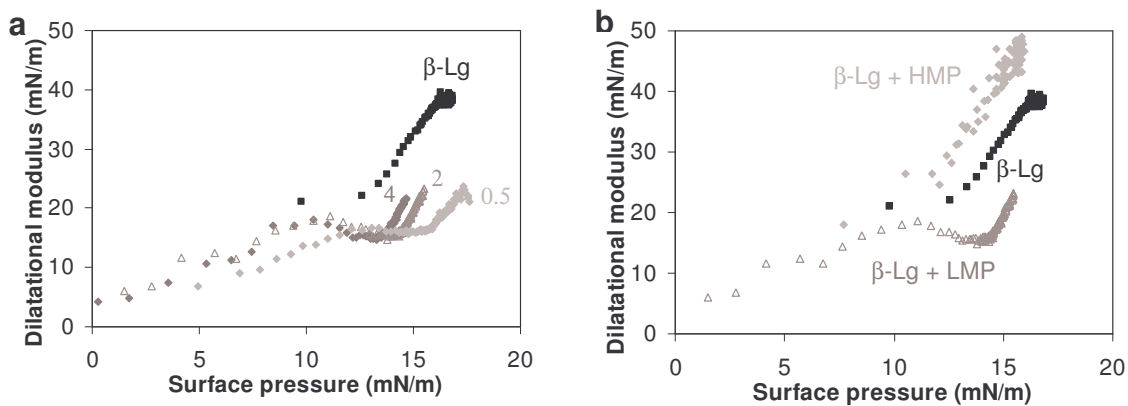


Figure 4.5: Dilatational modulus as a function of surface pressure at the oil/water interface as a function of time for a) pure β -lactoglobulin and β -lactoglobulin/LMP mixtures at different mixing ratios (as indicated) and b) pure β -lactoglobulin and β -lactoglobulin/(LM- or HM-) pectin mixtures, w/w ratio 2; for all samples the protein concentration was 0.1 g/L, pH 4.5 and I 2 mM

In figure 4.5b the effect of the two pectins with different charge densities on dilatational modulus is compared at a mixing ratio of 2 w/w. Surprisingly, whereas the presence of LMP decreases the dilatational modulus, in the presence of HMP the dilatational modulus is higher - both compared to the pure protein layer. The same trend was observed at the air/water interface (not shown). A possible explanation is that since HMP has a lower charge density than LMP, and therefore the binding of protein molecules to HMP is weaker, HMP is not able to prevent the protein molecules from forming a dense protein layer at the interface. An adsorbed complex layer with HMP could therefore quickly transform into a layer like D in figure 3.8 (chapter 3); a dense protein layer, reinforced by coadsorption of HMP, and possibly with that more β -lactoglobulin as compared to a pure protein layer. This hypothesis is supported by the observation that when a protein layer was formed at the air/water interface from a pure protein solution and subsequently LMP was injected into the bulk solution, the dilatational modulus increased to a value higher than that of a pure protein layer (chapter 3). Apparently, when LMP is present from the beginning of adsorption, it can prevent the

formation of a dense protein layer at the air/water (and presumably also at the oil/water) interface, whereas it can reinforce a protein layer formed previous to LMP addition. For the air/water interface the effect of different mixing ratios with LMP as well as the effect of the sequence of adsorption (chapter 3, simultaneous versus sequential adsorption) have been shown to affect surface shear rheology even stronger than dilatational rheology. Since the build-up of the mixed layers seems to be at least qualitatively the same at air/water and oil/water interfaces, with respect to adsorption kinetics and surface dilatational rheology, also the surface shear rheology at the oil/water interface is expected to depend strongly on mixing ratio and adsorption sequence.

4.5 CONCLUDING REMARKS

Protein adsorption in the presence of polysaccharides is retarded to a similar extent (up to a factor of 300 with LMP and a factor of 10 with HMP) at air/water and oil/water interfaces. Small changes in ionic strength or pH can change protein adsorption kinetics by changing the amount of complexed/free protein or the binding strength. In addition to system properties (protein/polysaccharide mixing ratio, ionic strength and pH), the mechanism can be controlled by molecular properties; charge density of the polysaccharide (and presumably also by charge density of the protein).

Similar to what was observed for air/water interfaces, also the rheological behaviour of the adsorbed layers at oil/water interfaces are affected by mixing ratio and protein/polysaccharide binding affinity (and thus polysaccharide charge density, pH and ionic strength). Understanding the mechanism of mixed protein/polysaccharide adsorption is of great value to manipulate adsorption kinetics and surface rheological properties at both air/water and oil/water interfaces. This could help to better control foam and emulsion formation and stability.

ACKNOWLEDGEMENTS

The authors thank Jan Benjamins for many valuable discussions and Frouke Duijzer for performing surface tension and surface rheological measurements at oil/water interfaces.

REFERENCES

- (1) Lee, Y. C.; Lee, R. T., Carbohydrate-Protein Interactions - Basis of Glycobiology. *Accounts of Chemical Research* **1995**, 28, (8), 321-327.
- (2) Pereyra, R.; Schmidt, K. A.; Wicker, L., Interaction and stabilization of acidified casein dispersions with low and high methoxyl pectins. *Journal of Agricultural and Food Chemistry* **1997**, 45, (9), 3448-3451.
- (3) Syrbe, A.; Bauer, W. J.; Klostermeyer, H., Polymer science concepts in dairy systems - An overview of milk protein and food hydrocolloid interaction. *International Dairy Journal* **1998**, 8, (3), 179-193.
- (4) Maroziene, A.; de Kruif, C. G., Interactions of pectin and casein micelles. *Food Hydrocolloids* **2000**, 14, (4), 391-394.
- (5) Weinbreck, F.; de Vries, R.; Schrooyen, P.; de Kruif, C. G., Complex coacervation of whey proteins and gum arabic. *Biomacromolecules* **2003**, 4, (2), 293-303.
- (6) MacRitchie, F.; Alexander, A. E., Kinetics of Adsorption of Proteins at Interfaces.1. Role of Bulk Diffusion in Adsorption. *Journal of Colloid Science* **1963a**, 18, (5), 453-457.

- (7) MacRitchie, F.; Alexander, A. E., Kinetics of Adsorption of Proteins at Interfaces.2. Role of Pressure Barriers in Adsorption. *Journal of Colloid Science* **1963b**, 18, (5), 458-463.
- (8) Graham, D. E.; Phillips, M. C., Proteins at Liquid Interfaces.1. Kinetics of Adsorption and Surface Denaturation. *Journal of Colloid and Interface Science* **1979**, 70, (3), 403-414.
- (9) Paulsson, M.; Dejmek, P., Surface-Film Pressure of Beta-Lactoglobulin, Alpha-Lactalbumin and Bovine Serum-Albumin at the Air-Water-Interface Studied by Wilhelmy Plate and Drop Volume. *Journal of Colloid and Interface Science* **1992**, 150, (2), 394-403.
- (10) Tripp, B. C.; Magda, J. J.; Andrade, J. D., Adsorption of Globular-Proteins at the Air/Water Interface as Measured Via Dynamic Surface-Tension - Concentration-Dependence, Mass-Transfer Considerations, and Adsorption-Kinetics. *Journal of Colloid and Interface Science* **1995**, 173, (1), 16-27.
- (11) Wierenga, P. A.; Meinders, M. B. J.; Egmond, M. R.; Voragen, A. G. J.; de Jongh, H. H. J., Quantitative description of the relation between protein net charge and protein adsorption to air-water interfaces. *Journal of Physical Chemistry B* **2005**, 109, (35), 16946-16952.
- (12) Wierenga, P. A.; Meinders, M. B. J.; Egmond, M. R.; Voragen, F. A. G. J.; de Jongh, H. H. J., Protein exposed hydrophobicity reduces the kinetic barrier for adsorption of ovalbumin to the air-water interface. *Langmuir* **2003**, 19, (21), 8964-8970.
- (13) Dickinson, E.; Pawlowsky, K., Effect of l-carrageenan on flocculation, creaming, and rheology of a protein-stabilized emulsion. *Journal of Agricultural and Food Chemistry* **1997**, 45, (10), 3799-3806.
- (14) Baeza, R.; Sanchez, C. C.; Pilosof, A. M. R.; Patino, J. M. R., Interactions of polysaccharides with beta-lactoglobulin adsorbed films at the air-water interface. *Food Hydrocolloids* **2005**, 19, (2), 239-248.
- (15) Schmitt, C.; da Silva, T. P.; Bovay, C.; Rami-Shojaei, S.; Frossard, P.; Kolodziejczyk, E.; Leser, M. E., Effect of time on the interfacial and foaming properties of beta-lactoglobulin/acacia gum electrostatic complexes and coacervates at pH 4.2. *Langmuir* **2005**, 21, (17), 7786-7795.
- (16) Sengupta, T.; Damodaran, S., Role of dispersion interactions in the adsorption of proteins at oil-water and air-water interfaces. *Langmuir* **1998**, 14, (22), 6457-6469.
- (17) Dickinson, E., Hydrocolloids at interfaces and the influence on the properties of dispersed systems. *Food Hydrocolloids* **2003**, 17, (1), 25-39.
- (18) Benichou, A.; Aserin, A.; Garti, N., Protein-polysaccharide interactions for stabilization of food emulsions. *Journal of Dispersion Science and Technology* **2002**, 23, (1-3), 93-123.
- (19) Moreau, L.; Kim, H. J.; Decker, E. A.; McClements, D. J., Production and characterization of oil-in-water emulsions containing droplets stabilized by beta-lactoglobulin-pectin membranes. *Journal of Agricultural and Food Chemistry* **2003**, 51, (22), 6612-6617.
- (20) Laplante, S.; Turgeon, S. L.; Paquin, P., Effect of pH, ionic strength, and composition on emulsion stabilising properties of chitosan in a model system containing whey protein isolate. *Food Hydrocolloids* **2005**, 19, (4), 721.
- (21) Einhorn-Stoll, U., Interactions of whey proteins with different pectins in O/W emulsions. *Nahrung* **1998**, 42, (3/4), 248-249.
- (22) Tokaev, E. S.; Gurov, A. N.; Rogov, I. A.; Tolstoguzov, V. B., Properties of oil/water emulsions stabilized by casein-acid polysaccharide mixtures. *Nahrung* **1987**, 31, (8), 825-834.
- (23) Ogawa, S.; Decker, E. A.; McClements, D. J., Production and characterization of O/W emulsions containing droplets stabilized by lecithin-chitosan-pectin multilayered membranes. *Journal of Agricultural and Food Chemistry* **2004**, 52, (11), 3595-3600.
- (24) Guzey, D.; Kim, H. J.; McClements, D. J., Factors influencing the production of o/w emulsions stabilized by β -lactoglobulin-pectin membranes. *Food Hydrocolloids* **2004**, 18, (6), 967.
- (25) Dickinson, E.; Semenova, M. G.; Antipova, A. S.; Pelan, E. G., Effect of high-methoxy pectin on properties of casein-stabilized emulsions. *Food Hydrocolloids* **1998**, 12, 425-432.

- (26) Ducel, V.; Richard, J.; Popineau, Y.; Boury, F., Rheological interfacial properties of plant protein-arabic gum coacervates at the oil-water interface. *Biomacromolecules* **2005**, 6, (2), 790-796.
- (27) Murray, B. S., Interfacial rheology of food emulsifiers and proteins. *Current Opinion in Colloid & Interface Science* **2002**, 7, (5-6), 426-431.
- (28) de Jongh, H. H. J.; Gröneveld, T.; de Groot, J., Mild isolation procedure discloses new protein structural properties of beta-lactoglobulin. *Journal of Dairy Science* **2001**, 84, (3), 562-571.
- (29) Smulders, P. E. A., *Formation and stability of emulsions made with proteins and peptides*. Thesis, Wageningen University, Wageningen, The Netherlands, 2000.
- (30) Berne, B. J.; Pecora, R., *Dynamic Light Scattering: with applications to Chemistry, biology, and Physics*. 2000 ed.; General Publishing Company, Ltd.: Toronto, 1976.
- (31) van der Burgh, S.; de Keizer, A.; Cohen Stuart, M. A., Complex coacervation core micelles. Colloidal stability and aggregation mechanism. *Langmuir* **2004**, 20, (4), 1073-1084.
- (32) Benjamins, J.; Cagna, A.; Lucassen-Reynders, E. H., Viscoelastic properties of triacylglycerol/water interfaces covered by proteins. *Colloids and Surfaces A* **1996**, 114, 245-254.
- (33) Benjamins, J. Static and dynamic properties of proteins adsorbed at liquid interfaces. PhD, Thesis, Wageningen University, Wageningen, The Netherlands, 2000.
- (34) Ward, A. F. H.; Tordai, L., Time-Dependence of Boundary Tensions of Solutions.1. The Role of Diffusion in Time-Effects. *Journal of Chemical Physics* **1946**, 14, (7), 453-461.
- (35) Le Bon, C.; Nicolai, T.; Kuil, M. E.; Hollander, J. G., Self-diffusion and cooperative diffusion of globular proteins in solution. *Journal of Physical Chemistry B* **1999**, 103, (46), 10294-10299.
- (36) Axelos, M. A. V.; Lefebvre, J.; Thibault, J. F., Conformation of a low methoxyl citrus pectin in aqueous solution. *Food Hydrocolloids* **1987**, 1, (5/6), 569-570.

Structure of mixed β -lactoglobulin/pectin adsorbed layers at air/water interfaces; a spectroscopy study

Renate A. Ganzevles, Remco Fokkink, Ton van Vliet, Martien A. Cohen Stuart
and Harmen H.J. de Jongh

ABSTRACT

As based on surface rheological behaviour and described in an earlier publication, two factors appeared to be important for the functional behaviour of mixed protein/polysaccharide adsorbed layers at air/water interfaces; protein/polysaccharide mixing ratio and the formation history of the layers. Complexes of β -lactoglobulin (positively charged at pH 4.5) and low methoxyl pectin (negatively charged) were formed at two different mixing ratios, chosen such that negatively charged complexes and nearly neutral complexes were formed. Neutron reflection showed that adsorption of negative complexes leads to more diffuse layers at the air/water interface than adsorption of neutral complexes. Besides adsorption of protein/polysaccharide complexes (simultaneous adsorption), a mixed layer can also be formed by adsorption of a pure protein layer and subsequent adsorption of protein/polysaccharide complexes to this previously formed protein layer (sequential adsorption). Although bulk concentrations were the same, adsorbed layer density profiles of simultaneously and sequentially formed layers were persistently different, as shown by neutron reflection. Time Resolved Fluorescence Anisotropy showed that the mobility of protein molecules at an air/water interface is hampered by the presence of pectin. This hampered mobility of protein through a complex layer could account for differences observed in density profiles (and surface rheological behaviour) of simultaneously and sequentially formed mixed layers. These insights substantiated previously proposed organisations of the different adsorbed layers based on surface rheological data.

5.1 INTRODUCTION

A combination of proteins and polysaccharides is often used for stabilisation of foams and emulsions, for instance in food- or pharmaceutical applications. Non-surface-active anionic polysaccharides like pectin, carrageenan, and dextran sulphate have been reported to affect surface rheological properties by interaction with protein adsorbed at interfaces^{1, 2}. Not only surface rheological properties, but also the net charge and the thickness of adsorbed layers are affected by co-adsorption of anionic polysaccharides^{3, 4}. An increased net charge and an increased layer thickness at the oil/water interface provides, respectively, electrostatic and steric repulsion between emulsion droplets⁵⁻⁸. Because emulsion stability is increased due to the latter effects, foam stability may be enhanced by similar effects at the air/water interface⁹. In a chapter 3 we discussed surface rheological measurements on several protein and mixed protein/polysaccharide adsorbed layers at air/water interfaces. On the basis of these data, we proposed the following hypothetical organisations of the various layers (Figure 5.1).

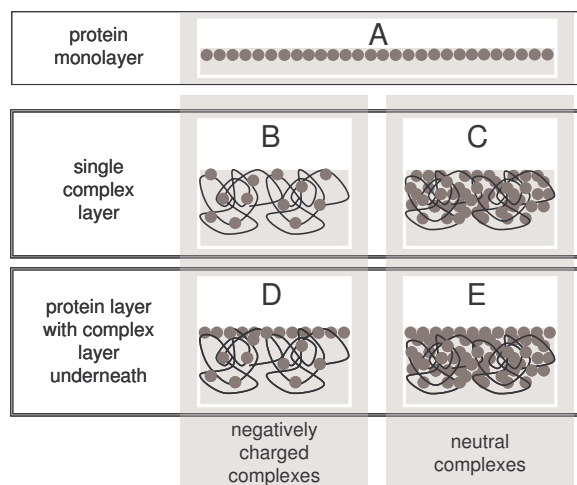


Figure 5.1: Schematic representation of different adsorbed layers at the air/water interface A: protein monolayer, B and C: mixed layers from simultaneous adsorption where B is from negatively charged complexes and C from net neutral complexes, D and E: complexes adsorbed at previously formed protein layer where D are negatively charged complexes and E net neutral complexes.

Two factors determine the functional behaviour of the adsorbed layers: (i) the net charge of the protein/polysaccharide complexes and (ii) the formation history of the layers. Negatively charged protein/polysaccharide complexes form adsorbed layers (Figure 5.1B) with lower dilatational modulus than a pure protein layer (1A). It was suggested that the presence of an excess of anionic polysaccharide is able to prevent the formation of a dense protein layer at the air/water interface. A layer formed from neutral protein polysaccharide complexes had a similar dilatational modulus as a pure protein layer, while its surface shear modulus was much higher than that of the pure protein layer. This indicated that dense and thick layers may be formed from neutral complexes (1C). When mixed layers were prepared in an alternative way, by sequential adsorption, a dense adsorbed protein layer could be formed before the polysaccharide was introduced: adsorption of the polysaccharide, or protein/polysaccharide complexes, to a previously formed protein layer increased both the dilatational and surface

shear modulus (1D and E). Although final protein and polysaccharide concentrations in the bulk solution were the same in 1B and 1D, surface rheological behaviour suggested that even after 20 hours, the density of layer B was still lower than that of layer D. This history dependent behaviour suggested that the layer structures may not quickly reorganise to a thermodynamically equilibrium situation. This model is, however, based on interpretation of system properties and thus a more molecular substantiation is lacking.

Specular neutron reflectivity may give insight in the structure (layer thickness and density profile) of adsorbed layers at air/water interfaces by providing scattering length density profiles normal to the interface at Angstrom resolution. An advantage of the technique is that it is possible to vary the contrast between the protein and the solvent by varying the H₂O/D₂O ratio. Simultaneous fitting of measurements performed on the same system at two different solution contrasts yields more reliable fit results; with this contrast variation technique a detailed density profile of the layer can be obtained¹⁰.

Time resolved fluorescence anisotropy (TRFA) has proven to be a useful tool to probe mobility of protein molecules at an air/water interface¹¹. With this technique fluorescently-labelled protein molecules (either free in solution or complexed with polysaccharide) are adsorbed to an air/water interface. Subsequently an excitation pulse of polarised light is aimed at the interface. Labels parallel to the polarisation angle are preferentially excited. After the excitation pulse, the anisotropy (which is - in 2D experiments as these - equal to the polarisation) of emitted light was followed during the lifetime of the label. Emitted light is polarised unless the labels (or the labelled protein molecules) have reoriented before emission takes place (within the lifetime of the fluorophore). Hence, anisotropy decay in time gives information about rotational mobility of protein molecules. Changes in protein mobility at the interface as a result of the presence of polysaccharide may provide insight in the molecular interactions and thus the structural organisation.

The combination of thicknesses and density profiles of the different layers to be obtained by neutron reflection and the mobility of protein molecules in these layers to be determined by TRFA may elucidate the molecular structure of mixed protein/polysaccharide adsorbed layers at air/water interfaces. The aim of this work is to validate the hypothesised mixed layer structures (as shown in figure 5.1), depending on protein/polysaccharide mixing ratio and the sequence of adsorption to the air/water interface.

5.2 MATERIALS AND METHODS

5.2.1 Materials

Bovine β -lactoglobulin was purified using a non-denaturing method as described previously¹². Low methoxyl pectin was supplied by CP Kelco (Lille Skensved, Denmark). The degree of methylation is 30.4 % (the non-methylated galacturonic acid monomers possess a free carboxyl group) and the uronic acid content is 78.5 %¹³. The average molar mass (M_n) is 1.5·10⁵ g/mol, the polydispersity (M_w/M_n) 2.4 (chapter 2) and the pKa ~ 4.5 (based on proton titration curves, not shown). Pectin solutions in H₂O (deionised water, Barnstead EASYpure UV, USA) and in D₂O (99 atom %, Sigma-Aldrich) were prepared by slowly dispersing the

powder on the surface of the thoroughly stirred (magnetic stirrer) and heated (~50°C) H₂O/D₂O and subsequently heating at 70°C for 30 minutes. After overnight storage at 35°C, the samples were centrifuged at 6000g for 10 minutes and stored at 4°C until further use. Solubility of pectin in H₂O and D₂O did not differ more than 10% as measured by an automated colorimetric m-hydroxydiphenyl method^{14, 15}. For the samples in Null Reflecting Water (NRW) stock solutions in H₂O and D₂O were mixed to 8.73 w/w % (corresponding to NRW at 22°C) D₂O in H₂O and stored overnight at 4°C to equilibrate H/D exchange ratio between pectin and solvent. Protein stock solutions were prepared by dissolving the freeze dried material in D₂O and NRW (pH after dissolution ~6.8) and storing overnight to equilibrate H/D exchange ratio between the protein and solvent. Protein solubility in D₂O did not deviate more than 2% compared to solubility in H₂O, as measured by UV spectrophotometry (at 280 nm, assuming that molar extinction coefficient in D₂O and H₂O are equal). Acetate buffers (5 mM acetate, I 2 mM) were prepared from analytical grade acetic acid (Merck, Germany) and deionised water/D₂O. The pH was adjusted to 4.5 for the NRW buffer, using concentrated NaOH and to 4.1 (which is equivalent to pD 4.5¹⁶) for the D₂O buffer using concentrated NaOH in D₂O. After dilution with buffer and mixing, protein/polysaccharide samples were equilibrated for 30 min before use in order to allow protein/polysaccharide complex formation to occur.

5.2.2 Neutron reflection

Neutron reflection measurements were performed on the white beam reflectometer SURF at ISIS (Didcot, UK) using a range of incident wavelengths (λ) of 0.5 to 6.5 Å which, in combination with varying glancing angle of incidence (θ) between 0.3° and 1.5°, covers a range of scattering vectors (Q_z , $Q_z = (4\pi/\lambda) \sin \theta$) between 0.01 and 0.66 Å⁻¹. The measuring procedure was similar to that described before by Brown et al.¹⁷. The beam intensity was calibrated with respect to the reflectivity of pure D₂O. A flat background (as determined by extrapolation to high values of Q_z) was subtracted from RQ⁴ data. Depending on beam intensity, total measuring times (sum of two or three angles of incidence) were approximately 70 minutes for samples in D₂O and 140 minutes for samples in NRW. Measurements were done in a thermostated (22±1 °C) teflon trough mounted on an antivibration bench and equipped with a movable barrier which separates the surface into two sections, one for introduction of the sample and one for collection of data. After filling the trough, the area of the measuring compartment was expanded by at least a factor of 5 to start with a clean interface. For the sequential protein/polysaccharide adsorbed layers, polysaccharide was injected with a (5 mL) pipette underneath the interface ~2 hours after the formation of a protein layer from a pure protein solution commenced. The sample was carefully mixed by three times flushing the pipette with some of the sample close to the bottom of the trough. It was ensured that the troughs were cleaned well between measurements and that the adsorbed protein layers were not distorted upon injection of polysaccharide by measuring surface tension (Wilhelmy plate tensiometer, NIMA technology Ltd, England) before and during the experiments. All samples were measured at two contrasts: namely in NRW and in D₂O. Negatively charged complexes as referred to in the text, prepared from a 2 w/w

β -lactoglobulin/pectin mixture, typically have a ζ -potential of -27 mV (chapter 3). Complexes formed from a 6 w/w mixture have a ζ -potential of -14 mV (chapter 3) and are referred to as neutral complexes (although they are not completely neutral, mixing ratio is close to the transition point at 7 w/w where complexes become insoluble). Samples (Table 5.1) are labelled corresponding to their hypothesised layer structures as presented in figure 5.1.

Table 5.1: Overview of samples as measured with neutron reflection, pH was 4.5 and 12 mM. Samples are labelled corresponding to their hypothesised layer structures as presented in figure 5.1.

sample	β -lactoglobulin concentration (g/L)	pectin concentration (g/L)	complex charge	order of adsorption
A	0.1	-	-	-
B	0.1	0.050	negative	simultaneous
C	0.1	0.017	neutral	simultaneous
D	0.1	0.050	negative	sequential
E	0.1	0.017	neutral	sequential

Neutron reflectivity profiles were analysed by means of the optical matrix formalism described before^{17, 18}. The software calculates reflectivity from a given starting point of adsorbed layer thicknesses and densities at an interface and uses a least-square-method to compare the calculations to the data and arrive at a final model. Sets of two reflectivity profiles of one sample measured in the two different contrasts (D₂O and NRW) were always fitted simultaneously. This simultaneous fitting procedure reduces non-uniqueness of the fit: fitting one spectrum with one contrast may give multiple solutions of layer thickness due to lack of phase information. The combination of two contrasts reduces the number of possible solutions. The pure protein films (to avoid confusion the word ‘film’ is used for an adsorbed layer as a whole and the word ‘layer’ is reserved for the layers in the fits) were fitted to a single-layer model. The adjustable parameters were: thickness and the scattering length density (SLD) of the adsorbed layer, air-film roughness, film-solvent roughness and solvent SLD. Of these parameters only SLD of the layer and the solvent were allowed to differ between the two contrasts. The mixed protein/polysaccharide films were fitted to a two-layer model with the air-film roughness constrained to 4 Å and second-layer-solvent roughness constrained to 50 Å; again only SLD of the layer and the solvent were allowed to differ between the two contrasts. The advantage of the measurements in D₂O is that not only the adsorbed material but also the solvent reflects neutrons, leading to a high reflected intensity over a larger Q_z-range. This makes the measurement more sensitive to layer thicknesses and mass distribution over the thickness of the film¹⁹. In the case of NRW, reflected light intensity may be low, but all reflection is due to adsorbed material at the interface. Therefore we chose to use D₂O data to guide the fitting procedure to reliable layer thicknesses and to get information on adsorbed amounts from the NRW fit parameters.

5.2.3 Time Resolved Fluorescence Anisotropy

For the time-resolved fluorescence anisotropy (TRFA) measurements, β -lactoglobulin was labelled with an N-hydroxysuccinimidyl ester of acridone 14, according to the ‘Molecular Probes’ protocol for labelling of proteins with amine-reactive probes¹¹. After removal of the

unreacted label, the average degree of modification was 1 mol of fluorophore per mol β -lactoglobulin, as determined by comparing fluorophore concentration with protein concentration; the first was obtained from absorbance at its absorbance maximum 413 nm and the second was obtained from absorbance (in the range 196-260 nm). The native conformation of the protein was not affected by the modification as could be concluded from far-UV circular dichroism (secondary structure, data not shown) and tryptophan fluorescence (tertiary structure, data not shown).

TRFA measurements were carried out using mode-locked continuous wave lasers for excitation (at 390 nm) and time-correlated single photon counting (at 430 nm) as the detection technique²⁰. The 2D-anisotropy reflection mode setup that enables measuring TRFA at an air/water interface of a sample in a Langmuir trough has been described in detail elsewhere^{11, 21}. Acetate buffer solution (5 mM, pH 4.5) was poured in the Langmuir trough after which concentrated stock solutions of (pectin and) labelled β -lactoglobulin were injected to a protein concentration of 0.03 g/L, and for the mixture a to protein/polysaccharide w/w ratio of 4. Complexes formed at this ratio are negatively charged (ζ -potential -21 mV, chapter 3), but somewhat less than sample B as used for neutron reflection (ζ -potential -27 mV). This mixture will therefore be referred to as B'. By adjusting the height of the interface to the position where a maximum in anisotropy was detected, it was ensured that the focus was in the interface. Measurements were performed at room temperature.

The total fluorescence $I(t)$ is the sum of the parallel $I_{\parallel}(t)$ and perpendicular $I_{\perp}(t)$ components relative to the polarisation direction of the exciting beam. The total fluorescence anisotropy $r(t)$ is determined from $I_{\parallel}(t)$ and $I_{\perp}(t)$ by $r(t) = \frac{I_{\parallel}(t) - I_{\perp}(t)}{I_{\parallel}(t) + I_{\perp}(t)}$. Total

fluorescence and anisotropy decay curves were analysed using the TRFA Data Processing Package of the Scientific Software Technologies Centre (Belarusian State University, Minsk, Belarus)^{11, 21}. The software simultaneously retrieves N fluorescence lifetimes (τ_i) with their relative contributions (α_i) from the total fluorescence and the instrumental response function $E(t)$, using $I(t) = E(t) \sum_{i=1}^N \alpha_i e^{-t/\tau_i}$ and M anisotropy correlation times (ϕ_j) with their relative contributions (β_j), using $r(t) = \sum_{j=1}^M \beta_j e^{-t/\phi_j}$. The software was used in an iterative

way; data were first fitted with the infinite anisotropy (the remaining anisotropy after the fluorescence of the labels has extinguished, r_{∞}) forced at 0. Afterwards the fluorescence lifetimes and contributions were fixed, r_{∞} released and other parameters reset to the default starting parameters. By subsequent restarting of the fitting procedure it was determined whether a fraction of initial anisotropy was retained at the end of the measuring time. The pure protein data were fitted with three fluorescence ($N=3$) and two anisotropy components ($M=2$). For the mixture an additional fluorescence component ($N=4$) was necessary to satisfactorily fit the data. The smallest fluorescence lifetime and anisotropy correlation time of each fit was always of the order of 1 to 3 photon counts and were therefore attributed to

scattering during the first few counts (during ~ 0.06 ns). These components were therefore disregarded in the interpretation of the data.

5.3 RESULTS

5.3.1 Neutron reflection measurements

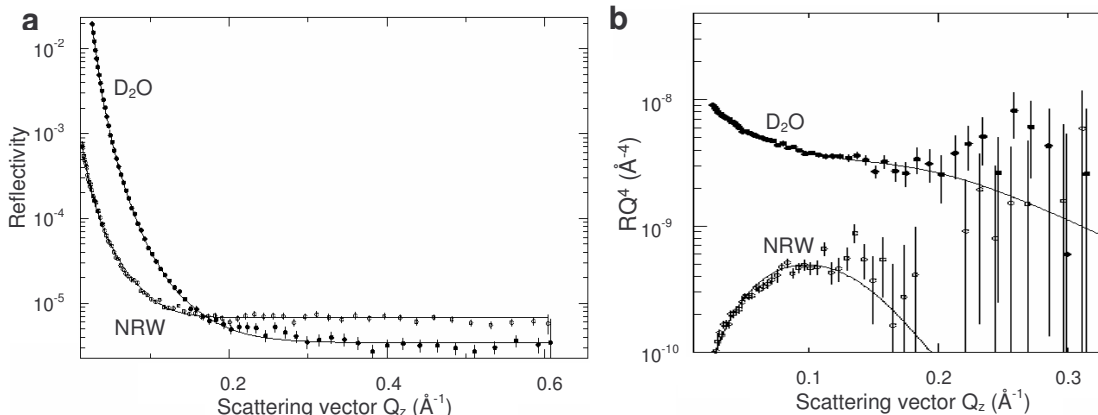


Figure 5.2: Typical example of a) (log) reflectivity data in D_2O and in NRW simultaneous fitted; lines represent the fits b) same as a but plotted as RQ^4 to illustrate the quality of the fits. The sample was a mixed β -lactoglobulin/pectin film formed from negatively charged complexes (sample B). The β -lactoglobulin concentration was 0.1 g/L, pH 4.5 and I 2mM.

Neutron reflectivity profiles of mixed β -lactoglobulin/pectin layers were measured and subsequently fitted to get information on layer thickness and layer densities. To avoid confusion we use the word ‘film’ for an adsorbed layer as a whole and reserve the word ‘layer’ for the layers used in the fits. Figure 5.2a shows a typical example of a mixed β -lactoglobulin/pectin film measured both in D_2O and in NRW. These two spectra were fitted simultaneously using a two-layer model; lines through the data represent the fits. In figure 5.2b the same data are plotted as RQ^4 to illustrate the quality of the fits¹⁷.

5.3.2 Pure protein film (sample A)

Before considering mixed protein/polysaccharide films in detail, first the pure protein adsorbed film (sample A) will be discussed. It should be mentioned that β -lactoglobulin adsorption kinetics in D_2O were up to 3 times slower than that in H_2O , as was observed with ellipsometry measurements (data not shown). A reduced adsorption rate as shown before for different proteins by Grunwald and coworkers²² was attributed to stronger hydrogen bonding in D_2O . This may reduce the exposed hydrophobicity on the protein. For the mixed protein/polysaccharide films the adsorption kinetics in D_2O were only a factor of 1.5-2 slower than in H_2O . It was tried to match aging times (time between the onset of adsorption to a clean interface and the actual measurement) to adsorption kinetics in D_2O and in NRW, but due to practical limitations this was not always possible. However, since SLD is allowed to differ between NRW and D_2O , adsorbed amount is also free to differ between the two contrasts.

Figure 5.3 shows volume fraction profiles of β -lactoglobulin adsorbed films in NRW, obtained by fitting with a single layer model. The thin line is a 75 minutes aged film in NRW

(which was fitted with a 30 minutes aged film measured in D₂O) and the thick line a 6.5 hours old film in NRW (fitted with a 12 hours old film in D₂O). The density of the film slightly increased with aging time of the interface, indicating an increasing amount of protein at the interface in time. The major part of adsorption occurred within the first hour. The thickness found for the adsorbed β -lactoglobulin film (~4 nm) corresponds with the diameter of β -lactoglobulin dimers in solution²³ and thus with a β -lactoglobulin monolayer. Similar values for the thickness of a β -lactoglobulin adsorbed film have been found by others²⁴. Moreover, the total adsorbed amount of β -lactoglobulin (after 6.5 hours in NRW), 3.2 mg/m² corresponds with ellipsometry data (3.4 mg/m² after 3.5 hours in water, unpublished results).

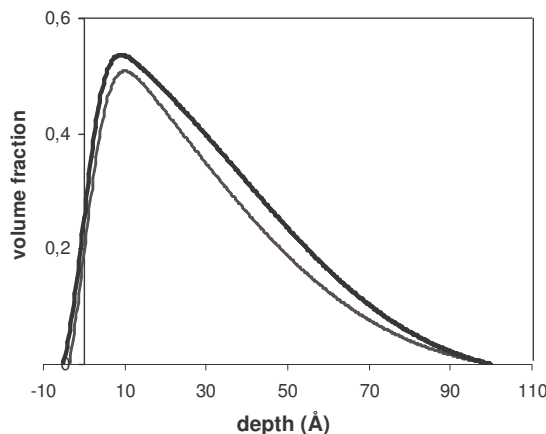


Figure 5.3: Fitted volume fraction profiles for sample A, pure β -lactoglobulin in NRW (thin line after 75 minutes, thick line after 6.5 hours), β -lactoglobulin concentration was 0.1 g/L, pH 4.5 and I 2 mM.

5.3.3 Effect of complex net charge on layer density profile (sample B and C)

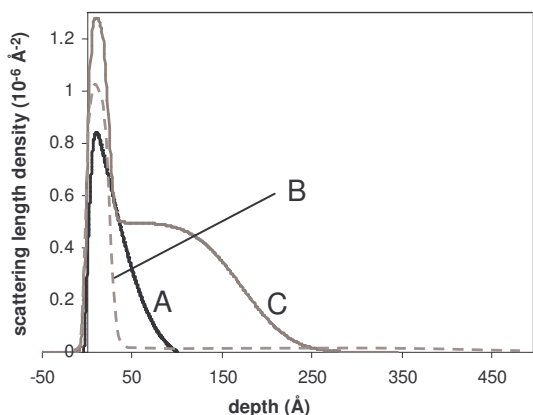


Figure 5.4: Fitted scattering length density profile in NRW for sample A after 75 minutes (pure β -lactoglobulin, solid black), sample B after ~2 hours (negatively charged β -lactoglobulin/pectin complexes, dashed grey) and sample C after ~2 hours (neutral complexes solid grey), β -lactoglobulin concentration was 0.1 g/L, pH 4.5 and I 2 mM.

In contrast to the protein film, the mixed protein/polysaccharide films could not be fitted with a single layer model, indicating that the complexes do not form a homogeneous thick film at the interface. On the other hand, fitting the pure protein film with the two-layer model used

for the mixed films, did not yield reproducible values. It has been reported before that β -lactoglobulin was best fitted with a single layer at solvent pH close to the iso-electric point²⁴.

From our data it is not possible to distinguish between protein and polysaccharide in the adsorbed films. Since both components have different scattering length densities (respectively $1.78 \cdot 10^{-6} \text{ \AA}^{-2}$ and $2.47 \cdot 10^{-6} \text{ \AA}^{-2}$, calculated based on atomic composition and density of the components) scattering length density cannot unambiguously be converted to volume fractions. Results are therefore presented in terms of scattering length density (SLD) profiles. In figure 5.4 the adsorbed protein layer profile in NRW after 1 hour (sample A, solid black) can be compared to profiles of mixed protein/polysaccharide films at two different mixing ratios after ~ 2 hours (please note the difference in the scale of the x-axis, compared to figure 5.3). The negatively charged complexes (sample B, dashed grey) form a dense thin layer (~ 4 nm) at the air/water interface, with a very diffuse layer of ~ 40 nm below it. The films of the neutral complexes (sample C, solid grey) were fitted with the same two-layer model and the same starting parameters. The resulting profile shows that the first and especially the second layer is much denser than the film formed by negatively charged complexes. The thickness of the second layer is smaller in case of neutral complexes than observed with negatively charged complexes.

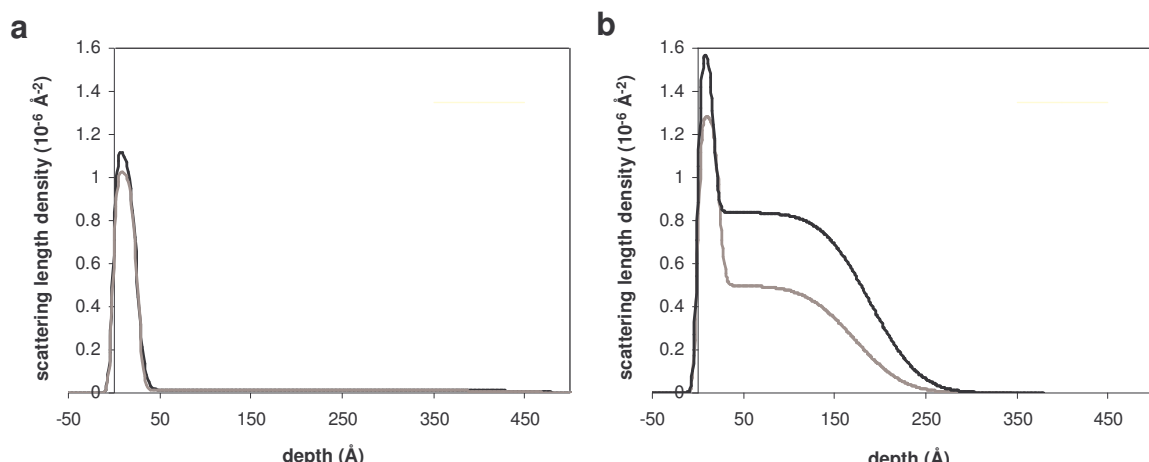


Figure 5.5: Effect of aging time (grey ~ 2 hours, black ~ 6.5 hours) on fitted scattering length density profile in NRW for a) Sample B, negatively charged and b) sample C, neutral β -lactoglobulin/pectin complexes; β -lactoglobulin concentration was 0.1 g/L , pH 4.5 and 12 mM .

In figure 5.5 it is shown how the films of negative and neutral complexes change in time. To determine the effect of time, a measurement of sample B in NRW after 2 hours was fitted with a measurement of B in D_2O after 3 hours and separately a measurement of B in NRW after 6.5 hours was fitted with the same measurement of B in D_2O after 3 hours. This procedure was chosen due to a lack of measurements in D_2O (after longer aging times) and was applied in the same way for measurements of sample C. Layer thicknesses at two different aging times in NRW are thus constrained to the layer thicknesses of one D_2O film, which may obscure growth of the film thickness in time. However, in fitting reflectivity

profiles with a uniform layer model, it is usually found that layer thickness and density can be varied over a limited range, but their variations cancel in their contribution to the total adsorbed amount (Γ)²⁵. Hence, since layer densities are not constrained between fits of NRW and D₂O, the fitting procedure does not obscure film growth in terms of adsorbed amount. Figure 5.5a shows SLD profiles of adsorbed films of negatively charged complexes (sample B) after ~2 hours (grey) and after ~6.5 hours (black) in NRW. It appears that the adsorbed amount in case of negative complexes hardly increases in time; both the first as well as the second layer hardly change in time. In contrast, the films formed from neutral complexes (sample C, figure 5.5b), which are already more dense after 2 hours, clearly become even more dense in time.

5.3.4 Simultaneous versus sequential adsorption (sample B & C versus D & E)

As mentioned in chapter 3, it is known that films formed by simultaneously adsorbing protein and polysaccharide in the form of complexes have surface rheological behaviour that differs from films where complexes are adsorbed to a previously formed protein layer (sequential adsorption). Therefore we compare in figure 5.6 films formed by simultaneous adsorption (as shown in figure 5.5) with films formed by sequential adsorption. The films D and E were fitted with the same two-layer model and the same starting parameters as used for B and C. Compared to film B, the first layer in film D resembles more the pure protein film (A). The second layers from B and D are both very diffuse and have comparable thicknesses. The second layers of film C and E (formed from neutral complexes) are both more dense, with the difference that the layers of C are more compact than those of E.

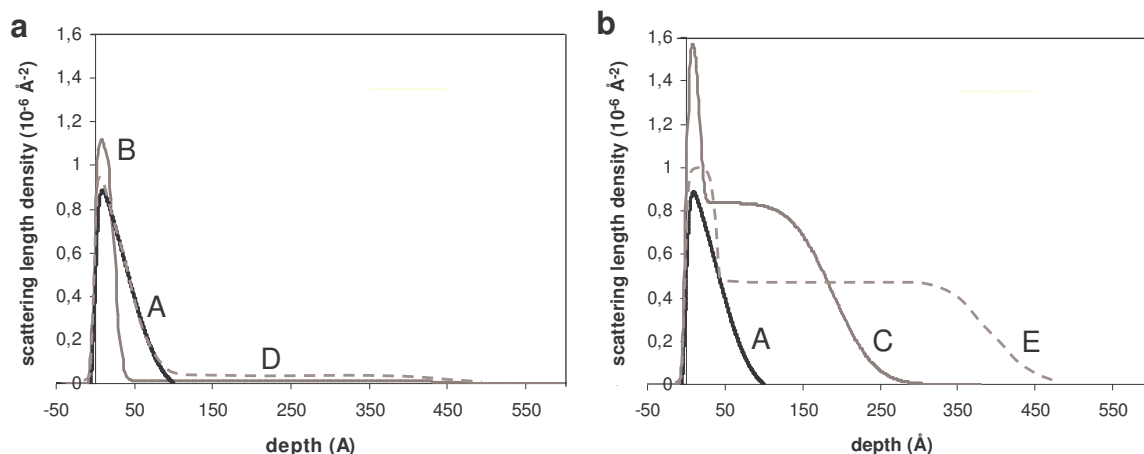


Figure 5.6a: Fitted scattering length density profile in NRW for simultaneously (B, solid grey) and sequentially (D, dashed grey) formed films from negatively charged complexes, compared to pure β -lactoglobulin film (A, solid black) and b: scattering length density profile in NRW for simultaneously (C, solid grey) and sequentially (E, dashed grey) formed films from neutral complexes, compared to pure β -lactoglobulin film (A, solid black) after ~6.5 hours; β -lactoglobulin concentration was 0.1 g/L, pH 4.5 and 12 mM.

The adsorbed mass in the films can be calculated from the SLD profile $\rho(Q_z)$ according to $\rho(Q_z) = \phi_a \rho_a + (1-\phi_a) \rho_s$, where ϕ_a is the volume fraction of adsorbed material. The equation reduces to $\rho(Q_z) = \phi_a \rho_a$ for NRW because the SLD of the solvent is zero. As protein and

polysaccharide cannot be distinguished, the SLD of β -lactoglobulin ($1.78 \cdot 10^{-6} \text{ \AA}^{-2}$ in NRW) was used for ϕ_a and the specific volume of β -lactoglobulin ($0.750 \cdot 10^{-3} \text{ m}^3 \text{ kg}^{-1}$)²⁶ was used to convert volume fraction to adsorbed mass. Although scattering length densities for β -lactoglobulin and pectin differ, these differences are reduced to ~20% in adsorbed mass, as also specific volumes of both ingredients differ ($\sim 0.625 \cdot 10^{-3} \text{ m}^3 \text{ kg}^{-1}$ for pectin, estimated on the basis of the density of saccharose).

In figure 5.7 an overview is given of all the different films (at an aging time of approximately 6.5 hours) that are in this case converted to adsorbed amounts and layer thicknesses. The first layers from the two-layer fits (black) of the sequentially adsorbed films (D and E) resemble the pure protein film, fitted with a single layer, of A; this holds for both adsorbed amount (figure 5.7a) and layer thickness (figure 5.7b). The first layers from B and C, the simultaneously adsorbed films, are thinner and contain less material than the first layers of the sequentially adsorbed films. It can be concluded that 6.5 hours after starting with a clean interface, film B and D are not the same. In all cases the total film thickness (sum of first and second layer) is much thicker in the presence of the polysaccharide (figure 5.7b). However, the (final) protein/polysaccharide mixing ratio (determining the net charge of the soluble complexes) seems to govern the total adsorbed amount (figure 5.7a). Adsorption of neutral complexes (both simultaneous and sequential) leads to much denser second layers (C and E) than adsorption of negative complexes (B and D) and so very high values of adsorbed mass are reached.

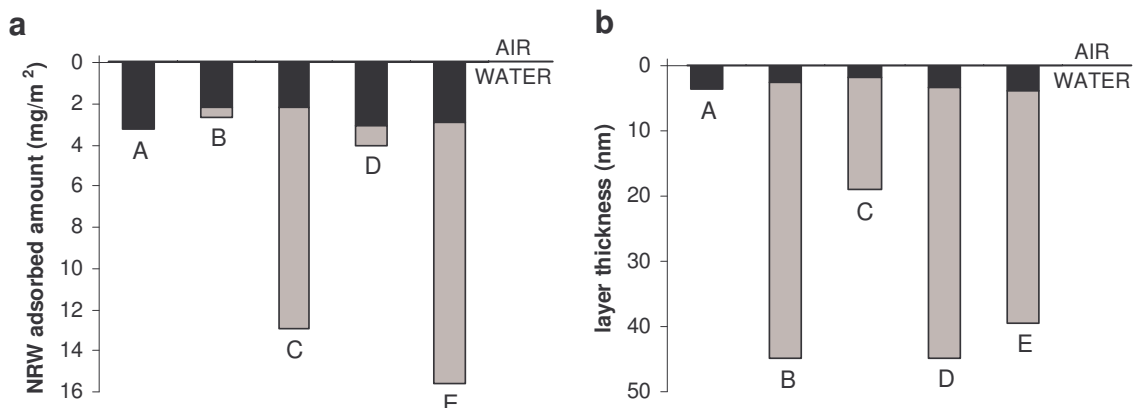


Figure 5.7: a) Adsorbed amounts and b) Layer thicknesses estimated from two-layer fits, first layer in black, second layer in grey (only A is a 1-layer fit); A: protein monolayer, B: mixed film by simultaneous adsorption of negatively charged complexes, C: mixed film by simultaneous adsorption of neutral complexes, D: negatively charged complexes adsorbed at previously formed protein film (sequential adsorption) and E: neutral complexes adsorbed at previously formed protein film; all 6.5 hours after the experiment was started with a clean interface.

5.3.5 Time resolved fluorescence anisotropy (sample A and B)

The question arises why there is a history dependence in the properties of the adsorbed films. Why are the simultaneously (B) and sequentially (D) adsorbed films different, as observed with both neutron reflection and surface rheology (chapter 3), even though bulk solution concentrations are the same? Possibly the polysaccharides hinder the protein molecules to reach the interface by substantially reducing their mobility. A technique to study mobility of protein molecules at an air/water interface is time-resolved fluorescence anisotropy (TRFA).

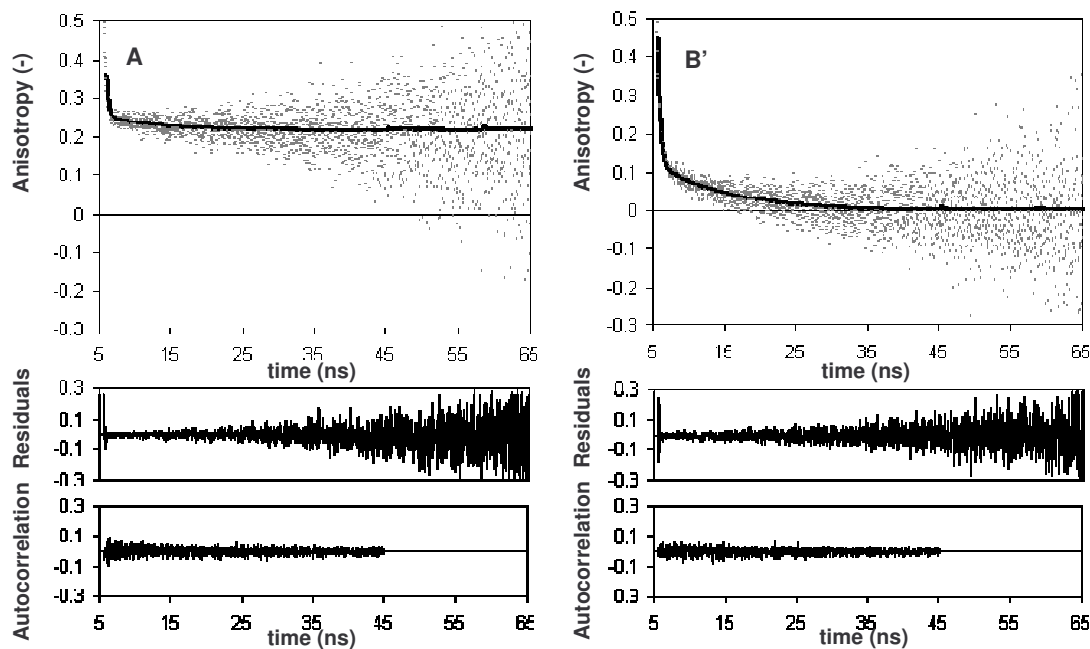


Figure 5.8: Anisotropy decay curves (with residuals and autocorrelation) of a pure β -lactoglobulin film after 6 min (sample A) and a film formed by adsorption of negatively charged β -lactoglobulin/pectin complexes after 11 min (sample B'), the dots are data points and the lines represent their fits; the β -lactoglobulin concentration was 0.1 g/L, pH 4.5 and I 2 mM.

Figure 5.8 shows the anisotropy decay curves, for a pure β -lactoglobulin film (sample A) and a film adsorbed from negatively charged β -lactoglobulin/pectin complexes (with somewhat less net charge than sample B; therefore indicated with B'). In the pure protein film all anisotropy disappears within the fluorescence lifetime of the label. This is not at all the case for the film formed by adsorption of negatively charged complexes. Both curves start with a fast decay in the first few nanoseconds which is attributed to scattering (since the parallel detection is more sensitive to scatter, apparent anisotropy at the start of the measurement is high: also the high residuals indicate that this is a random effect). In the pure protein case the fast decay is followed by a slower decay (figure 5.8, between 8 and 25 ns) assigned to rotation of the protein molecule. This curvature is not clearly visible in the decay curve of the mixture. By fitting the anisotropy decay, correlation times can be derived that correspond to the mass of a rotating unit. The black lines in figure 5.8 (top panels) represent the fits, whereas the bottom panels illustrate the quality of the fits. In Table 5.2 all rotational correlation times with their relative contributions, as well as all the fluorescence lifetimes and their relative contributions are listed with the corresponding aging time of the film. The χ^2 values illustrate the quality of the fits. The dominant fluorescence lifetime (τ_3) is close to the expected value of 14 ns for this label (small differences can be due to a different polarity of the surrounding of the label²⁰). Furthermore similar values of the fluorescence lifetimes (τ_3 , τ_2 and τ_1 in the presence and τ_3 and τ_2 in the absence of pectin) have been found by others for labelled ovalbumin²⁰. An anisotropy correlation time (ϕ_1) of approximately 10 ns corresponds to the molecular weight of a protein monomer. In the pure protein film after 6 min the contribution (β_1 0.11) of this correlation time is larger than that in the mixed film after 11 min

(β_1 0.04, ϕ_1 7 ns). For both samples the contribution seems to decrease with aging time of the film. Measurements that were performed after longer aging times (1 to 2 hours) could not be adequately fit, as anisotropy did not at all decay after the first 2 or 3 nanoseconds (the ‘scatter regime’).

Table 5.2: Fitted total fluorescence and anisotropy decay parameters: rotational correlation times (ϕ_1) and its contributions (β_1) fluorescence lifetimes (τ_i) and their contributions (α_i) for pure β -lactoglobulin film adsorbed at the air/water interface (sample A) and mixed β -lactoglobulin/pectin film adsorbed from β -lactoglobulin/pectin complexes (sample B') at different aging times. The χ^2 indicate the quality of the fits. β_1' is the relative contribution of ϕ_1 to the theoretical anisotropy decay to zero.

Sample	time (min)	β_1 ϕ_1 (ns)	α_3	α_2	α_1	χ^2	r_∞	β_1' (%)
			τ_3 (ns)	τ_2 (ns)	τ_1 (ns)			
A (β -Ig)	6	0.11 10	0.08 13.1	0.04 4.6		1.09	0.00	100
A (β -Ig)	14	0.11 11	0.10 13.2	0.05 4.6		1.11	0.06	64
A (β -Ig)	22	0.08 10	0.10 13.2	0.05 4.7		1.10	0.01	89
B' (β -Ig/pectin)	11	0.04 7	0.07 12.8	0.06 6.8	0.05 2.2	1.08	0.22	14
B' (β -Ig/pectin)	19	0.02 7	0.08 12.5	0.07 6.3	0.06 2.1	1.13	0.42	5

5.4 DISCUSSION

Comparison of the proposed schematic model for adsorbed film structures, derived from surface rheological measurements and shown in figure 5.1, with neutron reflection measurements leads to a number of conclusions. These will be discussed on the basis of figure 5.9, a slightly adapted version of figure 5.1. The observation that in the presence of polysaccharide the total film thickness is always larger than the pure protein monolayer formed in the absence of polysaccharide agrees well with the model. The hydrodynamic radius of complexes in solution, as measured by dynamic light scattering, is $\sim 55 \pm 1$ nm (chapter 8). Taking into account that the average size of complexes as measured by dynamic light scattering is presumably overestimated due heterodispersity in the system, the thickness of the layers corresponds to the size of the complexes in solution.

Adsorption of negatively charged complexes leads to thick but very diffuse films at the air/water interface as depicted in figure 5.9B; the presence of the polysaccharide somewhat lowers protein adsorption at the air/water interface in layer I compared to protein adsorption from a pure protein solution. Adsorption of neutral complexes leads to the formation of thick and much more dense films (9C). In the original model (figure 5.1) the simultaneously adsorbed mixed films (from protein/polysaccharide complexes) were schematically depicted as films with a homogeneous density. However, neutron reflection data have shown that the mixed films can always be subdivided in a first layer (figure 5.9, layer I) with the thickness of a protein monolayer and a second layer (figure 5.9, layer II) which is always less dense than the first layer.

The difference between simultaneously adsorbed mixed films (by adsorption of complexes, figure 5.9 B and C) and sequentially adsorbed films (by adsorption of complexes below a previously formed protein layer, figure 5.9 D and E) is the amount of adsorbed

material in layer I. Since this layer is always denser than layer II, it may dominate surface pressure and surface rheological behaviour as suggested in chapter 3. One may expect that a film formed from negatively charged complexes (9B) may in time change to a film as depicted in 9D. In other words, the density of layer I of B might increase in time because protein molecules move through the complex; once they reach the interface they will adsorb irreversibly. However, comparison of simultaneously (B) and sequentially adsorbed films (D) by neutron reflection after 6.5 hours (figure 5.8), and by surface rheology after up to 20 hours (chapter 3) reveals however that this is not the case. Despite the fact that total protein and polysaccharide concentrations are the same, the adsorbed films differ persistently. This means that at least in one case the adsorbed film is not in thermodynamic equilibrium. It seems that the presence of a polysaccharide (from the start of the adsorption) can hinder the formation of a dense layer I at the interface.

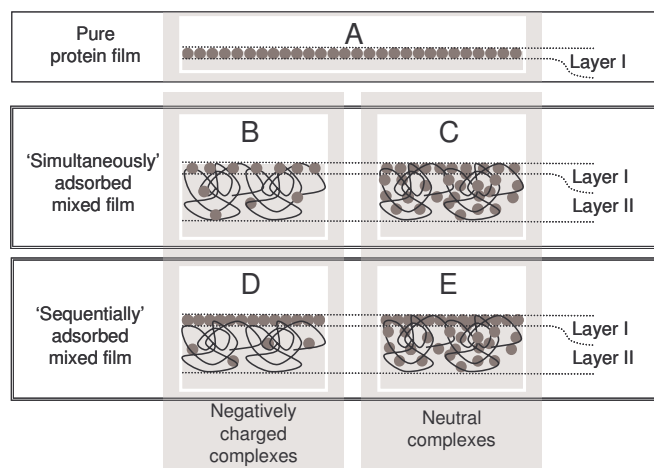


Figure 5.9: Adapted version of figure 5.1, based on neutron reflection data. The layers indicated on the right side refer to the layers used in the fits: Schematic representation of different adsorbed layers at the air/water interface A: protein monolayer, B and C: mixed layers from simultaneous adsorption where B is from negatively charged complexes and C from net neutral complexes, D and E: complexes adsorbed at previously formed protein layer where D are negatively charged complexes and E net neutral complexes.

From the TRFA data the protein mobility in the interface – and thus in the presence of polysaccharide the protein mobility through complexes in the interface – can be assessed. The rotation correlation time, ($\phi_1 = 10$ ns) is fast for a dimer, but it does correspond to the mass of a β -lactoglobulin monomer. In the presence of pectin the rotation correlation time is only 7 ns. This difference is not considered as significant since the quality of the fit did not change if this parameter was forced to 10 ns. In the presence of pectin the anisotropy does not decay to 0 within the measuring time ($r_\infty \neq 0$). To account for this an extra rotational correlation time should be added, which is infinitely large compared to the measuring time ($\phi_2 = \infty$). Since ϕ_2 is so large that it does not contribute to the anisotropy decay within the measuring time (~ 65 ns), its contribution (β_2) can be estimated as equal to r_∞ . To estimate which fraction of initial anisotropy decays due to rotation of protein molecules, a relative contribution (β_1' in %) of ϕ_1 to the total theoretical anisotropy decay (at infinite aging time of the film) can now be estimated by $\beta_1' = 100\% \cdot \beta_1 / (\beta_1 + \beta_2)$; values are given in table 5.2. The value of β_1' seems to decrease in time for both samples. More importantly, in the presence of pectin β_1' is up to a

factor of ~ 18 lower than in the absence of pectin. This illustrates that rotation of protein molecules is clearly reduced in the presence of polysaccharides. Although it is rotational, rather than translational mobility which is probed by this technique, it is quite reasonable to assume that if rotational mobility is largely reduced, translational mobility will be reduced as well. Hence, protein transport through the mixed layer to the air/water interface is hampered (compared to transport through the bulk solution).

The mechanism of protein/polysaccharide complexes (simultaneous adsorption) could now be imagined as follows: Presumably, negatively charged complexes in close vicinity to the interface adsorb via some protein molecules at the outside of the complexes such that the polysaccharide sticks to these adsorbed protein molecules (the polysaccharide itself is not surface active). The more protein molecules are (irreversibly) adsorbed, the more connections a polysaccharide molecule can make with the (protein at the) interface. Interaction of the polysaccharide with a collection of immobilized protein molecules (that have already lost their translational entropy) at the interface is much stronger than interaction of the polysaccharide with individual protein molecules in bulk (because there is less entropic penalty). Polysaccharide adsorption may hence become irreversible. As made plausible by TRFA measurements, protein molecules cannot easily move through the complex layer. This probably prevents further adsorption of protein molecules. The multi-point-interaction of polysaccharides with protein at the interface, in combination with a reduced protein mobility may be responsible for the thermodynamic non-equilibrium character of the films. One can easily imagine that a protein layer formed prior to polysaccharide injection, and therefore not hindered by the presence of polysaccharide, will be more dense. When after injection of polysaccharide in the bulk solution, instantaneously formed complexes adsorb to this protein layer, the first layer at the interface still contains more material; injection of pectin does not lead to desorption of protein, as was also shown in chapter 3. When neutral complexes adsorb to the air/water interface, there is no repulsion between the interface and complexes remaining in bulk. As neutral complexes in solution tend to aggregate (phase separate), the interface could serve as a substrate for the formation of a thick dense aggregated film, or complex coacervate film. Depending on the structure of this coacervate phase (liquid or semi-solid), this layer could be considered as a wetting or pre-wetting film.

5.5 CONCLUSIONS

Although the neutron reflection measurements could not distinguish between protein and polysaccharide, they form a valuable addition to surface rheological measurements to characterise mixed adsorbed films. The hypothesised film structures are now substantiated to a more molecular level: the net charge of protein/polysaccharides largely determines the layer density and adsorbed amount and thus the presence of an excess polysaccharide can hinder the formation of a dense protein layer at the interface. In the latter case, a kinetic barrier for further protein adsorption, is constituted by the reduced mobility of protein molecules at or in close vicinity to the interface (as illustrated with TRFA) presumably in combination with an irreversible character of polysaccharide adsorption at the adsorbed protein at the interface.

ACKNOWLEDGEMENTS

We greatly acknowledge NWO for granting our proposal RB52099 and herewith giving us the opportunity to perform the neutron reflection measurements. We thank Stephen Holt from ISIS Pulsed Neutron & Muon Source, Rutherford Appleton Laboratory, Chilton, Didcot, United Kingdom for his help with the neutron reflection measurements and for his support in analysing the data. Furthermore we thank Elena Kudryashova (WCFS, Wageningen) and Jan Willem Borst and Ton Visser (MicroSpectroscopy Centre, Wageningen) for their help with TRFA measurements and data analysis.

REFERENCES

- (1) Baeza, R.; Sanchez, C. C.; Pilosof, A. M. R.; Patino, J. M. R., Interactions of polysaccharides with beta-lactoglobulin adsorbed films at the air-water interface. *Food Hydrocolloids* **2005**, 19, (2), 239-248.
- (2) Dickinson, E.; Semenova, M. G.; Antipova, A. S.; Pelan, E. G., Effect of high-methoxy pectin on properties of casein-stabilized emulsions. *Food Hydrocolloids* **1998**, 12, 425-432.
- (3) Guzey, D.; Kim, H. J.; McClements, D. J., Factors influencing the production of o/w emulsions stabilized by β -lactoglobulin-pectin membranes. *Food Hydrocolloids* **2004**, 18, (6), 967.
- (4) Ogawa, S.; Decker, E. A.; McClements, D. J., Production and characterization of O/W emulsions containing droplets stabilized by lecithin-chitosan-pectin multilayered membranes. *Journal of Agricultural and Food Chemistry* **2004**, 52, (11), 3595-3600.
- (5) Benichou, A.; Aserin, A.; Garti, N., Protein-polysaccharide interactions for stabilization of food emulsions. *Journal of Dispersion Science and Technology* **2002**, 23, (1-3), 93-123.
- (6) Dickinson, E., Hydrocolloids at interfaces and the influence on the properties of dispersed systems. *Food Hydrocolloids* **2003**, 17, (1), 25-39.
- (7) Einhorn-Stoll, U., Interactions of whey proteins with different pectins in O/W emulsions. *Nahrung* **1998**, 42, (3/4), 248-249.
- (8) Tokaev, E. S.; Gurov, A. N.; Rogov, I. A.; Tolstoguzov, V. B., Properties of oil/water emulsions stabilized by casein-acid polysaccharide mixtures. *Nahrung* **1987**, 31, (8), 825-834.
- (9) Schmitt, C.; da Silva, T. P.; Bovay, C.; Rami-Shojaei, S.; Frossard, P.; Kolodziejczyk, E.; Leser, M. E., Effect of time on the interfacial and foaming properties of beta-lactoglobulin/acacia gum electrostatic complexes and coacervates at pH 4.2. *Langmuir* **2005**, 21, (17), 7786-7795.
- (10) van Well, A. A.; Brinkhof, R., Protein adsorption at a static and expanding air-water interface: a neutron reflection study. *Colloids and Surfaces A-Physicochemical and Engineering Aspects* **2000**, 175, (1-2), 17-21.
- (11) Kudryashova, E. V.; Meinders, M. B. J.; Visser, A.; van Hoek, A.; de Jongh, H. H. J., Structure and dynamics of egg white ovalbumin adsorbed at the air/water interface. *European Biophysics Journal with Biophysics Letters* **2003**, 32, (6), 553-562.
- (12) de Jongh, H. H. J.; Gröneveld, T.; de Groot, J., Mild isolation procedure discloses new protein structural properties of beta-lactoglobulin. *Journal of Dairy Science* **2001**, 84, (3), 562-571.
- (13) Daas, P. J. H.; Boxma, B.; Hopman, A. M. C. P.; Voragen, A. G. J.; Schols, H. A., Nonesterified galacturonic acid sequence homology of pectins. *Biopolymers* **2001**, 58, (1), 1-8.
- (14) Blumenkrantz, N.; Asboe-Hansen, G., New Method For Quantitative-Determination Of Uronic Acids. *Analytical Biochemistry* **1973**, 54, (2), 484-489.
- (15) Thibault, J. F., Automated-Method For The Determination Of Pectic Substances. *Lebensmittel-Wissenschaft & Technologie* **1979**, 12, (5), 247-251.
- (16) Salomaa, P.; Schaleger, L. L.; Long, F. A., Solvent Deuterium Isotope Effects On Acid-Base Equilibria. *Journal of The American Chemical Society* **1964**, 86, (1), 1-8.

- (17) Brown, A. S.; Holt, S. A.; Reynolds, P. A.; Penfold, J.; White, J. W., Growth of Highly Ordered Thin Silicate Films at the Air-Water Interface. *Langmuir* **1998**, 14, (19), 5532-5538.
- (18) Penfold, J. In *Neutron, X-ray and Light Scattering*, 1991; 1991; pp 223-236.
- (19) Lu, J. R.; Perumal, S.; Zhao, X. B.; Miano, F.; Enea, V.; Heenan, R. R.; Penfold, J., Surface-induced unfolding of human lactoferrin. *Langmuir* **2005**, 21, (8), 3354-3361.
- (20) Kudryashova, E. V.; Gladilin, A. K.; Izumrudov, V. A.; van Hoek, A.; Visser, A.; Levashov, A. V., Formation of quasi-regular compact structure of poly(methacrylic acid) upon an interaction with alpha-chymotrypsin. *Biochimica et Biophysica Acta-Protein Structure And Molecular Enzymology* **2001**, 1550, (2), 129-143.
- (21) Kudryashova, E. V.; Visser, A. J. W. G.; van Hoek, A.; De Jongh, H. H., Molecular details of pectin-ovalbumin complexes at the air/water interface; a spectroscopic study. submitted, 2006.
- (22) Grunwald, C.; Kuhlmann, J.; Woll, C., In Deuterated Water the Unspecific Adsorption of Proteins Is Significantly Slowed Down: Results of an SPR Study Using Model Organic Surfaces. *Langmuir* **2005**, 21, (20), 9017-9019.
- (23) Verheul, M.; Pedersen, J. S.; Roefs, S.; de Kruif, K. G., Association behavior of native beta-lactoglobulin. *Biopolymers* **1999**, 49, (1), 11-20.
- (24) Atkinson, P. J.; Dickinson, E.; Horne, D. S.; Richardson, R. M., Neutron Reflectivity Of Adsorbed Beta-Casein And Beta-Lactoglobulin At The Air/Water Interface. *Journal of The Chemical Society-Faraday Transactions* **1995**, 91, (17), 2847-2854.
- (25) Lu, J. R.; Su, T. J.; Thomas, R. K.; Penfold, J.; Webster, J., Structural conformation of lysozyme layers at the air/water interface studied by neutron reflection. *Journal of The Chemical Society-Faraday Transactions* **1998**, 94, (21), 3279-3287.
- (26) Valdez, D.; Le Huerou, J. Y.; Gindre, M.; Urbach, W.; Waks, M., Hydration and protein folding in water and in reverse micelles: Compressibility and volume changes. *Biophysical Journal* **2001**, 80, (6), 2751-2760.

Pullulan charge density controlled β -lactoglobulin complexation in relation to surface activity

Renate A. Ganzevles, Hans A. Kosters, Ton van Vliet, Martien A. Cohen Stuart
and Harmen H.J. de Jongh

ABSTRACT

Non-surface active anionic polysaccharides can adsorb to air/water interfaces along with proteins as a result of attractive interaction with the proteins. Since the formation of protein/polysaccharide complex is dominated by electrostatic interaction, the charge density of the polysaccharide plays a major role in the adsorption behaviour of the complexes. In this study pullulan (a non-charged polysaccharide) carboxylated to four different charge densities (fraction of carboxylated subunits: 0.1, 0.26, 0.51 and 0.56) was used to investigate the effect of charge density on the properties of mixed protein/polysaccharide adsorbed layers at air/water interfaces. Protein/polysaccharide complexation in solution was studied by light scattering and electrophoretic mobility. With all pullulan samples soluble complexes could be formed. Complex coacervation occurred only with the highest three charge densities if sufficient amounts of positively charged protein were added to compensate for the negative charge of the pullulan. The higher the pullulan charge density, the more the increase of surface pressure at the air/water interface in time was retarded compared to that for pure protein. This delaying trend with pullulan charge density was even more pronounced for the development of the dilatational modulus. The lower dilatational modulus can be explained by the ability of the polysaccharides to prevent the formation of a compact protein layer at the air/water interface due to electrostatic repulsion. This ability of the polysaccharides to prevent 'layer compactness' increases with the negative net charge of the complexes. When the charge density is high enough (≥ 0.26) the polysaccharide may enhance the cohesion between complexes within the adsorbed layer. The charge density of polysaccharides regulates the solubility of protein/polysaccharide complexes as well as their adsorption kinetics and the resulting surface rheological behaviour of the mixed layers formed.

6.1 INTRODUCTION

Attractive protein polysaccharide interaction, or in a broader sense protein polyelectrolyte interaction, has been extensively studied both fundamentally¹⁻³ as well as in many applications^{4, 5}. Another well explored field of research is protein adsorption to air/water⁶⁻⁹ and oil/water interfaces¹⁰⁻¹². When trying to relate properties of the mixed adsorbed layers to protein/polysaccharide interaction, knowledge from both fields should be combined. Many authors report an increased emulsion stability¹³⁻¹⁷ in the presence of polysaccharides, which may be related to the properties of the mixed adsorbed layers at the oil/water interface. Also at air/water interfaces protein/polysaccharide interaction has been studied^{18, 19}. As electrostatic interaction plays a dominant role in these processes, charge density of the polysaccharide is likely to be an important parameter.

Interaction of proteins with anionic polyelectrolytes has often been studied as a function of pH, at constant composition. Going from high to low pH (or from low to high pH in case of cationic polyelectrolytes) at constant protein/polyelectrolyte mixing ratio, three regimes are commonly distinguished: (i) formation of soluble or intrapolymer complexes (carrying excess net charge), (ii) aggregation of these soluble complexes to interpolymer complexes on decreasing net charge, (iii) formation of coacervate droplets^{1-3, 20}. If a system (e.g. β -lactoglobulin and low methoxyl pectin) is studied as a function of composition at constant pH (below the iso-electric point of the protein), by titrating an anionic polysaccharide with protein, two of the stages can be distinguished: (i) soluble complexes are formed when the negative charge of the polysaccharide is in excess with respect to the net positive charge of the protein, (ii/iii) by further uptake of proteins the net charge of the complexes decreases until, eventually, the complexes lose their negative net charge, after which they aggregate and become insoluble; i.e. complex coacervation²¹ (chapter 2). The nature of the concentrated phase depends on the strength of the interaction between the protein and polysaccharide; weak polyacids (e.g. carboxylated polysaccharides) form a liquid complex coacervate phase, whereas strong polyacids (e.g. sulphated polysaccharides) form precipitates².

By complexation with protein in the bulk solution, non-surface active polysaccharides can coadsorb at air/water interfaces along with proteins and in doing so affect adsorption kinetics and the surface rheology of the adsorbed layer^{18, 19, 22, 23}. It is presently unknown how this depends on the protein/polysaccharide binding affinity. In chapter 3 and 5 the properties of adsorbed mixed β -lactoglobulin/pectin layers have been shown to depend on protein/polysaccharide mixing ratio and adsorption sequence, which resulted in the schematic representation shown in figure 5.9 (chapter 5). At low mixing ratios, such that protein/polysaccharide complexes are highly negatively charged, the polysaccharide is assumed to prevent the formation of a densely packed protein layer at the interface resulting in a low dilatational modulus. In case of neutral complex adsorption or pure protein adsorption in the absence of polysaccharides, the adsorbed layers may become denser, resulting in a higher dilatational modulus. Adsorption of polysaccharides or complexes to a

previously formed (dense) protein layer can reinforce the latter and result in higher dilatational modulus than that of the pure protein layer. Insight in this mechanism provides a way to control the properties of the composite adsorbed layer by protein/polysaccharide interaction. As the influence of polysaccharides is likely to depend on the protein/polysaccharide binding affinity, polysaccharide charge density is a crucial parameter.

The aim of this work is to study how protein adsorption to air/water interfaces, and the rheological properties of these interfaces, can be controlled by polysaccharide charge density. The use of pullulan, a naturally non charged polysaccharide, that was carboxylated to four different charge densities²⁴ has a number of advantages. (1) Distribution of charges is relatively random, as the carboxylation is a chemical and not an enzymatic reaction. Moreover only two glucose units out of each repeating glucose trimer can be carboxylated. (2) Since all samples were prepared from the same pullulan batch, molar mass of all samples is similar; this is often not the case when e.g. comparing ι -carrageen and κ -carrageen. (3) Moreover, there are no chemical differences between the samples other than charge density; e.g. high- and low methoxyl pectin differ in polarity since besides charge density, also the amount of methyl groups differs. In order to better understand the effect of polysaccharide charge density on complex adsorption at the air/water interface, first the effect of polysaccharide charge density on protein/polysaccharide complexation in solution is studied. Subsequently surface rheological behaviour is studied as a function of polysaccharide charge density, protein/polysaccharide mixing ratio and order of adsorption.

6.2 MATERIALS AND METHODS

6.2.1 Pullulan oxidation and characterization

Desalinated pullulan ($M_n \sim 150\ 000$ g/mol) was purchased from Polysciences, Inc. (Warrington, PA, USA). Pullulan is a linear, water-soluble polysaccharide, consisting of repeating glucose trimers; the trimers are α -1,6 connected and within the trimers the glucose monomers are α -1,4 connected, leaving two primary alcohol groups per three monomers. Using catalytic amounts of TEMPO (2,2,6,6-tetramethylpiperidine-1-oxyl) these primary alcohol groups of native pullulan could be oxidized such that they transformed into carboxyl groups, following the method of de Nooy et al.²⁴. Four batches of carboxylated pullulan with different charge densities were obtained by keeping the pH constant at 9.4 and registering the OH^- uptake during the reaction, using a pH-stat (from which the charge density can be estimated: table 6.1). After extensive dialysis the samples were freeze-dried and stored at room temperature until further use. Stock solutions were prepared by subsequently dissolving the material in deionised water, storing overnight and filtering through 0.45 μm filters (Acrodisc, Gelman sciences, MI, USA). For each sample the total glucuronic acid content (using an automated colorimetric *m*-hydroxydiphenyl method^{25, 26}) and glucose content (using an automated orcinol method²⁷) were determined, from which the charge density (CD) was calculated (Table 6.1). The charge density values calculated from the glucose and galacturonic acid content correspond well to the values estimated from OH^- uptake during the reaction. Since the charge density is defined as the fraction of charged monomers from the

total number of glucose monomers, the maximum charge density possible for pullulan is 0.67. Charge densities calculated from glucose and glucuronic acid content were used for calculations of protein/polysaccharide charge ratios. Using High Pressure Size Exclusion Chromatography no systematic alteration of the molar mass with degree of oxidation could be detected (data not shown).

Table 6.1: Characterisation of the carboxylated pullulan samples: charge density (fraction of charged glucose monomers) as estimated by the OH- uptake during the reaction and charge density as determined by glucuronic acid content and glucose content. Accuracy is within 5 to 10%.

Pullulan sample name	charge density OH- uptake	charge density
		glucose/glucuronic acid content
pul1	0.10	0.10
pul2	0.29	0.26
pul3	0.54	0.51
pul4	0.61	0.56

6.2.2 Sample preparation

Acetate buffers (pH 4.5, ionic strength 9 mM) were prepared from analytical grade chemicals and deionised water (Barnstead EASYpure UV, USA). Please note that values for ionic strength mentioned in the text represent ionic strength of the buffer. Bovine β -lactoglobulin was purified using a non denaturing method as described previously²⁸. Protein stock solutions (for light scattering and ζ -potential 15 g/l, for all other measurements 1 or 2 g/l) were prepared freshly by dissolving the freeze dried protein in water. The pH of the protein stock solutions was 6.8 ± 0.2 . After dilution of the pullulan stock solution with buffer, protein stock solution was added to a protein concentration of 0.1 g/L. After mixing, the protein/polysaccharide samples were equilibrated for 30 min before use in order to allow formation of protein/polysaccharide complexes.

6.2.3 Light scattering

Protein-, pullulan- and buffer (25 mM acetate buffer, ionic strength 9 mM, pH 4.5) solutions were filtered through 0.45 μ m filter (Acrodisc, Gelman Sciences, MI, USA). Protein (using absorbance at 280 nm with an extinction coefficient of $9.56 \cdot 10^2 \text{ m}^2 \text{g}^{-1}$) and pullulan (using the glucose and glucuronic acid method as described in the pullulan modification and characterization section) stock concentrations were determined after filtration. In the titration cell of the light scattering setup small aliquots of a concentrated β -lactoglobulin stock solution (15 g/l) were added to a buffered pullulan solution (0.05 g/l, ionic strength 9 mM, pH 4.5). After each addition the mixture was stirred for 30 s, and equilibrated for 10 s. Subsequently scattered light intensity (at 90°) and second cumulant diffusion coefficients²⁹ were determined, using an ALV light scattering instrument equipped with a 400 mW argon laser tuned at a wavelength of 514.5 nm, as described before³⁰. Hydrodynamic radii were calculated according to the Stokes-Einstein relation, assuming that the complexes were spherical. Averages and standard deviations were calculated from sets of 10 measurements. Temperature was controlled at $20 \pm 1 \text{ }^\circ\text{C}$ using a thermostated water bath.

6.2.4 Electrophoretic mobility

The electrophoretic mobility of soluble protein/polysaccharide complexes was measured with a zetasizer 2000 HS (Malvern instruments Ltd., UK) at 150 V applied voltage, using a He-Ne laser at 633 nm. The ζ -potential was calculated using the Helmholtz-Smoluchovski equation. Stock β -lactoglobulin and stock pullulan solutions were mixed with buffer (ionic strength 9 mM, pH 4.5) to a final total concentration - (protein concentration varying from 0.01 to 0.05 g/L) depending on mixing ratio - such that the signal retrieved was optimal and only a single narrow peak was observed in the scattered light intensity versus electrophoretic mobility curve. Average values and standard deviations were calculated over 5 up to 10 measurements.

6.2.5 Drop tensiometry/surface dilatational rheology

Surface tension as a function of time was measured (for single component and mixed solutions of protein and polysaccharide) using a drop tensiometer (ADT, ITCONCEPT, Longessaigne, France), where an air bubble (7 μ l) is formed in aqueous solution on the tip of a needle as described before ¹¹. Surface tension was determined by bubble shape analysis. All results are presented in terms of surface pressure $\Pi = \gamma_0 - \gamma$, where γ_0 is the surface tension of the solvent (72 mN/m) and γ is the measured surface tension. Surface dilatational moduli (ϵ) as a function of time were determined by applying sinusoidal area (A) oscillations (amplitude 4%, frequency 0.1 Hz) and recording the resulting change in surface tension: $\epsilon = d\gamma/d\ln A = -d\Pi/d\ln A$. Periods of 5 oscillations were alternated with equally long resting periods. Average dilatational moduli, as well as the average surface pressure during the oscillations, were determined using the last three oscillations of each oscillation set. All experiments were performed at least in duplicate; differences were within 5 to 10%. Temperature was controlled at 21 ± 1 °C using a water bath. Experiments were performed at low ionic strength (2 mM) in order to optimise rheological differences between the samples. In case of sequential adsorption, an air bubble was formed in a protein solution (0.1 g/l) and the protein was allowed to adsorb for approximately 2 hours (after which the dilatational modulus for a pure protein layer remains constant). Subsequently a concentrated polysaccharide solution was added and mixed in the bulk solution.

6.2.6 Surface shear rheology

Surface shear rheological behaviour of adsorbed protein/polysaccharide layers at air/water interfaces was investigated using a strain-controlled Couette-type interfacial shear rheometer, as described elsewhere ^{31, 32}. Buffer solution was poured into the sample holder and subsequently, at time zero, a 10 fold concentrated protein or protein/polysaccharide solution was injected in the bulk solution at the bottom of the sample beaker to a final protein concentration of 0.1 g/L. After injection, a disc was suspended from a torsion wire until it just touched the interface. The sample was left to adsorb and equilibrate for 3 hours at 21 ± 1 °C (using climate control in the room), during which surface tension was monitored using a Wilhelmy plate. For the sequentially adsorbed samples pullulan was injected to the protein solution after ~45 minutes. Mixing was promoted by injecting the pullulan with a high force, without distorting the interface as monitored by the surface pressure. From previous

experiments it is known that in this way the injected solution spreads through the whole sample volume. Deformation of the interface is achieved by turning the sample holder at an angular velocity of $1.27 \cdot 10^{-3}$ rad/s and the resulting stress on the interfacial layer near the disc was recorded by the rotation of the disc. Stress-strain curves were calculated from these values. Since the relative deformation of the interface is not uniform due to the large gap width relative to the disc diameter, the ratio of stress and strain is to be considered as an apparent surface shear modulus. All experiments were performed in duplicate or triplicate.

6.3 RESULTS

6.3.1 β -lactoglobulin pullulan complexation

Before investigating the effect of polysaccharide charge density on mixed protein/polysaccharide adsorption behaviour, it is relevant to consider the complexation of the different charge density pullulan samples with β -lactoglobulin in solution. Since complexation is dominated by electrostatic interaction, the different charge density samples should not be compared at equal protein/polysaccharide weight ratio. In that case the ratio of positive charge on the proteins over the negative charge on the polysaccharides would be different for each pullulan sample. In order to isolate the effect of charge density on the polysaccharide, samples are compared at equal charge ratio. To that end the positive net charge per gram β -lactoglobulin at pH 4.5 was determined from a proton titration curve and found to be $2.5 \cdot 10^{-4}$ mol/g (data not shown). For the four pullulan samples the number of carboxyl groups in order of increasing charge density was $0.63 \cdot 10^{-3}$, $1.6 \cdot 10^{-3}$, $3.0 \cdot 10^{-3}$, $3.3 \cdot 10^{-3}$ mol/g respectively, as calculated from the charge density. We assumed that 50% of the carboxyl groups are dissociated at pH 4.5 (a pK_a of 4.5 was obtained from a titration curve of pectin, a similar carboxylated polysaccharide). Using these numbers any β -lactoglobulin/pullulan weight ratio can be recalculated into a β -lactoglobulin/pullulan charge ratio, which will be referred to as CR (-). A CR of 1 means that the total net positive charge on the proteins equals the total negative charge on the polysaccharides. Please note that with CR we always refer to the ratio at which both components were added to the solution, and not necessarily to the charge ratio within the complexes.

Scattered light intensity (at 90°) and hydrodynamic radius of β -lactoglobulin/pullulan complexes were measured as a function of CR (Figure 6.1) at pH 4.5 and an ionic strength of 9 mM. All pullulan samples show an increase in scattered light intensity upon addition of protein. The higher the charge density of the pullulan, the more steeply the intensity increases. The hydrodynamic radius can be determined only after the first protein addition because pullulan on its own does not scatter enough light. Further addition of protein does not affect the hydrodynamic radius until a CR of 0.5. Between CR 0.5 and 1 the radius slightly increases, while the scattered light intensity levels off or decreases in case of pul3 and pul4. From a CR of about 1 the radius steeply increases for all β -lactoglobulin/pullulan mixtures except for the mixture with the lowest charge density pullulan (pul1). The steeper increase in hydrodynamic radius from CR 1 onwards is indicative of coacervation of the complexes; macroscopic phase separation occurred that could also be observed with the naked eye. CR 1

is the point where the negative charge on the pullulan is compensated by the positive net charge on the protein if all would molecules take part in the complexation. To illustrate the fact that the amount of protein needed to provoke phase separation increases with increasing charge density, the hydrodynamic radius is plotted as a function protein/polysaccharide *weight* ratio in the inset in figure 6.1. For pullulan with the lowest charge density both the increase in intensity and the increase in hydrodynamic radius (max $\sim 0.4 \mu\text{m}$) at higher mixing ratio are very small compared to the other samples and the solution remains optically clear; no macroscopic phase separation occurs.

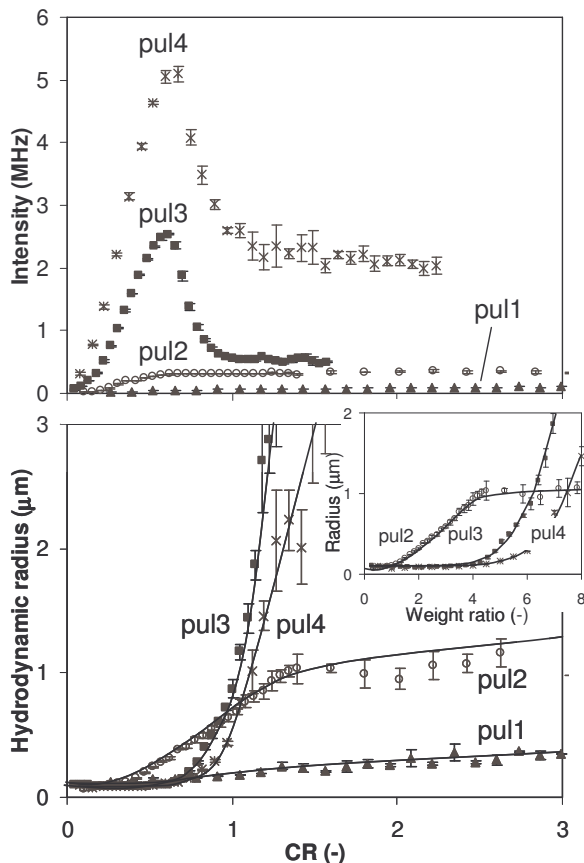


Figure 6.1: Hydrodynamic radius (bottom) and scattered light intensity (top) for complexes of β -lactoglobulin with the different charge density pullulan samples as a function of CR, pH 4.5, 19 mM. Inset: hydrodynamic radius as a function of β -lactoglobulin/pullulan weight ratio. Lines serve to guide the eye

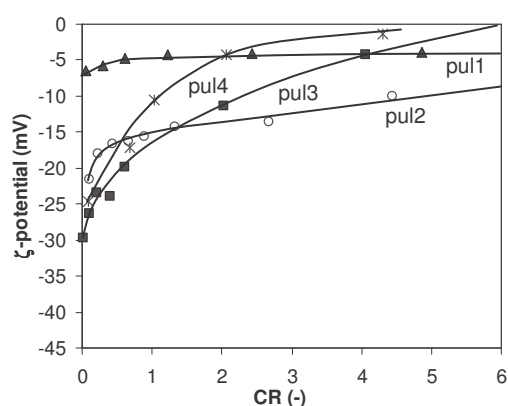


Figure 6.2: ζ -potential of complexes of β -lactoglobulin with the different charge density pullulan samples as a function of CR, pH was 4.5 and 19 mM. Lines serve to guide the eye

To check whether the net charge of soluble complexes changes upon uptake of protein, the ζ -potential of the complexes is measured as a function of CR (Figure 6.2). The pullulan samples in absence of protein do not scatter enough light to allow measuring a ζ -potential. The ζ -potential at low CR, (close to 0) is most negative for the complexes with pul4 and pul3, and becomes less negative with decreasing charge density. For all samples the ζ -potential increases with increasing CR and approaches 0 at CR values well above 1.

6.3.2 Effect of charge density on surface rheology

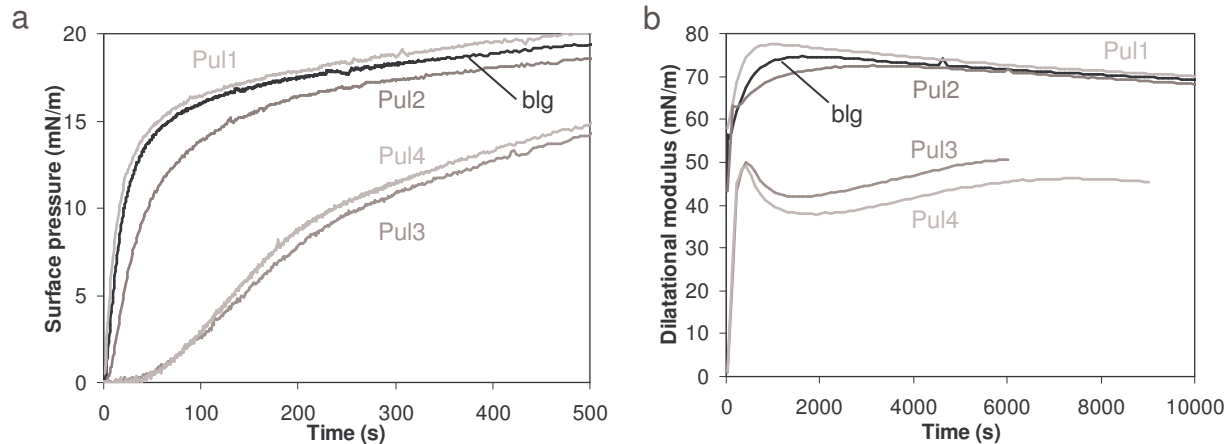


Figure 6.3a: Surface pressure and b: Dilatational modulus as a function of time for mixtures of β -lactoglobulin with pullulan with different charge density; pullulan concentrations were chosen such that the β -lactoglobulin/pullulan charge ratio was 0.5 for all samples at a β -lactoglobulin concentration 0.1 g/l, pH 4.5, 12 mM; Please note the difference in scale of the x-axis.

Since the charge density of pullulan affects the net charge and phase behaviour of complexes in solution, adsorption behaviour of the soluble complexes at the air/water interface is likely to be affected as well. It was shown in previous work that due to complexation of β -lactoglobulin to pectin (an anionic polysaccharide with a charge density of 0.7) surface pressure at the air/water interface increases at a much smaller rate than for β -lactoglobulin on its own. Pullulan is expected to have this ability as well. To assess how this delaying effect depends on charge density of the polysaccharide, surface pressure was measured as a function of time for mixtures of β -lactoglobulin with the different pullulan samples at a CR of 0.5 (Figure 6.3a). At this ratio only 50% of the negative charge on the pullulan can be compensated by the positive charge on the protein if all proteins take part in the complex formation. Since protein is the surface active component in the mixture, protein concentration was kept constant (0.1 g/L) for all mixtures (pullulan by itself is not surface active and therefore does not affect surface rheology in the absence of protein, data not shown). The pullulan samples with the highest charge density (pul3 and pul4) cause a lag time (defined as the time between formation of the clean interface and the increase in surface pressure) of about 50 s. The lag time established by pul2 is much shorter, only a few seconds. With pul1 no lag time was observed at all. The steady state value of surface pressure was 27 ± 1 mN/m for all mixtures.

To determine how the properties of the adsorbed layer depend on pullulan charge density, the dilatational modulus was measured as a function of time for the same β -lactoglobulin/pullulan mixtures as used for the surface pressure measurements (Figure 6.3b). The pure β -lactoglobulin layer reaches a steady state value of approximately 70 mN/m within 1000 s. The presence of pul4 and pul3 clearly decreases the steady state value of the dilatational modulus from 70 mN/m for the pure protein layer to respectively 45 mN/m and 50 mN/m. Also the time to reach the steady state value is longer with these pullulan samples. The presence of pul2 and pul1 does not significantly affect the dilatational modulus as compared to the pure protein layer.

Surface shear rheology is a suitable technique to probe the coherence within and between complexes in the adsorbed layers. As opposed to surface dilatational rheology, the area of the interface, and therefore also the surface pressure does not change upon deformation of the interface. Maximal coherence in the layers is expected at a CR close to 1, as from this ratio the complexes in solution start to aggregate. In chapter 3 indeed a maximum in surface shear modulus and steady state stress was observed just below CR 1 for β -lactoglobulin/pectin complexes. In order to prevent insolubility and sedimentation of complexes, a CR of 0.8 was chosen to compare surface shear rheology for the mixtures with different pullulan charge densities (protein concentration was 0.1 g/l for all samples, complexes with pul1 were tested at CR 0.6 and 1.8). Figure 6.4 shows that the apparent surface shear modulus for all mixtures with pullulan is slightly higher than that of a pure protein layer. No trend with pullulan charge density was observed. Also the steady state stress shows no trend with increasing charge density. However, steady state stress of the complexes with pul2, pul3 and pul4 is 2 to 3 times higher than that of the pure protein layer and the complexes with pul1 (Figure 6.4b).

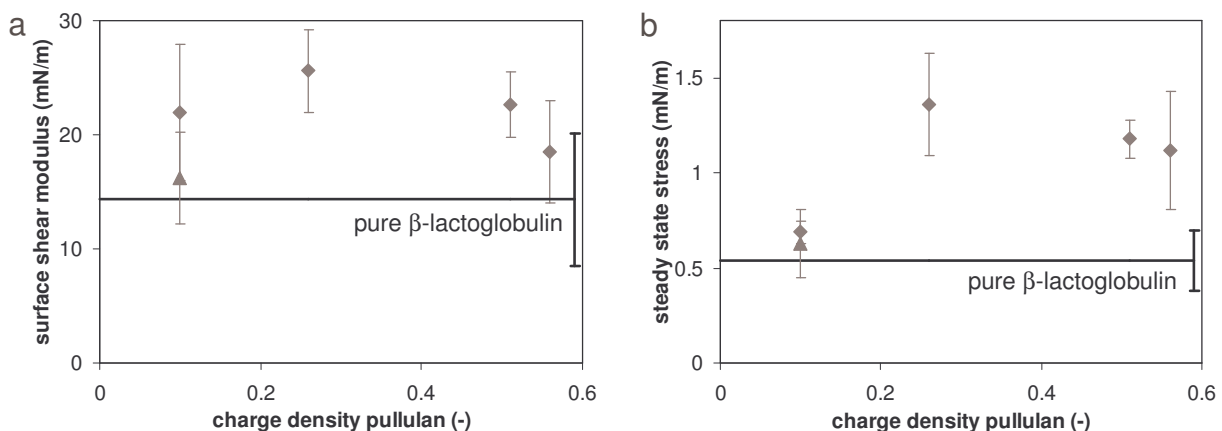


Figure 6.4: Apparent surface shear modulus (a) and steady state shear stress (b) as a function of the charge density of pullulan. Pullulan concentrations were chosen such that the β -lactoglobulin/pullulan charge ratio was 0.8 for all samples (except for the lowest charge density, where diamond is CR 0.6 and triangle CR 1.8) β -lactoglobulin concentration was 0.1 g/l, pH 4.5 and 19 mM.

6.3.3 Effect of charge ratio on surface rheology

The ζ -potential measurements showed that the net charge of the soluble complexes depends on the CR (Figure 6.2). Because this net charge is likely to affect surface rheological

behaviour, dilatational modulus was determined as a function time for a range of CR values. The pullulan sample with the highest charge density (pul4) was selected for this purpose because it had - out of the four pullulan samples - the largest effect on the dilatational modulus. Figure 6.5a shows that the dilatational modulus clearly depends on the CR. The more polysaccharide is present, the stronger the dependence of the dilatational modulus as on time is affected. To exclude the effect of adsorption kinetics, the dilatational modulus was also plotted as a function of surface pressure (Figure 6.5b). Comparison of the samples at a surface pressure of 20 mN/m shows that the higher the negative net charge of the complexes (i.e. the lowest CR) the lower the dilatational modulus. At a CR of 1.1, where the net charge is relatively small (ζ -potential approximately -10 mV, figure 6.2), and the complexes are no longer soluble (Figure 6.1a), the dilatational modulus versus surface pressure is rather similar to that of the pure protein.

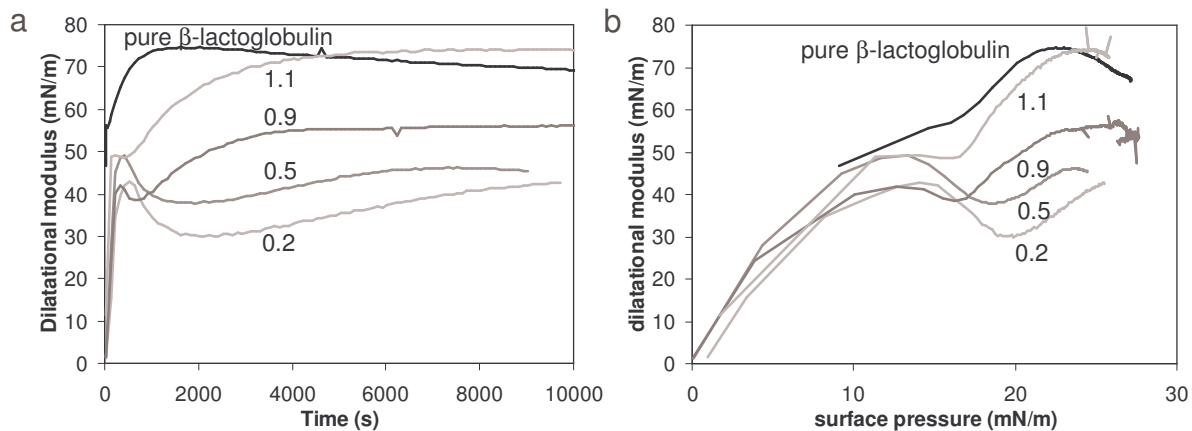


Figure 6.5: Dilatational modulus for different β -lactoglobulin/pul4 charge ratios (as indicated) as a function of a: time and b: surface pressure, β -lactoglobulin concentration was 0.1 g/L, pH was 4.5 and 12mM

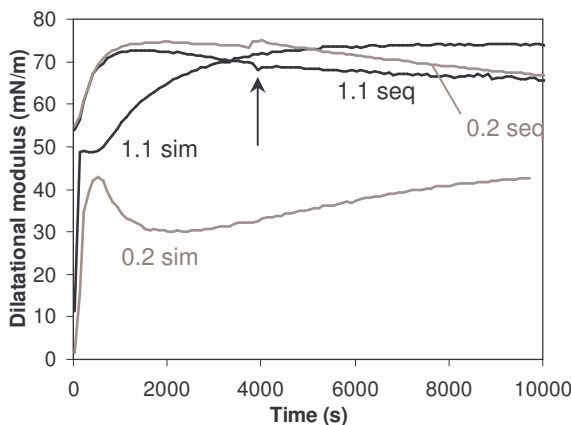


Figure 6.6: Comparison of dilatational modulus as a function of time for simultaneous and sequential adsorption; simultaneous adsorption is adsorption of β -lactoglobulin/pullulan complexes, with sequential adsorption β -lactoglobulin was allowed to adsorb before pullulan was added (indicated with the arrow), charge ratios are indicated in the graph; pH 4.5, 12mM

In the experiments described above, the protein and polysaccharide were allowed to adsorb to the interface simultaneously. Figure 6.6 shows the result of sequential adsorption; in that case first protein could adsorb from a pure protein solution, and subsequently a concentrated polysaccharide solution was added to the sample to reach final CR values of 0.2

and 1.1 respectively. Upon addition of the polysaccharide (as indicated by the arrows in figure 6.6) the dilatational modulus did not significantly change.

Finally the effect of CR on the cohesion in the adsorbed layer was investigated using surface shear rheology (Figure 6.7). Although the surface shear modulus of the mixtures is somewhat higher than for pure protein, there is no significant trend in the shear modulus as a function of CR. The steady state stress during continuous deformation is slightly higher for the mixtures with pullulan than for the pure protein layer. Again there is no clear trend with CR. Furthermore, there is no significant difference between a layer formed by simultaneous β -lactoglobulin/pullulan adsorption and a layer formed by sequential adsorption (Figure 6.7).

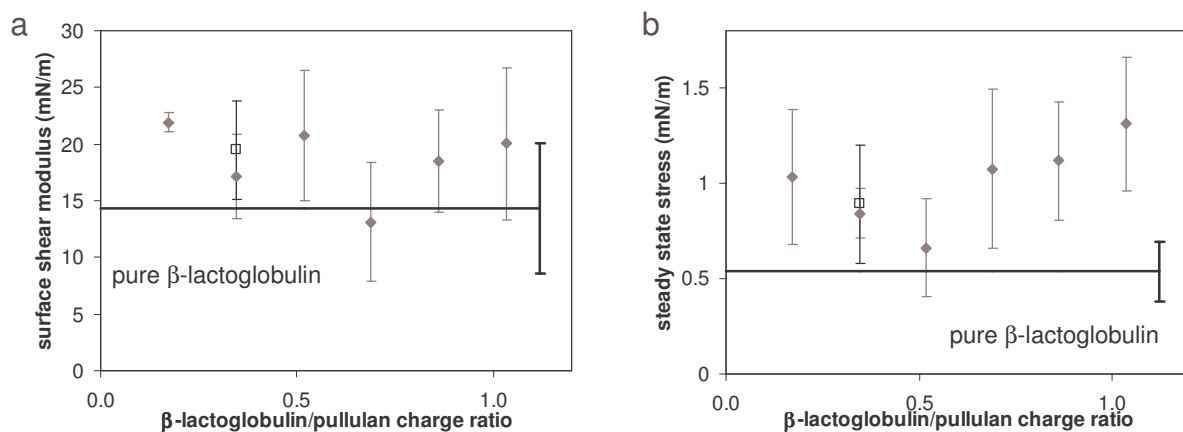


Figure 6.7: Surface shear modulus (a) and steady state shear stress (b) for mixtures of different protein/pullulan CR. The open square is a layer where protein was adsorbed at the interface before the pullulan was introduced in the solution below the interface (sequential adsorption). For all samples the protein concentration was 0.1 g/l, pH 4.5 and 19 mM.

6.4 DISCUSSION

6.4.1 Bulk complexation

The increase in scattered light intensity upon gradual addition of protein to pullulan together with a reduction in negative net charge (as concluded from ζ -potential measurements, figure 6.2), indicates that the pullulan molecules take up protein added to the solution. The sharp increase in hydrodynamic radius for the mixtures with pul4, pul3 and pul2, indicating the formation of insoluble complexes and/or the onset of complex coacervation (from our measurements we cannot distinguish these two cases) occurred at a CR of about 1 (Figure 6.1). At this CR the negative charge on the pullulan is compensated by the net positive charge on the protein. The observation that complex coacervation occurred at CR 1 both for pul3 and pul4 indicates that the majority of the protein is bound when the complexes aggregate (or in both cases the same fraction of protein binds but this is unlikely for two different pullulans). An increased turbidity hindering the light to pass through the sample at higher CR may account for the observed decrease in scattered light intensity with pul3 and pul4; due to the strong protein/polysaccharide interaction heterogeneity in the stoichiometry of complexes may occur upon addition of protein at pH 4.5. Association of some (close to) neutral complexes before the overall CR is 1 largely affects the scattered light intensity.

The ζ -potentials of the complexes did not reduce to zero at a CR of 1 (Figure 6.2). It approaches zero only when increasing CR above 1 and the point where it becomes zero shifts to higher CR in the order pul4, pul3, pul2, suggesting that higher charge density pullulan is more efficiently neutralised with protein than lower charge density pullulan. An explanation for this may be the distance between charges at the polysaccharide backbone. The higher the charge density, the higher the amount of diades: 2 carboxyl groups directly next to each other. The radius of a β -lactoglobulin molecule (dimer) is about 4.5 nm and the size of a monosaccharide ~0.5 nm. Because only two monosaccharides in each trimer can have a carboxyl group, there are maximal 2 charges per 1.5 nm contour length. Assuming that the charges are equally divided over the polysaccharide backbone, the lowest charge density pullulan contains only 1 carboxyl group on a chain section with the length of a protein diameter. The highest charge density pullulan has 6 carboxyl groups on the same stretch. A protein molecule may need a minimum number of carboxyl groups to interact with in order to bind sufficiently strongly to the polysaccharide. This could explain the more efficient neutralisation of complexes with increasing charge density. An alternative explanation could be that because the binding is weaker at lower charge density the complexes may be more easily disrupted by the electric field applied for the measurement of the ζ -potential.

Although the ζ -potential of the mixture with pul1 (the lowest charge density) at CR 1 is closer to neutral than for the other samples, the complexes do not macroscopically phase separate. This illustrates that a small net charge is able to prevent complexes from aggregation, but a reduction in net charge alone is not a driving force for the complexes to aggregate. Obviously, the solubility of complexes depends on the balance between complex-complex interaction and complex-solvent interaction. Pullulan on its own, also the non-carboxylated form, is well soluble. β -lactoglobulin self-associates at pH 4.5 in the absence of pullulan, as follows from a higher scattered light intensity in the absence of pullulan than in the presence of pul1 (data not shown). The sum of β -lactoglobulin-solvent interaction and pullulan-solvent interaction in a complex determines whether the complex is soluble or not. Not only a sufficient amount of net charge but also a sufficient amount of uncharged pullulan, as with pul1 above CR1, can make the total complex-complex affinity lower than complex-solvent affinity. In other words: pul1 is able to solubilise the protein (under conditions where protein would tend to aggregate). It seems that for the complexes to aggregate/coacervate, a sufficient amount of protein in/on the outside of the complexes, in combination with a small enough net charge is required. Complexes do not need to be completely neutral: aggregation of negatively charged complexes has also been shown by others^{33,34}.

6.4.2 Complexes at interfaces

Complexation of protein with polysaccharide can reduce the rate of surface pressure development in two ways. Firstly, it lowers the diffusion coefficient in bulk, due to the much larger hydrodynamic radius of the complexes compared to that of the free protein molecules. Secondly, complexation of the protein with pullulan may hinder an efficient packing of protein molecules at the interface by a hampered release of protein from the complex towards

the interface. The diffusion rate will not depend on the charge ratio; the size of the complexes is similar for all charge densities. However, the second effect, a hampered release of protein molecules from the complexes towards the interface (chapter 3), is presumably more important when interaction becomes stronger. This explains not only the increasing trend of the lag time with increasing charge density (Figure 6.3a), but also the decreasing trend of dilatational modulus with increasing charge density (Figure 6.3b). The presence of an excess of pullulan, which is the case at CR 0.5, ensures that all complexes are negatively charged and therefore repel each other. Since pullulan by itself is not surface active, the protein molecules in the complex are responsible for its adsorption at the interface. In chapter 3 it was shown that surface pressure of an adsorbed protein layer did not decrease after extensively rinsing the bulk solution with buffer. Due to their high affinity for the interface, β -lactoglobulin molecules tend to adsorb irreversibly. Multi-point interaction of the high charge density pullulan molecules (in an adsorbed complex) to several adsorbed β -lactoglobulin molecules at the same time makes also the adsorption of the pullulan irreversible. Especially when the complexes are strongly negatively charged, complexes in the interface will repel each other. This effect could hinder further adsorption of complexes (and thus also protein) to the interface, preventing the layer to become as compact as a pure protein layer. The result is a more compressible layer, resulting in a lower modulus (Figure 6.5). The compressibility of the layer increases with an increasing excess of polysaccharide, which explains the decrease of dilatational modulus with decreasing CR (Figure 6.5). Furthermore, the lower the charge density of the pullulan, the less binding sites it has for attaching to proteins at the interface. As a consequence the chance that the whole molecule detaches from the interface, making space for the adsorption of new complexes/protein molecules, increases. This will eventually lead to the formation of a denser protein layer, having a higher dilatational modulus. In effect, a high charge density of a polysaccharide, under conditions where complexes are (highly) negatively charged, constitutes a kinetic barrier for the formation of a dense protein layer. Addition of pullulan to the sample solution (up to a CR as low as 0.2) after a protein layer has been formed and the dilatational modulus has reached a steady state, did not affect the modulus (Figure 6.6). The modulus retained its value which was higher than in the situation where the pullulan was present before the protein was exposed to the interface. The fact that two different steady state values of dilatational modulus are found for systems with the same overall concentrations and solvent conditions, means that (at least) one of the two systems is thermodynamically not in equilibrium. It is presumably the irreversible character of protein adsorption that causes the system to be kinetically trapped.

Because with surface shear rheology the shape and not the size of interfacial area changes, surface pressure remains constant during deformation. Therefore, as compared to dilatational rheology, surface shear rheology is more sensitive to the cohesion within and between complexes in adsorbed layers. The surface shear modulus for all the mixtures is slightly higher than that of a pure protein layer, and no trend with charge density or CR is observed (figures 4a and 7a). Apparently the presence of polysaccharides in the interface only marginally influences the shear stress at small deformations in the interface. However, the

steady state shear stress, at large and continuous deformation, is significantly higher than that of a pure β -lactoglobulin layer for all β -lactoglobulin/pullulan mixtures, except for the lowest pullulan charge density. This may correspond to the fact that soluble complexes with the latter pullulan sample do not phase separate, even though the net charge of the complex at a charge ratio of 1 is lower than that with the higher charge density pullulans. If the complexes do not aggregate in bulk, they cannot form thick aggregated layers, nor show strong cohesion within the adsorbed layer, in contrast to the layers with the higher charge density pullulans.

Our conclusions concerning the influence of the pullulan charge density on complex behaviour and on adsorption as described in this work could be extrapolated to the behaviour of β -lactoglobulin in complexes with low methoxyl pectin, which has a higher charge density than the pullulan samples (chapter 3). The charge density of pectin is 0.7 and that of pul4 is 0.56. The molar mass of both polysaccharides is comparable ($\sim 150\ 000\ \text{g/mol}$). The ζ -potential of the pectin complexes at low CR is lower than that of pul4, and the approach to a zero net charge is steeper than that with pul4 (chapter 3). In both cases the onset of the increase in hydrodynamic radius is at the same CR (approximately at CR 1). The retarding effect on surface pressure and on dilatational modulus, which increases with pullulan charge density, is even stronger with pectin. Whereas with pectin a maximum in surface shear modulus and steady state stress was found around CR 1, such effect was not observed with pullulan. If these effects were less pronounced with pullulan due to its lower charge density, possibly the reproducibility of the surface shear measurements did not allow the observation of such a trend. One could imagine that two effects interfere. On the one hand, a high charge density polysaccharide, at conditions where the complexes are (strongly) negatively charged, may cause a higher kinetic barrier for the formation of a compact protein layer, as suggested before. A low charge density, on the other hand, could be less efficient in forming aggregated, cohesive complex layers.

6.5 CONCLUSIONS

Polysaccharide charge density largely affects the solubility of protein/polysaccharide complexes. Both a sufficient net charge, as well as a sufficient amount of uncharged (well soluble) pullulan in/on the outside of the complexes, can prevent complex coacervation. The higher the charge density, the more the protein molecules are hindered to form a compact adsorbed layer at the air/water interface at low CR, resulting in a stronger retardation in increase of surface pressure and dilatational modulus. This effect can be circumvented by introducing the polysaccharide after formation of an adsorbed protein layer. Close to CR 1, higher charge density polysaccharides (≥ 0.26) may provide stronger cohesion within the adsorbed layer. This study shows that the charge density of a polysaccharide is a powerful parameter to control properties of protein/polysaccharide complexes in solution and adsorbed complex layers at air/water interfaces. Hence, selecting a polysaccharide with a suitable charge density is a powerful alternative to changing protein/polysaccharide concentrations or system parameters like pH and ionic strength.

ACKNOWLEDGEMENTS

The authors would like to thank Renko de Vries and Stefan van der Burgh from SOFTLINK for the supply of the carboxylated pullulan samples and for their advice, and Bram Sperber for his help with the light scattering experiments.

REFERENCES

- (1) Cooper, C. L.; Dubin, P. L.; Kayitmazer, A. B.; Turkmen, S., Polyelectrolyte-protein complexes. *Current Opinion in Colloid & Interface Science* **2005**, 10, (1-2), 52-78.
- (2) de Kruif, C. G.; Weinbreck, F.; de Vries, R., Complex coacervation of proteins and anionic polysaccharides. *Current Opinion in Colloid & Interface Science* **2004**, 9, (5), 340-349.
- (3) Turgeon, S. L.; Beaulieu, M.; Schmitt, C.; Sanchez, C., Protein-polysaccharide interactions: phase-ordering kinetics, thermodynamic and structural aspects. *Current Opinion in Colloid & Interface Science* **2003**, 8, (4-5), 401-414.
- (4) Benichou, A.; Aserin, A.; Garti, N., Protein-polysaccharide interactions for stabilization of food emulsions. *Journal of Dispersion Science and Technology* **2002**, 23, (1-3), 93-123.
- (5) Dickinson, E., Hydrocolloids at interfaces and the influence on the properties of dispersed systems. *Food Hydrocolloids* **2003**, 17, (1), 25-39.
- (6) Graham, D. E.; Phillips, M. C., Proteins at Liquid Interfaces.1. Kinetics of Adsorption and Surface Denaturation. *Journal of Colloid and Interface Science* **1979**, 70, (3), 403-414.
- (7) MacRitchie, F.; Alexander, A. E., Kinetics of Adsorption of Proteins at Interfaces.1. Role of Bulk Diffusion in Adsorption. *Journal of Colloid Science* **1963a**, 18, (5), 453-457.
- (8) MacRitchie, F.; Alexander, A. E., Kinetics of Adsorption of Proteins at Interfaces.2. Role of Pressure Barriers in Adsorption. *Journal of Colloid Science* **1963b**, 18, (5), 458-463.
- (9) Tripp, B. C.; Magda, J. J.; Andrade, J. D., Adsorption of Globular-Proteins at the Air/Water Interface as Measured Via Dynamic Surface-Tension - Concentration-Dependence, Mass-Transfer Considerations, and Adsorption-Kinetics. *Journal of Colloid and Interface Science* **1995**, 173, (1), 16-27.
- (10) Beverung, C. J.; Radke, C. J.; Blanch, H. W., Protein adsorption at the oil/water interface: characterization of adsorption kinetics by dynamic interfacial tension measurements. *Biophysical Chemistry* **1999**, 81, (1), 59-80.
- (11) Benjamins, J.; Cagna, A.; Lucassen-Reynders, E. H., Viscoelastic properties of triacylglycerol/water interfaces covered by proteins. *Colloids and Surfaces A* **1996**, 114, 245-254.
- (12) Dickinson, E., Structure And Composition Of Adsorbed Protein Layers And The Relationship To Emulsion Stability. *Journal of The Chemical Society-Faraday Transactions* **1992**, 88, (20), 2973-2983.
- (13) Dickinson, E.; Pawlowsky, K., Effect of l-carrageenan on flocculation, creaming, and rheology of a protein-stabilized emulsion. *Journal of Agricultural and Food Chemistry* **1997**, 45, (10), 3799-3806.
- (14) Einhorn-Stoll, U., Interactions of whey proteins with different pectins in O/W emulsions. *Nahrung* **1998**, 42, (3/4), 248-249.
- (15) Tokaev, E. S.; Gurov, A. N.; Rogov, I. A.; Tolstoguzov, V. B., Properties of oil/water emulsions stabilized by casein-acid polysaccharide mixtures. *Nahrung* **1987**, 31, (8), 825-834.
- (16) Guzey, D.; Kim, H. J.; McClements, D. J., Factors influencing the production of o/w emulsions stabilized by β -lactoglobulin-pectin membranes. *Food Hydrocolloids* **2004**, 18, (6), 967.
- (17) Ogawa, S.; Decker, E. A.; McClements, D. J., Production and characterization of O/W emulsions containing droplets stabilized by lecithin-chitosan-pectin multilayered membranes. *Journal of Agricultural and Food Chemistry* **2004**, 52, (11), 3595-3600.

- (18) Baeza, R.; Sanchez, C. C.; Pilosof, A. M. R.; Patino, J. M. R., Interactions of polysaccharides with beta-lactoglobulin adsorbed films at the air-water interface. *Food Hydrocolloids* **2005**, 19, (2), 239-248.
- (19) Schmitt, C.; da Silva, T. P.; Bovay, C.; Rami-Shojaei, S.; Frossard, P.; Kolodziejczyk, E.; Leser, M. E., Effect of time on the interfacial and foaming properties of beta-lactoglobulin/acacia gum electrostatic complexes and coacervates at pH 4.2. *Langmuir* **2005**, 21, (17), 7786-7795.
- (20) Kaibara, K.; Okazaki, T.; Bohidar, H. B.; Dubin, P. L., pH-Induced Coacervation in Complexes of Bovine Serum Albumin and Cationic Polyelectrolytes. *Biomacromolecules* **2000**, 1, (1), 100-107.
- (21) Girard, M.; Turgeon, S. L.; Gauthier, S. F., Thermodynamic parameters of beta-lactoglobulin-pectin complexes assessed by isothermal titration calorimetry. *Journal of Agricultural And Food Chemistry* **2003**, 51, (15), 4450-4455.
- (22) Dickinson, E.; Semenova, M. G.; Antipova, A. S.; Pelan, E. G., Effect of high-methoxy pectin on properties of casein-stabilized emulsions. *Food Hydrocolloids* **1998**, 12, 425-432.
- (23) Duce, V.; Richard, J.; Popineau, Y.; Boury, F., Rheological interfacial properties of plant protein-arabic gum coacervates at the oil-water interface. *Biomacromolecules* **2005**, 6, (2), 790-796.
- (24) de Nooy, A. E. J.; Besemer, A. C.; van Bekkum, H.; van Dijk, J. A. P. P.; Smit, J. A. M., TEMPO-Mediated Oxidation of Pullulan and Influence of Ionic Strength and Linear Charge Density on the Dimensions of the Obtained Polyelectrolyte Chains. *Macromolecules* **1996**, 29, (20), 6541-6547.
- (25) Blumenkr.N; Asboehan.G, New Method For Quantitative-Determination Of Uronic Acids. *Analytical Biochemistry* **1973**, 54, (2), 484-489.
- (26) Thibault, J. F., Automated-Method For The Determination Of Pectic Substances. *Lebensmittel-Wissenschaft & Technologie* **1979**, 12, (5), 247-251.
- (27) Tollier, M. T.; Robin, J. P., Adaptation Of The Orcinol-Sulfuric Acid Method For The Automatic Titration Of Total Neutral Sugars - Conditions Of Application To Plant-Extracts. *Annales de Technologie Agricole* **1979**, 28, (1), 1-15.
- (28) de Jongh, H. H. J.; Groneveld, T.; de Groot, J., Mild isolation procedure discloses new protein structural properties of beta-lactoglobulin. *Journal of Dairy Science* **2001**, 84, (3), 562-571.
- (29) Berne, B. J.; Pecora, R., *Dynamic Light Scattering: with applications to Chemistry, biology, and Physics*. 2000 ed.; General Publishing Company, Ltd.: Toronto, 1976.
- (30) van der Burgh, S.; de Keizer, A.; Cohen Stuart, M. A., Complex coacervation core micelles. Colloidal stability and aggregation mechanism. *Langmuir* **2004**, 20, (4), 1073-1084.
- (31) Martin, A.; M., B.; Cohen Stuart, M.; Vliet, T. v., Stress-strain curves of adsorbed protein layers at the air/water interface measured with surface shear rheology. *Langmuir* **2002**, 18, 1238-1243.
- (32) Wierenga, P. A.; Kosters, H.; Egmond, M. R.; Voragen, A. G. J.; de Jongh, H. H. J., Importance of physical vs. chemical interactions in surface shear rheology. *Advances in Colloid and Interface Science* **2006**, 119, (2-3), 131.
- (33) Mekhloufi, G.; Sanchez, C.; Renard, D.; Guillemin, S.; Hardy, J., pH-induced structural transitions during complexation and coacervation of beta-lactoglobulin and acacia gum. *Langmuir* **2005**, 21, (1), 386-394.
- (34) Xia, J. L.; Dubin, P. L.; Kim, Y.; Muhoberac, B. B.; Klimkowski, V. J., Electrophoretic And Quasi-Elastic Light-Scattering Of Soluble-Protein Polyelectrolyte Complexes. *Journal of Physical Chemistry* **1993**, 97, (17), 4528-4534.

Complex coacervate morphology controlled by polysaccharide charge density

ABSTRACT

Upon mixing oppositely charged protein and polyelectrolyte, a complex coacervate phase can be formed. Since this process is dominated by electrostatic interaction the appearance of the coacervate phase presumably depends on the charge density of the protein and polysaccharide. This study shows that the distance between β -lactoglobulin molecules in a coacervate phase with carboxylated pullulan decreases upon increasing the charge density of the polysaccharide. The observation that the protein-protein distance is larger in a β -lactoglobulin/pectin coacervate while the charge density of pectin is higher than that of pullulan illustrates that charge density is not the only parameter involved.

The observation that with pullulan a liquid coacervate phase and with pectin a precipitate is formed suggests that reorganizations (e.g. mobility of protein through the complexes) within the coacervate phase with pectin are slower than with pullulan. A stronger interaction with pectin due to a more heterogeneous charge distribution and/or the higher charge density may account for this. Possibly the ‘frozen’ state of the concentrated β -lactoglobulin/pectin phase prevents the ‘shrinking’ to smaller protein-protein distances as would be expected based on the charge density.

7.1 INTRODUCTION

Due to electrostatic interaction, anionic polysaccharides can interact with protein molecules that bear positive (and negative) charges and form protein/polysaccharide complexes. Depending on the balance between complex-complex interaction and complex-solvent interaction, complexes may be soluble (e.g. when they are charged) or they may associate leading to phase separation to form a concentrated liquid phase. This type of phase separation is called complex coacervation; the concentrated or 'coacervate' phase contains both protein and polysaccharide and the dilute phase is the solvent with possibly an excess of either component. A coacervate phase of whey protein and gum arabic has been shown to have a viscous character¹ in which the protein and the polysaccharides can independently diffuse (with a lower diffusion coefficient than in dilute aqueous solutions due to the high viscosity and electrostatic interaction)². A certain regularity in the spatial distribution of proteins in the coacervate phase has been found for this system using small angle X-ray scattering³. From the typical distance between protein molecules, the protein density in the complex coacervate can be estimated. The morphology of the coacervate phase depends on the interaction between protein and polysaccharide and thus also on the type of protein and polysaccharide used⁴.

In previous work surface rheological behaviour of adsorbed β -lactoglobulin/pectin and β -lactoglobulin/pullulan complexes at the air/water interface was studied. These layers were formed from soluble complexes and the driving force for the accumulation of complexes at the interface is the affinity of protein (in the complexes) for the interface. This is different from complex coacervation where complex-complex affinity is the driving force for association of complexes. However, a better insight in the structure of coacervate phases may help to understand the structure of an adsorbed complex layer. Therefore the aim of this study is to investigate how the spatial distribution of β -lactoglobulin in (and the macroscopic appearance of) the coacervate phase depends on the charge density of the polysaccharide.

7.2 MATERIALS AND METHODS

7.2.1 Materials

Five polysaccharides with different charge densities were used for this study. Pullulan is an uncharged polysaccharide that was carboxylated to four different charge densities. See chapter 6 for the carboxylation procedure. The charge density (defined as the fraction of anionic monosaccharide units) of pul1, pul2, pul3 and pul4 was respectively 0.10, 0.26, 0.51 and 0.56. The last polysaccharide sample is low methoxyl pectin (Imp), which had a charge density of 0.70 (see chapter 3). The average molar mass of the polysaccharides is $\sim 1.5 \cdot 10^5$ g/mol. Pullulan stock solutions (10-15 g/L) were prepared by subsequently dissolving the freeze dried powder in deionised water (Barnstead EASYpure UV, USA), stirring (magnetic stirrer) for 30 min and heating at 70°C using a thermostated waterbath for 30 minutes. A pectin stock solution (8 g/L) was prepared by slowly dispersing the powder on the surface of thoroughly stirred (magnetic stirrer) and heated deionised water and subsequently heating at 70°C for 30 minutes. After overnight storage at 35°C, the pectin solution was centrifuged at

6000g for 10 minutes. All polysaccharide stock solutions were stored at 4°C until further use. A concentrated acetic acid solution (250 mM, pH 4.5) was prepared from analytical grade chemicals and deionised water. Bovine β -lactoglobulin was purified using a non denaturing method as described previously⁵. Protein stock solutions (40 g/L) were prepared freshly by dissolving the freeze dried protein in water. The pH of the protein stock solutions was 6.8 \pm 0.2.

Coacervate samples were prepared by subsequent addition of 1M NaOH or HCl, stock protein solution and stock acetic acid to the stock pectin solution and mixing (Vortex). The final conditions of the samples were pH 4.5, I ~9 mM and acetate concentration 25 mM. Protein and polysaccharide were mixed at a charge ratio (CR) of 1 (this means that the negative charge on the polysaccharide was just compensated by the positive net charge on the protein, based on proton titration curves of the individual components, see chapter 8). Only for the sample indicated with 'ImpCR0.25' protein and polysaccharide were mixed at a charge ratio of 0.25, which means a large excess of pectin. Phase separation was promoted by centrifugation of the mixtures at 4500g for 20 min after which measurements were performed on the concentrated phase.

7.2.2 Small angle X-ray scattering

Scattered X-ray intensities (I) were measured as a function of scattering wave vector (Q) at the Dutch-Belgian beam line (DUBBLE) at the European Synchrotron Radiation Facility (ESRF) in Grenoble (France). The wavelength of the X-rays was 0.93 Å and the (two-dimensional, 512x512 pixels, gas-filled) detector was placed at 5.5 m from the sample, which yielded scattering data in the Q-range: 0.07 - 1.1 nm⁻¹. The coacervate samples were placed in cuvettes with a sample volume of 20 mm³ and measurements were performed at room temperature.

7.2.3 Microscopy

Protein/polysaccharide mixtures were prepared as described in the materials section, with the difference that in this case the samples were not centrifuged. The samples were examined under a light microscope (Olympus BX 60, Olympus Nederland B.V., Zoeterwoude, The Netherlands) 30 min after mixing and 24 hours after mixing (separate microscopic preparations were prepared for the different times). Images were taken using an Olympus DP 70 camera.

7.3 RESULTS AND DISCUSSION

A peak in the X-ray scattering pattern is indicative of the presence of a dominant length scale in the sample. In the scattering patterns (I(Q) plots) of all the samples a peak is observed at around 0.7 nm⁻¹, except for the coacervate prepared with the lowest pullulan charge density (pul1): in this case the scattering intensity only steadily decreases from 0.07 to 1.1 nm⁻¹ (data not shown). A peak in the scattering pattern is indicative of the presence of a dominant length scale in the sample. The dominant length scales observed could either be the size of particles, or a preferred distance between particles. The size of β -lactoglobulin molecules is too small to be observed in the Q-range retrieved from the measurements. The size of complexes is not

observable since the concentration of the samples is above the overlap concentration. Therefore, the absence of peaks (in the pul1 sample) indicates that there is no preferred protein-protein distance and the coacervate phase is not structured. For this reason the coacervate with pul1 can serve as a blank. To emphasize the peaks observed with the other samples, the scattering patterns were normalized by the $I(Q)$ value of the pul1 sample.

7.3.1 Charge density dependence

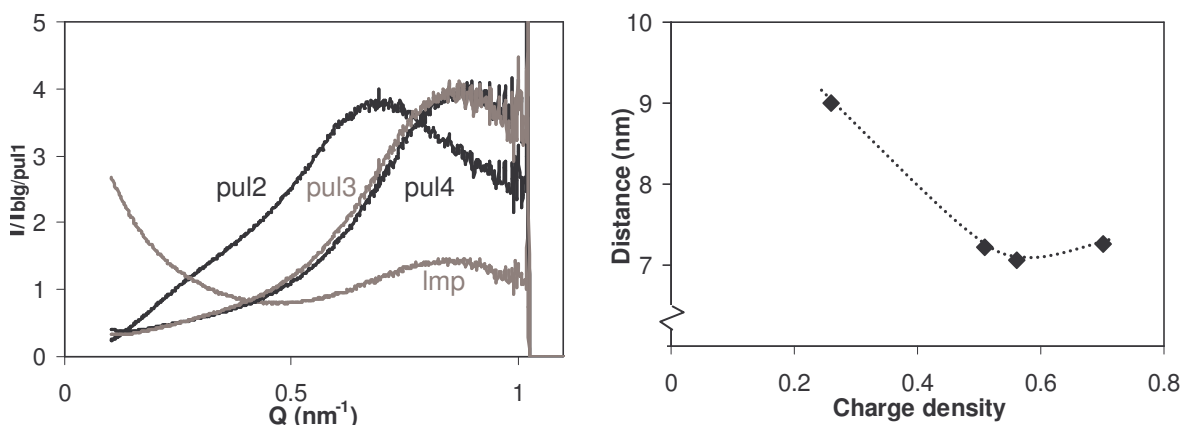


Figure 7.1: a) Normalised scattered X-ray intensity as a function of Q (wave vector) for coacervate phases of β -lactoglobulin and polysaccharides with different charge densities; all data were divided by the curve of the coacervate with the lowest charge density polysaccharide (pul1). b) Preferred distance between β -lactoglobulin molecules in the coacervate phase as a function of the charge density of the polysaccharide. The dotted line is to guide the eye. Please note that the y-axis does not start at the origin. The accuracy in distance is estimated to be within 2%. The pH was 4.5 and 19 mM, the age of the coacervate samples was 3 days.

In figure 7.1a the normalized scattering patterns are given for β -lactoglobulin/polysaccharide coacervates with polysaccharides with varying charge density. The preferred distance (d) between the protein molecules (the regularity in the spatial distribution) can now be determined from the position of the peak (Q_{max}) by $d = 2\pi/Q_{\text{max}}$ (figure 7.1b). It becomes then clear that the distance between protein molecules decreases with increasing charge density of pullulan from 9 nm for a charge density of 0.26 to 7.1 nm for a charge density of 0.56. Surprisingly, for the coacervates with pectin (with a charge density of 0.70) the distance between the protein molecules is larger than that of pullulan with the highest charge density. Furthermore, the peak observed with pectin in figure 7.1a is lower in intensity than that observed for pullulan. This could indicate that with pectin there is more heterodispersity in the spacing between the protein molecules in the coacervate phase.

From the distance between protein molecules, the volume fraction (ϕ) of protein in the coacervate phase can be estimated by:

$$\phi = 0.74 \cdot V_{\text{prot}} / \left(\frac{1}{6} \cdot \pi \cdot d^3 \right),$$

Where V_{prot} is the molecular volume of the β -lactoglobulin dimer (which is the predominant state of β -lactoglobulin at pH 4.5 and low ionic strength⁶). The value of 0.74 refers to the volume fraction of a hexagonal close packing of spheres and is arbitrarily selected since it is not known how the molecules are organised. The volume fractions were converted to the total

biopolymer concentration in w/w% (Table 7.1), by using the specific volume of protein ($0.750 \cdot 10^{-3} \text{ m}^3 \text{kg}^{-1}$)⁷ and the protein/polysaccharide w/w ratio at CR = 1. The obtained concentrations are in the same range as found for coacervate phases by others^{3,8}.

It is generally accepted that before a coacervate phase is formed, protein molecules bind to polysaccharide molecules to form intrapolymer complexes. These intrapolymer complexes subsequently associate (interpolymer complexes) to finally form a coacervate phase (see chapter 1). To estimate the total biopolymer concentration in a net neutral intrapolymer complex of β -lactoglobulin and pectin two assumptions are made: (1) the radius of the intrapolymer complex with pectin is ~20 nm (based on the 40 nm thickness of an adsorbed complex layer at the air/water interface, as determined using neutron reflection), (2) a soluble complex consists of a single pectin molecule and just enough protein molecules for a full charge compensation (CR in the complex is 1). This results in an estimation of the total biopolymer concentration in the intrapolymer complex of ~6.4% (protein volume fraction of ~4.3%), suggesting that solvent is exuded from the complexes upon formation of the coacervate phase, as previously described by Cooper et al⁸.

Table 7.1: Estimated β -lactoglobulin volume fractions and total biopolymer (β -lactoglobulin and pectin) concentrations in coacervate phases. The pH was 4.5 and 19 mM, the age of the coacervate samples was 3 days.

sample	protein volume fraction (%)	total biopolymer concentration (w/w%)
pul2	9	15
pul3	17	25
pul4	18	26
Imp	16	23

7.3.2 Charge ratio dependence

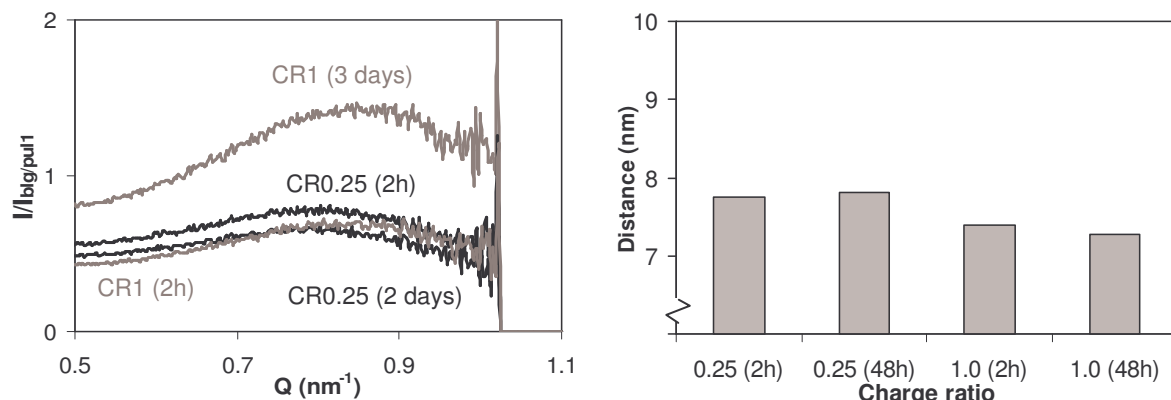


Figure 7.2: a) Normalised scattered X-ray intensity as a function of Q (wave vector) for coacervate phases of β -lactoglobulin and pectin prepared from different charge ratios and measured at different times after preparation; all data were divided by the curve of the coacervate with the lowest charge density polysaccharide (pul1). b) Preferred distance between β -lactoglobulin molecules in the coacervate phase as a function of the charge density of the polysaccharide. Please note that the y-axis does not start at the origin. The accuracy in distance is estimated to be within 2%. The pH was 4.5 and 19 mM.

An interesting question is whether complexes need to be net neutral before they can associate^{9, 10}. If this were the case, the composition of a coacervate phase would be independent of the initial charge ratio at which protein and polysaccharide are mixed. To

investigate whether this is true for the β -lactoglobulin/pectin coacervates, β -lactoglobulin and pectin were mixed at two different charge ratios: 0.25 and 1. At CR 0.25 pectin is in excess; only 25% of its charge can be compensated by protein. Two extreme situations could be imagined for the CR0.25 sample: (i) if protein molecules were equally distributed over the pectin molecules, no coacervate would be formed because all complexes would be strongly negatively charged, (ii) alternatively, a neutral coacervate phase is formed and the excess pectin will be in the dilute phase. In both samples (CR0.25 and CR1) a coacervate phase was formed and X-ray scattering data are shown in figure 7.2a, at \sim 2 hours and 2 or 3 days after preparation of the coacervate sample. The difference in protein-protein distance between the two samples (CR0.25 7.8 nm, CR1 7.3 nm) suggests that the structure of the coacervate depends on the ratio in which protein and polysaccharide were mixed before complex coacervation took place. An excess net charge in the CR0.25 coacervate could count for the larger protein-protein distance. If neutral complexes would be the most favourable state as reported by De Kruif et al.⁴, these data show that reorganizations within the coacervate are very slow (if occurring at all); there is no difference between a 2 hours and a 2 days old coacervate. Weinbreck and co-workers² showed that the diffusion rate of arabic gum and whey protein molecules through the coacervate phase decreased when protein/polysaccharide interaction became stronger. They measured a roughly 10 times smaller diffusion coefficient of whey protein in the coacervate phase than in aqueous solution. Since pectin has a higher charge density than arabic gum, the diffusion of components through the coacervate, and thus also rearrangements in the coacervate phase, is likely more delayed (see chapter 8).

7.3.3 Light microscopy

The macroscopic appearance of the coacervate phases of β -lactoglobulin/pul4 and β -lactoglobulin/lmp (CR1) was different. With pullulan a liquid coacervate phase was formed, that stuck to the bottom of a glass beaker. The ‘coacervate’ phase formed with pectin did not stick to the glass. Both samples were examined under a light microscope (figure 7.3). The coacervate phase with pullulan, after 30 min (top left panel, figure 7.3) appears like liquid droplets; many round shapes of a few micrometers are observed that seem to coalesce in time (within a few hours). After 24 hours, the coacervate phase looks like a single ‘coherent’ phase (with a rough surface, bottom left panel, figure 7.3). With pectin the structure looks more like a precipitate (no droplet like shapes). Although the concentrated phase sedimented after 24 hours, the microscopic picture reveals that the concentrated phase is not coherent; many separate aggregate like structures are observed in the bottom right panel in figure 7.3.

Besides a difference in charge density, pectin differs from pullulan in three other aspects: First, the distribution of the charged groups on pectin is more heterogeneous (resulting in longer sequences of charged groups¹¹) compared to pullulan. The latter polysaccharide always has one neutral glucose monomer on each monosaccharide trimer and carboxylation was a chemical reaction, which is more random than enzymatic de-methylation of pectin. Secondly, pectin has methyl groups, which may lead to hydrophobic interaction in addition to electrostatic interaction. Finally, pullulan is a more flexible chain compared to pectin; the persistence length of oxidized pullulan is 1.3 nm¹² and for low methoxyl pectin values of 4.5

nm¹³ and 6-13 nm¹⁴ were reported. Especially the first difference may lead to stronger interaction between the protein molecules and pectin. This may lead to a more frozen ‘coacervate’ structure in which the diffusion of protein molecules is strongly retarded. De Kruif et al.⁴ state that when attraction is strong as is the case with strong polyacids like carrageenan (with sulphate groups) a precipitate phase can be formed. Apparently this is also the case with pectin, which is a weak polyacid (with carboxyl groups).

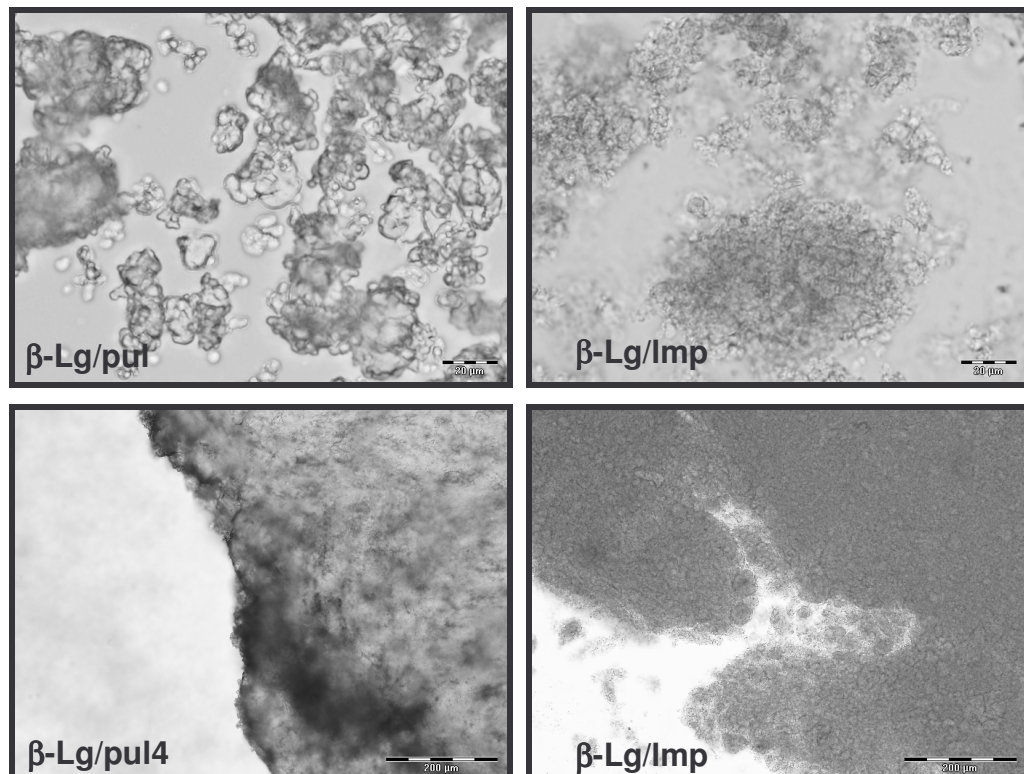


Figure 7.3: Coacervate phase of β -lactoglobulin (β -Lg) with pul4 (left) and Imp (right) as observed under the microscope; top frames 30 min after mixing the biopolymers, scale bar is 20 μm , bottom frame 24 hours after mixing, scale bar is 200 μm . The pH was 4.5 and 19 mM.

7.4 CONCLUSIONS

There is a regularity in spatial distribution of β -lactoglobulin molecules in a coacervate phase with carboxylated pullulan with a charge density of 0.26 or higher (up to 0.56). This preferred protein-protein distance increased with decreasing charge density until the regular structure had disappeared at a pullulan charge density of 0.10. The coacervate phases of β -lactoglobulin with pullulan appeared liquid. The concentrated phase (after associative phase separation) of β -lactoglobulin with pectin is more like a precipitate. This difference may indicate a much lower reorganization rate within the complexes with pectin due to the more heterogeneous charge distribution, or the higher charge density. Possibly the ‘frozen’ state of the concentrated β -lactoglobulin/pectin phase prevents the ‘shrinking’ to smaller protein-protein distances as would be expected based on the charge density. The structure of the concentrated phase formed from β -lactoglobulin and pectin depends on the initial mixing ratio; an excess of polysaccharide leads to a 7% larger preferred distance between the protein molecules in the

concentrated phase. The observed differences in the nature of coacervate phases formed from different polysaccharides and the estimated protein volume fractions may help to understand the structure of mixed adsorbed protein/polysaccharide layers at air/water interfaces.

ACKNOWLEDGEMENTS

We greatly acknowledge Kees de Kruif and Hans Tromp from NIZO food research for giving us the opportunity to do the SAXS measurements and for their help in interpreting the data. Furthermore we thank Renko de Vries and Stefan van der Burgh from the SOFTLINK program for supplying us with the carboxylated pullulan samples.

REFERENCES

- (1) Weinbreck, F.; Wientjes, R. H. W., Rheological properties of whey protein/gum arabic coacervates. *Journal of Rheology* **2004**, 48, (6), 1215-1228.
- (2) Weinbreck, F.; Rollema, H. S.; Tromp, R. H.; de Kruif, C. G., Diffusivity of whey protein and gum arabic in their coacervates. *Langmuir* **2004**, 20, (15), 6389-6395.
- (3) Weinbreck, F.; Tromp, R. H.; de Kruif, C. G., Composition and structure of whey protein/gum arabic coacervates. *Biomacromolecules* **2004**, 5, (4), 1437-1445.
- (4) de Kruif, C. G.; Weinbreck, F.; de Vries, R., Complex coacervation of proteins and anionic polysaccharides. *Current Opinion in Colloid & Interface Science* **2004**, 9, (5), 340-349.
- (5) de Jongh, H. H. J.; Gröneveld, T.; de Groot, J., Mild isolation procedure discloses new protein structural properties of beta-lactoglobulin. *Journal of Dairy Science* **2001**, 84, (3), 562-571.
- (6) Verheul, M.; Pedersen, J. S.; Roefs, S.; de Kruif, K. G., Association behavior of native beta-lactoglobulin. *Biopolymers* **1999**, 49, (1), 11-20.
- (7) Valdez, D.; Le Huerou, J. Y.; Gindre, M.; Urbach, W.; Waks, M., Hydration and protein folding in water and in reverse micelles: Compressibility and volume changes. *Biophysical Journal* **2001**, 80, (6), 2751-2760.
- (8) Cooper, C. L.; Dubin, P. L.; Kayitmazer, A. B.; Turksen, S., Polyelectrolyte-protein complexes. *Current Opinion in Colloid & Interface Science* **2005**, 10, (1-2), 52-78.
- (9) Mekhloufi, G.; Sanchez, C.; Renard, D.; Guillemin, S.; Hardy, J., pH-induced structural transitions during complexation and coacervation of beta-lactoglobulin and acacia gum. *Langmuir* **2005**, 21, (1), 386-394.
- (10) Xia, J. L.; Dubin, P. L.; Kim, Y.; Muhoberac, B. B.; Klimkowski, V. J., Electrophoretic And Quasi-Elastic Light-Scattering Of Soluble-Protein Polyelectrolyte Complexes. *Journal of Physical Chemistry* **1993**, 97, (17), 4528-4534.
- (11) Daas, P. J. H.; Boxma, B.; Hopman, A. M. C. P.; Voragen, A. G. J.; Schols, H. A., Nonesterified galacturonic acid sequence homology of pectins. *Biopolymers* **2001**, 58, (1), 1-8.
- (12) de Nooy, A. E. J.; Besemer, A. C.; van Bekkum, H.; van Dijk, J. A. P. P.; Smit, J. A. M., TEMPO-Mediated Oxidation of Pullulan and Influence of Ionic Strength and Linear Charge Density on the Dimensions of the Obtained Polyelectrolyte Chains. *Macromolecules* **1996**, 29, (20), 6541-6547.
- (13) Axelos, M. A. V.; Lefebvre, J.; Thibault, J. F., Conformation of a low methoxyl citrus pectin in aqueous solution. *Food Hydrocolloids* **1987**, 1, (5/6), 569-570.
- (14) Cros, S.; Garnier, C.; Axelos, M. A. V.; Imbert, A.; Perez, S., Solution conformations of pectin polysaccharides: Determination of chain characteristics by small angle neutron scattering, viscometry, and molecular modeling. *Biopolymers* **1996**, 39, (3), 339-352.

Polysaccharides as a kinetic barrier for protein accumulation at air/water interfaces

Renate A. Ganzevles, Jan Benjamins, Ton van Vliet, Martien A. Cohen Stuart
and Harmen H.J. de Jongh

ABSTRACT

The presence of anionic polysaccharides in a protein solution can affect protein adsorption to the air/water interface. Parameters affecting protein/polysaccharide interaction may therefore also influence adsorption kinetics. In this chapter in addition to surface pressure the adsorbed mass (using ellipsometry) is studied as a function of time (in addition to surface pressure) for complexes of β -lactoglobulin with different polysaccharides. By using a range of β -lactoglobulin/pectin complexes with different mixing ratios it was shown that compared to pure β -lactoglobulin the adsorption rate is two times slower for net neutral complexes and up to 200 times slower for negatively charged complexes. This retarding effect was observed in both surface pressure and adsorbed mass versus time, and increased with increasing molecular weight of the polysaccharide (10 times slower for a 5 times increase in M_w). Furthermore, the retarding effect also became stronger with increasing charge density on the polysaccharide (up to a factor of 100 for a 10 times increase in charge density). This work shows that the polysaccharide can constitute a kinetic barrier for protein adsorption at the air/water interface by electrostatic repulsion between and within complexes at the interface and a strongly reduced (up to 100 000 times) protein diffusion rate through the complex layer. This contributes to a more detailed insight in the dynamic character of protein/polysaccharide complexes at air/water interfaces.

8.1 INTRODUCTION

In chapter 2 it was shown that the presence of a polysaccharide can reduce the rate of surface pressure increase at the air/water interface. It was argued that this was due to decreased rate of mass accumulation at the interface. Two possible explanations can be given for a reduced adsorption rate: (i) a lower diffusion coefficient due to the larger size of the complexes compared to pure protein molecules, and (ii) adsorbed polysaccharide may provide electrostatic and steric hindrance for protein molecules to reach the interface once a complex is in close vicinity to the interface. When discussing adsorption kinetics, one should refer to adsorbed mass rather than to surface pressure. Between these two quantities there is no unambiguous quantitative relation, since this relation may be effected by the presence of the polysaccharide molecules at the interface. Co-adsorption of polysaccharides with proteins at the interface has been demonstrated by the different surface rheological behaviour in the presence of polysaccharides (chapter 3, 4 and 6) and by an increased adsorbed mass as shown by neutron reflection (chapter 5) both compared to a pure protein adsorbed layer. Neutron reflection is, however, not very suitable to follow adsorbed mass as a function of time, due to the long measuring times.

The aim of the study described in this chapter is to investigate how protein adsorption kinetics (in terms of adsorbed mass) can be controlled by protein/polysaccharide mixing ratio and by polysaccharide specificity; molecular weight and charge density. Although ellipsometry cannot distinguish protein and polysaccharide, following the total adsorbed mass as a function of time while simultaneously recording surface pressure may help to elucidate the nature of the retarding effect of polysaccharide on surface pressure increase (as was observed in chapter 2 and 6). Furthermore, the relation of surface pressure and adsorbed mass gives insight in the type of adsorbed layer.

8.2 MATERIALS AND METHODS

8.2.1 Materials

Low methoxyl pectin was supplied by CP Kelco (Lille Skensved, Denmark). The degree of methylation is 30.4 % (only the non-methylated galacturonic acid subunits have a free carboxyl group, $pK_a \sim 4.5$), the uronic acid content is 78.5 %¹, number averaged molecular weight (M_n) $1.5 \cdot 10^5$, polydispersity (M_w/M_n) 2.4 (chapter 2). Pectin stock solutions (1 g/l) were prepared by slowly dispersing the powder in thoroughly stirred (magnetic stirrer) and heated ($\sim 50^\circ\text{C}$) deionised water (Barnstead EASYPure UV, USA) and subsequently heating the dispersion at 60°C for 30 minutes. After overnight storage at room temperature, the samples were filtered (0.45 μm Acrodisc, Gelman Sciences, MI, USA) and stored at 4°C until further use.

A batch of the low methoxyl pectin was fractionated on molar mass, using gel-permeation-chromatography (two Sephadryl S500 columns in series: 4.3 + 3.5 liter, eluens 0.1 M Na-succinate buffer, flow rate 30 ml/min). Three fractions were collected; from 4000 – 4800 ml, 5200 – 5800 ml and 6200 – 7000 ml, corresponding to the left side, middle and right side of the peak observed in the elution pattern as measured by the refractive index (~ 5 to

10% of the material in the extreme left and right peak tail was not included). After ultra-filtration (cut-off 30 kDa) and extensive dialysis against deionised water to remove salts, the samples were freeze dried. Galacturonic acid content (71%) and neutral sugar content (0%) of the fractions were determined using an automated colorimetric m-hydroxydiphenyl method^{2,3} and orcinol method⁴, with galacturonic acid/galactose standards. Differences between the three fractions were within the accuracy of the method (< 5%). The degree of methylation of the different samples was determined by saponification of the ester groups by NaOH in water and subsequent analysis of the liberated methanol, using gas chromatography headspace analysis⁵. Differences between the fractions and the mother pectin were within the accuracy of the method (< 4%). Average molar mass of the fractions was determined by high-performance size-exclusion chromatography using three TSKgel columns (7.8 mm ID x 30 cm per column) in series (G4000 PWXL, G3000 PWXL, G2500 PWXL; Tosohas, Stuttgart, Germany), in combination with a PWX-guard column (Tosohas, Stuttgart, Germany). Elution of the material was performed with 0.2M NaNO₃ at 0.8 mL/min and was monitored by a refractive index detector (Shodex RI-101). Using a series of polygalacturonic acids for calibration, molecular weight of the fractions MW172, MW74 and MW39 was determined to be respectively 172·10³, 74·10³ and 39·10³.

Pullulan samples were carboxylated⁶ obtaining four different charge densities as described before (chapter 6). Pullulan stock solutions were prepared by dissolving the freeze dried material in water, stirring for 30 minutes, and subsequently heating at 60°C for 30 minutes. After overnight storage at room temperature, the samples were filtered and stored at 4°C until further use. After filtration pectin and pullulan stock concentrations were determined using an automated colorimetric m-hydroxydiphenyl method^{2, 3} and orcinol method⁴, with (for pectin) galacturonic acid/galactose and (for pullulan) glucuronic acid/glucose standards.

Bovine β -lactoglobulin (isoelectric point 5.1, molecular weight 36 600 in dimeric form) was purified using a non-denaturing method as described previously⁷. β -lactoglobulin stock solutions (1 g/l) were prepared freshly by overnight dissolving the freeze dried protein in deionised water. The pH of the protein stock solutions was 6.8 \pm 0.2. After filtration (0.45 μ m Acrodisc, Gelman Sciences, MI, USA) protein stock concentrations were determined using absorbance at 280 nm with an extinction coefficient of 9.56·10² m²g⁻¹.

Stock polysaccharide and protein solutions were diluted in a 5 mM sodium acetate solution to a protein concentration of 0.02 g/l and a polysaccharide concentration of 0.001 - 0.14 g/l (depending on the desired charge ratio). After adjustment of the solution pH to 4.5 (using 0.1 M HCl) under continuous stirring, protein/polysaccharide samples were equilibrated for 30 min before use in order to allow formation of protein/polysaccharide complexes. This procedure (first mixing at neutral pH and subsequent decreasing pH) promotes a homogenous distribution of protein over the polysaccharide molecules.

8.2.2 Dynamic light scattering

Second cumulant diffusion coefficients of the β -lactoglobulin/pectin complexes were determined by light scattering (at 90°)⁸, using an ALV 5000 light scattering instrument

(Langen, Germany) equipped with a 400 mW argon laser tuned at a wavelength of 514.5 nm, as described before⁹. From dynamic light scattering hydrodynamic radii were calculated according to the Stokes-Einstein relation, assuming that the complexes are spherical. Averages and standard deviations were calculated from sets of 10 measurements. Temperature was controlled at 20 ± 0.1 °C. Samples were prepared as described in the materials section, with the difference that protein concentration of these samples was 0.1 g/l. Hydrodynamic radii of the complexes with pullulan were deduced from chapter 6 where ionic strength was 9 mM, and protein was gradually titrated in the buffered polysaccharide solution.

8.2.3 Determination of ζ -potential

The electrophoretic mobility of soluble protein/polysaccharide complexes was measured using a zetasizer 2000 HS (Malvern instruments Ltd., UK) at 150 V applied voltage, using a He-Ne laser at 633 nm. The ζ -potential was calculated using the Helmholtz-Smoluchovski equation. Sample concentrations were chosen such that only a single narrow peak was observed in the scattered light intensity versus electrophoretic mobility curve. Protein concentration was 0.05 g/L for complexes with low methoxyl pectin, and 0.2 g/L for the fractionated pectin. Samples were prepared as described in the materials section, with the difference that in view of the higher protein/polysaccharide concentrations a more concentrated buffer was used (10 mM acetate). Average values and standard deviations were calculated over sets of 5 to 10 measurements.

8.2.4 Ellipsometry & Surface tensiometry

Adsorption kinetics of β -lactoglobulin and β -lactoglobulin/polysaccharide complexes to the air/water interface was studied using a combination of a multiskop ellipsometer (Optrell, Germany) and a Wilhelmy plate tensiometer (Nima Technology Ltd., England). Samples (prepared as described in the materials section) were placed in a teflon trough (sample volume 120 mL). Before the start of a measurement the air/water interface is cleaned by a custom made sucking device and subsequently expanded from 30 to 190 cm² in ~20s. Immediately after this procedure Δ (phase difference of light before and after reflection at the interface) and Ψ (reflecting the amplitude ratio of light parallel and perpendicular to the plane of interface) at an angle of incidence of 50°, a wavelength of 632.8nm and in two zones were measured and followed in time. Surface pressure was simultaneously recorded. Experiments were performed at least in triplicate and differences in Δ were within 10%. Only for the measurements at CR0.5 and CR1 (Table 8.1) differences in Δ up to 25% were observed, presumably due to aggregation and sedimentation of complexes. From the changes in Δ and Ψ (with respect to a clean air/water interface) a thickness and refractive index of the adsorbed layer can be calculated¹⁰. This can than be converted to adsorbed mass (Γ), using the refractive index increment (dn/dc) of the adsorbed material. At the angle of incidence used, the measurement of Δ is very accurate, unfortunately at the expense of the accuracy of Ψ . Due to large errors in the measured Ψ values, it appeared impossible to retrieve quantitative information on layer thickness and density.

By assuming a layer thickness, it is possible to determine Γ solely from the measured Δ values (and Γ does not strongly depend on the assumed layer thickness). All data for adsorbed mass were calculated with the assumption that layer thickness for pure protein layers is 4 nm. This value was obtained from neutron reflectivity (NR) measurements (chapter 5). For the mixed layers values varying from 20 to 40 nm were found using NR. In this work for all mixed layers a thickness of 20 nm was assumed to calculate the adsorbed mass. Using this assumption values of adsorbed mass are up to 16% underestimated if the layer thickness is in reality 40 nm or up to 15% overestimated if the layer thickness is in reality 4 nm. The dn/dc values (Table 8.1) needed for calculation of Γ were estimated from the dn/dc values of β -lactoglobulin (0.182¹¹), pectin (0.148, average from 14 pectin samples with an average degree of methylation of 28%¹²) and carboxylated pullulan (0.143⁶), using the Clausius-Mossotti relation¹³. The relative protein and polysaccharide volume fractions needed for this equation were calculated from the ratio in which protein and polysaccharide were mixed, specific protein volume ($0.750 \cdot 10^{-3} \text{ m}^3 \text{kg}^{-1}$)¹⁴ and specific polysaccharide volume ($\sim 0.625 \cdot 10^{-3} \text{ m}^3 \text{kg}^{-1}$ for pectin, estimated on the basis of the density of saccharose). Obviously ellipsometry cannot distinguish protein and polysaccharide and in reality the composition of the mixed layers may differ from the composition of complexes in solution. If the composition of the adsorbed layers is different, in the most extreme case adsorbed mass is 20% overestimated. Differences in adsorption kinetics between the different samples are larger than these uncertainties.

8.3 RESULTS

8.3.1 Selection of materials

To obtain more insight in the nature of the retarding effect of polysaccharide on protein adsorption, the effect of protein/polysaccharide complexation on adsorption kinetics to air/water interfaces was studied as a function of three parameters: protein/polysaccharide mixing ratio (expressed as charge ratio), the molar mass of the polysaccharide and the charge density of the polysaccharide. The effect of mixing ratio was investigated using β -lactoglobulin/pectin mixtures. The β -lactoglobulin/pectin weight ratios at which the samples were mixed were expressed in terms of charge ratio. To that end the positive net charge per gram β -lactoglobulin at pH 4.5 was determined to be 0.25 mol/kg, based on a proton titration curve (not shown). The number of carboxyl groups per gram pectin was 3.9 mol/kg, as calculated from the degree of methylation. Furthermore we assumed that 50% of the carboxyl groups were dissociated at pH 4.5 (a pK_a of 4.5 was obtained from a titration curve of pectin). Using these numbers the β -lactoglobulin/pectin weight ratio was recalculated into β -lactoglobulin/pectin charge ratio, which will be referred to as CR (Table 8.1). A CR of 1 means that the total amount of net positive charge on the protein equals the total amount of negative charge on the polysaccharide. In table 8.1 also the ζ -potential of the different complexes is listed. Only the size of the complex with the lowest charge ratio is given, since from a mixing ratio of roughly 1, complexes associate: large heterogeneities in size trouble a reliable measurement of the hydrodynamic radius. For the effect of molar mass the originally

heterogeneous mixture of pectins was fractionated according to size (table 8.1: MW172, MW74 and MW39). Since the degree of methylation of the fractions did not differ from that of the original pectin, the charge density was assumed to be the same. Finally, to study the effect of charge density a series of carboxylated pullulan samples with different charge densities was selected. For these samples the number of carboxyl groups/g was 0.63, 1.6, 3.0 and 3.3 mol/kg for pul0.6, pul1.6, pul3.0 and pul3.3 respectively, as calculated from the charge density (chapter 6). Also for these polysaccharides 50% of the carboxyl groups were assumed to be dissociated at pH 4.5.

Table 8.1: Characterization of protein/polysaccharide complexes in solution; ζ -potential and hydrodynamic radius (R_h) of β -lactoglobulin/polysaccharide complexes, dn/dc estimated based on dn/dc of individual ingredients and mixing ratio, pH 4.5 and 15 mM.

parameter	sample	CR	ζ complex (mV)	R_h complex (nm)	dn/dc
(β-lactoglobulin/pectin)	CR0.1/pec3.9	0.1	-32 ± 1	55 ± 1	0.167
	CR0.5	0.5	-23 ± 1	-	0.176
	CR1	1	-7 ± 1	-	0.180
	CR2	2	-2 ± 1	-	0.181
	CR3	3	-1 ± 1	-	0.181
molecular weight (pectin)	MW172	0.1	-39 ± 1	33 ± 1	0.167
	MW74	0.1	-35 ± 1	26 ± 1	0.167
	MW39	0.1	-32 ± 1	28 ± 4	0.167
charge density (pullulan)	pul0.6	0.1	-6 ± 1	108 ± 8	0.149
	pul1.6	0.1	-21 ± 1	74 ± 10	0.156
	pul3.0	0.1	-26 ± 1	98 ± 2	0.162
	pul3.3	0.1	-24 ± 1	90 ± 9	0.163

8.3.2 Complex charge ratio

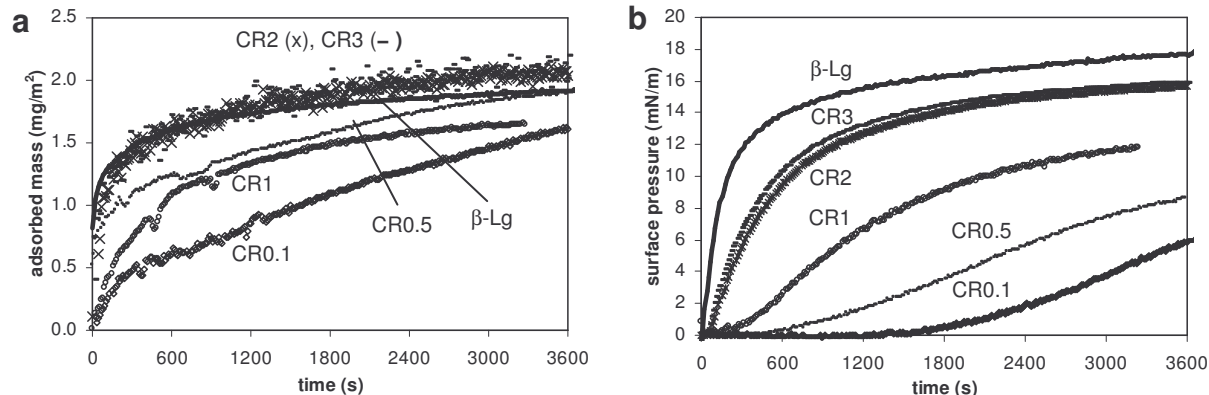


Figure 8.1: a) Adsorbed amount and b) surface pressure as a function of time for β -lactoglobulin/pectin complexes with different net charge, pH was 4.5, 15 mM

In previous work (chapter 3 and 6) the delaying effect of polysaccharide on protein adsorption kinetics has been partly ascribed to electrostatic repulsion. The adsorption rate (and corresponding increase in surface pressure) is therefore determined using ellipsometry as a function of the complex composition (CR), and thus as a function of the ζ -potential of the protein/polysaccharide complexes (Figure 8.1). For the pure β -lactoglobulin sample the adsorbed amount steeply increases directly from the start of the experiment with a cleaned

air/water interface (Figure 8.1a). Simultaneous measurement of the surface pressure shows that this also steeply increases right after the start (Figure 8.1b). Figure 8.1 also shows that the surface pressure increase rate decreases with decreasing complex charge ratio and, hence, with increasing negative net charge of the complexes. A similar trend is observed for the adsorbed mass as a function of time (with the exception that CR1 seems more retarded than CR0.5). The average adsorption rate of CR0.1 complexes (1 mg/m^2 in $\sim 2000\text{s}$) is roughly 100 times delayed compared to that of pure protein (1 mg/m^2 in the 20s before the first data point).

If electrostatic repulsion due to the high net charge of the complexes is responsible for the retarded adsorption rate, the effect should depend on the ionic strength of the solution. In chapter 2 it was indeed shown that increasing ionic strength diminished the effect of pectin and therefore increased the rate of surface pressure increase. At $\sim 1000\text{s}$ after the start of adsorption of strongly negatively charged complexes at a clean interface, the adsorbed mass at the air/water interface is $\sim 0.75 \text{ mg/m}^2$ while surface pressure still does not significantly deviate from zero (Figure 8.2). When NaCl is carefully (to minimize distortion of the interface) mixed in the solution up to an ionic strength of 100 mM, both adsorbed mass and surface pressure instantaneously increase, approaching the values of the pure protein layer much faster than the complexes without salt. The exact value of the adsorbed mass depends on the assumption made for the layer thickness. Before injection of NaCl, the layer thickness was assumed to be 20 nm. After injection, a thickness of 4 nm and a dn/dc of 0.182 (values for pure β -lactoglobulin) was assumed for the graph indicated with 'CR0.1+NaCl' (Figure 8.2). The dotted line illustrates what the adsorbed mass would be if a thickness of 20 nm and a dn/dc of 0.167 (as calculated based on the protein/polysaccharide mixing ratio) was assumed.

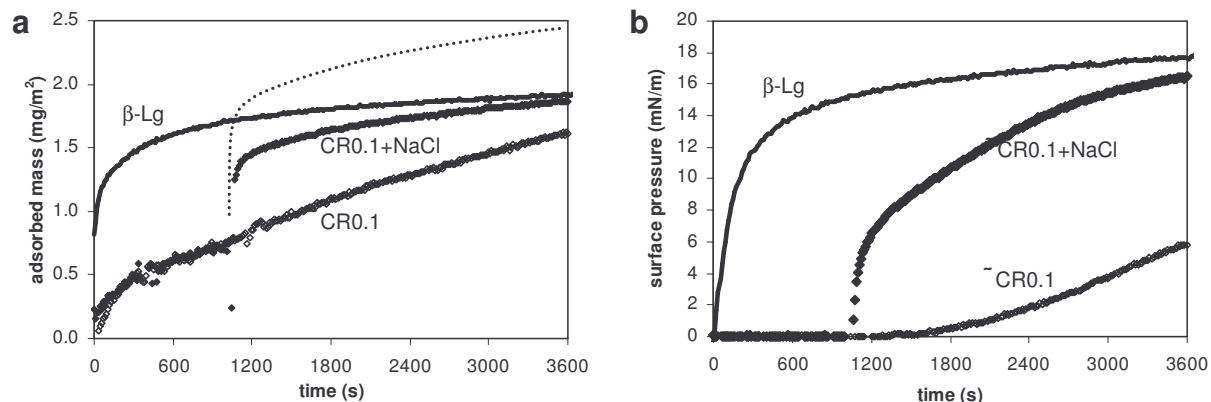


Figure 8.2: a) Adsorbed amount and b) surface pressure as a function of time for pure β -lactoglobulin and β -lactoglobulin/pectin complexes at a charge ratio of 0.12, pH was 4.5, 15 mM, in one of the experiments on complex adsorption NaCl was injected up to an ionic strength of 100 mM after $\sim 1000\text{s}$.

8.3.3 Polysaccharide molecular weight

Since adsorption kinetics is also expected to depend on the molar mass of the polysaccharide, adsorbed amount and surface pressure were recorded as a function of time for complexes of β -lactoglobulin with three pectin fractions with different molecular weights, respectively $172 \cdot 10^3$ (MW172), $74 \cdot 10^3$ (MW74) and $39 \cdot 10^3$ (MW39). Because the retarding effect of polysaccharide is in general most pronounced when complexes are negatively charged, the

effect of molecular weight of the polysaccharide was assessed at CR 0.1 (Figure 8.3a and b). The higher the molecular weight of the polysaccharide, the stronger the retarding effect on the increase of adsorbed mass. Also the rate of surface pressure increase decreases with increasing molecular weight. The adsorbed mass versus time curve for pure β -lactoglobulin is more smooth than those of the mixtures. Irregularities in the curves of the complexes may indicate heterogeneities in the adsorbed layers. The adsorbed mass of the mixtures linearly increases with time after \sim 500 seconds. Such a linear increase was not observed for pure β -lactoglobulin.

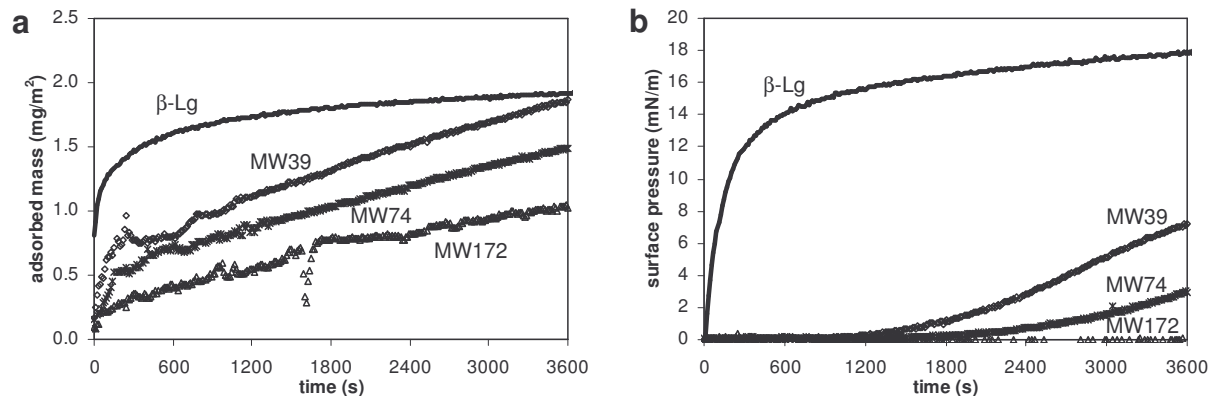


Figure 8.3: a) Adsorbed amount and b) surface pressure as a function of time for β -lactoglobulin/pectin complexes with three different molar masses, CR was 0.1, pH was 4.5 and 15 mM.

8.3.4 Polysaccharide charge density

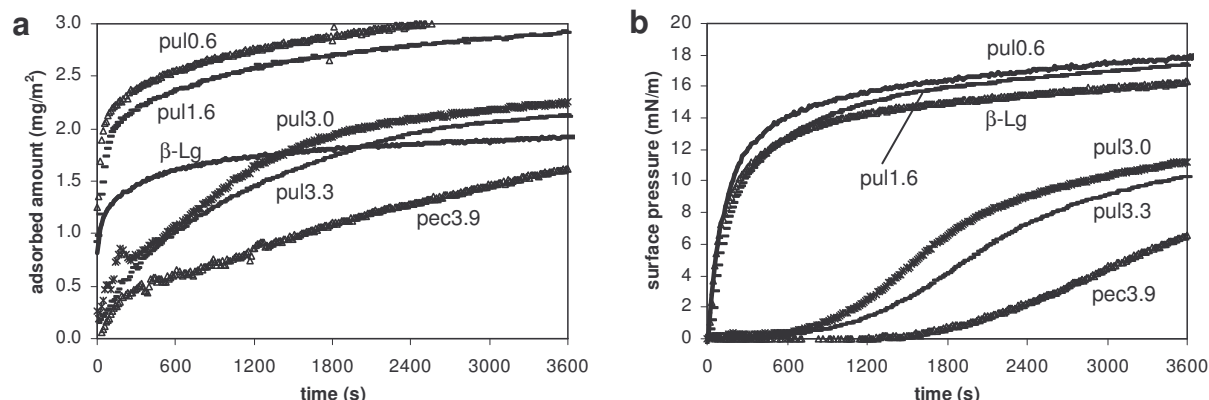


Figure 8.4: a) Adsorbed amount and b) surface pressure as a function of time for β -lactoglobulin/polysaccharide complexes with different charge density pullulans and pectin, CR was 0.1, pH was 4.5 and 15 mM

We finally considered the influence of charge density on adsorption kinetics. Figure 8.4 demonstrates that (at CR 0.1) the lower the charge density, the faster the increase in adsorbed amount and in surface pressure. For the two lowest charge densities the adsorbed amount increases even faster than that of the pure protein. Pectin has a higher charge density than pul3.3 (3.9 mol/kg versus 3.3 mol/kg, therefore referred to as pec3.9, table 8.1) which is why it was included in figure 8.4 in addition to the pullulan samples. The increase in adsorbed amount and surface pressure is more retarded for complexes with pectin than with pullulan. A linear increase of adsorbed mass versus time as observed for complexes with pectin is not so

clearly observed with the pullulan samples. The difference in adsorption kinetics between pul1.6 and pul3.3 is relatively large compared to differences between the other samples in the range pul0.6, pul1.6, pul3.0, pul3.3 and pec3.9.

8.3.5 Equation of state

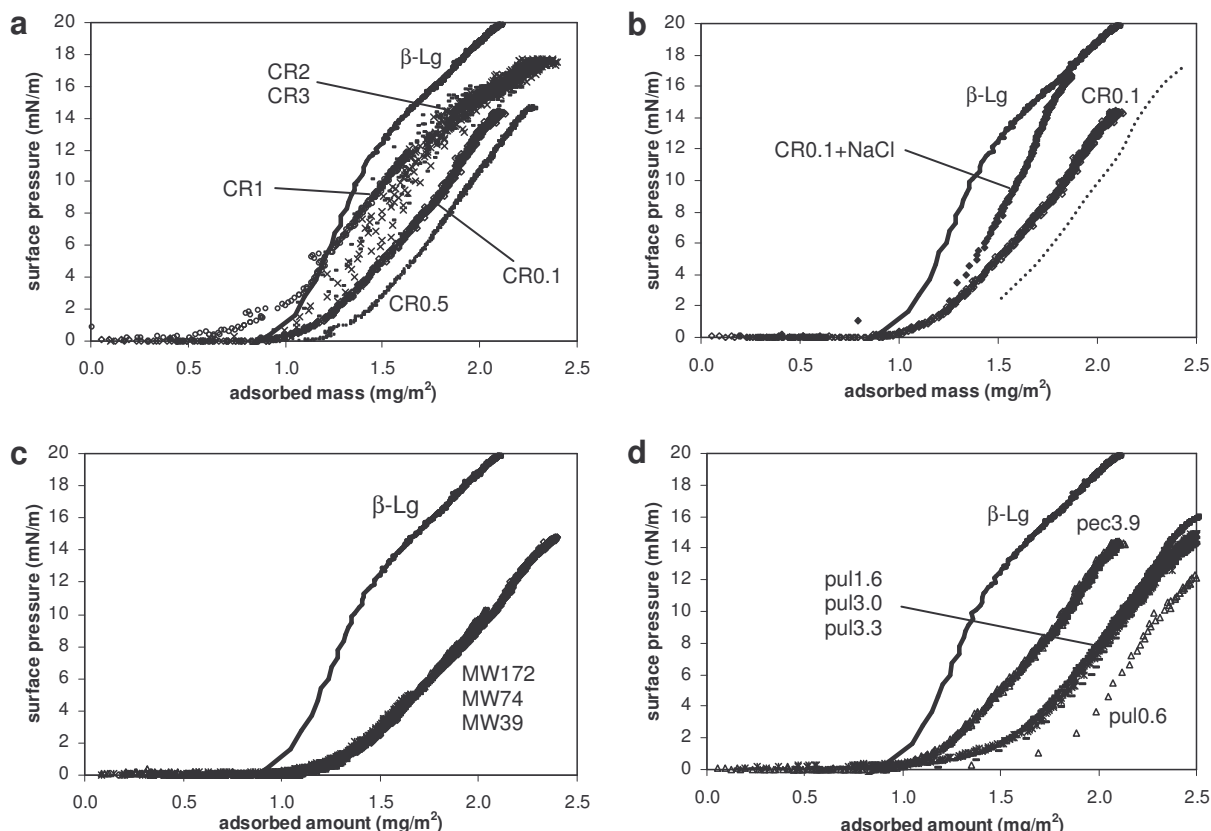


Figure 8.5: Surface pressure versus adsorbed mass at the air/water interface for a) β -lactoglobulin/pectin complexes of different charge ratio, b) negatively charged β -lactoglobulin/pectin complexes with and without addition of NaCl; for the graph indicated with '0.1+NaCl' a layer thickness of 4 nm and a dn/dc of 0.182 was assumed. (The dotted line represents a 20 nm layer with a dn/dc of 0.164). c) β -lactoglobulin/pectin complexes of pectin samples with varying molecular weight, CR = 1 and d) β -lactoglobulin/polysaccharide complexes with varying pullulan (and pectin) charge density, CR = 1. For all samples (unless mentioned otherwise) the pH was 4.5, 15 mM.

In figure 8.5 surface pressure is plotted as a function of the adsorbed mass (equation of state). The equation of state allows comparison of different layers independent of time. For the pure protein layer, an adsorbed mass of 0.9 mg/m^2 is needed before surface pressure deviates from zero. This value is often found for globular proteins¹⁵. From an adsorbed mass of $\sim 1.5 \text{ mg/m}^2$, the slope of the equation of state is lower than it was at lower adsorbed mass. The lower increase in surface pressure per gram adsorbed mass, and thus per adsorbed protein molecule may indicate a different state (conformation or molecular area) of the protein molecules above a surface pressure of $\sim 14 \text{ mN/m}$ (we will come back to this observation in chapter 9). In figure 8.5a it can be seen that the layers formed from negative complexes, indicated with (CR) 0.1 and 0.5 are less effective in increasing surface pressure; a higher adsorbed mass is necessary to reach a certain surface pressure (e.g. nearly 2 mg/m^2 for a surface pressure of 10 mN/m , whereas the pure protein layer reaches this surface pressure at an adsorbed amount of

less than 1.5 mg/m²). For the complexes with a lower net charge the equation of state resembles that of the pure protein layer better (Figure 8.5a). When NaCl is injected (to a final ionic strength of ~100 mM) in the sample with negatively charged complexes, the Π - Γ relation gradually approaches that of the pure protein layer (when a layer thickness of 4 nm and a $d\eta/dc$ of 0.182 is assumed). If complexes do not fall apart at this ionic strength, no polysaccharides detach from the interface and the layer retains its original thickness, the equation of state is like the dotted line in figure 8.5b. For the layers with different molecular weight polysaccharides the surface pressure versus adsorbed mass coincide (Figure 8.5c). For all molar masses the graphs have shifted to higher adsorbed masses, compared to that of the pure protein layer. The same shift to higher adsorbed masses is observed for the pullulan samples. No significant differences are found between pul1.6, pul3.0 and pul3.3.

8.4 DISCUSSION

Using the combination of all data described above and in previous chapters we now try to understand the mechanism by which anionic polysaccharides retard adsorption kinetics more deeply. The previously observed decreased rate of surface pressure development in the presence of polysaccharides always coincided with a decrease in adsorption kinetics in terms of adsorbed mass. In other words, the presence of polysaccharides retards accumulation of protein at the interface. We will first discuss the accumulation of mass at the interface and then elaborate on the relation between adsorbed mass and surface pressure (equation of state).

8.4.1 Accumulation of mass at the interface

Two possible explanations for a retarded mass accumulation at the interface in the presence of polysaccharides were suggested: Firstly, one may expect a decreased diffusion rate, due to the larger hydrodynamic radius of complexes (compared to that of protein molecules). Secondly, a strong negative net charge of the complexes can prevent a dense packing of complexes at the interface as previously observed with neutron reflection measurements (chapter 5).

Considering the first explanation, a decreased diffusion rate, two aspects need to be discussed: As posed in chapter 2 the hydrodynamic radius of complexes is presumably largely overestimated by dynamic light scattering (DLS). Association of a few complexes (at CR below 1) due to heterogeneity in the complex stoichiometry drastically increases the average hydrodynamic radius determined. This is illustrated by the fact that an average radius of a few hundred nanometers is found when protein is added to pectin at pH 4.5 (chapter 2), whereas the average radius is only 55 nm (Table 8.1) when protein and pectin were mixed at neutral pH and subsequently acidified. The radii of the complexes with pectins with different molecular weights are even lower (~30 nm, table 8.1). In the first case ideal mixing is hampered by the strong interaction acting immediately between the biopolymers upon addition of protein at pH 4.5. We believe that a more reliable estimation of the size of the complexes is that by the thickness of an adsorbed complex layer, measured by NR. The measured layer thickness of ~40 nm, suggests a complex radius of 20 nm. Complexes are then only a factor of 9 larger than pure protein molecules (with protein molecules we refer to β -lactoglobulin dimers, which is the predominant association degree of β -lactoglobulin at

these conditions, corresponding to a radius of $\sim 2.3^{16}$). A decrease in adsorption rate due to a smaller diffusion coefficient is therefore at most a factor of 9. A decreased diffusion rate can not account for the 100 times retarded adsorption rate of CR0.1 complexes compared to free protein molecules. Furthermore, the size of protein/polysaccharide complexes appeared to depend only marginally on the molecular weight of the polysaccharide (Table 8.1). The observed dependence of adsorption rate on polysaccharide molecular weight (Figure 8.3) can therefore not be ascribed to different diffusion rates

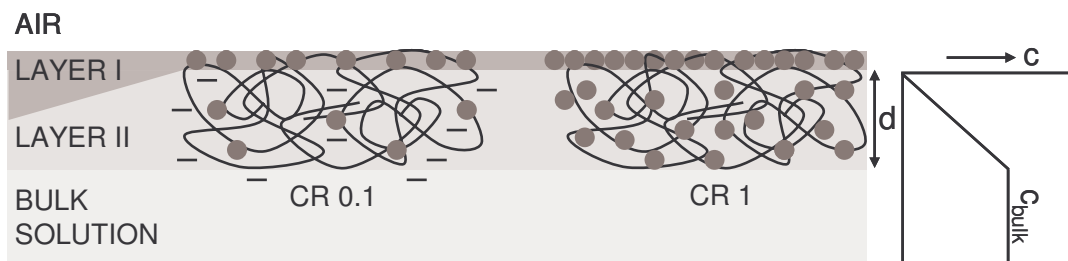


Figure 8.6: Schematic depiction of mixed adsorbed film consisting of two layers. Layer I has a thickness of ~ 4 nm and is in direct contact with air. Layer II is a thicker and more diffuse layer, the density of both layers depends on the protein/polysaccharide charge ratio (CR). For the estimation of an effective diffusion coefficient of protein through layer II (with a thickness 'd') the bulk protein concentration below layer II is indicated with (c_{bulk}). Layer I is considered as a 'perfect sink' for protein.

For the second explanation, we start with a schematic picture of a mixed adsorbed layer (Figure 8.6). In general protein/polysaccharide mixed adsorbed layers, from now on called 'films', always consist of two layers (as derived from neutron reflection, chapter 5). A dense first layer with a thickness of approximately 4 nm (Figure 8.6, layer I) is expected to be mainly responsible for the surface pressure. Below this first layer there is a second layer (II), which is more diffuse and thicker. The density of both layers depends on the CR, but due to the high affinity of protein for the interface, layer I is always more dense than layer II. Even when the film is formed from negatively charged complexes, the volume fraction of protein in this first layer in steady state is around 50 w/w% (as derived from NR, chapter 5). For comparison, the volume fraction of protein in a coacervate phase is only ~ 16 w/w% protein/polysaccharide (as demonstrated using small angle x-ray scattering, chapter 7). It is unlikely that a second layer, which has a maximum density when it is made up of neutral complexes is more dense than a coacervate phase. The density in layer I needs to reach a threshold density in order to increase surface pressure. If we imagine a protein/polysaccharide complex at the interface with a radius of 20 nm, it occupies an area larger by a factor of $9^2 = 81$, compared to a pure protein molecule with a radius of 2.3 nm¹⁶. Assuming a densely packed single layer of these complexes at the air/water interface, and supposing that all protein molecules in the complexes can access the air/water interface at some point in time, each complex should contain 81 protein molecules to form a closely packed protein monolayer at the interface. At a CR of 0.1 each (negatively charged) complex contains approximately only 4 protein molecules, assuming that complexes contain besides protein only one single polysaccharide molecule (according to the definition of intrapolymer complexes, chapter 1) with a molar mass of $\sim 1.5 \cdot 10^5$ g/mol. Hence, it is impossible that a

single complex layer provides enough protein to form a densely packed layer I. From the equation of state of the pure protein layer, it is deduced that the threshold adsorbed mass for the appearance of a finite surface pressure is 0.9 mg/m^2 . With a film thickness of 4 nm, this is a volume fraction of approximately 23 w/w%. Presumably in the presence of pectin the density in layer I needs to be similar for the surface pressure to increase. This means that the composition of the adsorbed film has to change; either pectin molecules have to desorb after delivering protein molecules to the interface, or protein from other complexes in the bulk solution has to penetrate through this layer II, before it can reach layer I. Since polysaccharide molecules have multi-point-interaction with the protein at the interface, they do not easily ‘desorb’: detach from the protein at the interface (even at 300 mM ionic strength a contribution of pectin at the interface to surface shear stress was demonstrated, chapter 3).

The observation that the adsorbed amount (Γ) linearly increases with time (t) for some samples (Figure 8.1a: CR0.1, Figure 8.3a: MW39, MW74 and MW172) indicates either convection, or a kinetic barrier for adsorption. Since the solution is not stirred, such a constant contribution of convection is not likely. Assuming that pectin molecules do not desorb, let us consider the diffusion of protein from (complexes in) the bulk solution through this polysaccharide layer (layer II) as a rate limiting step – a kinetic barrier for further protein adsorption (in the linear regime of the Γ - t curve). We consider layer I (Figure 8.6) as a perfect sink, due to the high affinity of protein for the interface (assuming that the affinity of protein for the interface is not dramatically different in the presence of pectin): because this assumption holds only when there is enough free space available for protein in layer I, we use the linear part of the Γ - t curves below $\Gamma = 1 \text{ mg/m}^2$. The curves level off between 1.0 and 1.5 mg/m^2 , which may indicate that due to a relatively high protein density layer I does no longer behave as a perfect sink. Although there is presumably electrostatic repulsion between complexes in the bulk solution and the adsorbed layer II, the thickness of the electric double layer is only a few nanometers, which is much smaller than the size of complexes. Hence, we assume a constant bulk concentration of protein ($c_{\text{bulk}} = 0.02 \text{ g/L}$) just below layer II (Figure 8.6). The effective diffusion coefficient (D_{eff}) of protein through the polysaccharide layer (layer II) can now be estimated using the slope of the Γ - t curve ($d\Gamma/dt$) and the thickness of layer II (d) by $D_{\text{eff}} = (d\Gamma/dt) \cdot d / c_{\text{bulk}}$. For CR0.1 D_{eff} is of the order of $1 \cdot 10^{-15} \text{ m}^2 \text{s}^{-1}$, which is 100 000 times lower than the diffusion of protein through the bulk solution. The strongly reduced protein mobility through complexes may also lead to heterogeneity in the adsorbed film causing the irregularities observed in the Γ - t . Brewster angle microscopy should be applied to confirm the presence of heterogeneity in the mixed film.

We suggest that two adsorption regimes can be distinguished in mixed protein/polysaccharide adsorption (if all protein in the bulk solution is bound to polysaccharide): (A) Adsorption of complexes from the bulk solution to the interface to form a single complex layer at the interface. The diffusion rate of complexes may be a rate limiting step in this regime, which is for all the different samples presumably at most a factor 10 slower than diffusion of protein molecules. Furthermore, adsorption in this regime may depend on the amount of protein on the outside of the complexes (since the affinity of protein

for the interface is much higher than that of polysaccharide for the interface) and on electrostatic repulsion within and between complexes (B) Diffusion of protein from complexes in the bulk solution through the complex/polysaccharide layer (layer II). The adsorption rate in regime B depends on the protein/polysaccharide binding affinity and thus on polysaccharide charge density. Whereas with pectin a linear regime in the Γ -t curve is clearly observed (Figure 8.4), with pul3.0 and pul3.3 the linear regime is less clear (but still visible around Γ is 1 mg/m²; the slope corresponds to a 33 000 times lower diffusion coefficient than for β -lactoglobulin in solution). With the lower charge densities (pul0.6 and pul1.6) adsorption is so fast that an adsorbed mass of 1 mg/m² is reached at the first data point. A possible fraction of free protein in these samples could contribute to the faster adsorption rate than that of pul3.0 and pul3.3 (for which there are indications that all protein is bound from dynamic light scattering, chapter 6) The two adsorption regimes may partly overlap in time and thus the total Γ at any point in time is the sum of adsorption from the first regime (Γ_A) and from the second regime ($\Gamma_B = c_{\text{bulk}} \cdot D_{\text{prot}} \cdot t / d$ as described above). The relative contribution of regime A to the total Γ increases with increasing protein density in the complexes and thus with increasing CR.

Also, polysaccharide molecular weight (Figure 8.3a) seems to affect mainly regime A. The slope of the linear parts of these curves (MW39, MW74 and MW172) does not differ much. The value of Γ from where regime B dominates (as from where the Γ -t curve linearly increases) is different. This difference may be attributed to a more efficient packing of complexes in regime A when the polysaccharide molecular weight is lower. The decreasing ζ -potential with decreasing molecular weight of polysaccharides supports this hypothesis.

8.4.2 Equation of state

The fact that the equation of state of pure protein increases more steeply than that of mixed films can be explained as follows: Accumulation of extra mass at the interface, in case of the pure protein sample takes place in layer I (the layer thickness of a β -lactoglobulin layer at the air/water interface observed with neutron reflection is 4 nm; layer II is absent in the absence of polysaccharides). This directly affects surface pressure. In case of the mixed films accumulation of extra mass initially takes place in layer II, which has much less effect on surface pressure, as layer II is always less dense than layer I. The higher the negative net charge in layer II, the more effectively the polysaccharide hinders protein to reach layer I. If the distribution of mass within the film is therefore less favoured to layer I the total adsorbed mass is less efficient in increasing surface pressure compared to films made of neutral complexes. This would explain the shift of equation of state to higher adsorbed mass, as observed with a charge ratio of 0.1 and 0.5. Finally, the lower the charge density, the lower is the electrostatic repulsion in layer II, allowing for more polysaccharide to remain attached to layer I. The observed shift of equation of state to higher adsorbed mass (at CR0.1) in the order pectin < pul1.6, pul3.0 and pul3.3 < pul0.6 may be a result of this. The observation that the initial steep increase in Γ -t for pul0.6 and pul1.6 continues till higher Γ than pure protein (Figure 8.4a) may also be explained by a higher amount of polysaccharide in the second layer.

The instantaneous increase in both adsorbed mass as well as surface pressure (Figure 8.2) upon increasing ionic strength (by injection of NaCl at a point in time where regime B dominates) confirms the strong impact of reduced protein mobility (at low ionic strength). Complexes in solution presumably fall apart at this ionic strength, making transport of extra 'free' protein to the interface easier. It is known that not all pectin desorbs from the interface at this ionic strength (an effect of pectin on surface shear stress was demonstrated up to 300 mM ionic strength, chapter 3) after injection of salt. However, presumably the pectin molecules that will remain at the interface orient more flat against the interface to interact with as many proteins at the interface as possible (multi-point interaction), resulting in a much thinner layer II. Assuming a total film thickness of 4 nm for the adsorbed film after salt has been injected, the equation of state gradually approaches that of a pure protein film (Figure 8.5b).

8.5 CONCLUSIONS

Not only the increase in surface pressure, but also the increase in adsorbed mass at the air/water interface is retarded by protein/polysaccharide interaction. Parameters influencing this interaction can therefore be used to manipulate adsorption kinetics at the air/water interface. A factor of 10 decrease in adsorption rate can be accomplished in three ways: i) by decreasing the protein/polysaccharide charge ratio by a factor of 20, ii) by increasing molecular weight of the polysaccharide by a factor of 4 or iii) by increasing the charge density on the polysaccharide by a factor of 2. The retarding effect of polysaccharides was subdivided in two stages: firstly, a reduced diffusion rate to the interface due to the large hydrodynamic radius of complexes (this can decrease the adsorption rate ~10 times at most), and secondly, the complex/polysaccharide layer constitutes a kinetic barrier for protein to reach the interface, by providing electrostatic repulsion within and between complexes and strongly reducing the diffusion of protein through this layer (up to a factor of 100 000).

ACKNOWLEDGEMENTS

We greatly acknowledge Renko de Vries and Stefan van der Burgh from SOFTLINK for the supply of the carboxylated pullulan samples and Marcel Meinders and Remco Fokkink for their help in interpreting the ellipsometry data.

REFERENCES

- (1) Daas, P. J. H.; Boxma, B.; Hopman, A. M. C. P.; Voragen, A. G. J.; Schols, H. A., Nonesterified galacturonic acid sequence homology of pectins. *Biopolymers* **2001**, 58, (1), 1-8.
- (2) Blumenkr.N; Asboehan.G, New Method For Quantitative-Determination Of Uronic Acids. *Analytical Biochemistry* **1973**, 54, (2), 484-489.
- (3) Thibault, J. F., Automated-Method For The Determination Of Pectic Substances. *Lebensmittel-Wissenschaft & Technologie* **1979**, 12, (5), 247-251.
- (4) Tollier, M. T.; Robin, J. P., Adaptation Of The Orcinol-Sulfuric Acid Method For The Automatic Titration Of Total Neutral Sugars - Conditions Of Application To Plant-Extracts. *Annales de Technologie Agricole* **1979**, 28, (1), 1-15.
- (5) Huisman, M. M. H.; Oosterveld, A.; Schols, H. A., Fast determination of the degree of methyl esterification of pectins by head-space GC. *Food Hydrocolloids* **2004**, 18, (4), 665-668.

- (6) de Nooy, A. E. J.; Besemer, A. C.; van Bekkum, H.; van Dijk, J. A. P. P.; Smit, J. A. M., TEMPO-Mediated Oxidation of Pullulan and Influence of Ionic Strength and Linear Charge Density on the Dimensions of the Obtained Polyelectrolyte Chains. *Macromolecules* **1996**, 29, (20), 6541-6547.
- (7) de Jongh, H. H. J.; Gröneveld, T.; de Groot, J., Mild isolation procedure discloses new protein structural properties of beta-lactoglobulin. *Journal of Dairy Science* **2001**, 84, (3), 562-571.
- (8) Berne, B. J.; Pecora, R., *Dynamic Light Scattering: with applications to Chemistry, biology, and Physics*. 2000 ed.; General Publishing Company, Ltd.: Toronto, 1976.
- (9) van der Burgh, S.; de Keizer, A.; Cohen Stuart, M. A., Complex coacervation core micelles. Colloidal stability and aggregation mechanism. *Langmuir* **2004**, 20, (4), 1073-1084.
- (10) de Feijter, J. A.; Benjamins, J.; Veer, F. A., Ellipsometry As A Tool To Study Adsorption Behavior Of Synthetic And Biopolymers At Air-Water-Interface. *Biopolymers* **1978**, 17, (7), 1759-1772.
- (11) Perlmann, G. E.; Longsworth, L. G., The Specific Refractive Increment Of Some Purified Proteins. *Journal of The American Chemical Society* **1948**, 70, (8), 2719-2724.
- (12) Hourdet, D.; Muller, G., Solution Properties Of Pectin Polysaccharides.2. Conformation And Molecular-Size Of High Galacturonic Acid Content Isolated Pectin Chains. *Carbohydrate Polymers* **1991**, 16, (2), 113-135.
- (13) Markov, K. Z., Elementary Micromechanics of Heterogeneous Media (chapter 1). In *Heterogeneous Media: Modelling and Simulation*, Markov, K. Z.; Preziosi, L., Eds. Birkhauser Boston: Boston, 1999; pp 1-162.
- (14) Valdez, D.; Le Huerou, J. Y.; Gindre, M.; Urbach, W.; Waks, M., Hydration and protein folding in water and in reverse micelles: Compressibility and volume changes. *Biophysical Journal* **2001**, 80, (6), 2751-2760.
- (15) Benjamins, J. Static and dynamic properties of proteins adsorbed at liquid interfaces. PhD, Thesis, Wageningen University, Wageningen, The Netherlands, 2000.
- (16) Verheul, M.; Pedersen, J. S.; Roefs, S.; de Kruif, K. G., Association behavior of native beta-lactoglobulin. *Biopolymers* **1999**, 49, (1), 11-20.

General discussion

In this chapter some general remarks and speculations are made based on the combination of all previously discussed data together with some additional observations. To respond to the aim of this thesis - to understand the influence of protein/polysaccharide interaction on the adsorption behaviour at air/water interfaces - we will complete and summarize the previously proposed schematic model for polysaccharide controlled protein adsorption in the first part of this chapter. In the second part, we will discuss the dynamic behaviour of protein/polysaccharide complexes and how this depends on several molecular parameters. In the last part we will place the model in a wider context of possible applications. The majority of measurements in this thesis were performed at pH 4.5, and at low ionic strength. For the applicability of the system we shall consider a wider range of conditions.

9.1 SCHEMATIC MODEL POLYSACCHARIDE CONTROLLED PROTEIN ADSORPTION

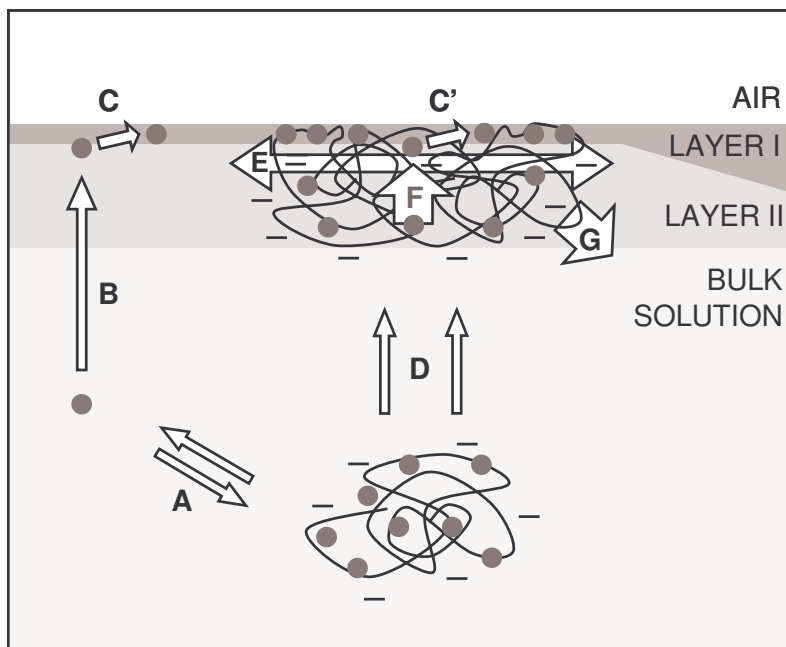


Figure 9.1: Model for polysaccharide controlled protein adsorption at the air/water interface; A) partition of free protein and protein bound to polysaccharide, B) diffusion of free protein in bulk, C) protein adsorption at interface, D) transport of protein/polysaccharide complexes in bulk, E) protein density in the complexes, F) mobility of protein through the complex layer, G) desorption of polysaccharide.

In chapter 2 a schematic model for mixed protein/polysaccharide adsorption was proposed. This model is slightly extended (Figure 9.1) in view of some new insights. The model was tested for anionic polysaccharides (pectin and pullulan) and β -lactoglobulin at pH 4.5 and low ionic strength (up to 80 mM) at the air/water and oil/water interface. In section 9.3 the applicability of the model will be discussed for a wider range of conditions. The combination of several simultaneously occurring processes determines the rate by which proteins adsorb to the air/water interface in the presence of polysaccharides. Furthermore, a number of these processes also influence the type and properties of the adsorbed layers. In figure 9.1 all relevant processes are indicated by arrows and will be discussed below. For each process the parameters that influence this process will be discussed.

Process A is the partition of free protein and protein in complexes with polysaccharides. This depends on the protein/polysaccharide binding affinity, which in turn depends on molecular parameters of the ingredients (protein and polysaccharide charge density and distribution) and system parameters like protein/polysaccharide mixing ratio (also expressed as charge ratio) solution pH, and ionic strength (chapter 2). Binding affinity is dominated by electrostatic interaction; at low ionic strength and when the polysaccharide charge density is high (> 0.5), the majority of protein ($> 90\%$) in solution is complexed with the polysaccharides up to a charge ratio of 1 (ratio of the amount of positive net charge on the protein and negative charge on the polysaccharide, chapter 6). Process B, transport of free proteins through the solution is determined by its diffusion coefficient (possibly in combination with convection). Since various types of protein molecules do not differ much in size, their diffusion rate does not differ by more than roughly a factor of 2 or 3. Process C, adsorption of protein to the interface may be determined by a kinetic barrier for adsorption. Since this barrier depends on the exposed hydrophobicity on the surface of the protein and the protein net charge^{1, 2}, it will be referred to as the ‘protein’ kinetic barrier. This is the process that accounts for large differences in adsorption rate between different protein molecules (e.g. β -lactoglobulin and lysozyme). For β -lactoglobulin, the adsorption rate is dominated by its diffusion rate; its adsorption is essentially barrier free (chapter 4). Depending on the kinetic barrier for unfolding, the protein molecule may change its conformation at the interface (β -lactoglobulin shows limited conformational changes at the air/water interface³, whereas ovalbumin does not⁴). Please note that process B and C do not depend on protein/polysaccharide interaction, only the amount of protein taking this path does, as determined by process A (Only an increased bulk viscosity at high polysaccharide concentrations could effect B, but this was not the case at the concentrations used in this thesis). Process D is transport of complexes to the air/water interface. This depends on the size of the complexes (through the diffusion coefficient). In general the radius of complexes is roughly 10 times larger than pure protein molecules, giving rise to at most a 10 times retarded adsorption rate. It should be noted that the size of complexes does not strongly depend on the molecular weight of polysaccharides (chapter 8).

The last three processes E, F and G determine the kinetic barrier for protein adsorption that can be constituted by polysaccharide. The amount of protein that is directly

available for the interface in layer I depends on the volume fraction of protein in the protein/polysaccharide complexes, E . This protein volume fraction is determined by the protein/polysaccharide charge ratio at which the complexes are mixed. The protein volume fraction in a soluble neutral complex is ~4% (chapter 7). The volume fraction of protein in a coacervate phase formed from neutral complexes is ~16% (based on Small Angle X-ray Scattering, chapter 7). Hence, the protein volume fraction in a film at the air/water interface formed from adsorption of these neutral complexes will initially be somewhere between 4 and 16%. In a film formed from negatively charged complexes, the initial protein density is much lower (e.g. ~0.4% for a charge ratio of 0.1) due to strong electrostatic repulsion within and between complexes. For comparison, a densely packed protein film has a protein volume fraction of ~60% (chapter 5). In mixed films it was observed that two layers can be distinguished (as demonstrated with neutron reflection, chapter 5); layer I is always more dense than layer II (Figure 9.1). At 6 hours after the start of negatively charged protein/polysaccharide complex adsorption this layer I contains a volume fraction of ~50% (chapter 5). This means that protein from layer II must have moved to layer I, where it is stuck due to its high affinity for the interface. The rate at which protein can move through the complex (Figure 9.1, process F) depends on how strong the protein is locally bound to the polysaccharide in the complex. Parameters that influence the protein/polysaccharide binding affinity are described at process A. The strong dependence of process F on charge density is illustrated using ellipsometry in chapter 8: with a high charge density polysaccharide, the diffusion coefficient of protein through such a complex layer can be up to 100 000 times lower than the diffusion coefficient through aqueous solution. Also in chapter 5 a reduced protein mobility in the presence of polysaccharides was demonstrated by time resolved fluorescence anisotropy measurements. A strong effect on the dynamic character of the complexes is expected of the charge distribution on protein and polysaccharide (chapter 7). In case of negatively charged complexes, a single complex layer does not contain enough protein to form a densely packed layer I. Two scenarios for further (protein) adsorption could be imagined: (i) the polysaccharide desorbs from the interface (Figure 9.1 G) making space for adsorption of new complexes from the bulk solution. However, since polysaccharides may simultaneously attach to many protein molecules at the interface (that have already lost their translational entropy by adsorption) its interaction with the interface is much stronger than with separate protein molecules in bulk solution. Therefore with increasing polysaccharide charge density (more attachments to protein at the interface) it becomes rather unlikely that this occurs. Alternatively (ii), protein from complexes in the bulk solution has to penetrate in layer II and then move towards layer I, which may be strongly retarded as explained for F. The more the mobility of protein through the complex is hindered (due to strong protein/polysaccharide interaction), the stronger also the polysaccharide is bound to the interface.

In short: a polysaccharide can constitute a kinetic barrier for protein adsorption at the interface by its irreversible attachment to (proteins at) the interface and a reduced protein mobility through a complex layer. If route B and C are minor, this ‘polysaccharide’ kinetic

barrier is the rate limiting step in adsorption. The barrier increases with decreasing CR, due to electrostatic repulsion within and between complexes at the interface and the resulting lower initial protein volume fraction at the interface. Also by increasing polysaccharide molecular weight the net charge of - and thus electrostatic repulsion between - the complexes increases (chapter 8).

It should finally be noted that a possible 'protein' kinetic barrier for protein adsorption, as explained at C, may be different when a protein adsorbs from a complex rather than from a pure protein solution. Therefore this process is indicated with C' in figure 9.1.

As the 'polysaccharide' kinetic barrier for protein adsorption (raised by the presence of a polysaccharide) takes place in layer II, the whole mechanism is presumably rather independent of the type of interface (air/water or oil/water). It was indeed shown that the proposed mechanism for mixed adsorption is also valid for oil/water interfaces (chapter 4). A different extent of protein unfolding at air/water and oil/water interfaces may raise differences in the effect of polysaccharide on protein adsorption at both interfaces. Obviously also the 'protein' kinetic barrier for protein adsorption (C and C') may be different at air/water and oil/water interfaces.

The density in layer I is expected to dominate surface pressure and surface dilatational modulus, since layer I is always more dense than layer II. Since polysaccharides can prevent a dense packing in layer I, the resulting dilatational modulus is lower than that of a neutral complex layer or a pure protein layer (chapter 3). This lowering effect on dilatational modulus can be circumvented by first allowing the formation of a pure protein layer and subsequent addition of polysaccharide (sequential adsorption, chapter 3). The surface pressure may be partly compensated by strong electrostatic repulsion (section 9.2.2). The cohesion between and within complexes at the interface is presumably important for the surface shear behaviour. Whereas in a pure protein layer protein molecules may shear along each other, if protein molecules are interconnected by polysaccharides, within layer I or by II, the shear stress may increase (chapter 3 and 6). The observation that layer I is always more dense than layer II may be an advantage of these electrostatic complexes compared to covalent protein/polysaccharide complexes. Since in the latter case the protein is covalently bound in the complexes, they cannot migrate to form a more dense layer I. This may lead to a weaker attachment of the complexes at the interface, lower surface pressure and dilatational modulus due to the a lower protein volume fraction at the interface and lower shear stress as a result of low cohesion between complexes.

In conclusion, protein/polysaccharide interaction can be exploited to control protein adsorption at air/water and also oil/water interfaces. Any parameter affecting protein/polysaccharide interaction (e.g. ingredient parameters like polysaccharide molecular weight, charge density and distribution or system parameters like charge ratio, pH and ionic strength) may be varied to obtain the desired adsorption kinetics, surface rheological behaviour, or net charge of the surface layer. To give a more quantitative description of adsorption kinetics, a more detailed description of the phase behaviour and

protein/polysaccharide binding affinities is necessary. In view of applications, section 9.3 provides an overview, explanation and examples on how different parameters may be used to get the desired functional behaviour.

9.2 COMPLEX DYNAMICS

A retarding effect of polysaccharides on protein adsorption at air/water interfaces has been demonstrated by kinetic measurements of surface pressure (chapter 1, 3, 6 and 8) and adsorbed mass (chapter 5 and 8). The retarding effect was even more pronounced while studying the increase in surface dilatational modulus as a function of time. In chapter 3 it was suggested that the dependence of the dilatational modulus on time may be understood in terms of reorganizations of protein and complexes at the air/water interface. We now revisit this issue, considering a collection of old and new results.

9.2.1 Results

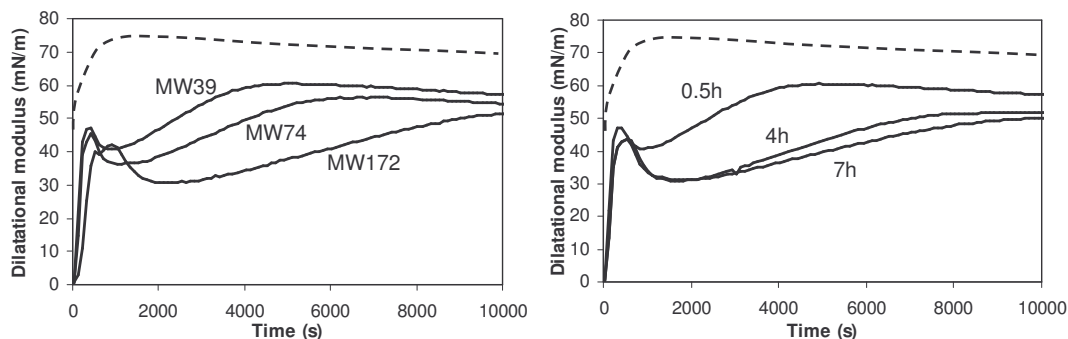


Figure 9.2: Dilatational modulus as a function of surface pressure for pure β -lactoglobulin (dashed lines) and for β -lactoglobulin/pectin complexes a) with pectin of three different molecular weights (172000, 74000 and 39000 indicated in the graph with MW172, MW74 and MW39 respectively) 30 minutes after mixing protein and polysaccharide, and b) with β -lactoglobulin/pectin complexes (with MW39 pectin) at different aging times of the complex in solution before adsorption takes place, β -lactoglobulin concentration was 0.1 g/L, pH 4.5 and 1 mM. Measurements were performed using a drop tensiometer that carried out sinusoidal oscillations (at 0.1Hz) of the interfacial area (A) of an air bubble in the sample solution; dilatational modulus (ε) was calculated from the resulting change in surface pressure (Π) by $\varepsilon = -d\Pi/d\ln A$

To get an idea of the extent and type of reorganizations within the adsorbed layers and thus in adsorbed protein/polysaccharide complexes, we will focus on surface dilatational rheology. In figure 9.2 the surface dilatational modulus as a function of time is shown for three β -lactoglobulin/pectin complex samples differing in molecular weight of the pectin involved (for the method of surface dilatational rheology we refer to chapter 3, for information on the pectin fractionation we refer to the materials section of chapter 8). The molecular weight of the pectin fractions was $172 \cdot 10^3$, $74 \cdot 10^3$ and $39 \cdot 10^3$, indicated in the graph with MW172, MW74 and MW39 respectively. After the start of a measurement with a clean interface the dilatational modulus first steeply increases, after which it goes through a maximum (within the first 1000s). After the maximum a minimum is observed and finally the modulus reaches a steady state value. The shape of the curve is similar for each sample, but the times it takes to go through the maximum and minimum and finally reach the steady state value are different. Also the depth of the minimum is somewhat different. A pure protein layer, formed in the absence of polysaccharide, reaches a steady state within 1000s (illustrated by the dashed lines

in figure 9.2). For the complexes, the time required for reaching a steady state value increases with increasing molecular weight of the polysaccharide. Similar trends have been observed with increasing aging time of the complexes (before adsorption takes place, figure 9.2b), increasing charge density (chapter 6), decreasing charge ratio (CR) (chapter 3 and 6), and decreasing ionic strength (chapter 3).

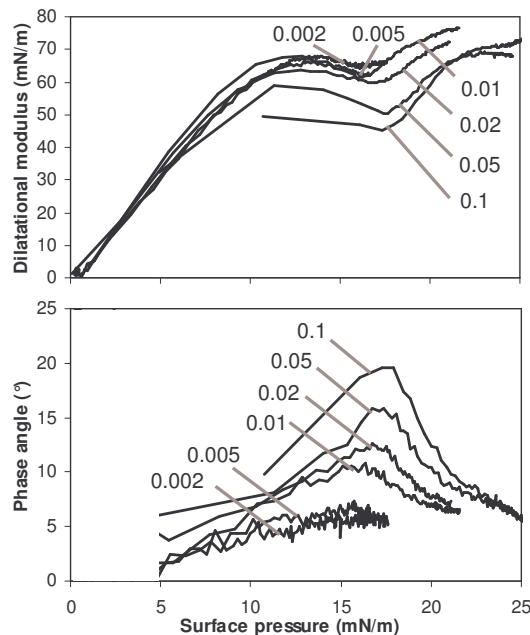


Figure 9.3: Dilatational modulus (top) and phase angle (i.e. phase difference between $d\Pi$ and dA , bottom) as a function of surface pressure for β -lactoglobulin at different bulk concentrations. Concentrations in g/L are indicated in the graphs, pH was 4.5 and $I = 2$ mM.

The minima as shown in figure 9.2 are not unique for the mixed protein/polysaccharide systems, but are also observed for pure protein layers (although not resolved in figure 9.2). The dilatational modulus as a function of time obviously depends on protein concentration. The higher the concentration, the faster the modulus increases and the faster a steady state value is reached. To compare the dilatational modulus for different protein concentrations, it is plotted as a function of surface pressure (Figure 9.3, top panel); this enables comparison of the layers formed from different bulk solution concentrations independent of time. One sees that the minimum in dilatational modulus becomes less deep with decreasing protein concentration. The (complex) dilatational modulus consists of an elastic and a viscous component. The phase angle, which is the measured phase difference in the imposed area oscillations of the interface and the response in surface pressure, reflects the ratio between the viscous and elastic component. If the surface pressure instantaneously changes according to the static Π - Γ dependence (equation of state) upon changing Γ as a result of area oscillations, the modulus is purely elastic and the phase angle is zero. If the surface pressure does not follow the equation of state completely within the time scale of the imposed oscillations, there is a viscous contribution, or ‘loss’ contribution to the modulus, and the phase angle (or loss angle) is finite. We assume that protein does not desorb within the timescale of the oscillations and therefore the phase angle indicates in-surface relaxations at

the relevant timescale, i.e. of the order of 2 s for the frequency used (0.1 Hz). The bottom panel in figure 9.3 shows the phase angle as a function of surface pressure for the different protein concentrations. It appears that the minimum in dilatational modulus corresponds to a maximum in phase angle. Furthermore, whereas the minimum becomes deeper with increasing concentration, the maximum in the phase angle becomes higher. This means that at the surface pressure of e.g. 17 mN/m the layers formed from different bulk concentrations are not the same.

Now let us return to the complexes with pectin. In figure 9.4 (top panel) the dilatational moduli from figure 9.2a, as well as the corresponding phase angles (bottom panel) are plotted as a function of surface pressure. It appears that for the complexes the phase angle also shows a maximum at the point where the modulus shows a minimum. However, there is also a new maximum in the phase angle. The new maximum, at a surface pressure of \sim 11 mN/m is lower than the familiar one at \sim 17 mN/m. The minimum in dilatational modulus becomes deeper with increasing molecular weight of the polysaccharide.

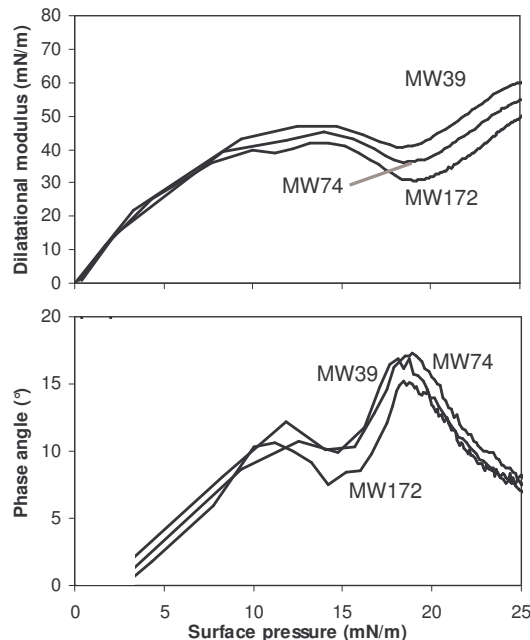


Figure 9.4: Dilatational modulus (top) and phase angle (bottom) as a function of surface pressure for β -lactoglobulin/pectin complexes with pectin of three different molecular weights, β -lactoglobulin concentration was 0.1 g/L, pH 4.5 and 15 mM.

Since dilatational modulus and phase angle depend on protein concentration and thus on adsorption kinetics, it may be interesting to see how both quantities respond to variation of protein/polysaccharide charge ratio (at constant protein concentration and thus variation of polysaccharide concentration); it is known that charge ratio affects adsorption kinetics. Furthermore, to see if the effects are system specific the same measurements were performed with pullulan, a different polysaccharide. In figure 9.5 the dilatational modulus (top) and phase angle (bottom) are shown for different protein/polysaccharide mixing ratios with pectin (left, measurements described in chapter 3) and pullulan (right, measurements described in chapter 6). The charge density (fraction of monosaccharide subunits with a carboxyl group) of pectin and pullulan is 0.7 and 0.56 respectively (the pullulan sample with the highest charge

density was used for these measurements, chapter 6). The maximum in the phase angle seems to depend on the charge ratio (ratio at which protein and polysaccharide were mixed). For both types of polysaccharides it can be observed that with increasing charge ratio, the minimum in dilatational modulus becomes less deep, whereas the maximum in phase angle becomes higher. Note that in this respect the dependence of protein concentration, figure 9.3, was different; in that case a deeper minimum in dilatational modulus corresponded to a higher phase angle. The data of complexes with pectin look very similar to those of complexes with pullulan. However, taking the kinetics into account we observe a difference. In figure 9.6 the same data are presented as in figure 9.5(top), but here as a function of time. The dilatational modulus - time dependence observed for complexes with pectin (figure 9.6, left) and that for complexes with pullulan (figure 9.6, right) qualitatively look similar again, with respect to the minima observed. However, the x-axis differs by a factor of 4; with pectin it takes about 4 times as long to reach a steady state than it does with pullulan. In chapter 3 it was found that also with increasing ionic strength the time it takes to reach a steady state value decreased.

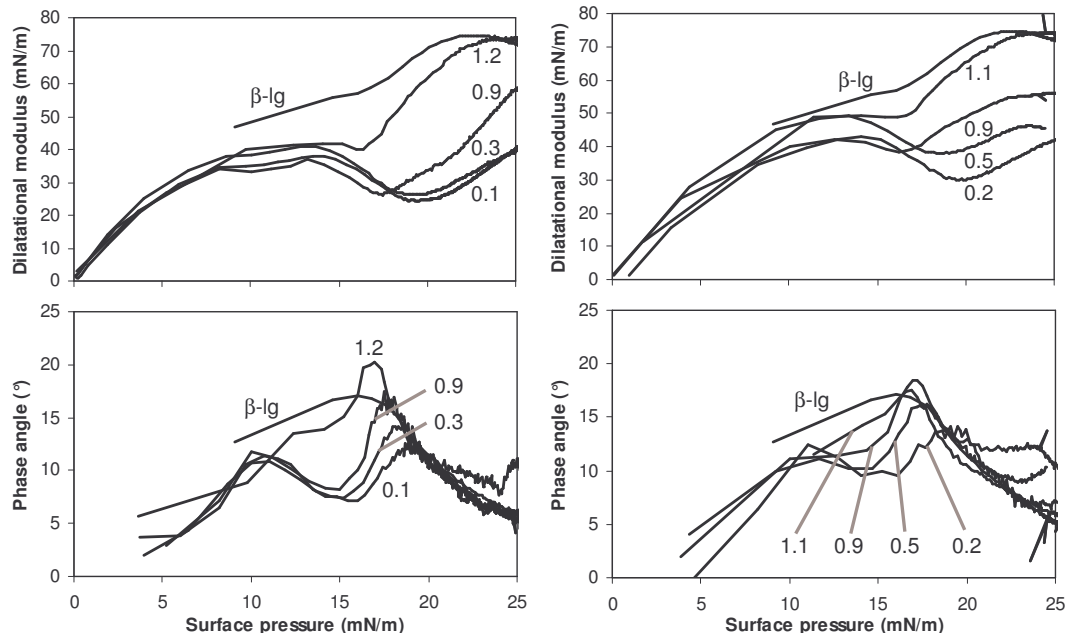


Figure 9.5: Dilatational modulus (top) and phase angle (bottom) as a function of surface pressure at various charge ratios for β -lactoglobulin/pectin complexes (left) and β -lactoglobulin/pullulan complexes (right), β -lactoglobulin concentration was 0.1 g/L, pH 4.5 and 12 mM.

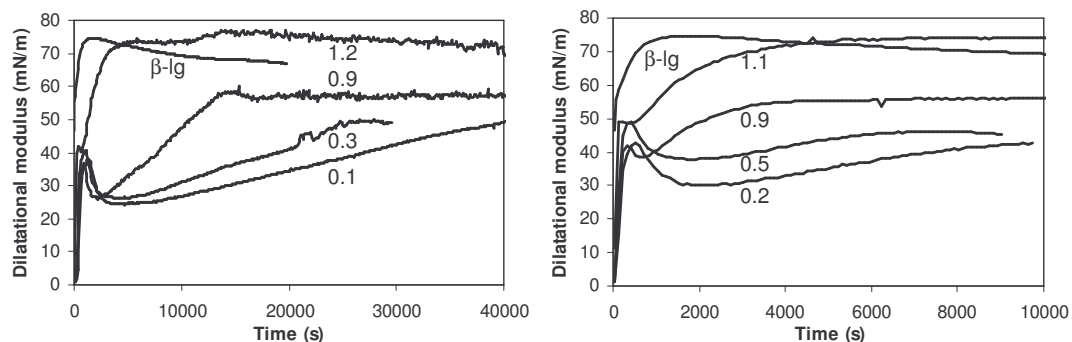


Figure 9.6: Dilatational modulus as a function of time at various charge ratios for β -lactoglobulin/pectin complexes (left) and β -lactoglobulin/pullulan complexes (right), β -lactoglobulin concentration was 0.1 g/L, pH 4.5 and 12 mM.

In addition to measurements with different polysaccharides, some measurements were performed with a different protein; ovalbumin and ovalbumin/pectin complexes. In contrast to what we find for β -lactoglobulin (a concentration dependency of the dilatational modulus and phase angle), the rather featureless curves for two different concentrations of ovalbumin coincide (Figure 9.7). It should be mentioned here that variation between duplicate measurements of dilatational modulus and phase angle is 5 to 10%. Furthermore, corresponding to what was observed by others⁵, no distinguishable peaks are observed in the phase angle. With β -lactoglobulin/pectin complexes the dilatational modulus at low charge ratios was always lower than that of the pure protein in the absence of pectin. With ovalbumin this is not the case. The modulus in the presence of pectin is higher than that of pure ovalbumin. Only in the initial stage of adsorption (just after the formation of a clean interface) the increase of surface pressure was delayed in the presence of pectin (see lag time, chapter 2, table 2.2). During this stage, e.g. 30s after formation of the clean interface, the modulus of the complex layer is also lower than that of the pure ovalbumin layer (at equal ovalbumin bulk concentration). A few minutes later, the modulus versus surface pressure curves of the mixtures cross that of the pure ovalbumin layer and reach higher values than pure ovalbumin.

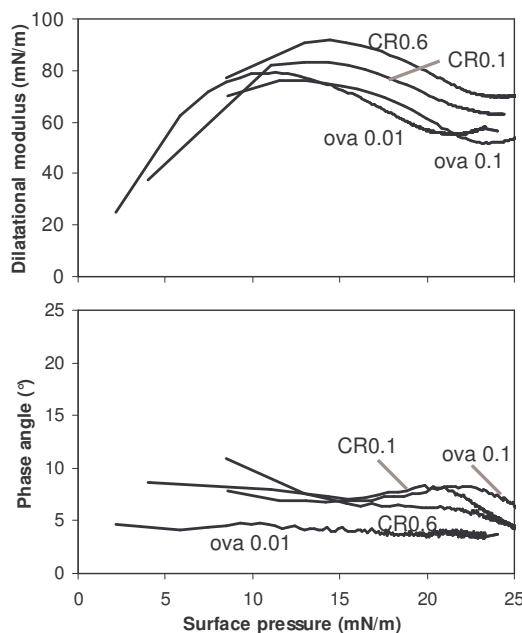


Figure 9.7: Dilatational modulus (top) and phase angle (bottom) as a function of surface pressure for ovalbumin at two concentrations (0.01 and 0.1 g/L) and ovalbumin/pectin complexes at two charge ratios (~0.1 and ~0.6, ovalbumin concentration 0.1 g/L), pH 4.5 and 12 mM.

It should finally be noted that with ovalbumin and pectin complex coacervation (macroscopic phase separation) upon mixing both ingredients occurred very rapidly compared to the phase separation observed with β -lactoglobulin/pectin and β -lactoglobulin/pullulan; with ovalbumin large liquid like coacervate droplets appeared almost instantaneously. A microscopic picture of an ovalbumin/pectin coacervate phase is shown in figure 9.8. This picture may be compared to the pictures of β -lactoglobulin/pectin and β -lactoglobulin/pullulan coacervate phases in chapter 7.

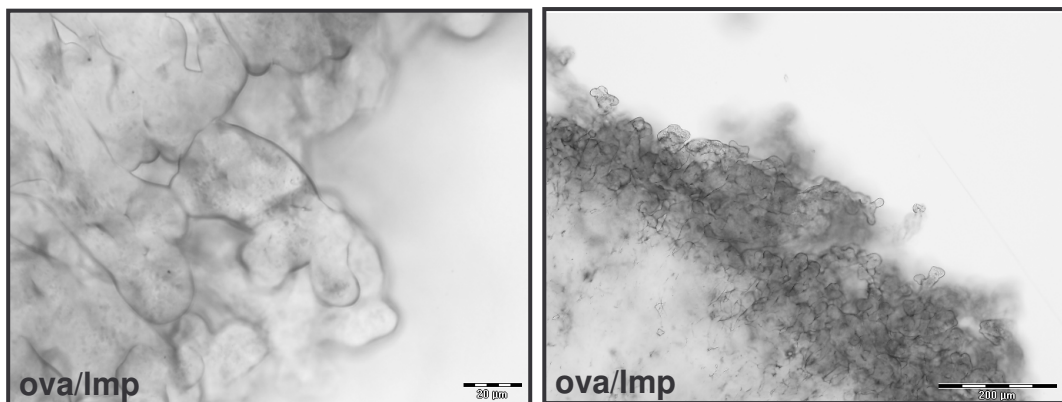


Figure 9.8: Microscopic picture of a ovalbumin/pectin (ova/Imp) coacervate phase ~30 min after mixing the biopolymers, scale bar left is 20 μm , right 200 μm . The pH was 4.5 and the ionic strength ~9 mM.

9.2.2 Discussion

Before trying to understand the surface rheological behaviour of the complexes we first consider the behaviour of pure β -lactoglobulin layers. If the dependence of dilatational modulus on surface pressure completely coincided for all concentrations, and only the adsorption rates were different, the layer structures could be the same for all β -lactoglobulin concentrations. The fact that dilatational modulus and phase angle versus surface pressure depend on the bulk concentration indicates that a second process occurs during adsorption, presumably at a rate independent of adsorption rate. This second process may be either conformational changes of protein in the adsorbed layer, occurring to a different extent at different bulk protein concentrations, or a time dependent interaction between protein molecules or ordering of protein molecules in the surface layer. Recently, a very similar β -lactoglobulin concentration dependence of the phase angle was reported by Benjamins et al.⁶. Limited conformational changes upon adsorption of β -lactoglobulin (10% loss of β -sheet) were previously demonstrated using infra-red reflection adsorption spectroscopy³ (In this work no concentration dependence was shown, but the lowest concentration used was a factor of 5 higher than our highest concentration). Fainerman and coauthors⁷ proposed a model for calculating the dilatational modulus of adsorbed protein layers (the elastic part) based on the idea that different molecular areas are occupied at different surface pressures. Cohen Stuart et al.⁸ relate the extent to which different protein molecules may spread at an interface to the protein conformational stability. In figure 9.9 (top right) the transition between two different molecular areas, A_{\min} (minimum area occupied per molecule) and A_{\max} (maximum area occupied per molecule), is schematically depicted, indicated with A-reorganisations. These A-reorganisations - which is a form of in surface relaxation - could account for the observation of a phase angle. However, this does not yet explain the bulk concentration dependence of the maximum value of the phase angle. Let us therefore assume that the longer the maximum molecular area is occupied by a protein molecule at the interface, the more difficult becomes the return to a smaller molecular area; the occupation of A_{\max} may even become irreversible. The concentration dependence of the phase angle can now be explained by the presence of two populations of protein molecules at the surface: one population formed by molecules that arrived at the surface before the surface pressure reached ~15 mN/m so that

they could irreversibly spread to some extent (occupying A_{\max}) and a second population ('late arrivals') that adsorb in a more compact conformation, closer to the native state (occupying only A_{\min}). In particular at high concentrations, adsorption is fast and the second population is relatively large. These are the molecules that can reversibly spread at the relevant timescale (during oscillations), giving rise to a significant phase angle. A larger population irreversibly occupying A_{\max} at lower bulk concentration corresponds to the observation that the equation of state shifts to lower adsorbed mass by adsorption at lower bulk concentration⁴. Furthermore, the decreasing slope of the equation of state observed at ~ 15 mN/m (chapter 8, e.g. figure 8.5c) is in line with the fact that the population of protein molecules arriving after surface pressure has increased to ~ 15 mN/m occupy a smaller molecular area.

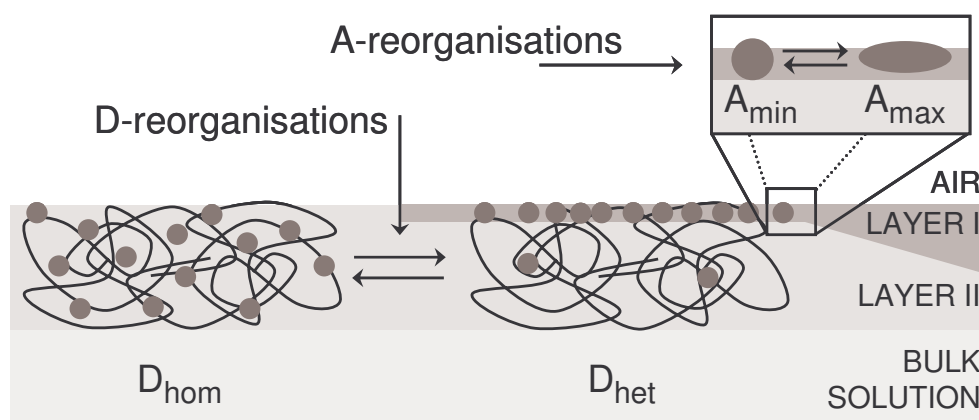


Figure 9.9: Schematic depiction of two types of reorganisations within adsorbed protein/polysaccharide layers. Left: reorganisation within the complex layer from a homogeneous distribution of adsorbed mass (D_{hom}) perpendicular to the interface to a heterogeneous distribution (D_{het}): layer I and layer II (indicated as D-reorganisations). Right: reorganisations of protein in layer I to a different area occupied per molecule (indicated as A-reorganisations).

In mixed protein/polysaccharide layers two peaks were observed in the phase angle (Figure 9.4 and 9.5). We first focus on the second peak, which is observed in the same surface pressure range as that for the pure protein layers (between 15 and 20 mN/m). We assume that layer I, as depicted in figure 9.9, dominates the surface pressure, because the density of this layer is in all cases higher than that of its adjacent layer II (as demonstrated by neutron reflection, chapter 5). This layer has the thickness of a protein monolayer, but most likely also contains some (parts of) polysaccharides. The amount of polysaccharide depends on the charge ratio (and with that on the net charge) of the complexes. If negatively charged complexes adsorb at an interface, the rate at which protein molecules arrive at the interface is much lower than in the absence of the polysaccharide. This may lead to irreversible occupation of a larger molecular area by the protein molecules in the complexes. When a neutral complex arrives at the interface it delivers more protein molecules at the same time than a negatively charged complex (the volume fraction of protein in neutral complexes is higher). In this case arrival of neighbouring protein molecules takes less time, resulting in a higher population of protein molecules occupying smaller molecular area (A_{\min}). These molecules may reversibly spread at the relevant timescale (the timescale of the oscillations), indicated by a higher phase angle when the charge ratio approaches 1 (Figure 9.5). While the

maximum in phase angle decreases with decreasing charge ratio (and thus higher net charge), the peak position shifts to higher surface pressures. Since electrostatic repulsion within an adsorbed layer contributes to surface pressure (as demonstrated for protein molecules with varying net charge by Wierenga et al.⁴), part of the surface pressure in case of the negatively charged complexes could originate from the presence of negatively charged polysaccharides. (It should be noted that pectin does not increase surface pressure in the absence of protein, but the presence of protein may force a higher polysaccharide concentration in the adsorbed layer). Although the presence of polysaccharides may contribute to surface pressure, it is not likely to force protein molecules to adopt a smaller molecular area. Adsorption of ‘second population’ protein molecules, adopting only A_{\min} , therefore occurs at higher surface pressure than in the absence of polysaccharides. Hence, the shift of phase angle peak position to higher surface pressures observed with decreasing charge ratio may be explained by an increasing contribution by (negatively charged) polysaccharides to the surface pressure.

Whereas with pure protein layers the lower peak height of the phase angle corresponded to a higher dilatational modulus, in the mixed layers the lower peak height (observed at low CR) corresponds to lower dilatational modulus. The suggested increasing contribution of electrostatic repulsion by polysaccharides with decreasing charge ratio may account for the lower modulus; the polysaccharides are presumably easier compressible than protein. In summary, an excess of polysaccharide (i.e. low CR) may facilitate protein spreading by reducing the rate at which proteins reach layer I. This results in a lower ‘second population’ of protein molecules that can spread at the timescale of the oscillations, leading to a high phase angle. At the same time, although the polysaccharide may contribute to surface pressure by electrostatic repulsion, the dilatational modulus remains relatively low, due to its higher compressibility of polysaccharide compared to protein.

To discuss the first peak in phase angle observed at $\Pi \sim 11$ mN/m we return to figure 9.9. Before surface pressure is sufficiently high that ‘second population’ protein molecules adsorb occupying A_{\min} , giving rise to the second peak in phase angle (observed at $\Pi \sim 17$ mN/m), reorganisations within the complex layer need to occur; when complexes arrive at the interface, the protein molecules are presumably homogeneously distributed through the complex, resulting in a homogeneous density profile in the adsorbed layer perpendicular to the interface (figure 9.9, D_{hom}). At this stage surface pressure is low, the volume fraction of protein molecules in direct contact with the interface is low (see chapter 8) and hence, the protein molecules can spread to A_{\max} . At this stage surface pressure may be determined by the complete thickness of the film. To reach a further increase in surface pressure, reorganisation in the complexes has to take place. In figure 9.9, reorganisations within the adsorbed complex layer (indicated as D-reorganisations) is considered as the transition from a homogeneous protein distribution in the complex layer normal to the interface (D_{hom}) to a more dense layer I formed with extra protein from layer II (D_{het}). This type of reorganisation starts at lower surface pressures than the reorganisation within protein molecules (A-reorganisations). Although the D-reorganisations continue till high surface pressures (as it is the rate limiting step for adsorption in layer I) the transition of a homogeneous density distribution over the

film that determines surface pressure as a whole, to a heterogeneous film in which layer I dominates surface pressure may account for the first peak in phase angle as observed for the complex layers (Figure 9.4 and 9.5, bottom panels).

Considering all the discussions above, the dilatational modulus as a function of time responds clearly to a variation in any parameter affecting protein/polysaccharide interaction (charge ratio, charge density and molecular weight of the polysaccharides, ionic strength, aging time of the complex before adsorption). Previously described D-reorganisations, i.e. the increase of the protein volume fraction in layer I at the expense of layer II (and the bulk solution), are a rate limiting step in the increase of surface pressure and dilatational modulus. The dilatational modulus seems to give information on the rate in which this happens. The relatively simple measurement of dilatational modulus and corresponding phase angle may provide an opportunity to get information on conformational reorganisation in soluble complexes at interfaces since both quantities respond differently to the different types of reorganisations. For instance, with β -lactoglobulin/pectin complexes it takes much more time to reach a steady state dilatational modulus than it does with β -lactoglobulin/pullulan complexes. This suggests faster reorganisations in the complexes with pullulan compared to those in complexes with pectin; reorganisations in terms of protein diffusion through the complexes. In chapter 7 the same was suggested (faster protein diffusion through the complexes with pullulan than with pectin) on the basis of the more liquid character of a β -lactoglobulin/pullulan coacervate compared to a β -lactoglobulin/pectin coacervate (as concluded from small angle X-ray scattering and light microscopy).

Another example is the fact that the increase in dilatational modulus with ovalbumin is much less retarded by the presence of pectin than β -lactoglobulin is. This suggests faster reorganisations, or a faster diffusion of ovalbumin through the complex with pectin compared to the diffusion rate of β -lactoglobulin through the complex with pectin. Indeed time resolved fluorescence anisotropy (TRFA) measurements on ovalbumin in the presence of pectin at an air/water interface suggest that the rotational mobility of ovalbumin molecules in the presence of pectin is not hampered⁹. In contrast, a strongly decreased mobility of β -lactoglobulin molecules in the presence of pectin at an air/water interface was shown using TRFA (chapter 5). From a faster ovalbumin mobility through complexes with pectin (compared to β -lactoglobulin through complexes with pectin) one would predict that an ovalbumin/pectin coacervate phase has a more liquid character than a β -lactoglobulin/pectin coacervate. This is indeed shown in figure 9.8; see chapter 7 for a picture of the more solid-like β -lactoglobulin/pectin coacervate.

As to the question why ovalbumin, compared to β -lactoglobulin, may diffuse faster through a complex or coacervate phase with pectin the following may be considered. Ovalbumin shows no concentration dependence in the dilatational modulus versus time, and the observed phase angles are very low. It has been shown before that ovalbumin shows less unfolding at the air/water interface (by coinciding equations of state for different ovalbumin bulk concentrations^{4, 10}, and by a larger required adsorbed mass for surface pressure

increase¹¹. Moreover the timescale at which ovalbumin unfolds in bulk solution (10-100s) is much larger than that of β -lactoglobulin unfolding ($\sim 1s$)^{4, 12}. A faster unfolding rate of β -lactoglobulin molecules (compared to that of ovalbumin), as manifested at the interface by the different conformations (A_{min} and A_{max}), may contribute to a stronger binding to polysaccharide molecules. Conformational changes of β -lactoglobulin in a coacervate phase with acacia gum¹³ and α -Gliadin and Globulin proteins in coacervates with arabic gum¹⁴ have been reported, but more research is necessary to convincingly prove this. Another possible explanation may be differences in charge distribution on both protein molecules. However, observed effects of conformational changes and charge distribution are generally only subtle compared to this remarkable difference in complex/coacervate dynamic behaviour.

In conclusion, the dynamic character of protein/polysaccharide complexes (in terms of diffusion of protein through the soluble complexes) seems very relevant for the adsorption kinetics and the behaviour of the resulting adsorbed layers. Diffusion of protein through complexes with polysaccharides (which may be qualitatively extended to diffusion through protein/polysaccharide coacervate phases) depends on many parameters that effect protein/polysaccharide interaction, like charge ratio and charge density on both biopolymers, ionic strength, and aging time of the complex before adsorption. Relatively simple measurements of dilatational modulus and corresponding phase angle at the air/water interface (as a function of all the parameters mentioned above) gives information about the dynamic character of protein/polysaccharide complexes and presumably also on that of the coacervate phase. Although the discussions given above on this topic are speculative, all indications are welcome since literature on the dynamic character of complexes and complex coacervates is scarce¹⁵⁻¹⁷. However, more work (e.g. time resolved fluorescent anisotropy on protein in bulk and at interfaces in the presence and absence of polysaccharides, and varying all parameters that affect protein/polysaccharide interaction) should be done to prove the concepts.

9.3 APPLICATIONS

In this last section we will summarize the outcome of the thesis in terms of potential applicability. Now more insight is gained on the mechanism of mixed protein/polysaccharide adsorption it is possible to use this insight to control product properties. Using protein/polysaccharide interaction it appears possible to control both protein adsorption kinetics and the macroscopic properties of adsorbed layers (surface rheology, layer thickness and density and net charge of the layer).

Table 9.1 gives an overview of which parameters can be used to improve the functionality of the protein/polysaccharide combination used. The table should not be read in such a way that always all requirements to all parameters need to be met. Even by adjustment of a single parameter, the desired functionality could be improved. For instance the minus in the first row (Table 9.1) below 'charge density polysaccharide' indicates that charge density should be decreased in order to obtain a faster increase of surface pressure. In figure 9.10 the impact of polysaccharide charge density on the rate of surface pressure increase is illustrated.

A faster increase in surface pressure may improve the foam capacity of a product (chapter 2). Conversely, when foaming should be prevented (as for instance with fermentation processes), e.g. an increase of molecular weight or charge density of the polysaccharide may be sufficient.

Table 9.1: Suggestions for improvement of combined protein/polysaccharide functionality at liquid interfaces and in bulk structures. The words 'solid' and 'liquid' refer to the nature of the coacervate phase in bulk or in the interfacial layer. For further explanation see text.

desired functionality		control parameter			molecular parameters			system parameters		
		molecular weight polysaccharide	charge density polysaccharide	heterogeneity in charge distribution on polysaccharide	charge ratio complexes	solution pH*	solution ionic strength			
liquid interface	fast increase surface pressure (e.g. foam capacity)	-	-	?	+	+	+			
	thick cohesive layers (e.g. build bulk structure)	+	+	+ solid - liquid	close to 1	-	***		-	
	negatively** charged droplets/bubbles (e.g. foam stability)	+	+	?	(< 1) -	-	***		-	
bulk structure	solubilise protein	?	-		(< 1) -					
	macroscopically phase separated coacervate structure			+ solid - liquid						
	macroscopically phase separated coacervate density		+	?	maximal at 1					

* for cationic polysaccharides -

** or positively charged for cationic polysaccharides

*** not below pH ~ $pK_{a,\text{polysaccharide}} - 0.5$

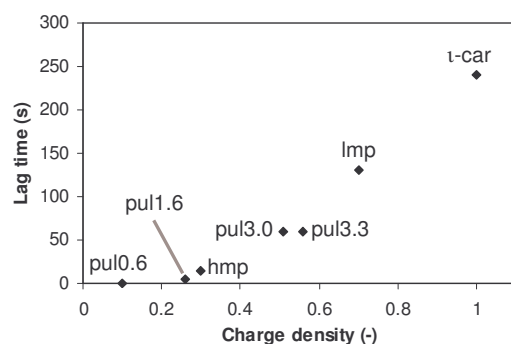


Figure 9.10: Charge density dependence of the lag time for surface pressure increase (i.e. the time between creation of a clean interface and a significant increase in surface pressure) for β -lactoglobulin/polysaccharide complexes with different polysaccharides. β -lactoglobulin concentration was 0.1 g/L, pH 4.5 and 12 mM. Pullulan samples (chapter 6) are indicated with 'pul', high methoxyl pectin with 'hmp', low methoxyl pectin with 'lmp' and ι -carrageenan with 't-car'. The charge density is the fraction of monosaccharide subunits with a carboxyl group (or sulphate group in case of ι -carrageenan), protein/polysaccharide charge ratio was 0.5 for most samples, only 0.2 for hmp and t-car.

When a combination of functionalities is desired, the ideal parameter conditions could contradict for two different functionalities. For instance one may be interested in a fast increase in surface pressure to make a foam or an emulsion. Subsequently a negative net charge on the air bubbles or emulsion droplets is desired to improve the stability of the

foam/emulsion. If both functionalities are not sufficiently met by the choice of a balance between e.g. low and high polysaccharide charge density and/or low and high polysaccharide molecular weight, one could think of a two step process. For example first creation of the foam or emulsion in the absence of a polysaccharide, and subsequent addition of the polysaccharide^{18, 19}. Alternatively, foam or emulsion could be created from a mixed protein/polysaccharide solution at a pH high enough that adsorption kinetics are not strongly retarded by the polysaccharide. A subsequent decrease in pH could then improve the stability by adsorption of the negatively charged polysaccharide on the densely packed protein layer formed during foaming/emulsification. If injection of acid after foam formation or emulsification is not possible in the production process, alternatively, acidification by glucono-delta-lactone or lactic acid bacteria may be a solution. All ingredients can in the latter case be added before the foaming or emulsification step, and acidification will (slowly) occur afterwards.

If the product formulation requires a certain pH or ionic strength at which the protein polysaccharide/interaction is not strong enough, selection of a polysaccharide with a higher charge density, and/or stronger acidic groups may be a solution. For instance λ -carrageenan has a charge density of 1.5 (3 charges in every disaccharide subunit) and instead of weak-acidic carboxyl groups (as in pectin and pullulan) it contains sulphate groups, which are strong acids.

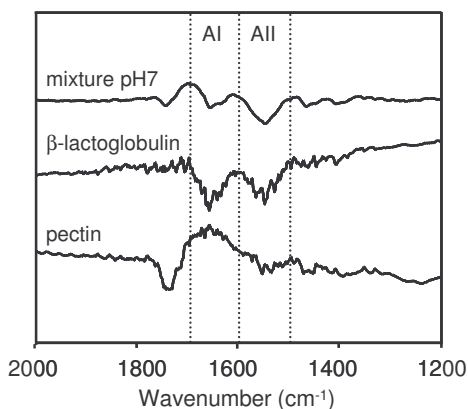


Figure 9.11: Infra-red reflection adsorption spectroscopy spectra at the air/water interface of a pure pectin (0.1 g/L, pH4.5), pure β -lactoglobulin solution (0.05 g/L, pH7) and a β -lactoglobulin(0.05 g/L)/pectin(0.025 g/L) mixture (pH7) after compression of the interface by a factor of 6. For a description of the method we refer to the work of Meinders et al.²⁰. The peaks in the amide I (AI) and amide II (All) region observed in the β -lactoglobulin spectrum were previously described³. The fact that the pectin spectrum showed different features enables to distinguish β -lactoglobulin and pectin at the air/water interface; the spectrum of the mixture at pH 7 indeed shows features from both the β -lactoglobulin and the pectin spectrum, especially in the AI region. (It should be mentioned that although pectin could be detected at the interface in the absence of protein, it did not affect surface pressure or surface rheological properties in the absence of protein.)

At conditions where complex formation could no longer be detected in bulk solution, binding of polysaccharide to an adsorbed protein layer may very well still occur. At an interface, polysaccharides can simultaneously bind to many protein molecules (that have already lost their translational entropy as a result of adsorption at the interface); this multi-point interaction is stronger than the binding of several 'loose' protein molecules in the bulk solution and therefore applicable over a wider range of conditions²¹. Whereas pectin does not

significantly delay the increase in surface pressure by β -lactoglobulin adsorption at ionic strengths above 80 mM (chapter 2), the presence of pectin affected surface shear rheology even up to an ionic strength of 300 mM (chapter 3). Whereas pectin does not delay the increase in surface pressure (by β -lactoglobulin adsorption) at a pH above 5.2, the presence of pectin at the air/water interface could still be observed with infra-red reflection adsorption spectroscopy (Figure 9.11). Also the rotational mobility at pH 7 is affected by the presence of pectin (table 9.2). In the presence of pectin β -lactoglobulin has an increased rotational mobility compared to that in the absence of pectin. The same was observed for ovalbumin⁹. This may be a useful functionality for the immobilisation of enzymes at interfaces; the polysaccharide may protect the native structure of the enzyme. Finally, if a stronger interaction at a pH above the iso-electric point of the protein is desired, one could use a cationic polysaccharide (e.g. chitosan) or cationic polyelectrolytes for non-food applications.

Table 9.2: Fluorescence anisotropy correlation times of pure β -lactoglobulin and β -lactoglobulin/pectin complex adsorbed layers at the air/water interface, pH 7 and $I \sim 2$ mM. For a description of the time resolved fluorescence anisotropy method and the α , τ , χ^2 and r_∞ we refer to chapter 5 and⁹. The rotational correlation time (ϕ_1) corresponds to the rotational mobility of β -lactoglobulin monomers. It appears that the contribution of this β -lactoglobulin rotation (β_1) is larger in the presence of pectin than in the pure protein layer; indicating an increased β -lactoglobulin rotational mobility in the presence of pectin.

Sample	time (min)	β_1 ϕ_1 (ns)	α_3 τ_3 (ns)	α_2 τ_2 (ns)	α_1 τ_1 (ns)	χ^2	r_∞
β -lg	8	0.09 8	0.10 13.4	0.03 6.5	0.02 2.2	1.06	0.00
β -lg/pectin	8	0.14 9	0.09 13.5	0.03 6.3	0.02 1.9	1.07	0.00
β -lg/pectin	17	0.14 8	0.07 14.2	0.06 10.4	0.03 3.0	1.07	0.00

REFERENCES

- (1) Wierenga, P. A.; Meinders, M. B. J.; Egmond, M. R.; Voragen, A. G. J.; de Jongh, H. H. J., Quantitative description of the relation between protein net charge and protein adsorption to air-water interfaces. *Journal of Physical Chemistry B* **2005**, 109, (35), 16946-16952.
- (2) Wierenga, P. A.; Meinders, M. B. J.; Egmond, M. R.; Voragen, F. A. G. J.; de Jongh, H. H. J., Protein exposed hydrophobicity reduces the kinetic barrier for adsorption of ovalbumin to the air-water interface. *Langmuir* **2003**, 19, (21), 8964-8970.
- (3) Meinders, M. B. J.; De Jongh, H. H. J., Limited conformational change of beta-lactoglobulin when adsorbed at the air-water interface. *Biopolymers* **2002**, 67, (4-5), 319-322.
- (4) Wierenga, P. A.; Egmond, M. R.; Voragen, A. G. J.; de Jongh, H. H., The adsorption and unfolding kinetics determines the folding state of proteins at the air-water interface and thereby the equation of state. *Journal of Colloid And Interface Science* **2006**, 299, (2), 850-857.
- (5) Benjamins, J.; Cagna, A.; Lucassen-Reynders, E. H., Viscoelastic properties of triacylglycerol/water interfaces covered by proteins. *Colloids and Surfaces A* **1996**, 114, 245-254.
- (6) Benjamins, J.; Lyklema, J.; Lucassen-Reynders, E. H., Compression/expansion rheology of oil/water interfaces with adsorbed proteins. Comparison with the air/water surface. *Langmuir* **2006**, 22, (14), 6181-6188.
- (7) Fainerman, V. B.; Lucassen-Reynders, E. H.; Miller, R., Description of the adsorption behaviour of proteins at water/fluid interfaces in the framework of a two-dimensional solution model. *Advances in Colloid and Interface Science* **2003**, 106, 237-259.

- (8) Cohen Stuart, M. A.; Norde, W.; Kleijn, J. M.; van Aken, G. A., Formation and properties of adsorbed protein films: importance of conformational stability. In *Food Colloids: interaction, microstructure and processing*, Dickinson, E., Ed. The Royal Society of Chemistry: Cambridge, 2005; pp 99-119.
- (9) Kudryashova, E. V.; Visser, A. J. W. G.; Hoek, A. v.; de Jongh, H. H. J., Molecular details of pectin-ovalbumin complexes at the air/water interface; a spectroscopy study. submitted, 2006.
- (10) Benjamins, J. Static and dynamic properties of proteins adsorbed at liquid interfaces. PhD, Thesis, Wageningen University, Wageningen, The Netherlands, 2000.
- (11) de Feijter, J. A.; Benjamins, J., Soft-Particle Model Of Compact Macromolecules At Interfaces. *Journal of Colloid and Interface Science* **1982**, 90, (1), 289-292.
- (12) Broersen, K.; Meinders, M. B. J.; Hamer, R. J.; Voragen, A. G. J.; de Jongh, H. H. J., Glycosylation affects protein unfolding/refolding mechanism and the formation of aggregation-prone intermediates. *manuscript in preparation*.
- (13) Mekhloufi, G.; Sanchez, C.; Renard, D.; Guillemin, S.; Hardy, J., pH-induced structural transitions during complexation and coacervation of beta-lactoglobulin and acacia gum. *Langmuir* **2005**, 21, (1), 386-394.
- (14) Chourpa, I.; Ducel, V.; Richard, J.; Dubois, P.; Boury, F., Conformational modifications of alpha gliadin and globulin proteins upon complex coacervates formation with gum arabic as studied by Raman microspectroscopy. *Biomacromolecules* **2006**, 7, (9), 2616-2623.
- (15) Bohidar, H.; Dubin, P. L.; Majhi, P. R.; Tribet, C.; Jaeger, W., Effects of protein-polyelectrolyte affinity and polyelectrolyte molecular weight on dynamic properties of bovine serum albumin-poly(diallyldimethylammonium chloride) coacervates. *Biomacromolecules* **2005**, 6, (3), 1573-1585.
- (16) Weinbreck, F.; Rollema, H. S.; Tromp, R. H.; de Kruif, C. G., Diffusivity of whey protein and gum arabic in their coacervates. *Langmuir* **2004**, 20, (15), 6389-6395.
- (17) Sanchez, C.; Mekhloufi, G.; Renard, D., Complex coacervation between beta-lactoglobulin and Acacia gum: A nucleation and growth mechanism. *Journal of Colloid and Interface Science* **2006**, 299, (2), 867-873.
- (18) Gu, Y. S.; Decker, A. E.; McClements, D. J., Production and characterization of oil-in-water emulsions containing droplets stabilized by multilayer membranes consisting of beta-lactoglobulin, iota-carrageenan and gelatin. *Langmuir* **2005**, 21, (13), 5752-5760.
- (19) McClements, D. J., Theoretical analysis of factors affecting the formation and stability of multilayered colloidal dispersions. *Langmuir* **2005**, 21, (21), 9777-9785.
- (20) Meinders, M. B. J.; van den Bosch, G. G. M.; de Jongh, H. H. J., IRRAS, a new tool in food science. *Trends in Food Science & Technology* **2000**, 11, (6), 218-225.
- (21) Neirynck, N.; Van der Meer, P.; Lukaszewicz-Lausecker, M.; Cocquyt, J.; Verbeken, D.; Dewettinck, K., Influence of pH and biopolymer ratio on whey protein - pectin interactions in aqueous solutions and in O/W emulsions. *Colloids and Surfaces A: Physicochemical and Engineering Aspects* In Press.

Summary

The aim of this thesis was to understand the influence of (attractive and non-covalent) protein/polysaccharide interaction on their adsorption behaviour at air/water interfaces. Having insight in the mechanism of mixed protein/polysaccharide adsorption could provide suggestions and predictions to control adsorption kinetics and the functional behaviour of mixed protein/polysaccharide adsorbed layers. The approach was to first identify the relevant parameters in the mixed protein/polysaccharide adsorption process. Subsequently, for each parameter a range of ingredients was selected/prepared allowing variation of only this one parameter (e.g. polysaccharide samples were chemically carboxylated to four different charge densities, all prepared from the same starting material). After investigation of the phase behaviour of all different protein/polysaccharide mixtures in bulk solution, the role of each parameter in mixed protein/polysaccharide adsorption was systematically studied. The parameters most thoroughly assessed were: protein/polysaccharide mixing ratio, polysaccharide charge density and molecular weight and the sequence of adsorption. The majority of the measurements were performed with β -lactoglobulin (in combination with various polysaccharides) at standard conditions of pH 4.5 and low ionic strength (< 10 mM). In addition, some experiments were done at higher ionic strengths, different pH's, with different proteins or at an oil/water interface, to extend the insight in mixed protein/polysaccharide adsorption. The selection of β -lactoglobulin was based on the fact that this protein is not significantly hindered by a kinetic barrier for adsorption, once it is in close vicinity of the interface. Furthermore, it is a widely used ingredient in the food industry.

In chapter 2 relevant parameters controlling mixed protein/polysaccharide adsorption kinetics (as monitored by surface pressure) are identified: pH, ionic strength, protein/polysaccharide mixing ratio and charge density of the protein and the polysaccharide. In chapter 3 it was shown that the density of adsorbed layers is determined by protein/polysaccharide mixing ratio and the sequence of adsorption (simultaneous or sequential - first protein, than polysaccharide - adsorption). Consequently, surface dilatational and shear rheology could be controlled by these parameters. In chapter 4 it is shown that protein/polysaccharide complex adsorption (both adsorption kinetics and surface rheological behaviour) at oil/water interfaces is similar to that at the air/water interface. By spectroscopic analysis of the surface layers, multiple layers could be identified (using neutron reflection) and a reduced protein mobility through adsorbed layers was illustrated (using time resolved fluorescence anisotropy) in chapter 5. In chapter 6, a strong charge density dependence of protein/polysaccharide complex behaviour in solution and at the air/water interface was demonstrated by

electrophoretic mobility, light scattering and surface rheology. The structure of macroscopically phase separated coacervate phases was examined using small angle X-ray scattering in chapter 7. Insight in the structure and density of coacervates helped understanding the structure of soluble complexes and adsorbed complex layers. In chapter 8 the adsorbed amount and surface pressure is followed as a function of time using ellipsometry while systematically varying charge ratio and polysaccharide charge density and molecular weight. Not only adsorption kinetics but also the relation between surface pressure and adsorbed amount (equation of state) differed between different samples. In chapter 9, entitled ‘general discussion’, the proposed mechanism for mixed adsorption and layer formation is discussed and extended. We present some speculations on the dynamic character of different protein/polysaccharide complexes inferred from surface dilatational modulus and phase angle data (viscous/elastic contribution). Finally we consider a number of possible applications of the newly gained insights.

A model for mixed protein/polysaccharide adsorption was proposed. The combination of several simultaneously occurring processes determines the rate by which proteins adsorb to air/water interface in the presence of polysaccharides. When considering adsorption kinetics it is important to control the partition of free protein and protein in complexes with polysaccharides. This depends on the protein/polysaccharide binding affinity, which in turn depends on molecular parameters of the ingredients (protein and polysaccharide charge density and distribution) and system parameters like protein/polysaccharide mixing ratio (also expressed as charge ratio) solution pH, and ionic strength. Binding affinity is dominated by electrostatic interaction; at low ionic strength and when the polysaccharide charge density is high (> 0.5), the majority of protein ($> 90\%$) in solution is present in complexes with the polysaccharides up to a charge ratio of ~ 1 (ratio between positive net charge on the protein and negative charge on the polysaccharide). Diffusion of free proteins from the solution to the interface is determined by the size of protein molecules, which does not vary much between different globular proteins. Protein present in a complex with a polysaccharide, like pectin, has a roughly ten times lower diffusion coefficient due to the large radius of the complexes (~ 20 nm). Hence, the polysaccharide may presumably retard protein adsorption by at most ten times by a retarded diffusion rate.

The much stronger decrease in adsorption rate observed for negatively charged complexes was explained by a kinetic barrier for protein adsorption by polysaccharide at the interface (chapter 8). Protein/polysaccharide complexes presumably adsorb at the interface by the protein molecules on the outside of the complexes (the polysaccharide on its own does not increase surface pressure). The volume fraction of protein in a soluble complex is, depending on its net charge, presumably only on the order of a few percent (chapter 7). From neutron reflection data (chapter 5) it was concluded that in steady state an adsorbed complex layer could always be subdivided in two layers. Layer I that is in direct contact with the actual air/water interface always had a higher density than layer II (adjacent to layer I on the solvent side). Especially the density of layer II depended on the net charge of the complexes. The

density of layer I was ~50%, which implies that reorganisations within the complex layer must have occurred. Due to the high affinity of protein for the interface, the density of layer I increased at the expense of layer II. In case of negatively charged complexes a single complex layer does not supply enough protein to reach such high volume fractions in layer I, and hence, adsorption of extra protein from (complexes in) the bulk solution is necessary. This extra protein from the bulk solution has to penetrate in layer II and move towards layer I. Depending on the strength of protein/polysaccharide interaction, the mobility of protein molecules through the complex layer may be up to 100 000 times retarded (chapter 5 and 8). An alternative way to increase the density in layer I would be desorption of the polysaccharide from the interface making space for adsorption of new complexes from the bulk solution. However, the more the mobility of protein through the complex is hindered (due to strong protein/polysaccharide interaction), the stronger also the polysaccharide is bound to the interface due to multi-point interaction: since polysaccharides may simultaneously attach to many protein molecules at the interface (that have already lost their translational entropy by adsorption) their interaction with the interface is much stronger than with separate protein molecules in bulk solution. Hence, a polysaccharide can constitute a kinetic barrier for protein adsorption at the interface by its irreversible attachment to (proteins at) the interface in combination with a reduced protein mobility through the complex layer. In case of strong protein/polysaccharide interaction, this kinetic barrier is the rate limiting step in adsorption. The barrier increases with decreasing charge ratio between the complexed protein and polysaccharide, due to electrostatic repulsion within and between complexes at the interface and the resulting lower initial protein volume fraction at the interface. Also by increasing polysaccharide molecular weight the net charge of - and thus electrostatic repulsion between - the complexes increases (chapter 8).

As the kinetic barrier for protein adsorption (raised by the presence of a polysaccharide) mainly takes place in layer II, the whole mechanism is presumably rather independent of the type of interface (air/water or oil/water). It was indeed shown that the proposed mechanism for mixed adsorption is also valid for oil water interfaces (chapter 4).

The density in layer I is expected to dominate surface pressure and surface dilatational modulus, since layer I is always more dense than layer II. Since polysaccharides can prevent a dense packing in layer I, the resulting dilatational modulus in case of negative complexes is lower than that of a neutral complex layer or a pure protein layer (chapter 3). This lowering effect on dilatational modulus can be circumvented by first allowing the formation of a pure protein layer and subsequent addition of polysaccharide (sequential adsorption, chapter 3). The cohesion between and within complexes at the interface is presumably important for the surface shear behaviour. Whereas in a pure protein layer protein molecules may shear along each other, if protein molecules are interconnected by polysaccharides, within layer I or by II, the required shear stress may be higher (chapter 3 and 6).

In conclusion, protein/polysaccharide interaction can be exploited to control protein adsorption at air/water and also oil/water interfaces. Any parameter affecting

protein/polysaccharide interaction (e.g. ingredient parameters like polysaccharide molecular weight, charge density and distribution or system parameters like charge ratio, pH and ionic strength) may be varied to obtain the desired adsorption kinetics, surface rheological behaviour, or net charge of the surface layer. The choice of simultaneous protein/polysaccharide adsorption (in the form of complexes) versus sequential adsorption (first the protein, than the polysaccharide) provides an extra control parameter in the functionality of mixed adsorbed layers.

Samenvatting

Eiwitten worden vaak gebruikt in levensmiddelen om een stabiel schuim of een stabiele emulsie te maken; oftewel om kleine luchtbellen of oliedruppeltjes in water te maken/houden. Polysachariden kunnen toegevoegd worden om het product wat dikker te maken (te ‘binden’). Als deze eiwitten en polysachariden tegelijk aanwezig zijn, kunnen ze interactie met elkaar hebben. Dit kan er voor zorgen dat de functionaliteit van beide ingrediënten verandert.

Het doel van dit proefschrift is het begrijpen van de invloed van (attractieve en niet-covalente) eiwit/polysacharide interactie op het adsorptie gedrag aan lucht/water grensvlakken. Inzicht in het mechanisme van simultane eiwit/polysacharide adsorptie verschafft voorspellingen en suggesties om adsorptiekinetiek en het functionele gedrag van eiwitten en polysachariden aan een grensvlak te sturen. De benadering was het eerst identificeren van relevante parameters in het simultane eiwit/polysacharide adsorptie proces (b.v. ladingsdichtheid en molgewicht van het polysacharide, eiwit/polysacharide ratio). Vervolgens werd voor elke parameter een reeks van ingrediënten geselecteerd/vervaardigd zodat het mogelijk was slechts een enkele parameter te variëren. Nadat het fasegedrag van de eiwit/polysacharide mengsels in de oplossing opgehelderd was, werd de rol van elke afzonderlijke parameter in eiwit/polysacharide adsorptie systematisch bestudeerd. De grondigst bestudeerde parameters waren eiwit/polysacharide ratio, ladingsdichtheid en molgewicht van de polysacharides en de volgorde van adsorptie. Het merendeel van de experimenten werd uitgevoerd met β -lactoglobuline (in combinatie met verschillende polysachariden) aan een lucht/water grensvlak onder standaard condities van pH 4.5 en lage ionsterkte (<10 mM). Verder is een aantal experimenten gedaan bij andere ionsterktes, andere pH's, met andere eiwitten of met een olie/water grensvlak om het inzicht in gemengde eiwit/polysacharide adsorptie te verdiepen.

De combinatie van de resultaten heeft geleid tot een algemeen schematisch model voor gemengde eiwit/polysacharide adsorptie. Een samenspel van verschillende gelijktijdig optredende processen bepaalt de snelheid waarmee eiwitten aan een grensvlak kunnen adsorberen. De partitie van vrije en aan polysacharide gebonden eiwitten speelt een belangrijke rol in de adsorptiekinetiek. Dit hangt af van de eiwit/polysacharide bindingsaffiniteit, welke op zijn beurt weer afhankelijk is van moleculaire parameters van beide componenten (ladingsdichtheid en -verdeling op eiwit en polysacharide) en van systeemparameters als eiwit/polysacharide ratio, pH en ionsterkte. De bindingsaffiniteit wordt gedomineerd door elektrostatische interactie; bij lage ionsterkte en hoge ladingsdichtheid van het polysacharide (>0.5) is de meerderheid van het eiwit (>90%) aanwezig in complexen met

polysachariden zolang de ladings ratio niet hoger is dan 1 (de verhouding tussen de positieve nettolading op het eiwit en de negatieve lading op de polysachariden). Diffusie van vrije eiwitten hangt af van de straal van de eiwitmoleculen, welke niet veel varieert tussen verschillende globulaire eiwitten. Eiwit/polysacharide complexen hebben een grofweg 10 keer zo langzame disffusiecoofficient door de grote straal van de complexen (~20 nm). De aanwezigheid van polysachariden kan dus de eiwitadsorptie maximaal 10 keer vertragen door een vertraagde diffusiesnelheid. De veel sterker vertraagde adsorptiesnelheid werd verklaard door een kinetische barrière voor eiwitadsorptie veroorzaakt door het polysacharide op het grensvlak (hoofdstuk 8). Eiwit/polysacharide complexen adsorberen waarschijnlijk door de eiwitmoleculen aan de buitenkant van de complexen (polysachariden veroorzaken geen oppervlaktdruk in afwezigheid van eiwitten). De volumefractie eiwit in de complexen is, afhankelijk van hun nettolading, waarschijnlijk slechts enkele procenten (hoofdstuk 7).

Van neutronen reflectie data (hoofdstuk 5) werd afgeleid dat een geadsorbeerde laag in steady state altijd onderverdeeld kan worden in twee lagen. Laag I, welke in direct contact is met de luchtfase, had altijd een hogere dichtheid dan laag II (aan de water kant van laag I). Vooral de dichtheid van laag II hing af van de netto lading van de complexen. De volumefractie van laag I was ongeveer 50%, wat impliceert dat reorganisatie binnen de complexlaag plaats moet hebben gevonden. Door de hoge affiniteit van eiwit voor het lucht/water grensvlak is de dichtheid van laag I gestegen, ten koste van de dichtheid van laag II. In het geval van negatief geladen complexen bevat een enkele complexlaag niet voldoende eiwit om zulke hoge volumefracties te bereiken in laag I. Er moet extra adsorptie van eiwit (of complexen) uit de bulk oplossing plaats hebben gevonden. Dit 'extra' eiwit moet eerst door laag II om laag I bereiken. Afhankelijk van de sterkte van de eiwit/polysacharide interactie kan de mobiliteit van eiwit door de complex laag (laag II) tot een factor 100 000 vertraagd zijn (hoofdstuk 5 en 8). Een alternatieve manier om de dichtheid in laag I te vergroten is desorptie van polysacharide van het oppervlak, wat ruimte maakt voor de adsorptie van nieuw eiwit of complexen. Echter, hoe meer de mobiliteit van eiwit door de complexlaag wordt verhinderd (door sterke eiwit/polysacharide interactie), hoe sterker ook het polysacharide gebonden is aan het grensvlak door multi-punt-interactie: omdat polysachariden aan meerdere eiwitten op het grensvlak tegelijkertijd gebonden zijn, is de interactie met (eiwitten op) het grensvlak veel sterker dan met afzonderlijke eiwitten in oplossing. Polysachariden kunnen dus een kinetische barrière opwerpen voor eiwitadsorptie aan het grensvlak door middel van hun irreversibele binding aan (eiwitten op) het grensvlak in combinatie met een vertraagde eiwitmobiliteit door een complexlaag. In het geval van sterke interactie is deze kinetische barrière de snelheidsbepalende stap in adsorptie. De barrière neemt toe met afnemende ladings ratio tussen gecomplexeerd eiwit en polysacharide door elektrostatische repulsie binnen en tussen complexen op het oppervlak en de resulterende lagere initiële eiwit volumefractie op het grensvlak. Ook door middel van een grotere molmassa van de polysachariden en dus een grotere nettolading van de complexen (hoofdstuk 8) stijgt de elektrostatische repulsie tussen complexen.

Doordat de kinetische barrière voor eiwitadsorptie (veroorzaakt door de aanwezigheid van polysachariden) zich bevindt in laag II, hangt het hele mechanisme waarschijnlijk niet sterk af van het type grensvlak (lucht/water of olie/water). Het is inderdaad aangetoond dat het voorgestelde mechanisme voor simultane eiwit/polysacharide adsorptie ook geldig is voor olie/water grensvlakken (hoofdstuk 4).

De dichtheid in laag I domineert naar verwachting de oppervlakte druk en dilatatiemodus, omdat deze altijd hoger is dan de dichtheid in laag II. Omdat polysachariden een dichte pakking van eiwitten aan het grensvlak kunnen voorkomen, is de dilatatiemodus in het geval van negatieve complexen lager dan in het geval van neutrale complexen of puur eiwit (hoofdstuk 3). Het verlagende effect op dilatatiemodus kan omzeild worden door eerst een pure eiwitlaag te laten adsorberen en vervolgens polysacharide toe te voegen (sequentiële adsorptie, hoofdstuk 3 en 5). Cohesie binnen en tussen complexen op het grensvlak is waarschijnlijk belangrijk voor het surface shear gedrag. Waar in een pure eiwitlaag eiwitmoleculen wellicht makkelijk langs elkaar kunnen bewegen, kan dat in een gemengde laag moeilijker zijn als de eiwitmoleculen met elkaar verbonden zijn door de polysachariden. Dit kan de hogere shear stress in de gemengde systemen verklaren (hoofdstuk 3 en 6).

In conclusie, eiwit/polysacharide interactie kan gebruikt worden om eiwit adsorptie aan lucht/water en olie/water grensvlakken te sturen. Elke parameter die betrokken is bij de eiwit/polysacharide interactie (b.v. moleculaire parameters als de molmassa van de polysachariden, ladingsdichtheid en ladingsverdeling of systeem parameters als eiwit/polysacharide ratio, pH en ionsterkte) kan gevarieerd worden om hiermee de gewenste adsorptiekinetiek, oppervlakte reologisch gedrag of nettolading van de oppervlaklaag te verkrijgen. De keuze voor simultane eiwit/polysacharide adsorptie (in de vorm van complexen) of sequentiële adsorptie (eerst eiwit, dan polysacharide) creëert een extra mogelijkheid om de functionaliteit van de geadsorbeerde lagen te beïnvloeden.

Dankwoord

Het meest gelezen onderdeel met de meeste clichés: het zit erop! Vier jaar lang zelfstandig werken aan een aio-project, best een lange tijd, en toch vliegt het voorbij. Natuurlijk hoef je het gelukkig niet helemaal alleen te doen. Ten eerste wil ik graag mijn promotoren en co-promotoren bedanken. Ton, mede dankzij jou ben ik aan dit project begonnen. De rust die jij uitstraalt gaf mij altijd vertrouwen. Bedankt voor de fijne samenwerking. Martien, jouw heldere kijk op het geheel was erg nuttig evenals je mooie, heldere formuleringen. Ik heb veel van je geleerd en ben blij dat je mijn promotor bent. Fons, jouw inbreng lag vooral in het begin van het project. Ik heb de samenwerking met levensmiddelenchemie en fysische chemie en kolloïdkunde als zeer waardevol ervaren. Harmen, tja wat zal ik zeggen... (ondanks die twee diagonaal tegengestelde kwadranten) toppie?! Je had altijd tijd en aandacht voor me wanneer het nodig was, ook toen het WCFS project B009 al lang verleden tijd was (ja, ook jij hebt stiekem een zwak voor B009; laatste uitje, allerlaatste uitje, allerallerlaatste uitje, etc.) en tegelijkertijd liet je me heel zelfstandig mijn eigen gang gaan. Ik bewonder je aanstekelijke optimisme en het feit dat bij jou de ontwikkeling van je AIO's altijd centraal lijkt te staan.

Dan ga ik graag eerst even terug naar mijn middelbare school: dhr. van Lottum en dhr. Gradussen, jullie hebben mijn interesse gewekt in de natuur- en scheikunde; ik vind het nog steeds leuk! Tijdens mijn studie waren het vooral mijn afstudeerbegeleiders die mijn enthousiasme voor de fysische chemie van levensmiddelen warm hielden. Leonard, Erik en Natalie en George, bedankt daarvoor.

Alle team members van B009, oftewel het 'biopolymer stability and functionality' project van het WCFS, waarin ik tijdens mijn promotieonderzoek ondergebracht werd, bedankt! Ook al kwam ik pas twee jaar nadat (de meesten van) jullie begonnen waren, ik voelde me vanaf dag 1 op mijn plek. Peter en Kerensa, nog een keer met zijn drieën aan één touw? Peter, bedankt voor hulp bij de ellipsometer, IRRAS, etc. en voor alle discussies. Toch fijn te weten dat ik niet de enige ben die dat één artikel maar niet kan vinden, misschien schrijf jij m nog eens!? Ik vind het leuk dat je mijn paranimf bent. Marcel, bedankt voor alle leuke discussies over mijn project en van alles en nog wat, altijd lachen met jou! Hans K., bedankt voor alle hulp, ik vond het heel leuk om samen te werken. We konden de goede B009 sfeer nog leuk even voorzetten in het scheikunde gebouw, maar die surface shear, zucht... Jolan, je moest er misschien even aan wennen, die bijgehante opmerkingen van Bas en mij, maar stiekem kon je er zelf ook wat van! Bedankt voor de hulp op het lab, de gezelligheid en alle fijne tussen-het-werk-door praatjes. Helena, spaciba bolshoj for the help and advice with TRFA. I enjoyed working together and sawing the yolki palkies in the garden of the datscha! Thank you, Alex and Dasha (gurka, gurka for your wedding Dasha, congratulations!!) for the

great Moscow experience. Cristina, muchas gracias por las dias Valencianas, eating an orange will never be the same. Mijn twee studenten: Frouke, dankjewel voor jouw ‘vette’ bijdrage, de olie/water data zijn een mooie aanvulling op mijn proefschrift. Kiki, thanks for your colourful and inspiring input, you’ve been a great help. Good luck with your PhD! I have learned a lot from both of you! Jan B., op dezelfde dag begonnen bij LMC, meeverhuisd naar Fysko, even lang volgehouden, en nu zit ik op jouw ‘oude plek’! Bedankt voor goede nuttige discussies, de trip naar Berlijn en de gezelligheid.

De eerste helft van mijn promotietijd heb ik met veel plezier bij levensmiddelenchemie gezeten. Bas, Hauke, GerdJan en Karin, bedankt voor het organiseren van het geweldige Japan avontuur! Steph ‘MSN buddy’ G, GerdJan, Hauke, Sandra, en Mirjam, bedankt voor de hulp met skalar, HPLC, etc., Jan ‘meneer van de overkant’ C. voor de hulp met GC en Jolanda voor de goede organisatie. Evelien (XL?), Koen ‘san’, Gerrit vK., Steph P., Laurice, Lidwien, Wil, Aagje, bedankt voor de leuke koffiepauzes en de inbreng in de foute grappen top tien (ik denk dat er op deze pagina’s ook wel een aantal nominaties staan). Verder, ook iedereen die ik niet bij naam noem, bedankt voor de goede sfeer en de gezelligheid, zowel tijdens werk, als op wandelweekenden, labuitjes, etc.!

De tweede helft van mijn promotietijd zat ik bij fysische chemie en kolloïdkunde. Ook daar heb ik het altijd erg naar mijn zin gehad. Ik vond de werkbesprekingen een aangename en goede manier om over verschillende onderwerpen te discussiëren. Er hing altijd een goede sfeer in de labs, kantoren, gangen, en last but certainly not least, in het secretariaat. Josie, Willy, Bert en Anita, alles om het onderzoek heen verliep altijd op rolletjes dankzij jullie! Ronald, Mara, Remco (lichtverstrooier), Ab (zetaszter) en Franklin, mede dankzij jullie liepen vele experimenten gesmeerd. Herman, bedankt voor de goede discussies, Gert voor de hulp met de kaft. Remco, ‘to beam or not to beam’ that’s the question! Als jij niet tot drie keer toe met mij meegereisd was naar ISIS, was hoofdstuk 5 niet geweest wat het nu is, dankjewel daarvoor. Ik dank het hele B014 team voor het adopteren van mij als ‘weesAIO’. Olga, het was leuk samen op de kamer, ondanks de rotzooi ;-). Hans L., ik waardeer het zeer dat jij de taak van plaatsvervangend rector op je wilt nemen bij mijn verdediging. Iedereen bedankt voor de goede herinneringen aan o.a. het geven van practica, de chemie olympiade, de lange wandelingen in en rond ‘Han sur Lesse’, overdag en ’s nacht naar de lokale ‘openlucht bar’ in Han, de AIO-uitjes, de labuitjes, FICS- en ‘spontane’ borrels, dagelijkse lunches en koffiepauzes. Beter verse koffie op ‘gezette’ tijden dan de hele dag automaatkoffie!

Bram, bedankt voor de samenwerking in het ‘carbohydrate stabilised protein dispersions project’. Het was fijn om niet in mijn eentje tussen de eiwitten en polysacchariden in te staan! Verder ook Henk, Harry en Willem, bedankt voor jullie inbreng.

Verder is er nog een aantal andere mensen van andere groepen die ik wil bedanken: Harry Baptist van levensmiddelenbiologie, Jan Willem Borst en Ton en Nina Visser van het MicroSpectroscopy Centre, Wageningen voor de hulp bij TRFA experimenten en de uitwerking daarvan. Stephen Holt and John Webster of ISIS pulsed neutron & muon source, I thank you for your help with neutron reflection measurements and the interpretation of the data. Dirk Visser en NWO, bedankt voor de mogelijkheid om de neutronen experimenten te

doen. Ad van Well van het IRI, TU Delft bedankt voor de discussie over de neutronen data. Kees de Kruif en Hans Tromp van NIZO food research bedankt dat jullie mij de gelegenheid hebben gegeven SAXS experimenten te doen, het was een mooie ervaring. Theo, Anneke en Elke, bedankt voor het organiseren van de AIO-reis naar Engeland.

Verder wil ik al mijn vrienden bedanken voor al het leuks, altijd fijn om dat werk voor even te vergeten. Marieke, sinds we elkaar kennen hebben we (behalve de stages) nog nooit zover uit elkaar gewoond. Het was super op T14 (op het eind leek het wel een hotel) bedankt voor de leuke tijd daar! Janine, in jouw oude huisje voel ik me meteen thuis in Rotterdam, leuk, kom maar vaak langs! Marieke en Sander, worden we ooit nog weer buren, misschien in Rotterdam? Bas en Julia, ex-huisgenoten (+aanhang), ex-studiegenoten, ex-collega's, maar gelukkig geen ex-vrienden! Ik hoop jullie en Liese nog heel veel te zien. Bas, 'my brother', leuk dat je mijn paranimf bent, wie weet werken ooit we nog eens samen?! Guliana, kom je binnenkort 's lekker dansen in Rotterdam? Alle studiegenoten bedankt voor alle feestjes en de leuke pinksterweekenden, hopelijk blijft de traditie nog lang bestaan. Diane, het was leuk om samen 'verder te studeren' bij Fysko, succes nog! Jij en Annemarie, Arjon, Myrthe bedankt voor de hulp in m'n nieuwe huis. Josiene, Michel en Ise, meiden van ZVO, buren van de Thorbeckestraat, salsa vrienden, mensen van bodyline, opa, de rest van de familie en iedereen die ik vergeten ben (sorry).

Tenslotte, dank aan mijn ouders en broer(tje) en zus(je), altijd fijn om weer even in Zutphen te zijn, vooral 's zomers in de tuin. Rudie, bedankt voor de ict-ondersteuning, Sonja, voor het altijd voor me klaar staan 'om de hoek', wel wennen nu zo ver weg he? Pap en mam, bedankt voor al jullie steun en interesse en het mij bijbrengen van doorzettingsvermogen en nuchterheid. Ik ben trots op wat jullie allemaal bereiken/bereikt hebben, jullie zijn mijn goede voorbeeld!

Renate

List of publications

Sagis, L. M. C.; Veerman, C.; Ganzevles, R.; Ramaekers, M.; Bolder, S. G.; van der Linden, E., Mesoscopic structure and viscoelastic properties of beta-lactoglobulin gels at low pH and low ionic strength. *Food Hydrocolloids* **2002**, 16, (3), 207-213.

Ganzevles, R. A.; Cohen Stuart, M. A.; van Vliet, T.; de Jongh, H. H. J., Use of polysaccharides to control protein adsorption to the air-water interface. *Food Hydrocolloids* **2006**, 20, (6), 872-878.

Ganzevles, R. A.; Zinoviadou, K.; van Vliet, T.; Cohen Stuart, M. A.; de Jongh, H. H. J., Modulating Surface Rheology by Electrostatic Protein/Polysaccharide Interactions. *Langmuir* **2006**, 22, (24), 10089-10096.

Ganzevles, R. A.; van Vliet, T.; Cohen Stuart, M. A.; de Jongh, H. H. J., Manipulation of adsorption behaviour to liquid interfaces by protein polysaccharide electrostatic interactions. In *Food Colloids; Self-Assembly and Material Science*, Royal Society of Chemistry: Montreux, **2007**, 193-206, in press.

Ganzevles, R. A.; Fokkink, R.; van Vliet, T.; Cohen Stuart, M. A.; de Jongh, H. H. J., Structure of mixed β -lactoglobulin/pectin adsorbed layers at air/water interfaces; a spectroscopy study. to be submitted.

Ganzevles, R. A.; Kosters, H.; van Vliet, T.; Cohen Stuart, M. A.; de Jongh, H. H. J., Pullulan charge density controlled β -lactoglobulin complexation in relation to surface activity. to be submitted.

Ganzevles, R. A.; van Vliet, T.; Cohen Stuart, M. A.; de Jongh, H. H. J., Complex coacervate morphology controlled by polysaccharide charge density. to be submitted.

Ganzevles, R. A.; Benjamins, J.; van Vliet, T.; Cohen Stuart, M. A.; de Jongh, H. H. J., Polysaccharides as a kinetic barrier for protein accumulation at air/water interfaces. to be submitted.



Curriculum vitae

Renate Antonia Ganzevles werd geboren op 27 januari 1978 te Warnsveld. In 1996 behaalde ze haar VWO diploma aan het R.K. Isendoorn college te Warnsveld. In datzelfde jaar begon ze haar studie levensmiddelentechnologie aan de Wageningen Universiteit. Haar eerste afstudeervak deed ze bij de leerstoelgroep Levensmiddelennatuurkunde (*Fasegedrag en reologie van mengsels van β -lactoglobuline en dextraan*), gevolgd door een stage bij Quest International in Naarden (*Effect van hydrokolloïden en emulgatoren op de textuur van romige sauzen*). De tweede stage was aan de University of New South Wales in Sydney, Australië (*Het effect van ethanol op smaakwaarneming*). Ten slotte deed ze haar tweede afstudeervak bij de leerstoelgroep Fysische Chemie en Kolloïdkunde (*Insertie van emulsiedruppels in lucht/water grensvlakken*) en studeerde vervolgens af in 2002. Per september 2002 was zij in dienst bij de Wageningen Universiteit, leerstoelgroep Fysische Chemie en Kolloïdkunde, als promovendus. Hier voerde zij in opdracht van het Wageningen Centre for Food Sciences het in dit proefschrift beschreven werk uit. Sinds februari 2007 is zij werkzaam als ‘biopolymer physical scientist’ bij Unilever Research and Development in Vlaardingen.

Overview of completed training activities

Discipline specific activities

PhD study trip UK	VLAG	2002
Industrial protein conference	IOP	2003
Liquids and interfaces	NWO	2003
Physical chemistry winterschool 'Dynamics'	Han sur Lesse	2003
Liquids and interfaces	NWO	2004
Physical chemistry winterschool 'Statics'	Han sur Lesse	2004
International workshop: Bubble and drop interfaces	Genova, Italy	2004
PhD study trip Japan (Laboratory of Food Chemistry)	WUR	2004
Molecular modelling and statistical thermodynamics (Laboratory of Physical Chemistry and Colloid Science)	WUR	2005
European Conference on the Spectroscopy of Biological Molecules	Aschaffenburg, Germany	2005
Liquids and interfaces	NWO	2006
Food Colloids Conference	Montreux, Switzerland	2006

General courses

PhD introduction course	VLAG	2002
Scientific writing (The Language Centre)	WUR	2003
Philosophy and ethics of food science & technology (Product Design and Quality Management)	WUR	2003

The research presented in this PhD Thesis was part of the research programme ‘Structure and Functionality’ of the Wageningen Centre for Food Sciences and was carried out at Wageningen University, The Netherlands

Cover: Gert Buurman

Printing: Ponsen & Looijen bv, Wageningen